



Universidad  
Politécnica  
de Cartagena



PROGRAMA DE DOCTORADO EN TECNOLOGIAS INDUSTRIALES

TESIS DOCTORAL

INVESTIGACIÓN DE LAS PROPIEDADES DE UN OPERADOR DE RECONSTRUCCIÓN  
NO LINEAL EN MALLADOS NO UNIFORMES

Presentada por D. PEDRO ORTIZ HERRANZ para optar al  
grado de Doctor  
por la Universidad Politécnica de Cartagena

Dirigida por:  
Dr. JUAN CARLOS TRILLO MOYA

Cartagena, 2021



Universidad  
Politécnica  
de Cartagena

U ESCUELA  
P INTERNACIONAL DE  
C DOCTORADO  
T

DOCTORAL PROGRAMME IN INDUSTRIAL TECHNOLOGIES

PhD THESIS

RESEARCH ON CERTAIN PROPERTIES OF AN ADAPTED NONLINEAR  
RECONSTRUCTION OPERATOR ON NONUNIFORM GRIDS

Presented by D. PEDRO ORTIZ HERRANZ to the Technical  
University of Cartagena in fulfilment of the thesis  
requirement for the award of  
PhD

Supervisor:  
Dr. JUAN CARLOS TRILLO MOYA

Cartagena, 2021

Dedico esta tesis a la memoria de mis padres y a mi familia.

A mis padres, por su esfuerzo, cariño y por sus sabios consejos. A mi esposa, por su apoyo y comprensión durante estos años. A mis hijos para que les sirva de guía.

Quiero dar las gracias hoy y siempre a todas las personas que de una u otra forma han contribuido a mi formación, me han ayudado, me han acompañado en los momentos alegres y tristes y han hecho de mí la persona que soy.

A mis amigos cercanos y a mis amigos de la infancia y adolescencia, con quienes sigo compartiendo buenos momentos.

A Pepe y Leonor Sáez, a José María y María Raja, por recibirme en su casa con alegría infinita.

A mi profesor de instituto, Rafael Hostench, hombre de voz profunda y clara, quien encendió una luz que me permitió descubrir la belleza de las matemáticas. Siempre estaré en deuda con él.

Muchos profesores he tenido a lo largo de mi camino; a todos los recuerdo con afecto y agrado. Quiero plasmar aquí el nombre de algunos que de una u otra forma me han impactado, ya sea por su lucidez, por su exquisito trato, por su generosidad o por todo. Ahí están Ángel Rodríguez Rubio, José Tomás Díez Roche, catedrático de mecánica de fluidos, brillante y singular, sus clases fueron lecciones magistrales, José María Sáez de Benito, catedrático de resistencia de materiales, no solo por los conocimientos que transmitió, sino también por la elegancia y claridad con la que lo hizo.

De esto hace ya muchos años. Hace no tantos, decidí retomar los estudios y hacer la tesis doctoral, contacté con el departamento de Matemática Aplicada y Estadística de la Universidad Politécnica de Cartagena donde todo han sido facilidades y ayuda. Aquí he conocido a profesores de ésta y otras universidades, con los que he colaborado en algunos de los artículos presentes en esta tesis. A todos ellos, mi agradecimiento.

Para el final dejo a Juan Carlos Trillo, mi director de tesis. Siempre es un placer conocer personas brillantes de las que puedes aprender, desinteresadas y generosas. Le doy las gracias por su amistad, por abrirme nuevos caminos, por valorarme, ayudarme a mejorar y compartir conmigo parte de sus conocimientos. Mi más sincera gratitud.

Pedro Ortiz Herranz

# Resumen

Los esquemas de subdivisión y multiresolución se han utilizado en las últimas décadas en muchas aplicaciones que requieren del diseño geométrico. Estas aplicaciones son numerosas en la industria, por ejemplo para la fabricación de coches y barcos, y también en la industria cinematográfica para generar diferentes formas tanto en  $2D$  como en  $3D$ . Los esquemas de subdivisión se basan en un proceso de refinamiento sucesivo de un conjunto inicial de datos discretos. Se genera un nuevo conjunto de datos más denso de acuerdo con algunas reglas específicas. A su vez, este nuevo conjunto se refinará aún más. En este punto surgen diversas cuestiones matemáticas importantes, y que van desde asegurar la convergencia de los esquemas a estudiar la suavidad de la función límite, la estabilidad de los esquemas de subdivisión, el orden de aproximación y los requisitos necesarios para su aplicabilidad en problemas de la vida real. En particular, es importante el análisis de las capacidades de preservación de los esquemas para algunas propiedades cruciales que podrían estar presentes en el conjunto inicial de datos, tal como la convexidad.

Los esquemas de subdivisión generan algoritmos rápidos para la fácil construcción de curvas y superficies [26], [29]. Todas estas cualidades los convierten en una herramienta interesante para diversas aplicaciones industriales. Además, su estrecha relación con esquemas de multiresolución abre la puerta a más aplicaciones en el campo del procesamiento de datos y señales. Los procesos de compresión y eliminación de ruido son fáciles de implementar mediante el uso de esquemas de multiresolución y se ha comprobado que son bastante eficientes. Véase, por ejemplo [35], [5], [2].

Una cuestión principal a la hora de elegir un esquema de subdivisión adecuado es la propiedad de conservación de la convexidad, porque muchas aplicaciones la requieren. Se han hecho muchos esfuerzos en este sentido, véase por ejemplo [27], [32], [33], [37].

La estabilidad es también un problema principal en las aplicaciones de la vida real, ya que los diseños finales se generan mediante el refinamiento de un conjunto inicial de puntos que suele estar afectado por algún error. Por lo tanto, es esencial hacer un seguimiento del error y mantenerlo por debajo de una tolerancia prescrita. Algunas referencias recomendadas sobre la estabilidad de los esquemas de subdivisión y multiresolución pueden consultarse en [24], [9], [11], [1], [3], [15].

Harten derivó una teoría que conecta estrechamente los operadores de reconstrucción con los esquemas de subdivisión y multiresolución [35], [5]. Las reconstrucciones no lineales aparecen como una buena opción para minimizar los efectos adversos de las posibles singularidades y para mejorar la adaptación a los datos dados. Esta teoría no es tan fácil de estudiar como para el caso lineal. Los operadores de reconstrucción no lineales dan lugar a esquemas de subdivisión y multiresolución no lineales. Para dejar claro el tipo de dificultades que se pueden encontrar, mencionamos por ejemplo el caso del análisis de estabilidad. A este respecto, se ha demostrado que todos los esquemas de subdivisión y multiresolución lineales son estables, mientras que se necesita un análisis particular para cada esquema no lineal concreto.

Los esquemas de multiresolución están profundamente conectados con los esquemas de subdivisión y heredan muchas de sus propiedades. Para más información sobre estas herramientas se puede consultar [5] como primera referencia.

En [6] se introdujo una reconstrucción no lineal denominada PPH y se estudió el esquema de subdivisión asociado. Esta reconstrucción se definió con el fin de adaptarse a la presencia de potenciales singularidades. Consiste en una modificación ingeniosa de la interpolación centrada de cuarto orden de Lagrange a trozos. Para implementar la adaptación, la reconstrucción se realiza

localmente en un intervalo  $[x_j, x_{j+1}]$  usando los valores disponibles de la función en las cuatro abscisas centradas  $\{x_{j-1}, x_j, x_{j+1}, x_{j+2}\}$ , y teniendo en cuenta dos aspectos principales. El primer aspecto es que la modificación en un área donde la función subyacente es suave debe hacerse de tal manera que las cantidades alteradas no cambien significativamente, de modo que la modificación siga siendo  $O(h^4)$ , donde  $h$  representa el espaciado del mallado. El segundo aspecto es que en los intervalos adyacentes a una singularidad, pero que no la contienen, la reconstrucción conserve cierto orden de aproximación, de hecho  $O(h^2)$ , al contrario de lo que ocurre con su homólogo lineal que pierde completamente el orden de aproximación.

Esta tesis se dedica principalmente al estudio del operador de reconstrucción no lineal PPH en mallados no uniformes. En algunos casos y para demostrar determinados resultados teóricos haremos uso de mallados  $\sigma$  cuasi uniformes, que no son otra cosa que un tipo de mallados no uniformes que aparecen en casi todas las aplicaciones prácticas. La definición exacta se da más adelante.

Esta memoria está organizada con la estructura que a continuación se detalla. Obsérvese que todos los capítulos han sido redactados para permitir su lectura fácil, haciéndolos lo más autocontenidos posible. Cada capítulo ha dado lugar a un artículo de investigación. Dichos artículos han sido presentados para su publicación en diferentes revistas matemáticas indexadas en el Journal Citations Report (JCR) dentro del primer cuartil de revistas en los ámbitos de Matemáticas o Matemáticas Aplicadas. En algunos casos, los artículos ya han sido publicados y la referencia exacta se incluye tanto al principio del capítulo como en la bibliografía.

**Capítulo 2** En [11], se consideró el problema de estabilidad del esquema de subdivisión PPH en mallados uniformes mediante el uso de ciertas propiedades de contractividad de las diferencias divididas de segundo orden. En este capítulo proponemos un estudio paralelo utilizando diferencias divididas de primer orden en su lugar, obteniendo una menor constante de estabilidad, más ajustada a la realidad. El estudio se realiza para datos iniciales convexos procedentes de funciones suaves. Dado que el esquema de subdivisión PPH considerado preserva la convexidad [37], [10], la propiedad de convexidad de los datos iniciales está garantizada en todas las escalas de refinamiento. A lo largo de este capítulo introducimos el esquema de subdivisión PPH, damos el esquema resultante para las primeras diferencias, y el resultado que garantiza la convergencia del esquema. También estudiamos la contractividad del esquema para las diferencias, y probamos el resultado de estabilidad anunciado mejorando la constante de estabilidad en [11] y en [33] para datos iniciales estrictamente convexos que satisfacen una cierta restricción. Finalmente, damos un ejemplo numérico para mostrar las potenciales aplicaciones de la teoría presentada y algunas conclusiones.

**Capítulo 3** Damos una definición del operador de reconstrucción PPH para datos sobre mallados no uniformes, y estudiamos algunas propiedades de este operador en mayor profundidad. En particular, nos centramos en la suavidad de la reconstrucción y en la conservación de la convexidad de los datos iniciales. Demostramos que la reconstrucción PPH da una función  $C^\infty$ , excepto para los nodos en los que la función sigue siendo  $C^0$  y donde las diferencias entre la primera, segunda y tercera derivadas laterales son de tercer, segundo y primer orden respectivamente (véase la definición 7).

En [10], los autores demostraron que el esquema de subdivisión asociado en mallados uniformes preserva la convexidad de los puntos de control. En este artículo, intentamos determinar si este resultado sobre preservar la convexidad puede extenderse para el operador de

reconstrucción y no sólo en mallados uniformes, sino también en mallados  $\sigma$  cuasi-uniformes con  $\sigma \leq 4$ .

El capítulo comienza con la definición del operador de reconstrucción PPH sobre mallados no uniformes. Para ello, se hace uso de una media armónica ponderada con los pesos adecuados. A continuación, se muestra que el nuevo operador de reconstrucción equivale al operador de reconstrucción PPH original cuando se restringe a mallados uniformes. La definición se da para mallados generales no uniformes, aunque para establecer algunos resultados teóricos, se consideran mallados  $\sigma$  cuasi-uniformes. A continuación, se estudian algunas propiedades básicas de la reconstrucción PPH, como la reproducción de polinomios de segundo grado, el orden de aproximación, la suavidad, la acotación del operador, la continuidad de Lipschitz y la conservación de la convexidad. También se analiza la reconstrucción cuando se trata de datos iniciales estrictamente convexos (o cóncavos). Por último, se presentan algunas pruebas numéricas y se incluyen algunas conclusiones.

**Capítulo 4** En este capítulo, analizamos el comportamiento del operador de reconstrucción PPH en presencia de discontinuidades de salto. Probamos la adaptación a la presencia de una discontinuidad de salto en el sentido de que se mantiene algún orden de aproximación en la zona cercana a la discontinuidad, al contrario de lo que ocurre con los operadores lineales que pierden completamente el orden de aproximación. También demostramos, tanto teóricamente como en los experimentos numéricos, la ausencia de oscilaciones debidas al fenómeno de Gibbs.

**Capítulo 5** La media armónica original presenta dos características indeseables para nuestros fines. La primera es la posible división por cero en el denominador, y la segunda la necesidad de la hipótesis  $x = O(1)$ , e  $y = O(1)$ , junto con  $|x - y| = O(h)$  para poder asegurar que la media armónica se mantendrá cerca,  $O(h^2)$ , de la media aritmética. En el operador de reconstrucción los argumentos  $x$  e  $y$  de la media armónica son diferencias divididas de segundo orden, y entonces no es una sorpresa que los problemas mencionados surjan cerca de los puntos de inflexión o cerca de las singularidades de la función subyacente. Para resolver ambos problemas en este capítulo se presenta una definición general de lo que se entiende por un operador de traslación. A continuación, se hace uso de este operador para modificar la media armónica ponderada de tal manera que se obtiene una nueva media adaptada que conserva propiedades similares a la original, lo que es de vital importancia para ser empleada en la definición del operador de reconstrucción PPH adaptado. Se estudian varias opciones posibles de expresiones concretas para el operador de traslación para trabajar en combinación con el operador de reconstrucción PPH. En particular, se define una forma de elegir una buena opción en función de los datos específicos a los que se va a aplicar con el fin de adaptarse en presencia de discontinuidades y mantener el orden de la reconstrucción alrededor de los puntos de inflexión.

Los nuevos resultados contenidos en el capítulo parten de la mencionada definición y estudio del operador de traslación. A continuación, se analiza el comportamiento del operador de reconstrucción PPH mejorado con respecto al orden de aproximación. Posteriormente, se presentan algunos operadores de traslación específicos, y se da una forma de seleccionar un parámetro de traslación adecuado en función de los datos. Se presentan algunas pruebas numéricas para confirmar los resultados teóricos. Por último, se ofrecen algunas conclusiones.

**Capítulo 6** Dedicamos este capítulo a relacionar el operador de reconstrucción PPH con los splines suavizantes en un intervalo dado  $[a, b]$ . Los splines suavizantes se construyen mediante tro-

zos de reconstrucción polinómicos que se enlazan de forma suave en los nodos de control y satisfacen el problema de minimización

$$\min_{p \in \Pi_n} J(p) := \min_{p \in \Pi_n} \int_a^b p''(x)^2 dx + \sum_j \mu_j (p(x_j) - f_j)^2, \quad (1)$$

donde  $\Pi_n$  representa el espacio vectorial de los polinomios de grado menor o igual a  $n$ . El funcional considerado implica un compromiso, dominado por los pesos  $\mu_j$ , entre un término de baja curvatura y un valor pequeño de la distancia acumulada al conjunto inicial de datos  $(x_j, f_j)$ .

En concreto, se destacan dos propiedades principales que van a ser cruciales para los propósitos que se persiguen: La preservación de la convexidad cuando se parte de un conjunto discreto de datos convexos y un término de curvatura bajo. Esta última propiedad sobre la curvatura es parte de lo que se va a estudiar a lo largo del capítulo. Más concretamente, se estudia el término de curvatura del funcional para las reconstrucciones de Lagrange y PPH, tanto en el caso uniforme como en el no uniforme. Los resultados del estudio realizado parecen indicar que la conexión entre la reconstrucción PPH y los splines suavizantes podría dar lugar a aplicaciones muy interesantes.

**Capítulo 7** Los esquemas de subdivisión no lineales han surgido como variación de los esquemas lineales para adaptarse a los datos específicos en uso. La no linealidad se refiere a los esquemas de subdivisión dependientes de los datos que también pueden implicar operaciones no lineales en su definición. Entonces, inherentemente, están diseñados para superar ciertos inconvenientes que aparecen cuando se trata con sus homólogos lineales, como por ejemplo el mal comportamiento en presencia de discontinuidades aisladas. Un caso particular de este tipo de operadores se definió en [6] y se denominó PPH (Piecewise Polynomial Harmonic). Este esquema consiste básicamente en una ingeniosa modificación del clásico esquema de subdivisión de Lagrange con cuatro puntos. Se han realizado varios estudios sobre sus propiedades y rendimiento en diferentes aplicaciones, véase por ejemplo [6], [10], [32]. Dos objetivos principales de este esquema de subdivisión están relacionados con el tratamiento de datos que contienen discontinuidades aisladas, reduciendo los efectos indeseables, y con la preservación de la convexidad de los datos iniciales, mientras se mantiene un soporte centrado basado en cuatro puntos.

En el capítulo 3 se extendió la definición del operador de reconstrucción PPH a mallados no uniformes. A su vez, este hecho nos permite extender el esquema de subdivisión PPH a este tipo de mallados no uniformes, y realizar un estudio paralelo en este nuevo entorno. Para superar algunas dificultades técnicas en las pruebas teóricas, se ha considerado una restricción a mallados  $\sigma$  cuasi-uniformes en algunos resultados. El esquema resultante es bastante interesante en términos de aplicaciones debido a la suavidad casi  $C^1$  de la función límite, que permite aproximar con precisión funciones continuas con esquinas, y también debido a sus buenas propiedades en cuanto a la preservación de la convexidad de los datos iniciales.

A lo largo del capítulo se recuerda el operador de reconstrucción PPH sobre mallados no uniformes. Se presenta una breve reseña sobre el entorno de multirresolución interpolatoria de Harten, que está estrechamente relacionado con los esquemas de subdivisión interpolatoria. A continuación, se define un esquema de subdivisión asociado. Esta definición se da

para mallados generales no uniformes, aunque para establecer algunos resultados teóricos se consideran mallados  $\sigma$  cuasi-uniformes. A partir de este punto, se analizan las principales cuestiones sobre los esquemas de subdivisión. En particular, se demuestran algunos resultados sobre la convergencia del esquema, la suavidad de la función límite y la preservación de la convexidad. Además, se realizan algunas pruebas numéricas para comprobar la suavidad teórica de la función límite y el comportamiento del esquema de subdivisión no lineal.

**Capítulo 8** La media aritmética y la media armónica de números positivos aparecen en muchas aplicaciones científicas que van desde la estadística hasta el análisis numérico. La media armónica tiene la propiedad de penalizar los valores grandes, dando lugar, por esta razón, a varias aplicaciones interesantes. Además, cuando los argumentos no difieren mucho entre sí, ambas medias se mantienen cercanas, lo que constituye otra propiedad crucial para ciertas aplicaciones.

Este capítulo tiene por objetivo el presentar algunos ingredientes necesarios para extender el operador de reconstrucción PPH a varias dimensiones. Más concretamente, se necesita disponer de una media apropiada en varias variables que satisfaga las propiedades básicas mencionadas anteriormente, como lo hace la media armónica. De hecho, la media armónica ponderada de varios valores cumple el objetivo. Este estudio se acompaña de una interpretación gráfica de la media armónica ponderada de varios valores, que ayuda a comprender rápidamente los resultados teóricos.

El capítulo se inicia con las medias aritmética y armónica ponderadas de dos números positivos, demostrando los dos resultados esenciales sobre estas medias que nos permitirán definir operadores de reconstrucción adaptados. Estos resultados vienen acompañados de una interpretación gráfica intuitiva en  $2D$  según un resultado teórico correspondiente que también se prueba. Se sigue un camino similar para el caso de  $3D$ , que implica trabajar con medias ponderadas y armónicas de tres números positivos. A continuación, se aborda el caso general, considerando las medias aritmética y armónica ponderadas de  $n$  números positivos para cualquier valor entero  $n \geq 2$ . Se termina el capítulo esbozando algunas aplicaciones de estos resultados para permitir la definición de reconstrucciones adaptadas en varias dimensiones, y se define explícitamente una nueva reconstrucción en  $2D$  sobre mallados triangulares adaptada a las discontinuidades, es decir, una especie de método de reconstrucción PPH sobre triángulos.

**Capítulo 9** Se termina este documento con algunas perspectivas y propuestas de trabajos futuros que han ido apareciendo durante la realización de esta tesis, y cuya idea principal surge directamente en relación con los resultados contenidos en los capítulos anteriores.



This thesis is dedicated to the memory of my parents and my family.

To my parents, for their effort, affection and for their wise advice. To my wife, for her support and understanding during these years. To my children to serve as a guide for them.

Today and always I want to thank all the people who in one way or another have contributed to my training, have helped me, have shared happy and sad moments and have made me the person I am.

To my close friends and to my friends from childhood and adolescence, with whom I continue to share good times.

To Pepe and Leonor Sáez, to José María and María Raja, for receiving me in their home with infinite joy.

To my high school teacher, Rafael Hostench, a man with a deep and clear voice, who turned on a light that allowed me to discover the beauty of mathematics. I will always be in debt to him.

I have had many teachers along my path; I remember them all with affection and pleasure. I want to bring here the names of some who in one way or another have impacted me, either for their lucidity, for their exquisite treatment, for their generosity or for everything. There are Ángel Rodríguez Rubio, José Tomás Díez Roche, professor of fluid mechanics, brilliant and unique, his classes were master classes, José María Sáez de Benito, professor of resistance of materials, not only because of the knowledge he transmitted, but also for the elegance and clarity with which he did it.

This was many years ago. Not so long ago, I decided to continue my studies and write my doctoral thesis, I contacted the Department of Applied Mathematics and Statistics at the Universidad Politécnica de Cartagena where everything has been facilities and help. Here I have met professors from this and other universities, with whom I have collaborated on some of the articles in this thesis. To all of them my thanks.

For the end I leave Juan Carlos Trillo, my thesis advisor. It is always a pleasure to meet brilliant people you can learn from, selfless and generous. I thank him for his friendship, for opening new paths for me, for valuing me, helping me improve and sharing part of his knowledge with me. My most sincere gratitude.

Pedro Ortiz Herranz

# Contents

<b>1</b>	<b>Introduction</b>	<b>15</b>
<b>2</b>	<b>Improving the stability bound for the PPH nonlinear subdivision scheme for data coming from strictly convex functions</b>	<b>20</b>
2.1	Introduction . . . . .	20
2.2	PPH subdivision scheme . . . . .	21
2.3	Scheme for the differences. Convergence . . . . .	22
2.4	Lipchitz condition for the scheme $S_1$ for a class of strictly convex initial data . . . . .	22
2.5	Stability result for a set of strictly convex initial data . . . . .	32
2.6	Conclusions . . . . .	33
<b>3</b>	<b>On the convexity preservation of a quasi <math>C^3</math> nonlinear interpolatory reconstruction operator on <math>\sigma</math> quasi-uniform grids</b>	<b>34</b>
3.1	Introduction . . . . .	34
3.2	A nonlinear PPH interpolation procedure on nonuniform grids . . . . .	35
3.3	Main properties of the PPH reconstruction operator in nonuniform meshes . . . . .	41
3.3.1	Reproduction of polynomials up to degree 2 . . . . .	41
3.3.2	Approximation order for strictly convex (concave) functions . . . . .	41
3.3.3	Smoothness . . . . .	42
3.3.4	Boundedness and Lipschitz continuity . . . . .	44
3.3.5	Convexity preservation . . . . .	48
3.4	PPH reconstruction operator over $\sigma$ quasi-uniform meshes for strictly convex (concave) initial data . . . . .	50
3.5	Numerical experiments . . . . .	51
3.6	Conclusions . . . . .	52
<b>4</b>	<b>PPH nonlinear interpolatory reconstruction operator on nonuniform grids: Adaptation around jump discontinuities and elimination of Gibbs phenomenon</b>	<b>54</b>
4.1	Introduction . . . . .	54
4.2	A nonlinear PPH reconstruction operator on nonuniform grids . . . . .	55
4.3	Approximation order around jump discontinuities . . . . .	59
4.4	Analysis of Gibbs phenomena around jump discontinuities . . . . .	63
4.5	Numerical experiment . . . . .	68
4.6	Conclusions . . . . .	72

<b>5</b>	<b>Improving the approximation order around inflection points of the PPH non-linear interpolatory reconstruction operator on nonuniform grids.</b>	<b>75</b>
5.1	Introduction . . . . .	75
5.2	A nonlinear PPH reconstruction operator on nonuniform grids . . . . .	76
5.3	The translation operator . . . . .	80
5.4	Improved PPH reconstruction operator . . . . .	85
5.5	Nonlinear choice of the parameter $\epsilon$ in the translation operator . . . . .	88
5.6	Numerical experiments . . . . .	89
5.7	Conclusions . . . . .	91
<b>6</b>	<b>On certain inequalities associated to curvature properties of the nonlinear PPH reconstruction operator</b>	<b>100</b>
6.1	Introduction . . . . .	100
6.2	Study of the curvature term in uniform meshes . . . . .	101
6.2.1	Curvature term for the Lagrange reconstruction . . . . .	102
6.2.2	Curvature term for the PPH reconstruction . . . . .	102
6.3	Study of the curvature term in nonuniform meshes . . . . .	105
6.3.1	Curvature term for the Lagrange reconstruction in nonuniform meshes . . . . .	106
6.3.2	Curvature term for the PPH reconstruction in nonuniform meshes . . . . .	106
6.4	Conclusions and perspectives . . . . .	112
<b>7</b>	<b>Analysis of PPH interpolatory subdivision scheme on <math>\sigma</math> quasi-uniform grids.</b>	<b>113</b>
7.1	Introduction . . . . .	113
7.2	A nonlinear PPH reconstruction operator on nonuniform grids . . . . .	114
7.3	Harten's interpolatory multiresolution setting . . . . .	117
7.4	A nonlinear PPH subdivision scheme on nonuniform grids . . . . .	117
7.5	Main properties of the PPH subdivision scheme in nonuniform meshes . . . . .	118
7.6	Numerical experiments . . . . .	133
7.7	Conclusions . . . . .	135
<b>8</b>	<b>Graphical interpretation of the weighted harmonic mean of <math>n</math> positive values and applications.</b>	<b>138</b>
8.1	Introduction . . . . .	138
8.2	About specific results on the weighted harmonic mean of two positive values . . . . .	139
8.3	Geometrical interpretation of the weighted harmonic mean of three positive values . . . . .	142
8.4	Results on the weighted harmonic mean of $n$ values . . . . .	144
8.5	Examples of application . . . . .	155
8.6	Conclusions . . . . .	162
<b>9</b>	<b>Future works and perspectives</b>	<b>165</b>

# List of Figures

3.1	Solid line: Lagrange polynomial; dashed line: piecewise polynomial harmonic (PPH) polynomial. Circles stand for Lagrange values at the nodes, asterisks stand for PPH values at the nodes, and triangles stand for inflection points. . . . .	51
3.2	Solid line: function $f(x) = \sin(x)$ ; dashed line: PPH reconstruction obtained with the finest considered nonlinear grid. <b>(a)</b> : Original function and PPH reconstruction. <b>(b)</b> : Zoom of a part of the signal. . . . .	53
4.1	In black solid line: function $f(x)$ , in green solid line the straight line joining the extreme points of the jump interval $[x_j^k, x_{j+1}^k]$ , in blue dotted line: Lagrange reconstruction, in red dotted line: PPH reconstruction. Void circles stand for initial nodes, filled circles for nodes at the $k$ subdivision level and asterisks for points $P_1$ and $P_2$ . <b>(a)</b> : Lagrange $k = 0$ , <b>(b)</b> : PPH $k = 0$ , <b>(c)</b> : Lagrange $k = 1$ , <b>(d)</b> : PPH $k = 1$ , <b>(e)</b> : Lagrange $k = 2$ , <b>(f)</b> : PPH $k = 2$ . . . . .	73
4.2	Zoom of the region around the jump discontinuity for subdivision grid level $k = 3$ . <b>(a)</b> : Lagrange, <b>(b)</b> : PPH. . . . .	74
5.1	In black solid line: function $f(x)$ . In green solid line the straight line joining the extreme points of the jump interval $[x_j^k, x_{j+1}^k]$ . In blue dotted line: Lagrange reconstruction. In red dotted line: PPHT reconstruction with adapted $\epsilon_j$ . Void circles stand for initial nodes, filled circles for nodes at the $k$ subdivision level. <b>(a)</b> : Lagrange $k = 0$ , <b>(b)</b> : PPHT $k = 0$ , <b>(c)</b> : Lagrange $k = 1$ , <b>(d)</b> : PPHT $k = 1$ , <b>(e)</b> : Lagrange $k = 2$ , <b>(f)</b> : PPHT $k = 2$ . . . . .	97
5.2	Zoom of the region around the jump discontinuity for subdivision grid level $k = 3$ . <b>(a)</b> : Lagrange, <b>(b)</b> : PPHT with adapted $\epsilon_j$ . . . . .	98
5.3	Values of the $\epsilon$ parameter in (5.34) along different intervals for the $x$ variable. <b>(a)</b> : for $\beta = 1$ in the interval $[0, 2\pi]$ , <b>(b)</b> : for $\beta = 1$ in the interval $[3.7, 3.8]$ , <b>(c)</b> : for $\beta = 100$ in the interval $[0, 2\pi]$ , <b>(d)</b> : for $\beta = 100$ in the interval $[3.7, 3.8]$ . . . . .	99
7.1	<b>(a)</b> : Comparison of the subdivision curve after $k = 5$ subdivision levels for the Lagrange subdivision scheme, in dashed red line, and the PPH subdivision scheme in dash-dotted black line. The original function $f(x)$ is also plotted in solid blue line. The initial control points, plotted with red circles, come from one of the nonuniform grids $X$ considered in our two experiments, the one which consists on 30 abscissas in the interval $[0, 1]$ . <b>(b)</b> : Zoom of the area around the first jump discontinuity. . . . .	135

7.2	Comparison of the subdivision curve after $k = 5$ subdivision levels for the Lagrange subdivision scheme, in dashed red line, and the PPH subdivision scheme in dash-dotted black line. The original function is also plotted in solid blue line. The initial control points, plotted with red circles, come from one of the nonuniform grids $X$ considered in our two experiments, the one which consists on 20 abscissas in the interval $[0, 1]$ . <b>(a)</b> : Subdivision curve for data coming from $f(x)$ . <b>(b)</b> : Subdivision curve for data coming from $g(x)$ . . . . .	136
8.1	Representation of the weighted harmonic and arithmetic means. <b>(a)</b> : $w_1 = 0.7$ , $w_2 = 0.3$ , $a_1 = 14$ , $a_2 = 10$ . <b>(b)</b> : $w_1 = 0.5$ , $w_2 = 0.5$ , $a_1 = 14$ , $a_2 = 10$ . <b>(c)</b> : $w_1 = 0.7$ , $w_2 = 0.3$ , $a_1 = 14$ , $a_2 = 2$ . <b>(d)</b> : $w_1 = 0.5$ , $w_2 = 0.5$ , $a_1 = 14$ , $a_2 = 2$ . In black the weighted harmonic mean, in red the weighted arithmetic mean, in dashed magenta line the parabola $p_1(x)$ and in dashed green line the parabola $p_2(x)$ . . . . .	141
8.2	Representation of the three paraboloids considered in Theorem 13 for the representation of the harmonic mean of the values $a_1 = 3$ , $a_2 = 4$ , $a_3 = 6$ . <b>(a, c, e)</b> : weights $w_1 = 0.2$ , $w_2 = 0.2$ , $w_3 = 0.6$ . <b>(b, d, f)</b> : weights $w_1 = w_2 = w_3 = \frac{1}{3}$ . <b>(a, b)</b> : $V_1^*$ . <b>(c, d)</b> : $V_2^*$ . <b>(e, f)</b> : $V_3^*$ . . . . .	145
8.3	Representation of weighted harmonic mean of three positive values $a_1 = 3$ , $a_2 = 4$ , $a_3 = 6$ as the height of the prism through the intersection point of the three paraboloids considered in Theorem 13. Comparison with the weighted arithmetic mean for the representation of the harmonic mean of the values. <b>(a, c)</b> : weights $w_1 = 0.2$ , $w_2 = 0.2$ , $w_3 = 0.6$ . <b>(b, d)</b> : weights $w_1 = w_2 = w_3 = \frac{1}{3}$ . <b>(a, b)</b> : Intersection of the three paraboloids. <b>(c, d)</b> : Comparison between the weighted harmonic mean and the weighted arithmetic mean. . . . .	146
8.4	Representation of weighted harmonic mean according to Corollary 4. <b>(a)</b> : Weighted harmonic mean of the two positive values $a_1 = 3$ , $a_2 = 6$ , with weights $w_1 = 0.6$ , $w_2 = 0.4$ . <b>(b)</b> : Comparison among $H_{\frac{1}{n}}^*$ , $H_w$ , $M_{\frac{1}{n}}^*$ , $M_w$ , in the case of two arguments. <b>(c)</b> : Weighted harmonic mean of the three positive values $a_1 = 6$ , $a_2 = 7$ , $a_3 = 10$ with weights $w_1 = 0.4$ , $w_2 = 0.3$ , $w_3 = 0.3$ . <b>(d)</b> : Comparison among $H_{\frac{1}{n}}^*$ , $H_w$ , $M_{\frac{1}{n}}^*$ , $M_w$ , in the case of three arguments. In blue the harmonic mean, in red the weighted arithmetic mean of the original values, in yellow the arithmetic mean of the modified values. . . . .	155
8.5	Disposition of the considered domain to build the reconstruction inside the red triangle $S_R$ with vertices $BDF$ , using the point values of an underlying function $f(x, y)$ at the six points $A, B, C, D, E, F$ . . . . .	157
8.6	Disposition of the considered domain affected by a jump discontinuity along the blue curve. . . . .	158

8.7 **(a):** Disposition of the considered domain to build the linear and nonlinear reconstructions inside the triangles  $S_R$ ,  $S_Y$ , and  $S_G$ . **(b):** Disposition of the considered domain affected by a jump discontinuity along the blue curve for which we build the linear and nonlinear reconstructions inside the triangles  $S_R$ ,  $S_Y$ , and  $S_G$ . **(c):** Obtained reconstructions, and comparison with the original smooth function  $f(x, y)$  in the triangle  $S_R$ . **(d):** Obtained reconstructions, and comparison with the original discontinuous function  $g(x, y)$  in the triangle  $S_R$ . With blue circles the original function, with red asterisks the linear reconstruction and with black triangles the new nonlinear reconstruction. . . . . 163

# List of Tables

3.1	Approximation errors $E_k$ in $l_\infty$ norm and corresponding approximation orders $p$ obtained after $k$ iterations for the PPH reconstruction with $f(x) = \sin(x)$ , $k = 0, 1, \dots, 7$ .	52
4.1	Approximation errors obtained at iteration $k$ , $k = 1, \dots, 7$ for the considered cases $A_0$ , $A_1, A_2, A_3$ and $A_4$ using the Lagrange reconstruction.	70
4.2	Approximation errors obtained at iteration $k$ , $k = 1, \dots, 7$ for the considered cases $A_0$ , $A_1, A_2, A_3$ and $A_4$ using the PPH reconstruction.	70
4.3	Approximation orders obtained at iteration $k$ , $k = 1, \dots, 7$ for the considered cases $A_0$ , $A_1, A_2, A_3$ and $A_4$ using the PPH and Lagrange reconstructions.	71
4.4	Distances $r_{max}^k$ obtained at subdivision level $k$ , $k = 0, 1, 2, 3, 4, 5, 6, 7$ .	71
5.1	Approximation errors $E_k$ in the infinity norm obtained at iteration $k$ , $k = 0, \dots, 7$ by using the considered reconstruction operators, Lagrange PPH, PPHT with $\epsilon = 0.5$ , PPHT with $\epsilon = 0.05$ , and PPHT with adapted $\epsilon_j$ in the region $A_0$ .	91
5.2	Approximation orders $p$ in the infinity norm obtained at iteration $k$ , $k = 1, \dots, 7$ by using the considered reconstruction operators, Lagrange PPH, PPHT with $\epsilon = 0.5$ , PPHT with $\epsilon = 0.05$ , and PPHT with adapted $\epsilon_j$ in the region $A_0$ .	92
5.3	Approximation errors $E_k$ in the infinity norm obtained at iteration $k$ , $k = 0, \dots, 7$ by using the considered reconstruction operators, Lagrange PPH, PPHT with $\epsilon = 0.5$ , PPHT with $\epsilon = 0.05$ , and PPHT with adapted $\epsilon_j$ in the region $A_1$ .	92
5.4	Approximation orders $p$ in the infinity norm obtained at iteration $k$ , $k = 1, \dots, 7$ by using the considered reconstruction operators, Lagrange PPH, PPHT with $\epsilon = 0.5$ , PPHT with $\epsilon = 0.05$ , and PPHT with adapted $\epsilon_j$ in the region $A_1$ .	93
5.5	Approximation errors $E_k$ in the infinity norm obtained at iteration $k$ , $k = 0, \dots, 7$ by using the considered reconstruction operators, Lagrange PPH, PPHT with $\epsilon = 0.5$ , PPHT with $\epsilon = 0.05$ , and PPHT with adapted $\epsilon_j$ in the region $A_2$ .	93
5.6	Approximation orders $p$ in the infinity norm obtained at iteration $k$ , $k = 1, \dots, 7$ by using the considered reconstruction operators, Lagrange PPH, PPHT with $\epsilon = 0.5$ , PPHT with $\epsilon = 0.05$ , and PPHT with adapted $\epsilon_j$ in the region $A_2$ .	94
5.7	Approximation errors $E_k$ in the infinity norm obtained at iteration $k$ , $k = 0, \dots, 7$ by using the considered reconstruction operators, Lagrange PPH, PPHT with $\epsilon = 0.5$ , PPHT with $\epsilon = 0.05$ , and PPHT with adapted $\epsilon_j$ in the region $A_3$ .	94
5.8	Approximation orders $p$ in the infinity norm obtained at iteration $k$ , $k = 1, \dots, 7$ by using the considered reconstruction operators, Lagrange PPH, PPHT with $\epsilon = 0.5$ , PPHT with $\epsilon = 0.05$ , and PPHT with adapted $\epsilon_j$ in the region $A_3$ .	95

5.9	Approximation errors $E_k$ in the infinity norm obtained at iteration $k, k = 0, \dots, 7$ by using the considered reconstruction operators, Lagrange PPH, PPHT with $\epsilon = 0.5$ , PPHT with $\epsilon = 0.05$ , and PPHT with adapted $\epsilon_j$ in the region $A_4$ . . . . .	95
5.10	Approximation orders $p$ in the infinity norm obtained at iteration $k, k = 1, \dots, 7$ by using the considered reconstruction operators, Lagrange PPH, PPHT with $\epsilon = 0.5$ , PPHT with $\epsilon = 0.05$ , and PPHT with adapted $\epsilon_j$ in the region $A_4$ . . . . .	96
7.1	Estimations of the $C$ constant in the condition for Hölder continuity with exponent $\alpha$ for approximations of the limit function with $k$ levels of subdivision for initial data coming from 30 point-values of the function $f(x)$ at the grid $X_1$ of non equally spaced abscissas. . . . .	134
7.2	Estimations of the $C$ constant in the condition for Hölder continuity with exponent $\alpha$ for approximations of the limit function with $k$ levels of subdivision for initial data coming from 20 point-values of the function $f(x)$ at the grid $X_2$ of non equally spaced abscissas. . . . .	134
7.3	Estimations of the $C$ constant in the condition for Hölder continuity with exponent $\alpha$ for approximations of the limit function with $k$ levels of subdivision for initial data coming from 20 point-values of the function $g(x)$ at the grid $X_2$ of non equally spaced abscissas. . . . .	134
7.4	Subdivision errors $\ f^k - \mathcal{S}^k f^0\ _p, p = 1, 2, \infty$ , committed by approximating the original data $f^k$ with $\mathcal{S}^k f^0$ for $k = 5$ subdivision levels starting from the initial function point-values $f^0$ at the given grid $X_1$ with 30 points. . . . .	136
7.5	Subdivision errors $\ f^k - \mathcal{S}^k f^0\ _p, p = 1, 2, \infty$ , committed by approximating the original data $f^k$ with $\mathcal{S}^k f^0$ for $k = 5$ subdivision levels starting from the initial function point-values $f^0$ at the given grid $X_2$ with 20 abscissae. . . . .	136
7.6	Subdivision errors $\ g^k - \mathcal{S}^k g^0\ _p, p = 1, 2, \infty$ , committed by approximating the original data $g^k$ with $\mathcal{S}^k g^0$ for $k = 5$ subdivision levels starting from the initial function point-values $g^0$ at the given grid $X_2$ with 20 abscissae. . . . .	137
8.1	Numerical approximation errors $\ p(x, y) - g(x, y)\ _\infty$ and $\ \tilde{p}(x, y) - g(x, y)\ _\infty$ in infinity norm between the linear reconstruction and the original discontinuous function $g(x, y)$ and between the nonlinear reconstruction $\tilde{p}(x, y)$ and the original discontinuous function $g(x, y)$ in the triangle $S_G$ for the cases of building the reconstructions inside the triangles $S_R, S_Y$ and $S_G$ of decreasing side lengths. The approximation orders $p$ are also offered. . . . .	164
8.2	Numerical approximation errors $\ p(x, y) - f(x, y)\ _\infty$ and $\ \tilde{p}(x, y) - f(x, y)\ _\infty$ in infinity norm between the linear reconstruction and the original smooth function $f(x, y)$ and between the nonlinear reconstruction $\tilde{p}(x, y)$ and the original smooth function $f(x, y)$ in the triangle $S_G$ for the cases of building the reconstructions inside the triangles $S_R, S_Y$ and $S_G$ of decreasing side lengths. The approximation orders $p$ are also offered. . . . .	164



# Chapter 1

## Introduction

Subdivision and multiresolution schemes have been used in the last few decades in many applications that require from geometrical design. These applications are numerous in industry, for example for car and ship manufacturing, and also in the film industry in order to generate different shapes as much in  $2D$  as in  $3D$ . Subdivision schemes are based on a process of successive refinement of a given initial discrete data set. A new denser set of data is generated according to some specific rules. In turn, this new set will be further refined. A bunch of important mathematical questions arise at this point, and range from ensuring the convergence of the schemes, studying the smoothness of the limit function, the stability of the subdivision schemes and the order of approximation and the necessary requirements for their applicability in real life problems. In particular, it is important the analysis of the preservation capabilities of the schemes for some crucial properties which might be present in the initial set of data such as it could be the convexity.

Subdivision schemes generate fast algorithms to the easy construction of curves and surfaces [26], [29]. All these qualities make them an interesting tool for several industrial applications. Also, their close relation to multiresolution schemes opens the door to more applications in the fields of data and signal processing. Compression and denoising processes are easy to implement by using multiresolution schemes and they have been tested to be quite efficient. See for example [35], [5], [2].

A chief issue in choosing an adequate subdivision scheme is the property of convexity preservation, because many application require it. Many efforts have been done in this sense, see for example [27], [32], [33], [37].

Stability is also a main issue in real life applications, since the final designs are generated through the refinement of an initial set of points which usually is affected by some error. Therefore, keeping track of the error and maintaining it under a prescribed tolerance is essential. Some recommended references about stability of subdivision and multiresolution schemes can be consulted in [24], [9], [11], [1], [3], [15].

Harten derived a theory which closely connects reconstruction operators with subdivision and multiresolution schemes [35], [5]. Nonlinear reconstructions appear as a good option to minimize the adverse effects of potential singularities and to improve the adaptation to the given data. This theory is not as easy to study as for the linear case. Nonlinear reconstruction operators give rise to nonlinear subdivision and multiresolution schemes. In order to let clear the kind of difficulties to be encountered, we mention for example the case of stability analysis. In what stability issues regards, all linear subdivision and multiresolution schemes are proved to be stable, while a particular analysis is needed for each particular nonlinear scheme.

Multiresolution schemes are deeply connected with subdivision schemes and they inherit many of their properties. For more information about these useful schemes one can consult [5] as a first reference.

In [6] a nonlinear reconstruction called PPH was introduced, and the associated subdivision scheme was studied. This reconstruction was built in order to get adapted to the presence of potential singularities. It consists on a witty modification of the centered fourth order piecewise Lagrange interpolation. In order to implement the adaptation, the reconstruction is built also locally using a stencil of four centered data, but keeping in mind two main concerns. The first concern is that the modification in an area where the underlying function is smooth must be done in such a way that the modified quantities are not significantly changed, so that the modification remains  $O(h^4)$ , where  $h$  stands for the grid size. The second concern is that in the intervals adjacent to a singularity, but not containing it, the reconstruction retains some order of approximation, in fact  $O(h^2)$ , on the contrary to what happens with its linear counterpart that loses completely the approximation order.

This thesis is mainly devoted to the study of the PPH nonlinear reconstruction operator over nonuniform grids. In some cases, and in order to prove particular theoretical results we will make use of  $\sigma$  quasi uniform grids, that are nothing else but a kind of nonuniform grid that appears almost in all practical applications. The exact definition is given later.

This memoir is organized with the following structure. Notice that all chapters have been written in order to allow its reading without too many previous requirements, making them as self-contained as possible. In fact, each chapter has given rise to a whole research article submitted for publication to different mathematical journals. In some cases, the articles have been already published and the exact reference is included both at the beginning of the chapter and in the bibliography.

**Chapter 2** In [11], the stability issues of the PPH subdivision scheme in uniform grids were considered through the use of certain contractivity properties of second order divided differences. In this chapter we propose a parallel study using first order divided differences instead, giving rise to better stability bounds, more fitted to reality. The study is carried out for convex initial data coming from smooth functions. Since the considered PPH subdivision scheme is convexity preserving [37], [10], the convexity property of the initial data is ensured at all refinement scales. Along this chapter we introduce the PPH subdivision scheme, we give the resulting scheme for the first differences, and the result ensuring the convergence of the scheme. We also study the contractivity of the scheme for the differences, and we prove the announced stability result improving the stability constant in [11] and in [33] for strictly convex initial data satisfying a certain restriction. Finally, we give a numerical example to show the potential applications of the presented theory and some conclusions.

**Chapter 3** We give a definition of the PPH reconstruction operator for data over nonuniform grids, and we study some properties of this operator in greater depth. In particular, we focus on the smoothness of the reconstruction and the convexity-preserving properties of the initial data. We show that PPH reconstruction gives a  $C^\infty$  function, except for the knots where the function remains  $C^0$  and the differences between the first, second, and third one-sided derivatives are of the third, second, and first order, respectively (see Definition 7).

In [10], the authors proved that the related subdivision scheme in uniform meshes preserves the convexity of the control points. In this chapter, we attempt to determine if this result

about preserving convexity can be extended for the reconstruction operator and not only in uniform meshes, but also in  $\sigma$  quasi-uniform meshes with  $\sigma \leq 4$ .

The chapter deals with the definition of the PPH reconstruction operator over nonuniform grids. For this purpose, we will use the weighted harmonic mean with appropriate weights. Then, we show that the new reconstruction operator amounts to the original PPH reconstruction operator when we restrict to uniform grids. The definition is given for general nonuniform meshes, although in order to establish some theoretical results, we consider  $\sigma$  quasi-uniform meshes. Then, we study some basic properties of PPH reconstruction, such as the reproduction of polynomials of the second degree, approximation order, smoothness, boundedness of the operator, Lipschitz continuity, and convexity preservation. We also analyze the reconstruction when dealing with strictly convex (or concave) initial data. Finally, we present some numerical tests and some conclusions are included.

**Chapter 4** In this chapter, we analyze the behavior of the PPH reconstruction operator in presence of jump discontinuities. We prove adaptation to the presence of a jump discontinuity in the sense that some order of approximation is maintained in the area close to the discontinuity, on the contrary to what happens with linear operators that lose completely the approximation order. We also prove, as much theoretically as in numerical experiments, the absence of any Gibbs phenomena.

**Chapter 5** The original harmonic mean presents two undesirable characteristics for our purposes. The first one is the possible division by zero at the denominator, and the second one the need of the hypothesis  $x = O(1)$ , and  $y = O(1)$ , together with  $|x - y| = O(h)$  in order to be able to ensure that the harmonic mean will stay close,  $O(h^2)$ , to the arithmetic mean. In the reconstruction operator the arguments of  $x$  and  $y$  of the harmonic mean are taken by second order differences, and then it is not a surprise that the mentioned problems arise either close to inflexion points or close to singularities of the underlying function. In order to solve both problems, in this chapter we introduce a general definition of what we call a translation operator. Then, we make use of this operator to modify the weighted harmonic mean in such a way that we obtain a new adapted mean which retains similar properties as the original one, what is of chief importance in order to be employed into the construction of the adapted PPH reconstruction operator. We study several possible options to work in combination with the PPH reconstruction operator. In particular we define a way of choosing a good option depending on the specific data to which it is going to be applied with the purpose of both adapting in presence of discontinuities and maintaining the reconstruction order around inflexion points.

The new results contained in the chapter start with a proper definition and study of the translation operator. Then, we analyze the behavior of the improved PPH reconstruction operator with respect to the approximation order. Later, we present some specific translation operators, and we give a way of selecting an adequate translation parameter depending on the data. Some numerical tests are presented in order to confirm the theoretical results. Finally, some conclusions are given.

**Chapter 6** We dedicate this chapter to connect the PPH reconstruction operator with smoothing splines in a given interval  $[a, b]$ . Smoothing splines are built through polynomial reconstruction pieces

that are linked in a smooth way at the control knots and satisfy the minimization problem

$$\min_{p \in \Pi_n} J(p) := \min_{p \in \Pi_n} \int_a^b p''(x)^2 dx + \sum_j \mu_j (p(x_j) - f_j)^2, \quad (1.1)$$

where  $\Pi_n$  stands for the polynomials of degree less or equal to  $n$ . The considered functional implies a balance, dominated by the weights  $\mu_j$ , between a low curvature term and a small value of the accumulated distance to the initial set of data  $(x_j, f_j)$ .

We specifically remark two main properties which are going to be crucial for our purposes. The convexity preservation when dealing with initial discrete set of convex data and a low curvature term. This last property about the curvature is part of what is going to be proven along the chapter. More precisely we study the term of curvature of the functional for the Lagrange and PPH reconstructions, in the uniform and the nonuniform case. Due to these suitable properties, we think that connecting the PPH reconstruction with smoothing splines could result in very interesting applications.

**Chapter 7** Nonlinear subdivision schemes have emerged as good candidates to adapt to the specific data in use. Nonlinearity means data dependent subdivision schemes which may also involve nonlinear operations in their definition. Then, by definition, they are designed to overcome certain drawbacks that appear when dealing with their linear counterparts, such as bad behavior in presence of isolated discontinuities for instance. An example of these kind of operators was defined in [6] and was named as PPH (Piecewise Polynomial Harmonic). This scheme basically consists on a witty modification of the classical four points Lagrange subdivision scheme. Several studies have been carried out about their properties and performance in different applications, see for example [6], [10], [32]. Two main purposes of this subdivision scheme are related to dealing with data containing isolated discontinuities, reducing the undesirable effects, and preserving the convexity of the initial data, while maintaining a centered support based on four points.

In chapter 3 we extend the definition of the PPH reconstruction operator to nonuniform grids. In turn, this fact allows us to extend the PPH subdivision scheme to nonuniform grids, and carry out a parallel study in this new setting. In order to overcome some technical difficulties in the theoretical proofs, we have restricted to  $\sigma$  quasi-uniform grids for some results. The resultant scheme is quite interesting in terms of applications due to the almost  $C^1$  smoothness of the limit function, allowing to approximate accurately continuous functions with corners, and also due to appropriate properties regarding convexity preservation of the initial data.

Along the chapter we remind the PPH reconstruction operator over nonuniform grids. We present a short review about Harten's interpolatory multiresolution setting, which is closely connected to interpolatory subdivision schemes. Then, we define an associated subdivision scheme. This definition is given for general nonuniform meshes, although in order to establish some theoretical results we consider  $\sigma$  quasi-uniform meshes. We analyze the main issues about subdivision schemes. In particular, we prove some results about convergence, smoothness of the limit function, and convexity preservation. In addition, we carry out some numerical tests to check the theoretical smoothness of the limit function, and the performance of the nonlinear subdivision scheme.

**Chapter 8** The arithmetic and the harmonic mean of positive numbers appear in many scientific applications ranging from statistics to numerical analysis. The harmonic mean has the property of

penalizing large values, giving rise, because of this reason, to several interesting applications. Moreover, when the arguments do not differ much from each other, both means remain close, which is another crucial property in applications.

In this chapter our aim is to introduce some necessary ingredients to extend in turn this last reconstruction operator to several dimensions. More specifically speaking, we need to dispose of an appropriate mean in several dimensions which satisfies the required basic properties, the two mentioned above, as the harmonic mean does. We carry out this study accompanied by a graphical interpretation of the weighted harmonic mean of several values, which helps to quickly understand the theoretical results.

We begin the chapter with the weighted arithmetic and harmonic means of two positive numbers, proving two essential results about these means which will allow us to define adapted reconstruction operators. These results come accompanied with an intuitive graphical interpretation in  $2D$  according to a corresponding theoretical result that will be also proven. A similar path will be followed for the  $3D$  case, which involves working with weighted and harmonic means of three positive numbers. After this, we deal with the general case of considering the weighted arithmetic and harmonic mean of  $n$  positive numbers for whatever integer value  $n \geq 2$ . Some applications of these results are outlined in order to allow the definition of adapted reconstructions in several dimensions, and we explicitly define a new reconstruction in  $2D$  over triangular meshes adapted to discontinuities, that is, a kind of PPH reconstruction method on triangles.

**Chapter 9** We finish this thesis document with some perspectives and future works that we have in mind, whose main idea emerge directly in relation to the results contained in previous chapters.

## Chapter 2

# Improving the stability bound for the PPH nonlinear subdivision scheme for data coming from strictly convex functions

The contents of this chapter are the result of collaboration with other colleagues from the Universidad Politécnica de Cartagena (UPCT) and Universidad de Valencia (UV). This chapter corresponds with the first submission to the journal. Later, it was published under the following reference [36]

- Jiménez, I.; Ortiz, P.; Ruiz, J.; Trillo, J. C.; Yáñez, D. F. Improving the stability bound for the PPH nonlinear subdivision scheme for data coming from strictly convex functions. *Applied Mathematics and Computations*. **2021**, <https://doi.org/10.1016/j.amc.2021.126042>

### 2.1 Introduction

Subdivision schemes give rise to fast algorithms to generate curves and surfaces [26], [29]. Therefore they are used in car and ship manufacturing and in the design of cartoons for films among a variety of applications. They conform also the heart of multiresolution schemes, and therefore more applications are found such as signal and image compression and denoising [35], [5], [2].

A crucial issue in the selection of an appropriate subdivision scheme is the preservation of the convexity property of initial data, since many components and parts of the body in cars and other engineering manufactures precise of this requirement. Many studies in this direction have been carried out in the last decades, see for example some interesting works [27], [32], [33], [37].

Stability is also crucial in applications since the different curves and surfaces are generated through the refinement of an initial set of points which in most cases is affected of some error. Therefore maintaining the error under control and getting valid output data is of utmost importance. Some nice references about stability of subdivision schemes can be found in [24], [9], [11], [1], [3], [15].

Nonlinear reconstruction and subdivision schemes [35] appear as good candidates to avoid

potential singularities and to improve the adaptation to the given data. Theory is in general not so well studied as for linear stationary schemes. In what stability issues regards, all linear subdivision schemes are proved to be stable, while a particular analysis is needed for each particular nonlinear scheme.

Multiresolution schemes are deeply connected with subdivision schemes and they inherit many of their properties. For more information about these useful schemes one can consult [5] as a first reference.

In [6] a nonlinear reconstruction called PPH was introduced, and the associated subdivision scheme was studied. The stability issues were considered in [11] through the use of certain contractivity properties of second order divided differences. In this work we propose a parallel study using first order divided differences instead, giving rise to better stability bounds, more fitted to reality. The study is carried out for convex initial data coming from smooth functions. Since the considered PPH subdivision scheme is convexity preserving [37], [10], the convexity property of the initial data is ensured at all refinement scales.

This chapter is organized as follows: in Section 2.2 we introduce the PPH subdivision scheme, in Section 2.3 we give the scheme for the differences, and the result ensuring the convergence of the scheme, in Section 2.4 we study the contractivity of the scheme for the differences, in Section 2.5 we prove the announced stability result improving the stability constant in [11] and in [33] for strictly convex initial data satisfying a certain restriction. Finally in Section 2.6 we give some conclusions.

## 2.2 PPH subdivision scheme

Let us consider a set of nested grids in  $\mathbb{R}$ :

$$X^k = \{x_j^k\}_{j \in \mathbb{Z}}, \quad x_j^k = jh_k, \quad h_k = 2^{-k}.$$

The PPH subdivision scheme is described in detail [6], and we refer the interested reader to this paper for more specific details. We would like to remark that it had been already studied following different approaches by F. Kuijt and R. van Damme in [37], and independently by M.S. Floater and C.A. Michelli in [32]. In both of these papers, and opposed to the development in [6] the subdivision scheme is completely defined outside of the environment provided by Harten's framework for multiresolution.

In this section, we introduce the scheme given in [6] and express it as follows

$$(Sf^k)_{2j} = f_j^k, \tag{2.1}$$

$$(Sf^k)_{2j+1} = \begin{cases} \frac{f_{j+1}^k + f_j^k}{2} - \frac{1}{4} \frac{\Delta_j f^k \Delta_{j+1} f^k}{\Delta_j f^k + \Delta_{j+1} f^k} & \text{if } \Delta_j f^k \Delta_{j+1} f^k > 0, \\ \frac{f_{j+1}^k + f_j^k}{2} & \text{else,} \end{cases} \tag{2.2}$$

where  $\Delta_j f = f_{j-1} - 2f_j + f_{j+1}$ .

This scheme is proven to be uniformly convergent, to attained fourth order accuracy in smooth convex regions, and to maintain convexity in the following sense.

**Definition 1.** *An univariate data set  $\{f_j\}$  is said to be strictly convex if and only if  $\Delta f_j > 0 \forall j$ .*

**Definition 2.** *An interpolatory subdivision scheme is said to be convexity preserving for a set of sequences  $\mathcal{A}$  if and only if the data set  $\{f_j^k\} = S^k f^0$  is strictly convex for any strictly convex initial data  $f^0 \in \mathcal{A}$  for all subdivision levels. The subdivision scheme is said convexity preserving if the requirement is satisfied for all strictly convex initial data.*

A general proof for convexity preserving schemes through the use of associated reconstruction operators can be found in [10].

### 2.3 Scheme for the differences. Convergence

In [6] a nonlinear scheme  $S_1$  for the first order differences  $\delta_j f^k := f_j^k - f_{j-1}^k$  was defined, and we can express it in the following way

$$(S_1 \delta f^k)_{2j+1} = \begin{cases} \left( \frac{1}{2} - \frac{1}{4} \frac{\Delta_{j+1} f^k}{\Delta_j f^k + \Delta_{j+1} f^k} \right) \delta_{j+1} f^k + \frac{1}{4} \left( \frac{\Delta_{j+1} f^k}{\Delta_j f^k + \Delta_{j+1} f^k} \right) \delta_j f^k & \text{if } \Delta_j f^k \Delta_{j+1} f^k > 0, \\ \frac{\delta_{j+1} f^k}{2} & \text{else.} \end{cases} \quad (2.3)$$

And similarly for the even indexes,

$$(S_1 \delta f^k)_{2j} = \begin{cases} \left( \frac{1}{2} - \frac{1}{4} \frac{\Delta_{j-1} f^k}{\Delta_{j-1} f^k + \Delta_j f^k} \right) \delta_j f^k + \frac{1}{4} \left( \frac{\Delta_{j-1} f^k}{\Delta_{j-1} f^k + \Delta_j f^k} \right) \delta_{j+1} f^k & \text{if } \Delta_j f^k \Delta_{j+1} f^k > 0, \\ \frac{\delta_j f^k}{2} & \text{else.} \end{cases}$$

The following two results were proof in [6], which proof that the operator  $S_1$  is contractive in  $l_\infty(\mathbb{Z})$  and that the PPH subdivision scheme is uniformly convergent.

**Proposition 1.** *Associated to the PPH nonlinear reconstruction, there exists a nonlinear subdivision scheme  $S_1$  for the differences that satisfies*

$$\|S_1 \delta f^k\|_{l_\infty(\mathbb{Z})} \leq \frac{1}{2} \|\delta f^k\|_{l_\infty(\mathbb{Z})} \quad \forall f^k \in l_\infty(\mathbb{Z}),$$

where  $\delta_j f^k := f_j^k - f_{j-1}^k$ .

**Proposition 2.** *The nonlinear subdivision scheme associated to the PPH reconstruction is uniformly convergent. Moreover, for any  $f \in l_\infty(\mathbb{Z})$  the limit function  $S^\infty(f)$  satisfies*

$$\exists C \text{ such that } \forall x, y \in \mathbb{R}, \quad |S^\infty(f)(x) - S^\infty(f)(y)| \leq C|x - y|.$$

### 2.4 Lipchitz condition for the scheme $S_1$ for a class of strictly convex initial data

For the rest of the chapter we are going to work with strictly convex initial data satisfying

$$|\Delta_j f^k - \Delta_{j+1} f^k| \leq \frac{1}{2^n} |\Delta_j f^k + \Delta_{j+1} f^k|, \quad \forall j, \quad n = -\log_2\left(\frac{1}{\sqrt{2}} - \frac{1}{2}\right), \quad (2.4)$$

$$\exists a > 0 : \min_j \{\Delta_j f^k\} \geq a > 0 \quad (\exists a > 0 : \max_j \{\Delta_j f^k\} < -a < 0). \quad (2.5)$$

Notice that conditions (2.4) and (2.5) are true for initial data coming from the point value discretization of smooth strictly convex functions with compact support for a sufficiently small step of discretization. This kind of functions are the most common in practical cases.



The first result that we need to prove is that after one step of subdivision the data still satisfy the conditions (2.4) and (2.5).

**Lemma 1.** *Let  $x, y,$  and  $z$  be any positive real numbers and let us define the functions  $H(x, y) = \frac{2xy}{x+y}$ , and  $Z(x, y, z) = \frac{x}{2} - \frac{1}{8}(H(x, y) + H(x, z))$ . If  $|x - y| \leq \frac{1}{2^n}(x + y)$ ,  $|x - z| \leq \frac{1}{2^n}(x + z)$  with  $n = -\log_2(\frac{1}{\sqrt{2}} - \frac{1}{2})$ , then*

$$|\frac{1}{4}H(x, y) - Z(x, y, z)| \leq \frac{1}{2^n}(\frac{1}{4}H(x, y) + Z(x, y, z)). \quad (2.6)$$

*Proof.* In first place we see that (2.6) is equivalent to

$$\frac{x}{8} |4 - \frac{6y}{x+y} - \frac{2z}{x+z}| \leq \frac{x}{2^{n+2}} (2 + \frac{y}{x+y} - \frac{z}{x+z}). \quad (2.7)$$

Case 1:  $|4 - \frac{6y}{x+y} - \frac{2z}{x+z}| = \frac{6y}{x+y} + \frac{2z}{x+z} - 4$ .

Inequality (2.7) will be true if and only if

$$(3 \cdot 2^n - 1) \frac{y}{x+y} + (2^n + 1) \frac{z}{x+z} \leq 2 + 2^{n+1}.$$

Now using condition (2.4) we get that  $\frac{y}{x+y} \leq \frac{2^n+1}{2^{n+1}}$ , and  $\frac{z}{x+z} \leq \frac{2^n+1}{2^{n+1}}$ . Thus

$$\begin{aligned} (3 \cdot 2^n - 1) \frac{y}{x+y} + (2^n + 1) \frac{z}{x+z} &\leq (3 \cdot 2^n - 1) \frac{2^n + 1}{2^{n+1}} + (2^n + 1) \frac{2^n + 1}{2^{n+1}} \\ &= 2 + 2^{n+1}, \end{aligned}$$

and Case 1 is proven.

Case 2:  $|4 - \frac{6y}{x+y} - \frac{2z}{x+z}| = 4 - \frac{6y}{x+y} - \frac{2z}{x+z}$ .

Inequality (2.7) will be true if and only if

$$(3 \cdot 2^n + 1) \frac{y}{x+y} + (2^n - 1) \frac{z}{x+z} \leq 2^{n+1} - 2. \quad (2.8)$$

Using again condition (2.4) we get that  $\frac{y}{x+y} \geq \frac{2^n-1}{2^{n+1}}$ , and  $\frac{z}{x+z} \geq \frac{2^n-1}{2^{n+1}}$ . Thus

$$\begin{aligned} (3 \cdot 2^n + 1) \frac{y}{x+y} + (2^n - 1) \frac{z}{x+z} &\geq (3 \cdot 2^n + 1) \frac{2^n - 1}{2^{n+1}} + (2^n - 1) \frac{2^n - 1}{2^{n+1}} \\ &= 2^{n+1} - 2. \end{aligned}$$

□

**Proposition 3.** *If the data  $f^k$  satisfy conditions (2.4) and (2.5) at a given level of subdivision  $k$  then the data  $f^{k+1} = Sf^k$  after one level of PPH subdivision satisfy also the same conditions.*

*Proof.* Let us suppose without lost of generalization that  $\Delta_j f^k > 0, \forall j$ . Computing  $\Delta_{2j} f^{k+1}$  and  $\Delta_{2j+1} f^{k+1}$  we get

$$\Delta_{2j} f^{k+1} = Z(\Delta_j f^k, \Delta_{j+1} f^k, \Delta_{j-1} f^k), \quad \Delta_{2j+1} f^{k+1} = \frac{1}{4} H(\Delta_j f^k, \Delta_{j+1} f^k).$$

Condition (2.4) is now directly obtained just by using Lemma 1. Condition (2.5) is immediate taking into account that

$$\left| \frac{1}{8}(H(\Delta_j f^k, \Delta_{j+1} f^k) + H(\Delta_j f^k, \Delta_{j-1} f^k)) \right| \leq \frac{\Delta_j f^k}{2},$$

and

$$\Delta_{2j+1} f^{k+1} = \frac{1}{4} H(\Delta_j f^k, \Delta_{j+1} f^k) \geq \frac{1}{4} \min\{\Delta_j f^k, \Delta_{j+1} f^k\} > 0.$$

□

We proof now a proposition of practical importance in applications, since the subdivision scheme is always run with initial data affected of some small errors.

**Proposition 4.** *If the initial data  $f^0$  satisfy conditions (2.4) and (2.5) and  $\epsilon > 0$  is such that for all  $j \in \mathbb{Z}$   $|\Delta_j f^0 - \Delta_{j+1} f^0| \leq \frac{a-4\epsilon}{2^{n-1}} - 8\epsilon > 0$ , with  $a = \min_j\{|\Delta_j f^0|\}$ , then any sequence  $g^0$  satisfying  $\|f^0 - g^0\|_\infty \leq \epsilon$  satisfies also conditions (2.4) and (2.5).*

*Proof.* Condition (2.5) comes from

$$|\Delta_j g^0| \geq |\Delta_j f^0| - 4\epsilon \geq a - 4\epsilon > 0,$$

due to the chose of  $\epsilon$ . The following chain of inequalities proves the condition (2.4),

$$\begin{aligned} |\Delta_j g^0 - \Delta_{j+1} g^0| &\leq 8\epsilon + |\Delta_j f^0 - \Delta_{j+1} f^0| \\ &\leq \frac{a-4\epsilon}{2^{n-1}} = \frac{(a-4\epsilon) + (a-4\epsilon)}{2^n} \\ &\leq \frac{1}{2^n} (\Delta_j g^0 + \Delta_{j+1} g^0). \end{aligned}$$

□

Now we are going to prove the Lipchitz property addressing separately two cases, convex-concave and convex-convex, in two respective propositions.

**Proposition 5.** *(convex-concave) If the data  $f^k, g^k \in l_\infty(\mathbb{Z})$  satisfy conditions (2.4) and (2.5) at a given level of subdivision  $k$  and  $\Delta_j f^k \Delta_{j+1} f^k > 0$ ,  $\Delta_j g^k \Delta_{j+1} g^k > 0$ , with  $\Delta_j f^k \Delta_j g^k < 0$ , then*

1.  $|\delta_{2j+1} f^{k+1} - \delta_{2j+1} g^{k+1}| \leq \frac{1}{2} \|\delta f^k - \delta g^k\|_\infty \quad \forall j \in \mathbb{Z}$ ,
2.  $|\delta_{2j} f^{k+1} - \delta_{2j} g^{k+1}| \leq \frac{1}{2} \|\delta f^k - \delta g^k\|_\infty \quad \forall j \in \mathbb{Z}$ .

*Proof.* We are going to prove the first point. Second point is derived in the same way. From (2.3) we get

$$\begin{aligned} \delta_{2j+1} f^{k+1} &= \left( \frac{1}{2} - \frac{1}{4} \frac{\Delta_{j+1} f^k}{\Delta_j f^k + \Delta_{j+1} f^k} \right) \delta_{j+1} f^k + \frac{1}{4} \left( \frac{\Delta_{j+1} f^k}{\Delta_j f^k + \Delta_{j+1} f^k} \right) \delta_j f^k, \\ \delta_{2j+1} g^{k+1} &= \left( \frac{1}{2} - \frac{1}{4} \frac{\Delta_{j+1} g^k}{\Delta_j g^k + \Delta_{j+1} g^k} \right) \delta_{j+1} g^k + \frac{1}{4} \left( \frac{\Delta_{j+1} g^k}{\Delta_j g^k + \Delta_{j+1} g^k} \right) \delta_j g^k. \end{aligned}$$

Operating algebraically we arrive to

$$\begin{aligned}
\delta_{2j+1}f^{k+1} - \delta_{2j+1}g^{k+1} &= \frac{1}{2}(\delta_{j+1}f^k - \delta_{j+1}g^k) \\
&+ \frac{1}{4} \frac{\Delta_{j+1}g^k}{\Delta_j g^k + \Delta_{j+1}g^k} ((\delta_{j+1}g^k - \delta_{j+1}f^k) + (\delta_j f^k - \delta_j g^k)) \\
&+ \frac{1}{4} \left( \frac{\Delta_{j+1}g^k}{\Delta_j g^k + \Delta_{j+1}g^k} - \frac{\Delta_{j+1}f^k}{\Delta_j f^k + \Delta_{j+1}f^k} \right) \Delta_j f^k.
\end{aligned}$$

Let us suppose  $\Delta_j f^k > 0$ , and  $\Delta_j g^k < 0$ . Otherwise we change the roles of  $f^k$  and  $g^k$ . We differentiate two main cases,

Case 1: If  $|\delta_{2j+1}f^{k+1} - \delta_{2j+1}g^{k+1}| = \delta_{2j+1}f^{k+1} - \delta_{2j+1}g^{k+1}$ ,

$$- \text{ If } \frac{\Delta_{j+1}g^k}{\Delta_j g^k + \Delta_{j+1}g^k} \leq \frac{\Delta_{j+1}f^k}{\Delta_j f^k + \Delta_{j+1}f^k},$$

$$\begin{aligned}
|\delta_{2j+1}f^{k+1} - \delta_{2j+1}g^{k+1}| &\leq \left( \frac{1}{2} - \frac{1}{4} \frac{\Delta_{j+1}g^k}{\Delta_j g^k + \Delta_{j+1}g^k} \right) (\delta_{j+1}f^k - \delta_{j+1}g^k) \\
&+ \frac{1}{4} \frac{\Delta_{j+1}g^k}{\Delta_j g^k + \Delta_{j+1}g^k} (\delta_j f^k - \delta_j g^k),
\end{aligned}$$

and therefore  $|\delta_{2j+1}f^{k+1} - \delta_{2j+1}g^{k+1}| \leq \frac{1}{2} \|\delta f^k - \delta g^k\|_\infty$ .

$$- \text{ If } \frac{\Delta_{j+1}g^k}{\Delta_j g^k + \Delta_{j+1}g^k} > \frac{\Delta_{j+1}f^k}{\Delta_j f^k + \Delta_{j+1}f^k},$$

$$\begin{aligned}
|\delta_{2j+1}f^{k+1} - \delta_{2j+1}g^{k+1}| &\leq \frac{1}{2} (\delta_{j+1}f^k - \delta_{j+1}g^k) \\
&+ \frac{1}{4} \frac{\Delta_{j+1}g^k}{\Delta_j g^k + \Delta_{j+1}g^k} ((\delta_{j+1}g^k - \delta_{j+1}f^k) + (\delta_j f^k - \delta_j g^k)) \\
&+ \frac{1}{4} \left( \frac{\Delta_{j+1}g^k}{\Delta_j g^k + \Delta_{j+1}g^k} - \frac{\Delta_{j+1}f^k}{\Delta_j f^k + \Delta_{j+1}f^k} \right) (\Delta_j f^k - \Delta_j g^k) \\
&= \left( \frac{1}{2} - \frac{1}{4} \frac{\Delta_{j+1}f^k}{\Delta_j f^k + \Delta_{j+1}f^k} \right) (\delta_{j+1}f^k - \delta_{j+1}g^k) \\
&+ \frac{1}{4} \frac{\Delta_{j+1}f^k}{\Delta_j f^k + \Delta_{j+1}f^k} (\delta_j f^k - \delta_j g^k),
\end{aligned}$$

and we easily get  $|\delta_{2j+1}f^{k+1} - \delta_{2j+1}g^{k+1}| \leq \frac{1}{2} \|\delta f^k - \delta g^k\|_\infty$ .

Case 2: If  $|\delta_{2j+1}f^{k+1} - \delta_{2j+1}g^{k+1}| = \delta_{2j+1}g^{k+1} - \delta_{2j+1}f^{k+1}$ ,

$$- \text{ If } \frac{\Delta_{j+1}g^k}{\Delta_j g^k + \Delta_{j+1}g^k} \leq \frac{\Delta_{j+1}f^k}{\Delta_j f^k + \Delta_{j+1}f^k},$$

$$\begin{aligned}
|\delta_{2j+1}f^{k+1} - \delta_{2j+1}g^{k+1}| &\leq \left( \frac{1}{2} - \frac{1}{4} \frac{\Delta_{j+1}f^k}{\Delta_j f^k + \Delta_{j+1}f^k} \right) (\delta_{j+1}g^k - \delta_{j+1}f^k) \\
&+ \frac{1}{4} \frac{\Delta_{j+1}f^k}{\Delta_j f^k + \Delta_{j+1}f^k} (\delta_j g^k - \delta_j f^k),
\end{aligned}$$

and therefore  $|\delta_{2j+1}f^{k+1} - \delta_{2j+1}f^{k+1}| \leq \frac{1}{2} \|\delta f^k - \delta g^k\|_\infty$ .

$$- \text{ If } \frac{\Delta_{j+1}g^k}{\Delta_j g^k + \Delta_{j+1}g^k} > \frac{\Delta_{j+1}f^k}{\Delta_j f^k + \Delta_{j+1}f^k},$$

$$\begin{aligned} |\delta_{2j+1}f^{k+1} - \delta_{2j+1}f^{k+1}| &\leq \frac{1}{2}(\delta_{j+1}g^k - \delta_{j+1}f^k) \\ &+ \frac{1}{4} \frac{\Delta_{j+1}f^k}{\Delta_j f^k + \Delta_{j+1}f^k} ((\delta_{j+1}f^k - \delta_{j+1}g^k) + (\delta_j g^k - \delta_j f^k)) \\ &+ \frac{1}{4} \left( \frac{\Delta_{j+1}g^k}{\Delta_j g^k + \Delta_{j+1}g^k} - \frac{\Delta_{j+1}f^k}{\Delta_j f^k + \Delta_{j+1}f^k} \right) (\Delta_j f^k - \Delta_j g^k) \\ &= \left( \frac{1}{2} - \frac{1}{4} \frac{\Delta_{j+1}g^k}{\Delta_j g^k + \Delta_{j+1}g^k} \right) (\delta_{j+1}g^k - \delta_{j+1}f^k) \\ &+ \frac{1}{4} \frac{\Delta_{j+1}g^k}{\Delta_j g^k + \Delta_{j+1}g^k} (\delta_j g^k - \delta_j f^k), \end{aligned}$$

and we easily get  $|\delta_{2j+1}f^{k+1} - \delta_{2j+1}f^{k+1}| \leq \frac{1}{2} \|\delta f^k - \delta g^k\|_\infty$ .

□

Before giving the convex-convex proposition, we introduce some previous lemmas and definitions.

**Lemma 2.** *The following equality holds*

$$\Delta_j f^k \Delta_{j+1} g^k - \Delta_j g^k \Delta_{j+1} f^k = N_{j+1}(\Delta_j f^k - \Delta_j g^k) + N_j(\Delta_{j+1} g^k - \Delta_{j+1} f^k),$$

with

$$N_j := \frac{\Delta_j f^k + \Delta_j g^k}{2}, \quad N_{j+1} := \frac{\Delta_{j+1} f^k + \Delta_{j+1} g^k}{2}.$$

*Proof.* Applying the mean value theorem to the function  $F(x, y) = xy$  we have that

$$F(x, y) - F(\tilde{x}, \tilde{y}) = F_x(\theta)(x - \tilde{x}) + F_y(\theta)(y - \tilde{y}),$$

with  $\theta = t(\tilde{x}, \tilde{y}) + (1-t)(x, y)$ , for some  $t \in (0, 1)$ . Since  $\nabla F = (F_x, F_y) = (y, x)$ , taking  $(x, y) = (\Delta_j f^k, \Delta_{j+1} g^k)$ ,  $(\tilde{x}, \tilde{y}) = (\Delta_j g^k, \Delta_{j+1} f^k)$ , we get the result after realizing that  $t = \frac{1}{2}$  works. □

We now introduce the following definitions for  $\Delta_j f^k > 0$ ,  $\Delta_{j+1} f^k > 0$ ,  $\Delta_j g^k > 0$ ,  $\Delta_{j+1} g^k > 0$ ,

$$\begin{aligned} A_{fg} &= \frac{1}{4} \frac{\Delta_{j+1} g^k}{\Delta_j g^k + \Delta_{j+1} g^k}, & C_{fg} &= \frac{1}{4} \frac{N_{j+1} \Delta_j f^k}{(\Delta_j f^k + \Delta_{j+1} f^k)(\Delta_j g^k + \Delta_{j+1} g^k)}, \\ D_{fg} &= \frac{1}{4} \frac{N_j \Delta_j f^k}{(\Delta_j f^k + \Delta_{j+1} f^k)(\Delta_j g^k + \Delta_{j+1} g^k)}, \end{aligned} \tag{2.9}$$

$$\begin{aligned}
E_{fg} &= \frac{1}{4} \frac{\Delta_j g^k}{\Delta_j g^k + \Delta_{j+1} g^k}, & F_{fg} &= \frac{1}{4} \frac{N_j \Delta_{j+1} f^k}{(\Delta_j f^k + \Delta_{j+1} f^k)(\Delta_j g^k + \Delta_{j+1} g^k)}, \\
G_{fg} &= \frac{1}{4} \frac{N_{j+1} \Delta_{j+1} f^k}{(\Delta_j f^k + \Delta_{j+1} f^k)(\Delta_j g^k + \Delta_{j+1} g^k)}.
\end{aligned} \tag{2.10}$$

And the corresponding to  $A_{gf}$ ,  $C_{gf}$ ,  $D_{gf}$ ,  $E_{gf}$ ,  $F_{gf}$ , and  $G_{gf}$ . With all these definitions we can proof the next lemmas.

**Lemma 3.** *Let us consider  $A_{fg}$ ,  $C_{fg}$ , and  $D_{fg}$ . If the condition  $0 < \Delta_j f^k \leq \min\{\Delta_{j+1} f^k, \Delta_j g^k, \Delta_{j+1} g^k\}$  hold, then*

1.  $0 < A_{fg} \leq \frac{1}{8}$  if  $\Delta_{j+1} g^k \leq \Delta_j g^k$ , and  $0 < A_{fg} < \frac{1}{4}$  if  $\Delta_{j+1} g^k > \Delta_j g^k$ .
2.  $0 < C_{fg} < \frac{1}{8}$ ,
3.  $0 < D_{fg} < \frac{1}{8}$ ,
4.  $A_{fg} - C_{fg} > 0$ ,
5.  $|A_{fg} - C_{fg} - D_{fg}| < \frac{1}{4}$ .

*Proof.* **1.** Since  $\Delta_j g^k > 0$ ,  $\Delta_{j+1} g^k > 0$ , it is trivial. **2.** Since  $\Delta_j f^k > 0$ ,  $\Delta_{j+1} f^k > 0$ ,  $\Delta_j g^k > 0$ ,  $\Delta_{j+1} g^k > 0$ , it is trivial that  $C_{fg} > 0$ . Let us suppose now that  $\max\{\Delta_{j+1} f^k, \Delta_{j+1} g^k\} = \Delta_{j+1} g^k$ . The other cases are similar. Then

$$C_{fg} \leq \frac{1}{4} \frac{\Delta_j f^k}{(\Delta_j f^k + \Delta_{j+1} f^k)} \frac{\Delta_{j+1} g^k}{(\Delta_j g^k + \Delta_{j+1} g^k)} < \frac{1}{4} \cdot \frac{1}{2} = \frac{1}{8}.$$

**3.** From  $\max\{\Delta_j f^k, \Delta_j g^k\} = \Delta_j g^k$ , we have

$$D_{fg} \leq \frac{1}{4} \frac{\Delta_j f^k}{(\Delta_j f^k + \Delta_{j+1} f^k)} \frac{\Delta_j g^k}{(\Delta_j g^k + \Delta_{j+1} g^k)} < \frac{1}{4} \cdot \frac{1}{2} = \frac{1}{8}.$$

**4.** In order to prove point 4 we use the following sequence of inequalities,

$$\begin{aligned}
A_{fg} - C_{fg} &= \frac{1}{4} \frac{\Delta_{j+1} g^k}{\Delta_j g^k + \Delta_{j+1} g^k} \left(1 - \frac{1}{2} \frac{\Delta_j f^k}{(\Delta_j f^k + \Delta_{j+1} f^k)}\right) \\
&\quad - \frac{1}{8} \frac{\Delta_{j+1} f^k \Delta_j f^k}{(\Delta_j f^k + \Delta_{j+1} f^k)(\Delta_j g^k + \Delta_{j+1} g^k)} \\
&\geq \frac{1}{4} \frac{\Delta_{j+1} f^k}{(\Delta_j f^k + \Delta_{j+1} f^k)(\Delta_j g^k + \Delta_{j+1} g^k)} (\Delta_{j+1} g^k - \frac{1}{2} \Delta_j f^k) > 0.
\end{aligned}$$

**5.** It follows from  $|A_{fg} - C_{fg} - D_{fg}| \leq \max\{A_{fg}, C_{fg} + D_{fg}\} < \frac{1}{4}$ . □

**Lemma 4.** *Let us consider  $E_{fg}$ ,  $F_{fg}$ , and  $G_{fg}$ . If the condition  $0 < \Delta_{j+1} f^k \leq \min\{\Delta_j f^k, \Delta_j g^k, \Delta_{j+1} g^k\}$  hold, then*

1.  $0 < E_{fg} \leq \frac{1}{8}$  if  $\Delta_j g^k \leq \Delta_{j+1} g^k$ , and  $0 < E_{fg} < \frac{1}{4}$  if  $\Delta_j g^k > \Delta_{j+1} g^k$ .
2.  $0 < F_{fg} < \frac{1}{8}$ ,
3.  $0 < G_{fg} < \frac{1}{8}$ ,
4.  $E_{fg} - F_{fg} > 0$ ,
5.  $|E_{fg} - F_{fg} - G_{fg}| < \frac{1}{4}$ .

*Proof.* It can be done with the same track as in Lemma 3. □

**Lemma 5.** *Let us consider data  $f^k, g^k$  satisfying conditions (2.4) and (2.5), and for a given  $j \in \mathbb{Z}$  let us define*

$$\begin{aligned}
c_j &= A_{fg} - C_{fg}, & c_{j+1} &= C_{fg} + D_{fg} - A_{fg}, & c_{j+2} &= -D_{fg}, \\
\tilde{c}_j &= A_{gf} - C_{gf}, & \tilde{c}_{j+1} &= C_{gf} + D_{gf} - A_{gf}, & \tilde{c}_{j+2} &= -D_{gf}, \\
d_j &= G_{fg}, & d_{j+1} &= E_{fg} - F_{fg} - G_{fg}, & d_{j+2} &= -E_{fg} + F_{fg}, \\
\tilde{d}_j &= G_{gf}, & \tilde{d}_{j+1} &= E_{gf} - F_{gf} - G_{gf}, & \tilde{d}_{j+2} &= -E_{gf} + F_{gf}.
\end{aligned}$$

*Then one of the quantities  $|c_j| + |c_{j+1}| + |c_{j+2}|$ ,  $|\tilde{c}_j| + |\tilde{c}_{j+1}| + |\tilde{c}_{j+2}|$ ,  $|d_j| + |d_{j+1}| + |d_{j+2}|$ , or  $|\tilde{d}_j| + |\tilde{d}_{j+1}| + |\tilde{d}_{j+2}|$  is strictly lower than  $\frac{1}{4}$ .*

*Proof.* • If  $0 < \Delta_j f^k$  is lower or equal than  $\Delta_{j+1} f^k, \Delta_j g^k, \Delta_{j+1} g^k$ ,  
Then using Lemma 3 we have  $A_{fg} - C_{fg} > 0$ .

– If  $c_{j+1} \geq 0$ , then

$$|c_j| + |c_{j+1}| + |c_{j+2}| = 2D_{fg} < \frac{1}{4}.$$

– If  $c_{j+1} < 0$ , then

$$|c_j| + |c_{j+1}| + |c_{j+2}| = 2(A_{fg} - C_{fg}),$$

$$\begin{aligned}
A_{fg} - C_{fg} &\leq \frac{1}{4} \frac{\Delta_{j+1} g^k}{\Delta_j g^k + \Delta_{j+1} g^k} - \frac{1}{4} \left( \frac{2^n - 1}{2^{n+1}} \right) \frac{N_{j+1}}{\Delta_j g^k + \Delta_{j+1} g^k} \\
&< \frac{1}{4} \left( 1 - \frac{2^n - 1}{2^{n+2}} \right) \frac{\Delta_{j+1} g^k}{\Delta_j g^k + \Delta_{j+1} g^k} \leq \frac{1}{4} \left( \frac{3 \cdot 2^n + 1}{2^{n+2}} \right) \left( \frac{2^n + 1}{2^{n+1}} \right) \\
&= \frac{1}{8} \frac{6\sqrt{2} + 7}{16} < \frac{1}{8}.
\end{aligned}$$

- If  $0 < \Delta_j g^k$  is lower or equal than  $\Delta_{j+1} g^k, \Delta_j f^k, \Delta_{j+1} f^k$ ,  
then following the same steps as in the previous supposition

$$|\tilde{c}_j| + |\tilde{c}_{j+1}| + |\tilde{c}_{j+2}| < \frac{1}{4}.$$

- If  $0 < \Delta_{j+1} f^k$  is lower or equal than  $\Delta_j f^k, \Delta_j g^k, \Delta_{j+1} g^k$ ,  
we consider several subcases:

– If  $d_{j+1} < 0$ ,

$$|d_j| + |d_{j+1}| + |d_{j+2}| = 2G_{fg} < \frac{1}{4}.$$

– If  $d_{j+1} \geq 0$ ,

\* If  $\Delta_{j+1}g^k > \Delta_jg^k$ ,

then using Lemma 4 we have that

$$|d_j| + |d_{j+1}| + |d_{j+2}| = 2(E_{fg} - F_{fg}) \leq 2 \max\{E_{fg}, F_{fg}\} < \frac{1}{4}.$$

\* If  $\Delta_jg^k \geq \Delta_{j+1}g^k \geq \Delta_jf^k \geq \Delta_{j+1}f^k$ ,

then  $\Delta_{j+1}g^k - \frac{1}{2}\Delta_jf^k \geq 0$ , and according to the proof of point 4 of Lemma 3  $A_{fg} - C_{fg} \geq 0$ . In this case either  $|c_j| + |c_{j+1}| + |c_{j+2}| = 2(A_{fg} - C_{fg}) < \frac{1}{4}$ , or  $|c_j| + |c_{j+1}| + |c_{j+2}| = 2D_{fg} < \frac{1}{4}$ , since

$$\begin{aligned} A_{fg} &= \frac{1}{4} \frac{\Delta_{j+1}g^k}{\Delta_jg^k + \Delta_{j+1}g^k} < \frac{1}{8}, \\ C_{fg} &= \frac{1}{8} \frac{\Delta_jf^k}{\Delta_jf^k + \Delta_{j+1}f^k} \frac{\Delta_{j+1}g^k}{\Delta_jg^k + \Delta_{j+1}g^k} \\ &\quad + \frac{1}{8} \frac{\Delta_jf^k}{\Delta_jf^k + \Delta_{j+1}f^k} \frac{\Delta_{j+1}f^k}{\Delta_jg^k + \Delta_{j+1}g^k} < \frac{1}{8}, \\ D_{fg} &= \frac{1}{4} \frac{N_j\Delta_jf^k}{(\Delta_jf^k + \Delta_{j+1}f^k)(\Delta_jg^k + \Delta_{j+1}g^k)} < \frac{1}{8} \frac{\Delta_jf^k}{\Delta_jf^k + \Delta_{j+1}f^k} < \frac{1}{8}. \end{aligned}$$

\* If  $\Delta_jf^k \geq \Delta_jg^k \geq \Delta_{j+1}g^k \geq \Delta_{j+1}f^k$ ,

$$\begin{aligned} E_{fg} - F_{fg} &= \frac{1}{4} \frac{\Delta_jg^k}{\Delta_jg^k + \Delta_{j+1}g^k} \left(1 - \frac{1}{2} \frac{\Delta_{j+1}f^k}{\Delta_jf^k + \Delta_{j+1}f^k}\right) \\ &\quad - \frac{1}{8} \frac{\Delta_{j+1}f^k \Delta_jf^k}{(\Delta_jf^k + \Delta_{j+1}f^k)(\Delta_jg^k + \Delta_{j+1}g^k)} \\ &\leq \frac{1}{4} \frac{\Delta_jg^k}{\Delta_jg^k + \Delta_{j+1}g^k} \left(1 - \frac{\Delta_{j+1}f^k}{\Delta_jf^k + \Delta_{j+1}f^k}\right) \\ &= \frac{1}{4} \frac{\Delta_jg^k}{\Delta_jg^k + \Delta_{j+1}g^k} \frac{\Delta_jf^k}{\Delta_jf^k + \Delta_{j+1}f^k} \\ &< \frac{1}{4} \left(\frac{1}{2^{n+1}} + \frac{1}{2}\right)^2 < \frac{1}{8}, \end{aligned}$$

and therefore  $|d_j| + |d_{j+1}| + |d_{j+2}| = 2(E_{fg} - F_{fg}) < \frac{1}{4}$ .

\* If  $\Delta_jg^k \geq \Delta_jf^k \geq \Delta_{j+1}g^k \geq \Delta_{j+1}f^k$ ,

then  $\Delta_jf^k - \frac{1}{2}\Delta_{j+1}g^k \geq 0$ , and therefore  $E_{gf} - F_{gf} \geq 0$ . Now again we separate two cases,

• If  $\tilde{d}_{j+1} < 0$ ,

$$|\tilde{d}_j| + |\tilde{d}_{j+1}| + |\tilde{d}_{j+2}| = 2G_{gf} \leq \frac{1}{2} \frac{\Delta_{j+1}g^k}{\Delta_jg^k + \Delta_{j+1}g^k} \frac{\Delta_{j+1}f^k}{\Delta_jf^k + \Delta_{j+1}f^k} < \frac{1}{4}.$$

• If  $\tilde{d}_{j+1} \geq 0$ , then  $|\tilde{d}_j| + |\tilde{d}_{j+1}| + |\tilde{d}_{j+2}| = 2(E_{gf} - F_{gf}) < \frac{1}{4}$ , since

$$\begin{aligned}
E_{gf} - F_{gf} &= \frac{1}{4} \frac{\Delta_j f^k}{\Delta_j f^k + \Delta_{j+1} f^k} \left(1 - \frac{1}{2} \frac{\Delta_{j+1} g^k}{\Delta_j g^k + \Delta_{j+1} g^k}\right) \\
&\quad - \frac{1}{8} \frac{\Delta_{j+1} g^k \Delta_j g^k}{(\Delta_j f^k + \Delta_{j+1} f^k)(\Delta_j g^k + \Delta_{j+1} g^k)} \\
&\leq \frac{1}{4} \frac{\Delta_j f^k}{\Delta_j f^k + \Delta_{j+1} f^k} \left(1 - \frac{\Delta_{j+1} g^k}{\Delta_j g^k + \Delta_{j+1} g^k}\right) \\
&= \frac{1}{4} \frac{\Delta_j f^k}{\Delta_j f^k + \Delta_{j+1} f^k} \frac{\Delta_j g^k}{\Delta_j g^k + \Delta_{j+1} g^k} \\
&< \frac{1}{4} \left(\frac{1}{2^{n+1}} + \frac{1}{2}\right)^2 < \frac{1}{8}.
\end{aligned}$$

- If  $0 < \Delta_{j+1} g^k$  is lower or equal than  $\Delta_j f^k$ ,  $\Delta_{j+1} f^k$ ,  $\Delta_j g^k$ , then the case is symmetrical to the previous one.

And since we have considered all possible cases the proof is finished.  $\square$

Now we are ready to prove the convex-convex proposition.

**Proposition 6.** (convex-convex) *If the data  $f^k, g^k \in l_\infty(\mathbb{Z})$  satisfy conditions (2.4) and (2.5) at a given level of subdivision  $k$  and  $\Delta_j f^k \Delta_{j+1} f^k > 0$ ,  $\Delta_j g^k \Delta_{j+1} g^k > 0$ , with  $\Delta_j f^k \Delta_j g^k > 0$ , for  $j \in \mathbb{Z}$ , then*

1.  $|\delta_{2j+1} f^{k+1} - \delta_{2j+1} g^{k+1}| \leq \frac{3}{4} \|\delta f^k - \delta g^k\|_\infty$ ,
2.  $|\delta_{2j} f^{k+1} - \delta_{2j} g^{k+1}| \leq \frac{3}{4} \|\delta f^k - \delta g^k\|_\infty$ .

*Proof.* We are going to prove the first point. Second point is derived in the same way. From (2.3) we get the four expressions,

$$\begin{aligned}
\delta_{2j+1} f^{k+1} - \delta_{2j+1} g^{k+1} &= \frac{1}{2} (\delta_{j+1} f^k - \delta_{j+1} g^k) \\
&\quad + \frac{1}{4} \frac{\Delta_{j+1} g^k}{\Delta_j g^k + \Delta_{j+1} g^k} ((\delta_{j+1} g^k - \delta_{j+1} f^k) + (\delta_j f^k - \delta_j g^k)) \\
&\quad + \frac{1}{4} \left( \frac{\Delta_{j+1} g^k}{\Delta_j g^k + \Delta_{j+1} g^k} - \frac{\Delta_{j+1} f^k}{\Delta_j f^k + \Delta_{j+1} f^k} \right) \Delta_j f^k,
\end{aligned} \tag{2.11}$$

$$\begin{aligned}
\delta_{2j+1} f^{k+1} - \delta_{2j+1} g^{k+1} &= \frac{1}{2} (\delta_{j+1} f^k - \delta_{j+1} g^k) \\
&\quad + \frac{1}{4} \frac{\Delta_j g^k}{\Delta_j g^k + \Delta_{j+1} g^k} ((\delta_{j+1} f^k - \delta_{j+1} g^k) - (\delta_{j+2} f^k - \delta_{j+2} g^k)) \\
&\quad - \frac{1}{4} \left( \frac{\Delta_{j+1} g^k}{\Delta_j g^k + \Delta_{j+1} g^k} - \frac{\Delta_{j+1} f^k}{\Delta_j f^k + \Delta_{j+1} f^k} \right) \Delta_{j+1} f^k,
\end{aligned} \tag{2.12}$$



$$\begin{aligned}
\delta_{2j+1}g^{k+1} - \delta_{2j+1}f^{k+1} &= \frac{1}{2}(\delta_{j+1}g^k - \delta_{j+1}f^k) \\
&+ \frac{1}{4} \frac{\Delta_{j+1}f^k}{\Delta_j f^k + \Delta_{j+1}f^k} ((\delta_{j+1}f^k - \delta_{j+1}g^k) + (\delta_j g^k - \delta_j f^k)) \\
&+ \frac{1}{4} \left( \frac{\Delta_{j+1}f^k}{\Delta_j f^k + \Delta_{j+1}f^k} - \frac{\Delta_{j+1}g^k}{\Delta_j g^k + \Delta_{j+1}g^k} \right) \Delta_j g^k,
\end{aligned} \tag{2.13}$$

$$\begin{aligned}
\delta_{2j+1}g^{k+1} - \delta_{2j+1}f^{k+1} &= \frac{1}{2}(\delta_{j+1}g^k - \delta_{j+1}f^k) \\
&+ \frac{1}{4} \frac{\Delta_j f^k}{\Delta_j f^k + \Delta_{j+1}f^k} ((\delta_{j+1}g^k - \delta_{j+1}f^k) - (\delta_{j+2}g^k - \delta_{j+2}f^k)) \\
&- \frac{1}{4} \left( \frac{\Delta_{j+1}f^k}{\Delta_j f^k + \Delta_{j+1}f^k} - \frac{\Delta_{j+1}g^k}{\Delta_j g^k + \Delta_{j+1}g^k} \right) \Delta_{j+1}g^k.
\end{aligned} \tag{2.14}$$

Now taking absolute values, that is computing  $|\delta_{2j+1}f^{k+1} - \delta_{2j+1}g^{k+1}|$ , we can use Lemma 2 and regroup terms to rewrite expressions (2.11), (2.12), (2.13), and (2.14) in the form,

$$\begin{aligned}
|\delta_{2j+1}f^{k+1} - \delta_{2j+1}g^{k+1}| &= |c_j(\delta_j f^k - \delta_j g^k) + \left(\frac{1}{2} + c_{j+1}\right)(\delta_{j+1}f^k - \delta_{j+1}g^k) \\
&+ c_{j+2}(\delta_{j+2}f^k - \delta_{j+2}g^k)|, \\
|\delta_{2j+1}f^{k+1} - \delta_{2j+1}g^{k+1}| &= |\tilde{c}_j(\delta_j f^k - \delta_j g^k) + \left(\frac{1}{2} + \tilde{c}_{j+1}\right)(\delta_{j+1}f^k - \delta_{j+1}g^k) \\
&+ \tilde{c}_{j+2}(\delta_{j+2}f^k - \delta_{j+2}g^k)|, \\
|\delta_{2j+1}f^{k+1} - \delta_{2j+1}g^{k+1}| &= |d_j(\delta_j f^k - \delta_j g^k) + \left(\frac{1}{2} + d_{j+1}\right)(\delta_{j+1}f^k - \delta_{j+1}g^k) \\
&+ d_{j+2}(\delta_{j+2}f^k - \delta_{j+2}g^k)|, \\
|\delta_{2j+1}f^{k+1} - \delta_{2j+1}g^{k+1}| &= |\tilde{d}_j(\delta_j f^k - \delta_j g^k) + \left(\frac{1}{2} + \tilde{d}_{j+1}\right)(\delta_{j+1}f^k - \delta_{j+1}g^k) \\
&+ \tilde{d}_{j+2}(\delta_{j+2}f^k - \delta_{j+2}g^k)|.
\end{aligned} \tag{2.15}$$

According to Lemma 5 either  $|c_j| + (\frac{1}{2} + |c_{j+1}|) + |c_{j+2}|$ ,  $|\tilde{c}_j| + (\frac{1}{2} + |\tilde{c}_{j+1}|) + |\tilde{c}_{j+2}|$ ,  $|d_j| + (\frac{1}{2} + |d_{j+1}|) + |d_{j+2}|$ , or  $|\tilde{d}_j| + (\frac{1}{2} + |\tilde{d}_{j+1}|) + |\tilde{d}_{j+2}|$  is strictly lower than  $\frac{3}{4}$ . Let us suppose then that  $|c_j| + (\frac{1}{2} + |c_{j+1}|) + |c_{j+2}| < \frac{3}{4}$ . Now applying the triangular inequality we get

$$\begin{aligned}
|\delta_{2j+1}f^{k+1} - \delta_{2j+1}g^{k+1}| &\leq |c_j||\delta_j f^k - \delta_j g^k| + \left(\frac{1}{2} + |c_{j+1}|\right)|\delta_{j+1}f^k - \delta_{j+1}g^k| \\
&+ |c_{j+2}||\delta_{j+2}f^k - \delta_{j+2}g^k| \\
&\leq (|c_j| + \left(\frac{1}{2} + |c_{j+1}|\right) + |c_{j+2}|)|\delta f^k - \delta g^k|_\infty \\
&< \frac{3}{4}|\delta f^k - \delta g^k|_\infty.
\end{aligned} \tag{2.16}$$

Operating with the even indexes in the same way we also get

$$|\delta_{2j}f^{k+1} - \delta_{2j}g^{k+1}| \leq \frac{3}{4}|\delta f^k - \delta g^k|_\infty. \tag{2.17}$$

Finally from (2.16) and (2.17) we get

$$\|\delta f^{k+1} - \delta g^{k+1}\|_\infty \leq \frac{3}{4} \|\delta f^k - \delta g^k\|_\infty.$$

□

**Theorem 1.** *If the initial data  $f^0, g^0 \in l_\infty(\mathbb{Z})$  satisfy conditions (2.4) and (2.5) then  $\|\delta f^{k+1} - \delta g^{k+1}\|_\infty \leq \frac{3}{4} \|\delta f^k - \delta g^k\|_\infty, \forall k \in \mathbb{N}$ .*

*Proof.* Since the data satisfy conditions (2.4) and (2.5) at the initial scale, applying Proposition 3 the same will be true for all successive scales with  $k \geq 0$ . At a given scale  $k$ , for any  $j \in \mathbb{Z}$  the data will satisfy the hypothesis of either Proposition 5 or Proposition 6 and from here it follows immediately the thesis given in the theorem. □

## 2.5 Stability result for a set of strictly convex initial data

In this section we proof the main result of the chapter ensuring stability with respect to slight perturbations in the initial data.

**Theorem 2.** *Let  $f^0, g^0 \in l_\infty(\mathbb{Z})$  initial data satisfying conditions (2.4) and (2.5) then*

$$\|S^k f^0 - S^k g^0\|_\infty \leq 3 \|f^0 - g^0\|_\infty. \quad (2.18)$$

*Proof.* Again we are going to deal with odd and even indexes of  $|S^k f^0 - S^k g^0|$  separately. Let us denote  $f^k = S^k f^0$ , and  $g^k = S^k g^0$ . From the expression of the PPH scheme in (2.1) and (2.2) we get

$$\begin{aligned} f_{2j}^k &= f_j^{k-1}, \\ g_{2j}^k &= g_j^{k-1}, \\ f_{2j+1}^k &= \frac{f_j^{k-1} + f_{j+1}^{k-1}}{2} - \frac{1}{4} \frac{\Delta_j f^{k-1}}{\Delta_j f^{k-1} + \Delta_{j+1} f^{k-1}} (\delta_{j+2} f^{k-1} - \delta_{j+1} f^{k-1}), \\ g_{2j+1}^k &= \frac{g_j^{k-1} + g_{j+1}^{k-1}}{2} - \frac{1}{4} \frac{\Delta_j g^{k-1}}{\Delta_j g^{k-1} + \Delta_{j+1} g^{k-1}} (\delta_{j+2} g^{k-1} - \delta_{j+1} g^{k-1}), \end{aligned}$$

and therefore

$$|f_{2j}^k - g_{2j}^k| = |f_j^{k-1} - g_j^{k-1}| \leq \|f^{k-1} - g^{k-1}\|_\infty, \quad (2.19)$$

and for the odd indexes using Lemma 5 and supposing without loss of generalization  $|c_j| + |c_{j+1}| + |c_{j+2}| < \frac{1}{4}$ , we get

$$\begin{aligned}
|f_{2j+1}^k - g_{2j+1}^k| &\leq \frac{|f_j^{k-1} - g_j^{k-1}|}{2} + \frac{|f_{j+1}^{k-1} - g_{j+1}^{k-1}|}{2} \\
&+ \frac{1}{4} \left| \frac{\Delta_j f^{k-1}}{\Delta_j f^{k-1} + \Delta_{j+1} f^{k-1}} (\delta_{j+2} f^{k-1} - \delta_{j+1} f^{k-1}) - \frac{\Delta_j g^{k-1}}{\Delta_j g^{k-1} + \Delta_{j+1} g^{k-1}} (\delta_{j+2} g^{k-1} - \delta_{j+1} g^{k-1}) \right| \\
&\leq \|f^{k-1} - g^{k-1}\|_\infty + |\delta_{2j+1} f^k - \delta_{2j+1} g^k - \frac{1}{2} (\delta_{j+1} f^{k-1} - \delta_{j+1} g^{k-1})| \\
&= \|f^{k-1} - g^{k-1}\|_\infty + |c_j (\delta_j f^{k-1} - \delta_j g^{k-1}) + c_{j+1} (\delta_{j+1} f^{k-1} - \delta_{j+1} g^{k-1})| \\
&+ c_{j+2} (\delta_{j+2} f^{k-1} - \delta_{j+2} g^{k-1}), \\
&< \|f^{k-1} - g^{k-1}\|_\infty + \frac{1}{4} \|\delta f^{k-1} - \delta g^{k-1}\|_\infty.
\end{aligned} \tag{2.20}$$

Joining (2.19) and (2.20) we get

$$\|f^k - g^k\|_\infty \leq \|f^{k-1} - g^{k-1}\|_\infty + \frac{1}{4} \|\delta f^{k-1} - \delta g^{k-1}\|_\infty. \tag{2.21}$$

Now from expression (2.21) using the Lipchitz property proven in Theorem 1

$$\begin{aligned}
\|f^k - g^k\|_\infty &\leq \|f^{k-1} - g^{k-1}\|_\infty + \frac{1}{4} \left(\frac{3}{4}\right)^{k-1} \|\delta f^0 - \delta g^0\|_\infty \\
&\leq \|f^{k-2} - g^{k-2}\|_\infty + \frac{1}{4} \left( \left(\frac{3}{4}\right)^{k-2} + \left(\frac{3}{4}\right)^{k-1} \right) \|\delta f^0 - \delta g^0\|_\infty \\
&\leq \|f^0 - g^0\|_\infty + \frac{1}{4} \left( 1 + \frac{3}{4} + \dots + \left(\frac{3}{4}\right)^{k-1} \right) \|\delta f^0 - \delta g^0\|_\infty \\
&\leq \left( 1 + \frac{1}{4} \cdot 2 \cdot 4 \right) \|f^0 - g^0\|_\infty = 3 \|f^0 - g^0\|_\infty.
\end{aligned}$$

□

## 2.6 Conclusions

We have improved the stability bound in [11] for initial data coming from strictly convex smooth functions, obtaining a value of the constant  $C = 3$  instead of 9. The stability result has been obtained by analyzing the scheme of the first order differences, while in [11] was done with second order differences.

## Chapter 3

# On the convexity preservation of a quasi $C^3$ nonlinear interpolatory reconstruction operator on $\sigma$ quasi-uniform grids

The contents of this chapter are wholly included in the already published paper [42]

- Ortiz, P.; Trillo, J.C. On the Convexity Preservation of a Quasi  $C^3$  Nonlinear Interpolatory Reconstruction Operator on  $\sigma$  Quasi-Uniform Grids. *Mathematics*. **2021**, *9(4)*, 310. <https://doi.org/10.3390/math9040310>

### 3.1 Introduction

Reconstruction operators are widely used in computer-aided geometric design. For simplicity, the functions that are typically used as operators are polynomials. In order to avoid undesirable phenomena generated by high-degree polynomials, reconstructions are usually built piecewise. Due to the bad behavior of linear operators in the presence of discontinuities, it has become necessary to design nonlinear operators to overcome this drawback. One of these operators was defined in [6] and was called the piecewise polynomial harmonic (PPH). This operator essentially consists of a clever modification of the classical four-point piecewise Lagrange interpolation. The initial purpose of this definition was to deal with discontinuities, reducing the undesirable effects to only one interval instead of the three intervals affected in a reconstruction built with a four-point stencil. In addition to that, as we will see throughout this chapter, the reconstruction may also play an important role in design purposes, since it keeps the convexity properties of the given starting data.

For the sake of simplicity, as much in the theoretical analysis as in the practical implementation and computational time, studies usually start with data given in uniform grids. Nevertheless, some applications require dealing with data over nonuniform grids. At times, it is not trivial to adapt operators defined over uniform grids to the nonuniform case. The above-mentioned PPH operator was defined over a uniform grid and some of its properties were studied in [6]. These reconstruction operators are the basis for the definition of associated subdivision and multi-resolution schemes. In this chapter, we use the definition that we made of the PPH reconstruction operator for data over

nonuniform grids in [41], and we study some properties of this operator in greater depth. In particular, we focus on the smoothness of the reconstruction and the convexity-preserving properties of the initial data. We show that PPH reconstruction gives a  $C^\infty$  function, except for the knots where the function remains  $C^0$  and the differences between the first, second, and third one-sided derivatives are of the third, second, and first order, respectively (see Definition 7).

In [10], the authors proved that the related subdivision scheme in uniform meshes preserves the convexity of the control points. In this chapter, we attempt to determine if this result about preserving convexity can be extended for the reconstruction operator and not only in uniform meshes, but also in  $\sigma$  quasi-uniform meshes with  $\sigma \leq 4$ .

The chapter is organized as follows: Section 3.2 is devoted to defining the PPH reconstruction operator over nonuniform grids. For this purpose, we will use the weighted harmonic mean with appropriate weights. Then, we show that the new reconstruction operator amounts to the original PPH reconstruction operator when we restrict to uniform grids. The definition is given for general nonuniform meshes, although in order to establish some theoretical results, we consider  $\sigma$  quasi-uniform meshes. In Section 3.3, we study some basic properties of PPH reconstruction, such as the reproduction of polynomials of the second degree, approximation order, smoothness, boundedness of the operator, Lipschitz continuity, and convexity preservation. In Section 3.4, we analyze the reconstruction when dealing with strictly convex (or concave) initial data. In Section 3.5, we present some numerical tests. Finally, some conclusions are included in Section 3.6.

## 3.2 A nonlinear PPH interpolation procedure on nonuniform grids

Let us define the nonuniform grid  $X = (x_i)_{i \in \mathbb{Z}}$ . Let us also denote the nonuniform spacing between abscissae as  $h_i := x_i - x_{i-1}$ . We will work with continuous piecewise reconstructions of a given underlying continuous function  $f(x)$  with, at most, a finite set of isolated corner or jump discontinuities, that is

$$R(x) = R_j(x), \quad x \in [x_j, x_{j+1}], \quad (3.1)$$

where  $R_j(x)$  is a third-degree polynomial satisfying

$$\begin{aligned} R_j(x_j) &= f(x_j), \\ R_j(x_{j+1}) &= f(x_{j+1}). \end{aligned} \quad (3.2)$$

From now on, we will use the notation  $f_i := f(x_i)$ .

Taking (3.1) into account, this implies that we are interested in building the appropriate polynomial piece  $R_j(x)$  in the interval  $[x_j, x_{j+1}]$ . Let us consider the set of values  $\{f_{j-1}, f_j, f_{j+1}, f_{j+2}\}$  for some  $j \in \mathbb{Z}$  corresponding to subsequent ordinates of a function  $f(x)$  at the abscissae  $\{x_{j-1}, x_j, x_{j+1}, x_{j+2}\}$  of a nonuniform grid  $X$ , and  $PL_j(x)$  is the Lagrange interpolatory polynomial built with the points  $(x_i, f_i)$ ,  $i = j - 1, j, j + 1, j + 2$ , that is, the unique polynomial of degree less or equal 3 satisfying

$$PL_j(x_i) = f_i \quad j - 1 \leq i \leq j + 2. \quad (3.3)$$

The polynomial  $PL_j(x)$  can be expressed as

$$PL_j(x) = a_{j,0} + a_{j,1} \left(x - x_{j+\frac{1}{2}}\right) + a_{j,2} \left(x - x_{j+\frac{1}{2}}\right)^2 + a_{j,3} \left(x - x_{j+\frac{1}{2}}\right)^3, \quad (3.4)$$

where  $x_{j+\frac{1}{2}} = \frac{x_j + x_{j+1}}{2}$ .

It is well known that from conditions (3.3), one obtains the following linear system of equations, where the coefficient matrix is a Vandermonde matrix with different nodes and is, therefore, invertible:

$$\begin{pmatrix} 1 & \left(-h_j - \frac{h_{j+1}}{2}\right) & \left(-h_j - \frac{h_{j+1}}{2}\right)^2 & \left(-h_j - \frac{h_{j+1}}{2}\right)^3 \\ 1 & -\frac{h_{j+1}}{2} & \frac{h_{j+1}^2}{4} & -\frac{h_{j+1}^3}{8} \\ 1 & \frac{h_{j+1}}{2} & \frac{h_{j+1}^2}{4} & \frac{h_{j+1}^3}{8} \\ 1 & \left(\frac{h_{j+1}}{2} + h_{j+2}\right) & \left(\frac{h_{j+1}}{2} + h_{j+2}\right)^2 & \left(\frac{h_{j+1}}{2} + h_{j+2}\right)^3 \end{pmatrix} \begin{pmatrix} a_{j,0} \\ a_{j,1} \\ a_{j,2} \\ a_{j,3} \end{pmatrix} = \begin{pmatrix} f_{j-1} \\ f_j \\ f_{j+1} \\ f_{j+2} \end{pmatrix}. \quad (3.5)$$

In order to express the solution of system (3.5) in a form that is convenient for our purposes, we introduce the definition of the second-order divided differences

$$\begin{aligned} D_j &:= f[x_{j-1}, x_j, x_{j+1}] = \frac{f_{j-1}}{h_j(h_j + h_{j+1})} - \frac{f_j}{h_j h_{j+1}} + \frac{f_{j+1}}{h_{j+1}(h_j + h_{j+1})}, \\ D_{j+1} &:= f[x_j, x_{j+1}, x_{j+2}] = \frac{f_j}{h_{j+1}(h_{j+1} + h_{j+2})} - \frac{f_{j+1}}{h_{j+1} h_{j+2}} + \frac{f_{j+2}}{h_{j+2}(h_{j+1} + h_{j+2})}, \end{aligned} \quad (3.6)$$

and a weighted arithmetic mean of  $D_j$  and  $D_{j+1}$ , defined as

$$M_j = w_{j,0}D_j + w_{j,1}D_{j+1}, \quad (3.7)$$

with the weights

$$\begin{aligned} w_{j,0} &= \frac{h_{j+1} + 2h_{j+2}}{2(h_j + h_{j+1} + h_{j+2})}, \\ w_{j,1} &= \frac{h_{j+1} + 2h_j}{2(h_j + h_{j+1} + h_{j+2})} = 1 - w_{j,0}. \end{aligned} \quad (3.8)$$

With these definitions, after solving the system (3.5), we get the following expressions for the coefficients of the polynomial (3.4):

$$\begin{aligned} a_{j,0} &= \frac{f_j + f_{j+1}}{2} - \frac{h_{j+1}^2}{4}M_j, \\ a_{j,1} &= \frac{-f_j + f_{j+1}}{h_{j+1}} + \frac{h_{j+1}^2}{2(2h_j + h_{j+1})}(D_j - M_j), \\ a_{j,2} &= M_j, \\ a_{j,3} &= -\frac{2}{2h_j + h_{j+1}}(D_j - M_j), \end{aligned} \quad (3.9)$$

which can also be expressed as

$$\begin{aligned}
a_{j,0} &= \frac{f_j + f_{j+1}}{2} - \frac{h_{j+1}^2}{4} M_j, \\
a_{j,1} &= \frac{-f_j + f_{j+1}}{h_{j+1}} + \frac{h_{j+1}^2}{2(2h_{j+2} + h_{j+1})} (-D_{j+1} + M_j), \\
a_{j,2} &= M_j, \\
a_{j,3} &= -\frac{2}{2h_{j+2} + h_{j+1}} (-D_{j+1} + M_j).
\end{aligned} \tag{3.10}$$

At this point, we give some more definitions and lemmas that we will need later.

**Lemma 6.** *Let us consider the set of ordinates  $\{f_{j-1}, f_j, f_{j+1}, f_{j+2}\}$  for some  $j \in \mathbb{Z}$  at the abscissae  $\{x_{j-1}, x_j, x_{j+1}, x_{j+2}\}$  of a nonuniform grid  $X = (x_i)_{i \in \mathbb{Z}}$ . Then, the values  $f_{j-1}$  and  $f_{j+2}$  at the extremes can be expressed as*

$$f_{j-1} = \frac{-1}{\gamma_{j,-1}} (\gamma_{j,0} f_j + \gamma_{j,1} f_{j+1} + \gamma_{j,2} f_{j+2}) + \frac{M_j}{\gamma_{j,-1}}, \tag{3.11a}$$

$$f_{j+2} = \frac{-1}{\gamma_{j,2}} (\gamma_{j,-1} f_{j-1} + \gamma_{j,0} f_j + \gamma_{j,1} f_{j+1}) + \frac{M_j}{\gamma_{j,2}}, \tag{3.11b}$$

with the constants  $\gamma_{j,i}$ ,  $i = -1, 0, 1, 2$  given by

$$\begin{aligned}
\gamma_{j,-1} &= \frac{h_{j+1} + 2h_{j+2}}{2h_j(h_{j+1} + h_j)(h_j + h_{j+1} + h_{j+2})}, \\
\gamma_{j,0} &= \frac{1}{2h_{j+1}(h_j + h_{j+1} + h_{j+2})} \left( \frac{h_{j+1} + 2h_j}{h_{j+1} + h_{j+2}} - \frac{h_{j+1} + 2h_{j+2}}{h_j} \right), \\
\gamma_{j,1} &= \frac{1}{2h_{j+1}(h_j + h_{j+1} + h_{j+2})} \left( \frac{h_{j+1} + 2h_{j+2}}{h_{j+1} + h_j} - \frac{h_{j+1} + 2h_j}{h_{j+2}} \right), \\
\gamma_{j,2} &= \frac{h_{j+1} + 2h_j}{2h_{j+2}(h_{j+1} + h_{j+2})(h_j + h_{j+1} + h_{j+2})}.
\end{aligned} \tag{3.12}$$

*Proof.* This proof is an immediate calculation just by expanding the expression of the weighted arithmetic mean in (3.7) in terms of  $f_i$ ,  $i = j - 1, j, j + 1, j + 2$ , that is

$$M_j = \gamma_{j,-1} f_{j-1} + \gamma_{j,0} f_j + \gamma_{j,1} f_{j+1} + \gamma_{j,2} f_{j+2}. \tag{3.13}$$

□

**Definition 3.** *A nonuniform mesh  $X = (x_i)_{i \in \mathbb{Z}}$  is said to be a  $\sigma$  quasi-uniform mesh if there exist  $h_{\min} = \min_{i \in \mathbb{Z}} h_i$ ,  $h_{\max} = \max_{i \in \mathbb{Z}} h_i$ , and a finite constant  $\sigma$  such that  $\frac{h_{\max}}{h_{\min}} \leq \sigma$ .*

In the presence of isolated singularities, predictions made using Lagrange reconstruction operators lose their accuracy in the vicinity of the discontinuity; in fact, three intervals are expected to

be affected, since we are considering a stencil of four points. In order to reduce the affected intervals to only one, the one containing the singularity, we introduce a weighted harmonic mean over nonuniform grids, which will be used in the general definition of the PPH reconstruction operator. Notice that it is not possible to recover the exact position of a jump discontinuity inside an interval by using point value discretization of an underlying function. For the case of a corner discontinuity, a strategy such as the subcell resolution technique [34] could be used to detect its position. This harmonic mean is built as the inverse of the weighted arithmetic mean of the inverses of the given values. We define the following function.

**Definition 4.** Given  $x, y \in \mathbb{R}$ , and  $w_x, w_y \in \mathbb{R}$  such that  $w_x > 0$ ,  $w_y > 0$ , and  $w_x + w_y = 1$ , we denote as  $\tilde{V}$  the function

$$\tilde{V}(x, y) = \begin{cases} \frac{xy}{w_x y + w_y x} & \text{if } xy > 0, \\ 0 & \text{otherwise.} \end{cases} \quad (3.14)$$

**Lemma 7.** If  $x > 0$  and  $y > 0$ , the harmonic mean is bounded as follows

$$\tilde{V}(x, y) < \min \left\{ \frac{1}{w_x} x, \frac{1}{w_y} y \right\}. \quad (3.15)$$

Before giving another important lemma for our purposes, we will introduce a definition about a basic concept that will be used throughout the rest of the chapter.

**Definition 5.** The expression  $e(h) = O(h^r)$  means that there exist  $h_0 > 0$  and  $M > 0$  such that  $\forall 0 < h \leq h_0$ ,

$$\frac{|e(h)|}{h^r} \leq M.$$

**Lemma 8.** Let  $a > 0$  be a fixed positive real number and let  $x \geq a$ ,  $y \geq a$ . If  $|x - y| = O(h)$ , then the weighted harmonic mean is also close to the weighted arithmetic mean  $M(x, y) = w_x x + w_y y$ ,

$$|M(x, y) - \tilde{V}(x, y)| = \frac{w_x w_y}{w_x y + w_y x} (x - y)^2 = O(h^2). \quad (3.16)$$

**Remark 1.** The smaller the value of  $a > 0$  in Lemma 8, the smaller the  $h_0$  in Definition 5 required to attain the expected theoretical order.

It is well known that the divided differences (3.6) work as smoothness indicators [5, 7, 11, 26, 29, 27, 32, 35, 37, 50]. If a potential singularity appears at the interval  $[x_{j+1}, x_{j+2}]$ , we propose that the data  $(x_{j+2}, f_{j+2})$  are not interpolated, and that the ordinate  $f_{j+2}$  is exchanged for another value that is more convenient for what happens in the target interval  $[x_j, x_{j+1}]$ , where we want to implement the local polynomial piece according to (3.1). In the same manner, if a potential singularity lies in the interval  $[x_{j-1}, x_j]$ , a symmetrical modification is carried out. According to these observations, we can give the following definition for the PPH reconstruction on nonuniform meshes.

**Definition 6** (PPH reconstruction). Let  $X = (x_i)_{i \in \mathbb{Z}}$  be a nonuniform mesh. Let  $f = (f_i)_{i \in \mathbb{Z}}$  be a sequence in  $l_\infty(\mathbb{Z})$ . Let  $D_j$  and  $D_{j+1}$  be the second-order divided differences, and for each  $j \in \mathbb{Z}$ , let us consider the modified values  $\{\tilde{f}_{j-1}, \tilde{f}_j, \tilde{f}_{j+1}, \tilde{f}_{j+2}\}$  built according to the following rule:



- *Case 1: If  $|D_j| \leq |D_{j+1}|$ ,*

$$\begin{cases} \tilde{f}_i = f_i, & j-1 \leq i \leq j+1, \\ \tilde{f}_{j+2} = \frac{-1}{\gamma_{j,2}}(\gamma_{j,-1}f_{j-1} + \gamma_{j,0}f_j + \gamma_{j,1}f_{j+1}) + \frac{\tilde{V}_j}{\gamma_{j,2}}. \end{cases} \quad (3.17)$$

- *Case 2: If  $|D_j| > |D_{j+1}|$*

$$\begin{cases} \tilde{f}_{j-1} = \frac{-1}{\gamma_{j,-1}}(\gamma_{j,0}f_j + \gamma_{j,1}f_{j+1} + \gamma_{j,2}f_{j+2}) + \frac{\tilde{V}_j}{\gamma_{j,-1}}, \\ \tilde{f}_i = f_i, & j \leq i \leq j+2, \end{cases} \quad (3.18)$$

where  $\gamma_{j,i}$ ,  $i = -1, 0, 1, 2$  are given in (3.12) and  $\tilde{V}_j = \tilde{V}(D_j, D_{j+1})$ , where  $\tilde{V}$  is the weighted harmonic mean defined in (3.14) with the weights  $w_{j,0}$  and  $w_{j,1}$  in (3.8). We define the PPH nonlinear reconstruction operator as

$$PPH(x) = PPH_j(x), \quad x \in [x_j, x_{j+1}], \quad (3.19)$$

where  $PPH_j(x)$  is the unique interpolation polynomial that satisfies

$$PPH_j(x_i) = \tilde{f}_i, \quad j-1 \leq i \leq j+2. \quad (3.20)$$

According to Definition 6, and establishing a parallelism with expression (3.4), we can write the PPH reconstruction as

$$PPH_j(x) = \tilde{a}_{j,0} + \tilde{a}_{j,1} \left(x - x_{j+\frac{1}{2}}\right) + \tilde{a}_{j,2} \left(x - x_{j+\frac{1}{2}}\right)^2 + \tilde{a}_{j,3} \left(x - x_{j+\frac{1}{2}}\right)^3, \quad (3.21)$$

where the coefficients  $\tilde{a}_{j,i}$ ,  $i = 0, \dots, 3$  are calculated by imposing conditions (3.20). Depending on the local case, Case 1 or Case 2, the coefficients will have different expressions.

Case 1:  $|D_j| \leq |D_{j+1}|$ , i.e., the possible singularity lies in  $[x_{j+1}, x_{j+2}]$ . The replacement of  $f_{j+2}$  with  $\tilde{f}_{j+2}$  by exchanging the weighted arithmetic mean in Equation (3.11b) for its corresponding weighted harmonic mean has been proposed. It is also important to point out that Equation (3.17) shows that  $\tilde{f}_{j+2}$  is not significantly affected by a potential singularity at the interval  $[x_{j+1}, x_{j+2}]$ , since, by property (3.15) in Lemma 7,  $|\tilde{V}_j| \leq \frac{1}{w_{j,0}}|D_j|$ , and in turn,  $D_j$  is not affected by this discontinuity. Therefore, the influence of  $f_{j+2}$  on the values of the reconstruction in the interval  $[x_j, x_{j+1}]$  will be limited. In this case, the coefficients of the new polynomial (3.21) come from solving the linear system

$$\begin{pmatrix} 1 & \left(-h_j - \frac{h_{j+1}}{2}\right) & \left(-h_j - \frac{h_{j+1}}{2}\right)^2 & \left(-h_j - \frac{h_{j+1}}{2}\right)^3 \\ 1 & -\frac{h_{j+1}}{2} & \frac{h_{j+1}^2}{4} & -\frac{h_{j+1}^3}{8} \\ 1 & \frac{h_{j+1}}{2} & \frac{h_{j+1}^2}{4} & \frac{h_{j+1}^3}{8} \\ 1 & \left(\frac{h_{j+1}}{2} + h_{j+2}\right) & \left(\frac{h_{j+1}}{2} + h_{j+2}\right)^2 & \left(\frac{h_{j+1}}{2} + h_{j+2}\right)^3 \end{pmatrix} \begin{pmatrix} \tilde{a}_{j,0} \\ \tilde{a}_{j,1} \\ \tilde{a}_{j,2} \\ \tilde{a}_{j,3} \end{pmatrix} = \begin{pmatrix} \tilde{f}_{j-1} \\ \tilde{f}_j \\ \tilde{f}_{j+1} \\ \tilde{f}_{j+2} \end{pmatrix}. \quad (3.22)$$

Thus, the coefficients  $\tilde{a}_{j,i}$ ,  $i = 0, \dots, 3$  take the form

$$\begin{aligned}
\tilde{a}_{j,0} &= \frac{f_j + f_{j+1}}{2} - \frac{h_{j+1}^2}{4} \tilde{V}_j, \\
\tilde{a}_{j,1} &= \frac{-f_j + f_{j+1}}{h_{j+1}} + \frac{h_{j+1}^2}{4h_j + 2h_{j+1}} (D_j - \tilde{V}_j), \\
\tilde{a}_{j,2} &= \tilde{V}_j, \\
\tilde{a}_{j,3} &= -\frac{2}{2h_j + h_{j+1}} (D_j - \tilde{V}_j).
\end{aligned} \tag{3.23}$$

Case 2:  $|D_j| > |D_{j+1}|$ , i.e., the possible singularity lies in  $[x_{j-1}, x_j]$ . In this case, in Definition 6, the value  $f_{j-1}$  is replaced with  $\tilde{f}_{j-1}$  by using expression (3.18). The net effect is again the exchange of the weighted arithmetic mean in Equation (3.11a) for the corresponding weighted harmonic mean. On this occasion, we get an adaptation of the reconstruction to a potential singularity in  $[x_{j-1}, x_j]$ , since the effect of the value  $f_{j-1}$  is largely reduced. In fact, by property (3.15) in Lemma 7,  $|\tilde{V}_j| \leq \frac{1}{w_{j,1}} |D_{j+1}|$ , and  $D_{j+1}$  is not affected by any discontinuity.

By solving the system (3.22), we obtain the following coefficients for the polynomial (3.21):

$$\begin{aligned}
\tilde{a}_{j,0} &= \frac{f_j + f_{j+1}}{2} - \frac{h_{j+1}^2}{4} \tilde{V}_j, \\
\tilde{a}_{j,1} &= \frac{-f_j + f_{j+1}}{h_{j+1}} + \frac{h_{j+1}^2}{2h_{j+1} + 4h_{j+2}} (-D_{j+1} + \tilde{V}_j), \\
\tilde{a}_{j,2} &= \tilde{V}_j, \\
\tilde{a}_{j,3} &= -\frac{2}{h_{j+1} + 2h_{j+2}} (-D_{j+1} + \tilde{V}_j).
\end{aligned} \tag{3.24}$$

**Remark 2.** *The replacement of the weighted arithmetic mean for the corresponding harmonic mean in Definition 6 does not only guarantee adaptation near singularities, but also enlarges the region where the reconstruction preserves convexity according to expressions (3.40) and (3.43), as we will see in the next section.*

**Remark 3.** *In both cases, the value of the PPH reconstruction at the midpoint  $x_{j+\frac{1}{2}}$  of  $x_j, x_{j+1}$  gets the value  $PPH_j(x_{j+\frac{1}{2}}) = \tilde{a}_{j,0}$ . This expression directly defines an associated subdivision scheme and, consequently, also an associated multi-resolution scheme in nonuniform meshes. The interested reader is referred to [5, 6] for more details in the context of uniform meshes.*

**Remark 4.** *Notice that, considering uniform meshes, i.e.,  $h_i = h \forall i$ , all the given expressions reduce to the equivalent expressions in [6], which are valid only for the uniform case.*

**Remark 5.** *Notice that Definition 6 of the PPH reconstruction operator has been given for general nonuniform meshes. From now on, one needs to take into account that some results are true for general grids, while others need the restriction to  $\sigma$  quasi-uniform meshes.*

### 3.3 Main properties of the PPH reconstruction operator in nonuniform meshes

In this section, we study some interesting properties of the new reconstruction operator. More precisely, we study the reproduction of polynomials, accuracy of the reconstruction, smoothness, boundedness, Lipschitz continuity, and convexity preservation. We start with the reproduction of polynomials up to degree 2.

#### 3.3.1 Reproduction of polynomials up to degree 2

If the underlying function  $f(x)$  is a polynomial of degree 2, then  $D_j = D_{j+1} = D$  is constant and  $D_j D_{j+1} = D^2 \geq 0$ . Using Equations (3.7), (3.10), (3.14), (3.23), and (3.24), we get

$$\begin{aligned} M_j &= w_{j,0}D + (1 - w_{j,0})D = D, \\ \tilde{V}_j &= \frac{D^2}{w_{j,0}D + (1 - w_{j,0})D} = D, \\ \tilde{a}_{j,i} &= a_{j,i} \quad \forall i = 0, 1, 2, 3. \end{aligned}$$

So,  $PPH_j(x) = PL_j(x)$ , i.e.,  $PPH_j(x)$ , reproduces polynomials of a degree less than or equal 2, since  $PL_j(x)$  does this.

#### 3.3.2 Approximation order for strictly convex (concave) functions

We will prove full-order accuracy, that is, fourth order, for a reconstruction that locally uses four centered points to get the approximation at a given interval  $[x_j, x_{j+1}]$  for any  $j \in \mathbb{Z}$ . In particular, we can enunciate the following proposition.

**Proposition 7.** *Let  $f(x)$  be a strictly convex (concave) function of class  $C^4(\mathbb{R})$  and let  $a \in \mathbb{R}, a > 0$  be such that  $f''(x) \geq a > 0, \forall x \in \mathbb{R}$  (let  $a \in \mathbb{R}, a < 0$  be such that  $f''(x) \leq a < 0, \forall x \in \mathbb{R}$ ). Let  $X = (x_i)_{i \in \mathbb{Z}}$  be a  $\sigma$  quasi-uniform mesh in  $\mathbb{R}$ , with  $h_i = x_i - x_{i-1}, \forall i \in \mathbb{Z}$ , and  $f = (f_i)_{i \in \mathbb{Z}}$ , the sequence of point values of the function  $f(x)$ ,  $f_i = f(x_i)$ . Then, the reconstruction  $PPH(x)$  satisfies*

$$|f(x) - PPH(x)| = O(h^4), \quad \forall x \in \mathbb{R}, \quad (3.25)$$

where  $h = \max_{i \in \mathbb{Z}} \{h_i\}$ .

*Proof.* Given  $x \in \mathbb{R}$ , there exist  $j \in \mathbb{Z}$  such that  $x \in [x_j, x_{j+1}]$ . This implies that  $PPH(x) = PPH_j(x)$ .

Now, let us suppose that the initial data  $f = (f_i)_{i \in \mathbb{Z}}$  come from a strictly convex function (for a concave function, the arguments remain the same) satisfying the given hypothesis  $f''(x) \geq a > 0, \forall x \in \mathbb{R}$  for some  $a > 0$ . Then,  $D_j D_{j+1} > 0$ , since second-order divided differences amount to second derivatives at an intermediate point divided by two, i.e.,

$$D_j = \frac{f''(\mu_1)}{2!} \geq \frac{a}{2}, \quad D_{j+1} = \frac{f''(\mu_2)}{2!} \geq \frac{a}{2},$$

with  $\mu_1 \in (x_{j-1}, x_{j+1})$  and  $\mu_2 \in (x_j, x_{j+2})$ . Moreover, we have

$$|D_{j+1} - D_j| \leq Mh = O(h),$$

where  $M$  is a bound of the third derivative of  $f(x)$  in the compact interval  $[x_{j-1}, x_{j+2}]$ .

Since from Equations (3.7) and (3.14), we can write

$$M_j - \tilde{V}_j = \frac{w_{j,0}w_{j,1}(D_{j+1} - D_j)^2}{w_{j,0}D_{j+1} + w_{j,1}D_j},$$

we get from Lemma 8 that

$$|M_j - \tilde{V}_j| = O(h^2). \quad (3.26)$$

Putting this information into (3.9) and (3.23), if  $|D_j| \leq |D_{j+1}|$ , or into (3.10) and (3.24), if  $|D_j| > |D_{j+1}|$ , we get that

$$|\tilde{a}_{j,i} - a_{j,i}| = O(h^{4-i}) \quad \forall i = 0, 1, 2, 3. \quad (3.27)$$

Thus

$$|PPH_j(x) - PL_j(x)| \leq \sum_{i=0}^3 |\tilde{a}_{j,i} - a_{j,i}| \left| \left( x - x_{j+\frac{1}{2}} \right)^i \right| = O(h^4),$$

where  $PL_j(x)$  is the Lagrange interpolatory polynomial. Taking the triangular inequality into account again

$$|f(x) - PPH_j(x)| \leq |f(x) - PL_j(x)| + |PL_j(x) - PPH_j(x)| = O(h^4),$$

and using that Lagrange interpolation also attains fourth-order accuracy. □

### 3.3.3 Smoothness

In this part, we study the smoothness of the resulting reconstruction, and for this purpose, we give the following definition.

**Definition 7** (Quasi  $C^s$  function). *A function  $f : \mathbb{R} \rightarrow \mathbb{R}$  is said to be quasi  $C^s(\mathbb{R})$  if it satisfies:*

- (a)  *$f(x)$  belongs to class  $C^s(\mathbb{R})$  except for a numerable set of points  $X = (x_i)_{i \in \mathbb{Z}}$  with  $h = \max_{i \in \mathbb{Z}} \{h_i\} < \infty$ , where  $h_i = x_i - x_{i-1}$ .*
- (b) *There exist one-sided derivatives until order  $s$ ,  $f^{(m)}(x_i^+)$  and  $f^{(m)}(x_i^-)$ ,  $m = 0, \dots, s$ , and these satisfy  $|f^{(m)}(x_i^+) - f^{(m)}(x_i^-)| = O(h^{s+1-m})$ ,  $m = 0, \dots, s$ .*

Before giving the main result regarding smoothness, we will prove an auxiliary lemma that we need.

**Lemma 9.** *Let  $f : [a, b] \rightarrow \mathbb{R}$  be a derivable function in  $(a, b)$ , and let us suppose that there exist  $h_0, M > 0$  and  $r \geq 1$  such that  $\forall 0 < h < h_0$ :*

$$\frac{|f(x)|}{h^r} \leq M, \quad \forall x \in (a, b),$$

*then, there exists  $K > 0$  such that  $\forall 0 < h < h_0$*

$$\frac{|f'(x)|}{h^{r-1}} \leq K, \quad \forall x \in (a, b).$$

*Proof.* From the fact that  $f$  is derivable in  $(a, b)$ , we have that given  $x \in (a, b)$  for all  $\varepsilon > 0$ , there exists  $h_\varepsilon > 0$  such that,  $\forall \tilde{h} : 0 < \tilde{h} < h_\varepsilon$ ,

$$\left| f'(x) - \frac{f(x + \tilde{h}) - f(x)}{\tilde{h}} \right| < \varepsilon.$$

Let  $h \in (0, h_0)$ ; then, we take  $\varepsilon_h := h^{r-1}$ , and there exists  $h_{\varepsilon_h} > 0$  such that,  $\forall \tilde{h} : 0 < \tilde{h} < h_{\varepsilon_h}$ ,

$$\left| \frac{f(x + \tilde{h}) - f(x)}{\tilde{h}} - f'(x) \right| < \varepsilon_h = h^{r-1}.$$

We now define  $h_1 = \min\{h, h_{\varepsilon_h}\}$ . Then, for all  $\tilde{h}$  with  $\tilde{h} \in (0, h_1)$ , we get:

$$\begin{aligned} \frac{|f'(x)|}{h^{r-1}} &\leq \frac{1}{h^{r-1}} \left| f'(x) - \frac{f(x + \tilde{h}) - f(x)}{\tilde{h}} \right| + \frac{1}{h^{r-1}} \left| \frac{f(x + \tilde{h}) - f(x)}{\tilde{h}} \right| \\ &< \frac{h^{r-1}}{h^{r-1}} + \frac{1}{h^{r-1}} \left| \frac{f(x + \tilde{h}) - f(x)}{\tilde{h}} \right| \\ &\leq 1 + \frac{|f(x + \tilde{h})|}{\tilde{h}^r} + \frac{|f(x)|}{\tilde{h}^r} = 1 + 2M =: K. \end{aligned}$$

□

We are now ready to present the following proposition with respect to the PPH reconstruction given in Definition 6.

**Proposition 8.** *Let  $f(x)$  be a strictly convex (concave) function of class  $C^4(\mathbb{R})$  and  $a \in \mathbb{R}, a > 0$  such that  $f''(x) \geq a > 0, \forall x \in \mathbb{R}$  ( $a \in \mathbb{R}, a < 0$  such that  $f''(x) \leq a < 0, \forall x \in \mathbb{R}$ ). Let  $X = (x_i)_{i \in \mathbb{Z}}$  be a  $\sigma$  quasi-uniform mesh in  $\mathbb{R}$ , with  $h_i = x_i - x_{i-1}, \forall i \in \mathbb{Z}$ , and  $f = (f_i)_{i \in \mathbb{Z}}$ , the sequence of point values of the function  $f(x)$ ,  $f_i = f(x_i)$ . Then, the reconstruction  $PPH(x)$  is quasi  $C^3(\mathbb{R})$ .*

*Proof.* By construction, the PPH reconstruction is  $C^\infty((x_i, x_{i+1}))$  for all  $i \in \mathbb{Z}$ , since it is nothing else but a piecewise polynomial. Let us study the situation at a grid point  $x_j$  where two polynomial pieces join. Again, by construction,  $PPH_{j-1}(x_j) = PPH_j(x_j)$ , and therefore, the reconstruction is a continuous function. Using the proof of Proposition 7, we know that

$$\begin{aligned} g_{j-1}(x) &:= f(x) - PPH_{j-1}(x) = O(h^4), \quad \forall x \in [x_{j-2}, x_{j+1}], \\ g_j(x) &:= f(x) - PPH_j(x) = O(h^4), \quad \forall x \in [x_{j-1}, x_{j+2}]. \end{aligned} \quad (3.28)$$

From (3.28), we get that

$$PPH_j(x) - PPH_{j-1}(x) = g_{j-1}(x) - g_j(x) = O(h^4), \forall x \in [x_{j-1}, x_{j+1}]. \quad (3.29)$$

Thus, from Lemma 9, we get that

$$PPH_j^{(m)}(x) - PPH_{j-1}^{(m)}(x) = O(h^{4-m}), \quad m = 1, 2, 3. \quad (3.30)$$

In particular, Equations (3.29) and (3.30) are true for the abscissa  $x_j$ , which proves the property of quasi  $C^3$  at the grid points.

□

### 3.3.4 Boundedness and Lipschitz continuity

We start by giving the exact definitions of the concepts treated in this section.

**Definition 8.** A nonlinear reconstruction operator  $\mathcal{R} : l_\infty(\mathbb{Z}) \rightarrow C(\mathbb{R})$  is called bounded if there exists a constant  $C > 0$  such that

$$\|\mathcal{R}(f)\|_\infty \leq C\|f\|_\infty \quad \forall f \in l_\infty(\mathbb{Z}).$$

**Definition 9.** A nonlinear reconstruction operator  $\mathcal{R} : l_\infty(\mathbb{Z}) \rightarrow C(\mathbb{R})$  is called Lipschitz continuous if there exists a constant  $C > 0$  such that  $\forall x, y \in \mathbb{R}$ , it is verified that

$$|\mathcal{R}(f)(x) - \mathcal{R}(f)(y)| \leq C|x - y|.$$

Before addressing these properties, we need to prove some lemmas.

**Lemma 10.** Let  $X = (x_i)_{i \in \mathbb{Z}}$  be a  $\sigma$  quasi-uniform mesh in  $\mathbb{R}$ , with  $h_i = x_i - x_{i-1} \forall i \in \mathbb{Z}$ , and let  $L_m(x)$   $m = -1, 0, 1, 2$  be the Lagrange basis for a four-point stencil  $\{x_{j-1}, x_j, x_{j+1}, x_{j+2}\}$ . Then

$$|L_m(x)| \leq \sigma \quad \forall x \in [x_j, x_{j+1}], \quad m = -1, 0, 1, 2.$$

*Proof.* As is well known, the Lagrange bases are given by

$$L_m(x) = \prod_{\substack{s=-1 \\ s \neq m}}^2 \frac{x - x_{j+s}}{x_{j+m} - x_{j+s}}, \quad m = -1, 0, 1, 2. \quad (3.31)$$

Denoting  $\alpha = x - x_j$ , we have

$$|L_{-1}(x)| = \left| \frac{\alpha}{h_j} \frac{h_{j+1} - \alpha}{h_{j+1} + h_j} \frac{h_{j+2} + h_{j+1} - \alpha}{h_{j+2} + h_{j+1} + h_j} \right| < \left| \frac{\alpha}{h_j} \right| \leq \sigma,$$

$$|L_0(x)| = \left| \frac{(h_j + \alpha)(h_{j+1} - \alpha)}{h_j h_{j+1}} \frac{h_{j+2} + h_{j+1} - \alpha}{h_{j+2} + h_{j+1}} \right| \leq \left| \frac{(\max\{h_j, h_{j+1}\})^2 - \alpha^2}{h_j h_{j+1}} \right| \leq \sigma,$$

$$|L_1(x)| = \left| \frac{h_j + \alpha}{h_j + h_{j+1}} \frac{\alpha}{h_{j+1}} \frac{h_{j+2} + h_{j+1} - \alpha}{h_{j+2}} \right|.$$

In order to obtain the bound for  $L_1(x)$ , we distinguish two cases.

1. If  $h_{j+2} \geq h_{j+1}$ ,  $\alpha \leq h_{j+2} - (h_{j+1} - \alpha)$ ,

$$\begin{aligned} |L_1(x)| &\leq \left| \frac{h_j + \alpha}{h_j + h_{j+1}} \frac{h_{j+2} - (h_{j+1} - \alpha)}{h_{j+1}} \frac{h_{j+2} + (h_{j+1} - \alpha)}{h_{j+2}} \right| \leq \left| \frac{(h_{j+2})^2 - (h_{j+1} - \alpha)^2}{h_{j+1} h_{j+2}} \right| \\ &\leq \left| \frac{(\max\{h_{j+1}, h_{j+2}\})^2}{h_{j+1} h_{j+2}} \right| \leq \sigma. \end{aligned}$$

2. If  $h_{j+1} > h_{j+2}$ ,  $\alpha < h_{j+1} - (h_{j+2} - \alpha)$ , working in a similar way, we also get  $|L_1(x)| \leq \sigma$ .

Finally,

$$|L_2(x)| \leq \left| \frac{h_j + \alpha}{h_j + h_{j+1} + h_{j+2}} \frac{\alpha}{h_{j+1} + h_{j+2}} \frac{h_{j+1} - \alpha}{h_{j+2}} \right| \leq \left| \frac{h_{j+1} - \alpha}{h_{j+2}} \right| \leq \sigma.$$

□

**Lemma 11.** *Let  $X = (x_i)_{i \in \mathbb{Z}}$  be a  $\sigma$  quasi-uniform mesh in  $\mathbb{R}$ , with  $h_i = x_i - x_{i-1} \forall i \in \mathbb{Z}$ , and let us consider the expressions  $|\tilde{f}_{j+2}|$  in (3.17) and  $|\tilde{f}_{j-1}|$  in (3.18). Then, we have the following bounds:*

$$|\tilde{f}_{j+2}| \leq (5 + 16\sigma)\sigma^3 \|f\|_{l_\infty(\mathbb{Z})}, \quad |\tilde{f}_{j-1}| \leq (5 + 16\sigma)\sigma^3 \|f\|_{l_\infty(\mathbb{Z})}.$$

*Proof.* From Equations (3.12), we get

$$\begin{aligned} \left| \frac{\gamma_{j,-1}}{\gamma_{j,2}} \right| &= \left| \frac{h_{j+2}}{h_j} \frac{h_{j+1} + h_{j+2}}{h_{j+1} + h_j} \frac{h_{j+1} + 2h_{j+2}}{h_{j+1} + 2h_j} \right| \leq \sigma^3, \\ \left| \frac{\gamma_{j,0}}{\gamma_{j,2}} \right| &= \left| \frac{h_{j+2}}{h_{j+1}} \frac{h_{j+1} + h_{j+2}}{h_{j+1} + 2h_j} \left( \frac{h_{j+1} + 2h_j}{h_{j+1} + h_{j+2}} - \frac{h_{j+1} + 2h_{j+2}}{h_j} \right) \right| \leq 2\sigma^3, \\ \left| \frac{\gamma_{j,1}}{\gamma_{j,2}} \right| &= \left| \frac{h_{j+2}}{h_{j+1}} \frac{h_{j+1} + h_{j+2}}{h_{j+1} + 2h_j} \left( \frac{h_{j+1} + 2h_{j+2}}{h_{j+1} + h_j} - \frac{h_{j+1} + 2h_j}{h_{j+2}} \right) \right| \leq 2\sigma^3. \end{aligned} \quad (3.32)$$

According to property (3.15) of the harmonic mean  $|\tilde{V}_j| \leq \frac{|D_j|}{w_{j,0}}$ , we also get

$$\begin{aligned} \left| \frac{\tilde{V}_j}{\gamma_{j,2}} \right| &\leq \left| \frac{D_j}{w_{j,0} \cdot \gamma_{j,2}} \right| = \frac{4h_{j+2}(h_{j+1} + h_{j+2})(h_j + h_{j+1} + h_{j+2})^2}{(h_{j+1} + 2h_{j+2})(h_{j+1} + 2h_j)} \\ &\left| \frac{f_{j-1}}{h_j(h_j + h_{j+1})} - \frac{f_j}{h_j h_{j+1}} + \frac{f_{j+1}}{h_{j+1}(h_j + h_{j+1})} \right| \leq 16\sigma^4 \|f^k\|_{l_\infty(\mathbb{Z})}. \end{aligned} \quad (3.33)$$

Plugging (3.32) and (3.33) into (3.17), we obtain

$$|\tilde{f}_{j+2}| \leq (5 + 16\sigma)\sigma^3 \|f^k\|_{l_\infty(\mathbb{Z})}.$$

Following a similar path for  $|\tilde{f}_{j-1}|$ ,

$$\begin{aligned} \left| \frac{\gamma_{j,0}}{\gamma_{j,-1}} \right| &= \left| \frac{h_j}{h_{j+1}} \frac{h_{j+1} + h_j}{h_{j+1} + 2h_{j+2}} \left( \frac{h_{j+1} + 2h_j}{h_{j+1} + h_{j+2}} - \frac{h_{j+1} + 2h_{j+2}}{h_j} \right) \right| \leq 2\sigma^3, \\ \left| \frac{\gamma_{j,1}}{\gamma_{j,-1}} \right| &= \left| \frac{h_j}{h_{j+1}} \frac{h_{j+1} + h_j}{h_{j+1} + 2h_{j+2}} \left( \frac{h_{j+1} + 2h_{j+2}}{h_{j+1} + h_j} - \frac{h_{j+1} + 2h_j}{h_{j+2}} \right) \right| \leq 2\sigma^3, \\ \left| \frac{\gamma_{j,2}}{\gamma_{j,-1}} \right| &= \left| \frac{h_j}{h_{j+2}} \frac{h_{j+1} + h_j}{h_{j+1} + h_{j+2}} \frac{h_{j+1} + 2h_j}{h_{j+1} + 2h_{j+2}} \right| \leq \sigma^3. \end{aligned}$$

Using the property (3.15) of the harmonic mean  $|\tilde{V}_j| \leq \frac{|D_{j+1}|}{w_{j,1}}$ , we get

$$\left| \frac{\tilde{V}_j}{\gamma_{j,-1}} \right| \leq \left| \frac{D_{j+1}}{w_{j,1} \cdot \gamma_{j,-1}} \right| = \frac{4h_j(h_{j+1} + h_j)(h_j + h_{j+1} + h_{j+2})^2}{(h_{j+1} + 2h_{j+2})(h_{j+1} + 2h_j)}$$

$$\left| \frac{f_j}{h_{j+2}(h_{j+2} + h_{j+1})} - \frac{f_{j+1}}{h_{j+2}h_{j+1}} + \frac{f_{j+2}}{h_{j+1}(h_{j+2} + h_{j+1})} \right| \leq 16\sigma^4 \|f^k\|_{l_\infty(\mathbb{Z})},$$

which leads us to

$$|\tilde{f}_{j-1}| \leq (5 + 16\sigma)\sigma^3 \|f^k\|_{l_\infty(\mathbb{Z})}.$$

□

**Proposition 9.** *The nonlinear PPH reconstruction operator is a bounded operator over  $\sigma$  quasi-uniform meshes.*

*Proof.* Let  $x \in \mathbb{R}$  and  $j \in \mathbb{Z}$  such that  $x \in [x_j, x_{j+1}]$ . Depending on the relative size of  $D_j$  and  $D_{j+1}$ , the PPH reconstruction operator replaces the value  $f_{j+2}$  with  $\tilde{f}_{j+2}$  or  $f_{j-1}$  by  $\tilde{f}_{j-1}$  as follows:

$$PPH_j(x) = \begin{cases} B_{-1}f_{j-1} + B_0f_j + B_1f_{j+1} + B_2\tilde{f}_{j+2} & \text{if } |D_j| \leq |D_{j+1}|, \\ B_{-1}\tilde{f}_{j-1} + B_0f_j + B_1f_{j+1} + B_2f_{j+2} & \text{if } |D_j| > |D_{j+1}|, \end{cases}$$

where  $B_m = L_m(x)$ ,  $m = -1, 0, 1, 2$ , stand for the Lagrange polynomials. Applying the triangular inequality for each case, we get

$$|PPH_j(x)| \leq \begin{cases} (|B_{-1}| + |B_0| + |B_1|) \|f\|_{l_\infty(\mathbb{Z})} + |B_2|\|\tilde{f}_{j+2}\| & \text{if } |D_j| \leq |D_{j+1}|, \\ |B_{-1}|\|\tilde{f}_{j-1}\| + (|B_0| + |B_1| + |B_2|) \|f\|_{l_\infty(\mathbb{Z})} & \text{if } |D_j| > |D_{j+1}|. \end{cases}$$

According to Lemmas 10 and 11, we obtain the following bound for both cases

$$|PPH_j(x)| \leq \sigma(3 + 5\sigma^3 + 16\sigma^4) \|f\|_{l_\infty(\mathbb{Z})}.$$

□

The following lemma will be used for proving the Lipschitz continuity.

**Lemma 12.** *Let  $X = (x_i)_{i \in \mathbb{Z}}$  be a  $\sigma$  quasi-uniform mesh in  $\mathbb{R}$ , with  $h_i = x_i - x_{i-1} \forall i \in \mathbb{Z}$ , and let  $f = (f_i)_{i \in \mathbb{Z}}$  be a sequence in  $l_\infty(\mathbb{Z})$ . Then, the nonlinear reconstruction operator defined in (6) satisfies that  $\forall j \in \mathbb{Z}$ ,*

$$|PPH'_j(x)| \leq C \|f\|_{l_\infty(\mathbb{Z})} \quad \forall x \in (x_j, x_{j+1}).$$

*Proof.* Since  $f \in l_\infty(\mathbb{Z})$ , there exists  $M \in \mathbb{R}$ ,  $M \geq 0$  such that  $|f_i| \leq M \quad \forall i \in \mathbb{Z}$ .



The reconstruction  $PPH_j(x)$  and its derivative read

$$PPH_j(x) = \tilde{a}_{j,0} + \tilde{a}_{j,1} \left(x - x_{j+\frac{1}{2}}\right) + \tilde{a}_{j,2} \left(x - x_{j+\frac{1}{2}}\right)^2 + \tilde{a}_{j,3} \left(x - x_{j+\frac{1}{2}}\right)^3, \quad (3.34)$$

$$PPH'_j(x) = \tilde{a}_{j,1} + 2\tilde{a}_{j,2} \left(x - x_{j+\frac{1}{2}}\right) + 3\tilde{a}_{j,3} \left(x - x_{j+\frac{1}{2}}\right)^2. \quad (3.35)$$

Without lost of generalization, we will suppose that  $|D_j| \leq |D_{j+1}|$ . The case  $|D_j| > |D_{j+1}|$  can be carried out similarly. First, we prove the following inequalities:

$$\begin{aligned} |D_j| &= \left| \frac{f_{j-1}}{h_j(h_j + h_{j+1})} - \frac{f_j}{h_j h_{j+1}} + \frac{f_{j+1}}{h_{j+1}(h_j + h_{j+1})} \right| \\ &\leq \left| \frac{h_{j+1} + (h_j + h_{j+1}) + h_j}{h_j h_{j+1} (h_j + h_{j+1})} \right| \|f\|_{l_\infty(\mathbb{Z})} = \frac{2}{h_j h_{j+1}} \|f\|_{l_\infty(\mathbb{Z})} \leq \frac{2}{(h_{min})^2} \|f\|_{l_\infty(\mathbb{Z})}, \\ |\tilde{V}_j| &\leq \frac{2}{(h_{min})^2} \|f\|_{l_\infty(\mathbb{Z})}, \\ |D_j - \tilde{V}_j| &\leq \max\{|D_j|, |\tilde{V}_j|\} \leq \frac{2}{(h_{min})^2} \|f\|_{l_\infty(\mathbb{Z})}, \end{aligned} \quad (3.36)$$

where  $h_{min} = \min_{i \in \mathbb{Z}} h_i$  depends on the particular  $\sigma$  quasi-uniform mesh.

Using the expressions (3.23) for the coefficients of the polynomial derivative in (3.35), we have

$$\begin{aligned} |\tilde{a}_{j,1}| &\leq \left| \frac{f_{j+1} - f_j}{h_{j+1}} \right| + \left| \frac{(h_{j+1})^2}{4h_j + 2h_{j+1}} \right| |D_j - \tilde{V}_j| \\ &\leq \frac{2}{h_{min}} \|f\|_{l_\infty(\mathbb{Z})} + \frac{(h_{max})^2}{6h_{min}} \frac{2}{(h_{min})^2} \|f\|_{l_\infty(\mathbb{Z})} \\ &\leq \frac{2}{h_{min}} \left(1 + \frac{\sigma^2}{6}\right) \|f\|_{l_\infty(\mathbb{Z})}, \\ |\tilde{a}_{j,2}| &= |\tilde{V}_j| \leq \frac{2}{(h_{min})^2} \|f\|_{l_\infty(\mathbb{Z})}, \\ |\tilde{a}_{j,3}| &\leq \left| \frac{2}{2h_j + h_{j+1}} \right| |D_j - \tilde{V}_j| \leq \frac{2}{3h_{min}} \frac{2}{(h_{min})^2} \|f\|_{l_\infty(\mathbb{Z})} \\ &= \frac{4}{3(h_{min})^3} \|f\|_{l_\infty(\mathbb{Z})}. \end{aligned}$$

Thus

$$\begin{aligned} |PPH'_j(x)| &= \left| \tilde{a}_{j,1} + 2\tilde{a}_{j,2} \left(x - x_{j+\frac{1}{2}}\right) + 3\tilde{a}_{j,3} \left(x - x_{j+\frac{1}{2}}\right)^2 \right| \\ &\leq \left( \frac{2}{h_{min}} \left(1 + \frac{\sigma^2}{6}\right) + 2 \frac{2}{(h_{min})^2} \frac{h_{max}}{2} + 3 \frac{4}{3(h_{min})^3} \frac{(h_{max})^2}{4} \right) \|f\|_{l_\infty(\mathbb{Z})} \\ &= \frac{1}{h_{min}} \left(2 + 2\sigma + \frac{4}{3}\sigma^2\right) \|f\|_{l_\infty(\mathbb{Z})} = C \|f\|_{l_\infty(\mathbb{Z})} \quad \forall x \in (x_j, x_{j+1}), \end{aligned}$$

where  $C = \frac{1}{h_{min}} \left(2 + 2\sigma + \frac{4}{3}\sigma^2\right)$  depends on the  $\sigma$  quasi-uniform mesh.  $\square$

**Proposition 10.** *The nonlinear PPH reconstruction operator is Lipschitz continuous over  $\sigma$  quasi-uniform meshes.*

*Proof.* Let us suppose first that there exists  $j \in \mathbb{Z}$  such that  $x, y \in [x_j, x_{j+1}]$ . Using the Lagrange mean value theorem,  $\exists \theta \in (x_j, x_{j+1})$ , such as

$$|PPH_j(x) - PPH_j(y)| = |PPH'_j(\theta)(x - y)|.$$

Thus, using Lemma 12 now, we get

$$|PPH_j(x) - PPH_j(y)| \leq C|x - y|.$$

In the general case, we can suppose that  $x < y$ ,  $x \in [x_{j_1}, x_{j_1+1}]$ ,  $y \in [x_{j_2}, x_{j_2+1}]$  with  $j_1 \leq j_2$ . If  $j_1 = j_2$ , we have already proved the result. For  $j_1 < j_2$ ,

$$\begin{aligned} |PPH(x) - PPH(y)| &= |PPH_{j_1}(x) - PPH_{j_2}(y)| \leq |PPH_{j_1}(x) - PPH_{j_1}(x_{j_1+1})| \\ &+ \sum_{j=j_1+1}^{j_2-1} |PPH_j(x_j) - PPH_j(x_{j+1})| + |PPH_{j_2}(x_{j_2}) - PPH_{j_2}(y)| \\ &\leq C|x - x_{j_1+1}| + \sum_{j=j_1+1}^{j_2-1} C|x_j - x_{j+1}| + C|x_{j_2} - y| = C|x - y|. \end{aligned}$$

□

### 3.3.5 Convexity preservation

We first introduce a definition concerning what we call strictly convex data and a strictly convexity-preserving reconstruction operator.

**Definition 10.** *Let  $X = (x_i)_{i \in \mathbb{Z}}$  be a nonuniform mesh in  $\mathbb{R}$ , with  $h_i = x_i - x_{i-1} \forall i \in \mathbb{Z}$ , and let  $f = (f_i)_{i \in \mathbb{Z}}$  be a sequence in  $l_\infty(\mathbb{Z})$ . We say that the data are strictly convex (concave) if, for all  $i \in \mathbb{Z}$ , it is satisfied that  $D_i > 0$  ( $D_i < 0$ ), where  $D_i$  stands for the second-order divided differences.*

**Definition 11.** *Let  $X = (x_i)_{i \in \mathbb{Z}}$  be a nonuniform mesh in  $\mathbb{R}$  with  $h_i = x_i - x_{i-1} \forall i \in \mathbb{Z}$ , and let  $f = (f_i)_{i \in \mathbb{Z}}$  be a strictly convex (concave) sequence. We say that an operator  $R : l_\infty(\mathbb{Z}) \rightarrow C(\mathbb{R})$  is strictly convexity preserving in the interval  $(a, b)$  if there exists  $R(f)''(x)$  and  $R(f)''(x) > 0$  ( $R(f)''(x) < 0$ )  $\forall x \in (a, b)$ .*

Next, we give a proposition that introduces sufficient conditions on the grid for convexity preservation of the proposed reconstruction.

**Proposition 11.** *Let  $X = (x_i)_{i \in \mathbb{Z}}$  be a  $\sigma$  quasi-uniform mesh in  $\mathbb{R}$ ,  $h_i = x_i - x_{i-1}$ ,  $\forall i \in \mathbb{Z}$ , and  $\sigma \leq 4$ . Let  $f = (f_i)_{i \in \mathbb{Z}}$  be a sequence of strictly convex data. Then, the reconstruction  $PPH(x)$  is strictly convexity preserving in each  $(x_j, x_{j+1})$ , that is, it is a piecewise convex function satisfying*

$$PPH''_j(x) > 0 \quad \forall x \in (x_j, x_{j+1}), \quad \forall j \in \mathbb{Z}. \quad (3.37)$$

*Proof.* Let  $x \in \mathbb{R}$  and  $j \in \mathbb{Z}$  such that  $x \in (x_j, x_{j+1})$ . Let us also consider that  $D_i > 0 \forall i \in \mathbb{Z}$ . The case  $D_i < 0 \forall i \in \mathbb{Z}$  is proved in the same way.

Computing derivatives in Equation (3.21), we get

$$PPH_j''(x) = 2\tilde{a}_{j,2} + 6\tilde{a}_{j,3} \left( x - x_{j+\frac{1}{2}} \right). \quad (3.38)$$

In order to analyze the sign of  $PPH_j''(x)$  we need to consider two cases due to the fact that the expression of  $PPH_j(x)$  is different for  $|D_j| \leq |D_{j+1}|$  than for  $|D_j| > |D_{j+1}|$ .

Case 1:  $|D_j| \leq |D_{j+1}|$ .

Replacing coefficients  $\tilde{a}_{j,2}, \tilde{a}_{j,3}$  coming from Equation (3.23) in expression (3.38) results in

$$PPH_j''(x) = 2\tilde{V}_j - \frac{12}{2h_j + h_{j+1}} (D_j - \tilde{V}_j) \left( x - x_{j+\frac{1}{2}} \right). \quad (3.39)$$

Taking into account that  $\tilde{V}_j - D_j \geq 0$ , from (3.39), we get that proving  $PPH_j''(x) > 0$  is trivial if  $\tilde{V}_j = D_j$ . Otherwise, the inequality  $PPH_j''(x) > 0$  reads

$$x > x_{j+\frac{1}{2}} - \frac{2h_j + h_{j+1}}{6} \frac{\tilde{V}_j}{\tilde{V}_j - D_j}. \quad (3.40)$$

Replacing  $\tilde{V}_j$  with its expression in Equation (3.14), we obtain

$$x > x_{j+\frac{1}{2}} - \frac{h_j + h_{j+1} + h_{j+2}}{3} \frac{D_{j+1}}{D_{j+1} - D_j}. \quad (3.41)$$

Evaluating the previous expression at  $x_j$ , we obtain the condition for convexity preservation in  $(x_j, x_{j+1})$ . This condition reads

$$(h_{j+1} - 2(h_j + h_{j+2})) D_{j+1} < 3h_{j+1} D_j. \quad (3.42)$$

Since  $X$  is a  $\sigma$  quasi-uniform mesh with  $\sigma \leq 4$ , we have  $h_{j+1} \leq 2(h_j + h_{j+2})$ , and therefore, the condition (3.42) is immediately satisfied. This proves the proposition in this case.

Case 2:  $|D_j| > |D_{j+1}|$ .

This time, by replacing the coefficients  $\tilde{a}_{j,2}, \tilde{a}_{j,3}$  coming from Equation (3.24) in expression (3.38) and following a similar track to that in Case 1, we obtain expressions similar to (3.40) and (3.41) for the abscissae verifying  $PPH_j''(x) > 0$ :

$$x < x_{j+\frac{1}{2}} + \frac{h_{j+1} + 2h_{j+2}}{6} \frac{\tilde{V}_j}{\tilde{V}_j - D_{j+1}}, \quad (3.43)$$

$$x < x_{j+\frac{1}{2}} + \frac{h_j + h_{j+1} + h_{j+2}}{3} \frac{D_j}{D_j - D_{j+1}}. \quad (3.44)$$

Now, evaluating at  $x_{j+1}$ , we get

$$(h_{j+1} - 2(h_j + h_{j+2})) D_j < 3h_{j+1} D_{j+1}. \quad (3.45)$$

Thus, since  $X$  is a  $\sigma$  quasi-uniform mesh with  $\sigma \leq 4$ , we get the result.  $\square$

**Remark 6.** As can be observed in expressions (3.41) and (3.44), the conditions that assure the strictly convexity-preserving property depend on the second-order divided differences of the initial data. The hypotheses of Proposition 11 are only sufficient conditions, but not necessary conditions.

**Remark 7.** Working in a similar way with the Lagrange reconstruction operator  $PL_j(x)$ , we obtain the following expression that is analogue to (3.41) for the abscissa-fulfilling condition  $PL_j''(x) > 0$ :

$$x > x_{j+\frac{1}{2}} - \frac{2h_j + h_{j+1}}{6} - \frac{h_j + h_{j+1} + h_{j+2}}{3} \frac{D_j}{D_{j+1} - D_j}. \quad (3.46)$$

Then, if we are under the supposition that  $D_j < D_{j+1}$ , calling  $x_{PPH}$  and  $x_{PL}$  to the second members of inequalities (3.41) and (3.46), respectively, we get

$$x_{PL} - x_{PPH} = \frac{h_{j+1} + 2h_{j+2}}{6} > 0, \quad (3.47)$$

i.e., PPH reconstruction operator preserves the strict convexity in a wider interval than the Lagrange reconstruction operator does. A similar conclusion can be reached under the supposition that  $D_j > D_{j+1}$ .

### 3.4 PPH reconstruction operator over $\sigma$ quasi-uniform meshes for strictly convex (concave) initial data

In this section, we gather the most important properties of the presented PPH reconstruction for strictly convex (concave) starting input data, and we give them in a unifying theorem. We want to emphasize the potential practical importance of the studied technique for designing processes.

**Theorem 3.** Let  $f(x)$  be a strictly convex (concave) function of class  $C^4(\mathbb{R})$  and let  $a \in \mathbb{R}, a > 0$  such that  $f''(x) \geq a > 0, \forall x \in \mathbb{R}$  ( $a \in \mathbb{R}, a < 0$  such that  $f''(x) \leq a < 0, \forall x \in \mathbb{R}$ ). Let  $X = (x_i)_{i \in \mathbb{Z}}$  be a  $\sigma$  quasi-uniform mesh in  $\mathbb{R}$  with  $h_i = x_i - x_{i-1}, \forall i \in \mathbb{Z}$ , and let  $f = (f_i)_{i \in \mathbb{Z}}$  be the sequence of point values of the function  $f(x)$ ,  $f_i = f(x_i)$ . Then, the reconstruction  $PPH(x)$  satisfies

1. Reproduction of polynomials up to the second degree.
2. Fourth-order accuracy.
3. It presents a quasi  $C^3$  smoothness.
4. It is bounded and Lipschitz continuous.
5. It is strictly convexity preserving in each  $(x_j, x_{j+1})$ .

*Proof.* Taking the previous results into account, the proof of this theorem is now immediate. In fact, the first affirmation is proven in Section 3.3.1, and the rest of the affirmations are proven in Propositions 7–11, respectively.  $\square$

### 3.5 Numerical experiments

In this section, we present three simple numerical experiments. The first one is dedicated to comparing the convexity preservation between the Lagrange and PPH reconstructions. Let us consider the initial convex set of points,  $(0, 10)$ ,  $(8, 9)$ ,  $(25, 12)$ , and  $(30, 30)$ , that is,  $D_j > 0$ ,  $D_{j+1} > 0$ . In Figure 3.1, we have depicted the reconstruction operators corresponding to Lagrange and PPH, and we have marked with triangles the inflection points for each reconstruction (5.66 and 10.16, respectively). We observe that PPH preserves convexity in a wider range  $\frac{h_{j+1} + 2h_{j+2}}{6} = 4.5$  than the Lagrange reconstruction does (see expression (3.47)). In fact, according to Theorem 3, PPH reconstruction is strictly convexity preserving for the abscissae corresponding with the central interval  $(8, 25)$ , while Lagrange reconstruction is not.

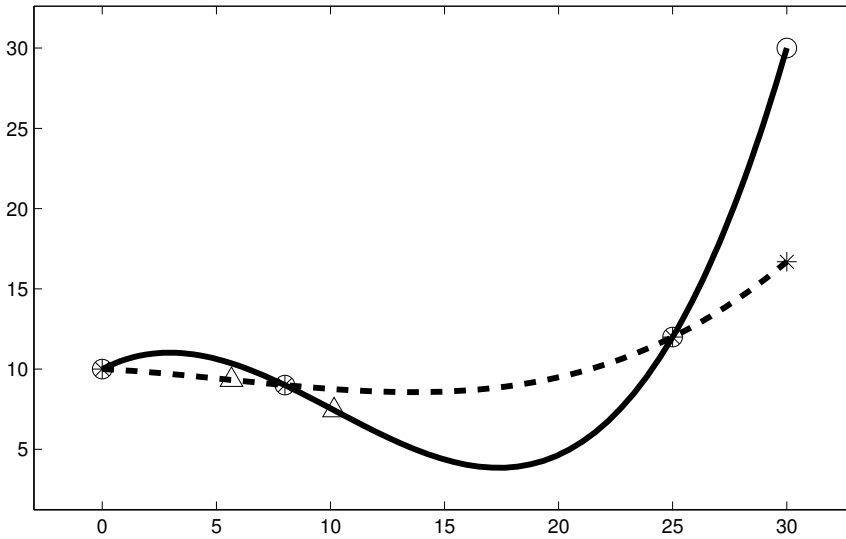


Figure 3.1: Solid line: Lagrange polynomial; dashed line: piecewise polynomial harmonic (PPH) polynomial. Circles stand for Lagrange values at the nodes, asterisks stand for PPH values at the nodes, and triangles stand for inflection points.

The next experiment computes the numerical approximation order of the considered reconstruction operator.

Let  $X$  be a nonuniform grid:

$$X = \left( \frac{22}{551}, \frac{28}{337}, \frac{28}{267}, \frac{79}{656}, \frac{149}{924}, \frac{47}{234}, \frac{67}{245}, \frac{92}{275}, \frac{98}{241}, \frac{113}{254}, \frac{185}{396}, \frac{251}{490}, \frac{141}{257}, \frac{134}{205}, \frac{469}{221}, \frac{316}{369}, \frac{1189}{1259} \right) \pi,$$

and let  $f(x) = \sin(x)$  be a smooth test function. Let us consider the set of initial points given by  $(x_i, f(x_i))$ ,  $i = 1, \dots, 17$ . In this experiment, we will measure the approximation errors and the numerical order of approximation of the presented PPH reconstruction. The numerical order of approximation  $p$  is calculated in an iterative way, just by considering at each new iteration  $k$ ,  $k = 1, 2, 3, 4, 5, 6, 7$  a nonuniform grid  $X_k$  built from the previous one by introducing a new node in the middle of each two consecutive existing nodes. The error  $E_k$  for the PPH reconstruction at

each iteration  $k$  is calculated as a discrete approximation to  $\|f(x) - PPH(x)\|_\infty$ , thus evaluating a much denser set of points. Both the errors and the approximation orders  $p$  for each iteration are shown in Table 3.1, where we can see that PPH reconstruction tends to fourth-order accuracy with this smooth concave function, as is expected according to Proposition 7.

Defining  $h := \max_{i=1, \dots, 16} \{h_i\}$ , we use the following formulae to compute the numerical order of approximation  $p$ :

$$E_{k-1} \approx C \left( \frac{h}{2^{k-1}} \right)^p,$$

$$E_k \approx C \left( \frac{h}{2^k} \right)^p.$$

Thus

$$\frac{E_{k-1}}{E_k} \approx 2^p \rightarrow p \approx \log_2 \frac{E_{k-1}}{E_k}, \quad k = 1, 2, 3, 4, 5, 6, 7.$$

The appropriate behavior of the reconstruction can be checked in Figure 3.2, where the preservation of the concavity and the accuracy of the approximation can be observed.

$k$	$E_k$	$p$	$k$	$E_k$	$p$
0	$4.6114 \times 10^{-4}$	-	4	$1.4165 \times 10^{-8}$	3.8226
1	$3.3727 \times 10^{-5}$	3.7732	5	$9.4710 \times 10^{-10}$	3.9027
2	$2.6009 \times 10^{-6}$	3.6968	6	$6.1330 \times 10^{-11}$	3.9488
3	$2.0042 \times 10^{-7}$	3.6979	7	$3.9035 \times 10^{-12}$	3.9737

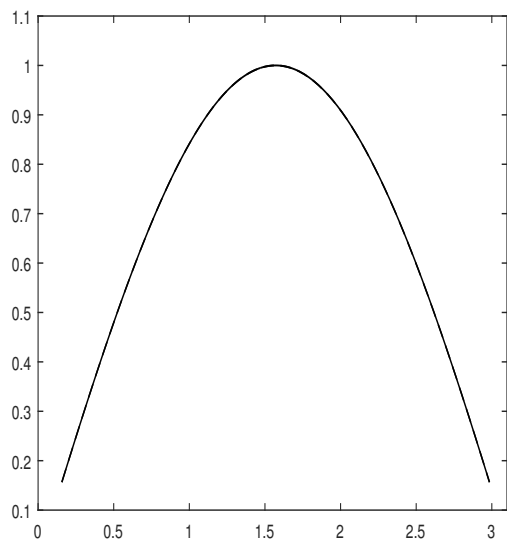
Table 3.1: Approximation errors  $E_k$  in  $l_\infty$  norm and corresponding approximation orders  $p$  obtained after  $k$  iterations for the PPH reconstruction with  $f(x) = \sin(x)$ ,  $k = 0, 1, \dots, 7$ .

### 3.6 Conclusions

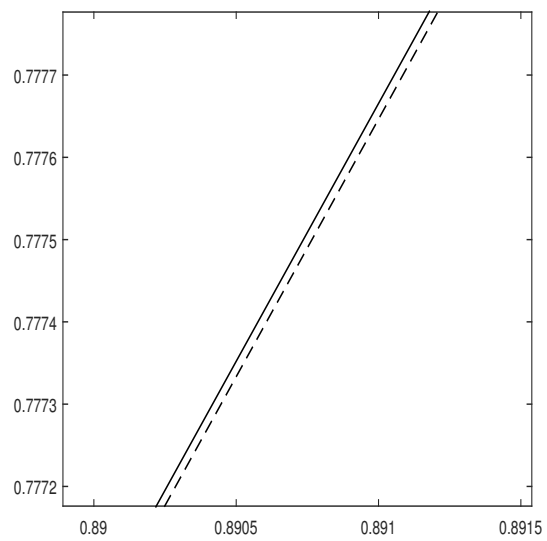
We have defined and studied the PPH reconstruction operator over nonuniform grids, paying special attention to the case of  $\sigma$  quasi-uniform grids and initial data coming from strictly convex (concave) underlying functions.

We have theoretically proven some very interesting properties of the new reconstruction operator from the point of view of a potential use in graphical design applications. These properties include the reproduction of polynomials up to the second degree, approximation order, smoothness, boundedness of the operator, Lipschitz continuity, and convexity preservation. In particular, we would like to emphasize the quasi  $C^3$  smoothness of the operator and the preservation of strict convexity according to the result contained in Theorem 3.

In the section on the numerical experiments, we checked that the behavior corresponded to the developed theory, in particular, the reconstruction attained fourth-order accuracy and preserved the convexity of the initial data. The results clearly show that the reconstruction introduces improvements in comparison with the Lagrange reconstruction. Therefore, the numerical experiments that we carried out reinforce the theoretical results.



(a)



(b)

Figure 3.2: Solid line: function  $f(x) = \sin(x)$ ; dashed line: PPH reconstruction obtained with the finest considered nonlinear grid. **(a)**: Original function and PPH reconstruction. **(b)**: Zoom of a part of the signal.

## Chapter 4

# PPH nonlinear interpolatory reconstruction operator on nonuniform grids: Adaptation around jump discontinuities and elimination of Gibbs phenomenon

The contents of this chapter are wholly included in the already published paper [43]

- Ortiz, P.; Trillo, J.C. A Piecewise Polynomial Harmonic Nonlinear Interpolatory Reconstruction Operator on Non Uniform Grids–Adaptation around Jump Discontinuities and Elimination of Gibbs Phenomenon. *Mathematics*. **2021**, *9*, 335. <https://doi.org/10.3390/math9040335>.

### 4.1 Introduction

Due to the extended use of reconstruction operators in many fields of application, ranging from hyperbolic conservation laws to computer aided geometric design, it is of great importance to dispose of efficient methods to build them for different situations. In general, and for the sake of simplicity, the considered functions are polynomials. High degree polynomials are, however, usually avoided because they are known to generate oscillations and undesirable effects.

Linear operators behave improperly in presence of jump discontinuities, so that different nonlinear operators have emerged to deal with this problematic. Recent approaches to deal with similar problems of functions affected by discontinuities can be found for example in [19, 13, 14, 8, 34]. And these nonlinear methods also give rise to interesting applications. To mention some of them one can refer to [16, 31, 25, 40, 26, 27].

In this chapter we pay attention to one of these operators that was defined in [6] under the name PPH (Piecewise Polynomial Harmonic). This operator can be seen as a nonlinear counterpart of the classical four points piecewise Lagrange interpolation. The theoretical analysis as much as the practical applications were developed in uniform grids in previous articles (see, for example, [6, 10, 50, 7, 11, 32, 37]). In turn these reconstruction operators are the heart of the definition of associated subdivision and multiresolution schemes [29, 5, 34, 35].



In this chapter, we extend the definition of the PPH reconstruction operator to data over nonuniform grids and we study some properties of this operator. In particular, we analyze the behavior of the operator in presence of jump discontinuities. We prove adaptation to the jump discontinuity in the sense that some order of approximation is maintained in the area close to the discontinuity, on the contrary to what happens with linear operators that lose completely the approximation order. We also prove, as much theoretically as in numerical experiments, the absence of any Gibbs phenomena.

The chapter is organized as follows: In Section 4.2 we remind the nonlinear PPH reconstruction operator [42] on nonuniform grids. Section 4.3 is dedicated to study the adaptation of the operator to the presence of jump discontinuities, making some emphasis in the order of approximation. In Section 4.4 we analyze the behavior of the operator with respect to the Gibbs phenomena. In Section 4.5 we present some numerical tests. Finally, some conclusions are given in Section 4.6.

## 4.2 A nonlinear PPH reconstruction operator on nonuniform grids

In this section we recall the definition of the nonlinear PPH reconstruction operator on nonuniform grids, see [42]. We include the necessary elements for the rest of the chapter. In [42] the reconstruction operator is designed to deal with strictly convex functions, albeit it is also of interest in the case of working with piecewise smooth functions affected by isolated jump discontinuities. This will be our case of interest in this section and in the rest of the chapter.

Let us define a nonuniform grid  $X = (x_i)_{i \in \mathbb{Z}}$  in  $\mathbb{R}$ . Let us also denote  $h_i := x_i - x_{i-1}$ , the nonuniform spacing between abscissae. We consider underlying piecewise continuous functions  $f(x)$  with at most a finite set of isolated corner or jump discontinuities, and let us call  $f_i := f(x_i)$  the ordinates corresponding to the point values of the function at the given abscissae. We also introduce the following notations. In first place, the second order divided differences

$$\begin{aligned} D_j &:= f[x_{j-1}, x_j, x_{j+1}] = \frac{f_{j-1}}{h_j(h_j + h_{j+1})} - \frac{f_j}{h_j h_{j+1}} + \frac{f_{j+1}}{h_{j+1}(h_j + h_{j+1})}, \\ D_{j+1} &:= f[x_j, x_{j+1}, x_{j+2}] = \frac{f_j}{h_{j+1}(h_{j+1} + h_{j+2})} - \frac{f_{j+1}}{h_{j+1} h_{j+2}} + \frac{f_{j+2}}{h_{j+2}(h_{j+1} + h_{j+2})}, \end{aligned} \quad (4.1)$$

in second place a weighted arithmetic mean of  $D_j$  and  $D_{j+1}$  defined as

$$M_j = w_{j,0} D_j + w_{j,1} D_{j+1}, \quad (4.2)$$

with the weights

$$\begin{aligned} w_{j,0} &= \frac{h_{j+1} + 2h_{j+2}}{2(h_j + h_{j+1} + h_{j+2})}, \\ w_{j,1} &= \frac{h_{j+1} + 2h_j}{2(h_j + h_{j+1} + h_{j+2})} = 1 - w_{j,0}. \end{aligned} \quad (4.3)$$

Given these ingredients in [42] we can find the following definitions, and results that we will use later.

**Lemma 13.** *Let us consider the set of ordinates  $\{f_{j-1}, f_j, f_{j+1}, f_{j+2}\}$  for some  $j \in \mathbb{Z}$  at the abscissae  $\{x_{j-1}, x_j, x_{j+1}, x_{j+2}\}$  of a nonuniform grid  $X = (x_i)_{i \in \mathbb{Z}}$ . Then, the values  $f_{j-1}$  and*

$f_{j+2}$  at the extremes can be expressed as

$$f_{j-1} = \frac{-1}{\gamma_{j,-1}}(\gamma_{j,0}f_j + \gamma_{j,1}f_{j+1} + \gamma_{j,2}f_{j+2}) + \frac{M_j}{\gamma_{j,-1}}, \quad (4.4a)$$

$$f_{j+2} = \frac{-1}{\gamma_{j,2}}(\gamma_{j,-1}f_{j-1} + \gamma_{j,0}f_j + \gamma_{j,1}f_{j+1}) + \frac{M_j}{\gamma_{j,2}}, \quad (4.4b)$$

with the constants  $\gamma_{j,i}$ ,  $i = -1, 0, 1, 2$  given by

$$\begin{aligned} \gamma_{j,-1} &= \frac{h_{j+1} + 2h_{j+2}}{2h_j(h_{j+1} + h_j)(h_j + h_{j+1} + h_{j+2})}, \\ \gamma_{j,0} &= \frac{1}{2h_{j+1}(h_j + h_{j+1} + h_{j+2})} \left( \frac{h_{j+1} + 2h_j}{h_{j+1} + h_{j+2}} - \frac{h_{j+1} + 2h_{j+2}}{h_j} \right), \\ \gamma_{j,1} &= \frac{1}{2h_{j+1}(h_j + h_{j+1} + h_{j+2})} \left( \frac{h_{j+1} + 2h_{j+2}}{h_{j+1} + h_j} - \frac{h_{j+1} + 2h_j}{h_{j+2}} \right), \\ \gamma_{j,2} &= \frac{h_{j+1} + 2h_j}{2h_{j+2}(h_{j+1} + h_{j+2})(h_j + h_{j+1} + h_{j+2})}. \end{aligned} \quad (4.5)$$

**Definition 12.** Given  $x, y \in \mathbb{R}$ , and  $w_x, w_y \in \mathbb{R}$  such that  $w_x > 0$ ,  $w_y > 0$ , and  $w_x + w_y = 1$ , we denote as  $\tilde{V}$  the function

$$\tilde{V}(x, y) = \begin{cases} \frac{xy}{w_x y + w_y x} & \text{if } xy > 0, \\ 0 & \text{otherwise.} \end{cases} \quad (4.6)$$

**Lemma 14.** If  $x \geq 0$  and  $y \geq 0$ , the harmonic mean is bounded as follows

$$\tilde{V}(x, y) < \min \left\{ \frac{1}{w_x}x, \frac{1}{w_y}y \right\} \leq \frac{1}{w_x}x. \quad (4.7)$$

Next definition, which is commonly used in numerical analysis, is going to be essential through the rest of the chapter.

**Definition 13.** An expression  $e(h) = O(h^r)$ ,  $r \in \mathbb{Z}$  means that there exist  $h_0 > 0$  and  $M > 0$  such that  $\forall 0 < h \leq h_0$

$$\frac{|e(h)|}{h^r} \leq M.$$

**Lemma 15.** Let  $a > 0$  a fixed positive real number, and let  $x \geq a$  and  $y \geq a$ . If  $|x - y| = O(h)$ , and  $xy > 0$ , then, the weighted harmonic mean is also close to the weighted arithmetic mean  $M(x, y) = w_x x + w_y y$ ,

$$|M(x, y) - \tilde{V}(x, y)| = \frac{w_x w_y}{w_x y + w_y x} (x - y)^2 = O(h^2). \quad (4.8)$$

**Definition 14** (PPH reconstruction). Let  $X = (x_i)_{i \in \mathbb{Z}}$  be a nonuniform mesh. Let  $f = (f_i)_{i \in \mathbb{Z}}$  a sequence in  $l_\infty(\mathbb{Z})$ . Let  $D_j$  and  $D_{j+1}$  be the second order divided differences, and for each  $j \in \mathbb{Z}$  let us consider the modified values  $\{\tilde{f}_{j-1}, \tilde{f}_j, \tilde{f}_{j+1}, \tilde{f}_{j+2}\}$  built according to the following rule

- **Case 1:** If  $|D_j| \leq |D_{j+1}|$

$$\begin{cases} \tilde{f}_i = f_i, & j-1 \leq i \leq j+1, \\ \tilde{f}_{j+2} = \frac{-1}{\gamma_{j,2}}(\gamma_{j,-1}f_{j-1} + \gamma_{j,0}f_j + \gamma_{j,1}f_{j+1}) + \frac{\tilde{V}_j}{\gamma_{j,2}}, \end{cases} \quad (4.9)$$

- **Case 2:** If  $|D_j| > |D_{j+1}|$

$$\begin{cases} \tilde{f}_{j-1} = \frac{-1}{\gamma_{j,-1}}(\gamma_{j,0}f_j + \gamma_{j,1}f_{j+1} + \gamma_{j,2}f_{j+2}) + \frac{\tilde{V}_j}{\gamma_{j,-1}}, \\ \tilde{f}_i = f_i, & j \leq i \leq j+2, \end{cases} \quad (4.10)$$

where  $\gamma_{j,i}$ ,  $i = -1, 0, 1, 2$  are given in (4.5) and  $\tilde{V}_j = \tilde{V}(D_j, D_{j+1})$ , with  $\tilde{V}$  the weighted harmonic mean defined in (4.6) with the weights  $w_{j,0}$  and  $w_{j,1}$  in (4.3). We define the PPH nonlinear reconstruction operator as

$$PPH(x) = PPH_j(x), \quad x \in [x_j, x_{j+1}], \quad (4.11)$$

where  $PPH_j(x)$  is the unique interpolation polynomial which satisfies

$$PPH_j(x_i) = \tilde{f}_i, \quad j-1 \leq i \leq j+2. \quad (4.12)$$

According to Definition 14, it is possible to establish a parallelism with Lagrange interpolation, in fact we can write the PPH reconstruction as

$$PPH_j(x) = \tilde{a}_{j,0} + \tilde{a}_{j,1} \left(x - x_{j+\frac{1}{2}}\right) + \tilde{a}_{j,2} \left(x - x_{j+\frac{1}{2}}\right)^2 + \tilde{a}_{j,3} \left(x - x_{j+\frac{1}{2}}\right)^3, \quad (4.13)$$

where the coefficients  $\tilde{a}_{j,i}$ ,  $i = 0, 1, 2, 3$  are calculated by imposing conditions (4.12). We explain each one of the two possible local cases, Case 1 or Case 2. The coefficients will have symmetrical expressions.

**Case 1.**  $|D_j| \leq |D_{j+1}|$ , which means that a potential singularity may lay in  $[x_{j+1}, x_{j+2}]$ . It has been proposed to replace  $f_{j+2}$  with  $\tilde{f}_{j+2}$  in Equation (4.9) by changing the weighted arithmetic mean in Equation (4.4b) for its corresponding weighted harmonic mean. This replacement has been performed to carry out a witty modification of the value  $\tilde{f}_{j+2}$  in such a way that its difference with respect to the original  $f_{j+2}$  is large in presence of a discontinuity, but remains sufficiently small in smooth areas maintaining the approximation order. Lemma 14 is crucial for the adaptation in case of dealing with the presence of a jump discontinuity, while Lemma 15 plays a fundamental part in proving fourth approximation order for smooth areas of an underlying function.

In this case the coefficients  $\tilde{a}_{j,i}$ ,  $i = 0, 1, 2, 3$  of the PPH polynomial read

$$\begin{aligned} \tilde{a}_{j,0} &= \frac{f_j + f_{j+1}}{2} - \frac{h_{j+1}^2}{4} \tilde{V}_j, \\ \tilde{a}_{j,1} &= \frac{-f_j + f_{j+1}}{h_{j+1}} + \frac{h_{j+1}^2}{4h_j + 2h_{j+1}} (D_j - \tilde{V}_j), \\ \tilde{a}_{j,2} &= \tilde{V}_j, \\ \tilde{a}_{j,3} &= -\frac{2}{2h_j + h_{j+1}} (D_j - \tilde{V}_j). \end{aligned} \quad (4.14)$$

For our purposes, in the next sections we need to examine deeper the relation with Lagrange interpolation. In particular we get that

$$|\tilde{f}_{j+2} - f_{j+2}| = \frac{2h_{j+2}(h_{j+1} + h_{j+2})(h_j + h_{j+1} + h_{j+2})}{2h_j + h_{j+1}} |M_j - \tilde{V}_j|, \quad (4.15)$$

and considering the Lagrange interpolation polynomial written in the same form as in (4.13), that is

$$PL_j(x) = a_{j,0} + a_{j,1} \left(x - x_{j+\frac{1}{2}}\right) + a_{j,2} \left(x - x_{j+\frac{1}{2}}\right)^2 + a_{j,3} \left(x - x_{j+\frac{1}{2}}\right)^3, \quad (4.16)$$

we get that the difference of these coefficients with the ones of  $PPH_j(x)$  is given by

$$\begin{aligned} \tilde{a}_{j,0} - a_{j,0} &= \frac{h_{j+1}^2}{4} (M_j - \tilde{V}_j), \\ \tilde{a}_{j,1} - a_{j,1} &= \frac{h_{j+1}^2}{4h_j + 2h_{j+1}} (M_j - \tilde{V}_j), \\ \tilde{a}_{j,2} - a_{j,2} &= -(M_j - \tilde{V}_j), \\ \tilde{a}_{j,3} - a_{j,3} &= -\frac{2}{2h_j + h_{j+1}} (M_j - \tilde{V}_j). \end{aligned} \quad (4.17)$$

**Case 2.**  $|D_j| > |D_{j+1}|$ , which means that a possible singularity lies in  $[x_{j-1}, x_j]$ . In this case, in Definition 14, the value  $f_{j-1}$  is replaced with  $\tilde{f}_{j-1}$  by using expression (4.10). Similar comments apply in this case due to symmetry considerations. The coefficients for the polynomial (4.13) now read

$$\begin{aligned} \tilde{a}_{j,0} &= \frac{f_j + f_{j+1}}{2} - \frac{h_{j+1}^2}{4} \tilde{V}_j, \\ \tilde{a}_{j,1} &= \frac{-f_j + f_{j+1}}{h_{j+1}} + \frac{h_{j+1}^2}{2h_{j+1} + 4h_{j+2}} (-D_{j+1} + \tilde{V}_j), \\ \tilde{a}_{j,2} &= \tilde{V}_j, \\ \tilde{a}_{j,3} &= -\frac{2}{h_{j+1} + 2h_{j+2}} (-D_{j+1} + \tilde{V}_j). \end{aligned} \quad (4.18)$$

The expressions relating the coefficients of the PPH polynomial with the Lagrange interpolation polynomial now write

$$|\tilde{f}_{j-1} - f_{j-1}| = \frac{2h_j(h_{j+1} + h_j)(h_j + h_{j+1} + h_{j+2})}{2h_{j+2} + h_{j+1}} |M_j - \tilde{V}_j|. \quad (4.19)$$

$$\begin{aligned}
\tilde{a}_{j,0} - a_{j,0} &= \frac{h_{j+1}^2}{4} (M_j - \tilde{V}_j), \\
\tilde{a}_{j,1} - a_{j,1} &= -\frac{h_{j+1}^2}{2h_{j+1} + 4h_{j+2}} (M_j - \tilde{V}_j), \\
\tilde{a}_{j,2} - a_{j,2} &= -(M_j - \tilde{V}_j), \\
\tilde{a}_{j,3} - a_{j,3} &= \frac{2}{2h_{j+2} + h_{j+1}} (M_j - \tilde{V}_j).
\end{aligned} \tag{4.20}$$

In next section, we will study the approximation order of the PPH reconstruction operator in presence of isolated jump discontinuities.

### 4.3 Approximation order around jump discontinuities

We are going to study the approximation order of the given reconstruction for functions of class  $C^4(\mathbb{R})$  with an isolated jump discontinuity at a given point  $\mu$ . We consider only the case of working with  $\sigma$  quasi-uniform grids, according with the following definition.

**Definition 15.** A nonuniform mesh  $X = (x_i)_{i \in \mathbb{Z}}$  is said to be a  $\sigma$  quasi-uniform mesh if there exist  $h_{\min} = \min_{i \in \mathbb{Z}} h_i$ ,  $h_{\max} = \max_{i \in \mathbb{Z}} h_i$ , and a finite constant  $\sigma$  such that  $\frac{h_{\max}}{h_{\min}} \leq \sigma$ .

In what follows we give a proposition proving full order accuracy for convex regions of the function, that is fourth order accuracy, and observing that the approximation order is reduced to second order close to the singularities and to third order close to inflection points. We would like to focuss especial attention to the intervals around the discontinuity where the order is reduced, but not completely lost.

**Theorem 4.** Let  $f(x)$  be a function of class  $C^4(\mathbb{R} \setminus \{\mu\})$ , with a jump discontinuity at the point  $\mu$ . Let  $X = (x_i)_{i \in \mathbb{Z}}$  be a  $\sigma$  quasi-uniform mesh in  $\mathbb{R}$ , with  $h_i = x_i - x_{i-1}$ ,  $\forall i \in \mathbb{Z}$ , and  $f = (f_i)_{i \in \mathbb{Z}}$ , the sequence of point values of the function  $f(x)$ ,  $f_i = f(x_i)$ . Let us consider  $j \in \mathbb{Z}$  such that  $\mu \in [x_j, x_{j+1}]$ ,  $a > 0$ , a fixed positive real number,  $\Omega$  the set of all inflexion points of  $f(x)$ , and  $d(x, \Omega)$  the distance function defined by

$$d(x, \Omega) := \begin{cases} \min\{|x - \omega| : \omega \in \Omega\} & \Omega \neq \emptyset, \\ +\infty & \Omega = \emptyset. \end{cases}$$

Then, the reconstruction  $PPH(x)$  satisfies

1. In  $x \in [x_i, x_{i+1}]$ ,  $i \neq j-1, j, j+1$ , if  $D_i D_{i+1} > 0$ , and  $d(x_{i-1}, \Omega) \geq a$ ,  $d(x_{i+2}, \Omega) \geq a$ , then

$$\max_{x \in [x_i, x_{i+1}]} |f(x) - PPH(x)| = O(h^4),$$

2. In  $x \in [x_i, x_{i+1}]$ ,  $i \neq j-1, j, j+1$ , if  $D_i D_{i+1} > 0$ , and  $d(x_{i-1}, \Omega) < a$ , or  $d(x_{i+2}, \Omega) < a$ , then

$$\max_{x \in [x_i, x_{i+1}]} |f(x) - PPH(x)| = O(h^{4-p}), \text{ with } 0 \leq p < 1.$$

3. In  $x \in [x_i, x_{i+1}]$ ,  $i \neq j-1, j, j+1$ , if  $D_i D_{i+1} \leq 0$ ,

$$\max_{x \in [x_i, x_{i+1}]} |f(x) - PPH(x)| = O(h^3),$$

4. In  $x \in [x_{j-1}, x_j] \cup [x_{j+1}, x_{j+2}]$ ,

$$\max_{x \in [x_{j-1}, x_j] \cup [x_{j+1}, x_{j+2}]} |f(x) - PPH(x)| = O(h^2),$$

where  $h = \max_{i \in \mathbb{Z}} \{h_i\}$ .

*Proof.* We do the proof point by point.

1. Given  $x \in [x_i, x_{i+1}]$ , the reconstruction operator is built as  $PPH(x) = PPH_i(x)$ .

From Equations (4.2) and (4.6) we can write

$$M_i - \tilde{V}_i = \begin{cases} \frac{w_{i,0} w_{i,1} (D_{i+1} - D_i)^2}{w_{i,0} D_{i+1} + w_{i,1} D_i} & \text{if } D_i D_{i+1} > 0, \\ M_i & \text{otherwise.} \end{cases} \quad (4.21)$$

From hypothesis we have that the initial data are strictly convex in the considered area  $[x_{i-1}, x_{i+2}]$  (for a concave function the arguments remain the same) and therefore they satisfy  $f''(x) \geq b > 0$ ,  $\forall x \in [x_{i-1}, x_{i+2}]$ , for some  $b > 0$ . Since second order divided differences amount to second derivatives at an intermediate point divided by two, i.e

$$D_i = \frac{f''(\mu_1)}{2!}, \quad D_{i+1} = \frac{f''(\mu_2)}{2!},$$

with  $\mu_1 \in (x_{i-1}, x_{i+1})$  and  $\mu_2 \in (x_i, x_{i+2})$ . Therefore, we have

$$D_i = O(1), \quad D_{i+1} = O(1) \text{ and } D_{i+1} - D_i = O(h),$$

and from (4.21) we get that

$$|M_i - \tilde{V}_i| = O(h^2). \quad (4.22)$$

Plugging this information into (4.17) if  $|D_i| \leq |D_{i+1}|$ , or into (4.20) if  $|D_i| > |D_{i+1}|$ , we get that

$$|\tilde{a}_{i,s} - a_{i,s}| = O(h^{4-s}), \quad s = 0, 1, 2, 3. \quad (4.23)$$

Thus

$$|PPH_i(x) - PL_i(x)| \leq \sum_{s=0}^3 |\tilde{a}_{i,s} - a_{i,s}| \left| \left( x - x_{i+\frac{1}{2}} \right)^s \right| = O(h^4),$$

where  $PL_i(x)$  is the Lagrange interpolatory polynomial. Taking into account again the triangular inequality

$$|f(x) - PPH_i(x)| \leq |f(x) - PL_i(x)| + |PL_i(x) - PPH_i(x)| = O(h^4),$$

using that Lagrange interpolation also attains fourth order accuracy.

**2.** We now prove Point 2. Since  $d(x_{i-1}, \Omega) < a$ , or  $d(x_{i+2}, \Omega) < a$ , and depending on the exact distance to the inflection point we encounter  $D_i = O(h^p)$ ,  $D_{i+1} = O(h^p)$ , with  $0 \leq p < 1$ . Then, from Equation (4.21), we directly get  $|M_i - \tilde{V}_i| = O(h^{2-p})$ , and the rest of the proof follows exactly the same track as in Point 1, giving the enunciated result.

**3.** For proving Point 3, we observe that in this case  $|M_i - \tilde{V}_i| = |M_i| = O(h)$ , and again following the same track as in previous points we get

$$\begin{aligned} |\tilde{a}_{i,s} - a_{i,s}| &= O(h^{3-s}), \quad s = 0, 1, 2, 3, \\ |PPH_i(x) - PL_i(x)| &\leq \sum_{s=0}^3 |\tilde{a}_{i,s} - a_{i,s}| \left| \left( x - x_{i+\frac{1}{2}} \right)^s \right| = O(h^3), \\ |f(x) - PPH_i(x)| &\leq |f(x) - PL_i(x)| + |PL_i(x) - PPH_i(x)| = O(h^3), \end{aligned}$$

and therefore in this case the accuracy is reduced to third order.

**4.** In order to prove Point 4, let us suppose without loss of generalization that  $x \in [x_{j-1}, x_j]$ . The other case it is proven analogously. Since by hypothesis the function  $f(x)$  is smooth in  $[x_{j-2}, x_j]$ , and it presents a jump discontinuity at the interval  $[x_j, x_{j+1}]$  we have  $D_{j-1} = O(1)$  and  $D_j = O(1/h^2)$ . Therefore  $|D_{j-1}| \leq |D_j|$ .

Let  $PL2_{j-1}(x)$  be the second degree Lagrange interpolatory polynomial built using the three pairs of values  $(x_{j-2}, f_{j-2})$ ,  $(x_{j-1}, f_{j-1})$ ,  $(x_j, f_j)$ .

$$PL2_{j-1}(x) = \hat{a}_{j-1,0} + \hat{a}_{j-1,1} \left( x - x_{j-\frac{1}{2}} \right) + \hat{a}_{j-1,2} \left( x - x_{j-\frac{1}{2}} \right)^2,$$

where

$$\begin{aligned} \hat{a}_{j-1,0} &= \frac{f_{j-1} + f_j}{2} - \frac{h_j^2}{4} D_{j-1}, \\ \hat{a}_{j-1,1} &= \frac{-f_{j-1} + f_j}{h_j}, \\ \hat{a}_{j-1,2} &= D_{j-1}. \end{aligned} \tag{4.24}$$

The difference between these coefficients and the ones of  $PPH_{j-1}(x)$  shown in Equation (4.14) is given by

$$\begin{aligned} \tilde{a}_{j-1,0} - \hat{a}_{j-1,0} &= \frac{h_j^2}{4} (D_{j-1} - \tilde{V}_{j-1}), \\ \tilde{a}_{j-1,1} - \hat{a}_{j-1,1} &= \frac{h_j^2}{4h_{j-1} + 2h_j} (D_{j-1} - \tilde{V}_{j-1}), \\ \tilde{a}_{j-1,2} - \hat{a}_{j-1,2} &= -(D_{j-1} - \tilde{V}_{j-1}), \\ \tilde{a}_{j-1,3} &= -\frac{2}{2h_{j-1} + h_j} (D_{j-1} - \tilde{V}_{j-1}). \end{aligned} \tag{4.25}$$

At this stage we distinguish two cases:

**4.1.**  $D_{j-1}D_j > 0$ .

Taking into account Equations (4.6), (4.7) and (4.25) and the triangular inequality we obtain

$$\begin{aligned}
|\tilde{V}(D_{j-1}, D_j)| &\leq \frac{1}{w_{j-1,0}} |D_{j-1}|, \\
|D_{j-1} - \tilde{V}_{j-1}| &\leq |D_{j-1}| + \frac{1}{w_{j-1,0}} |D_{j-1}| = \frac{1 + w_{j-1,0}}{w_{j-1,0}} |D_{j-1}| = O(1), \\
|\tilde{a}_{j-1,s} - \hat{a}_{j-1,s}| &= O(h^{2-s}), \quad s = 0, 1, 2, 3, \\
|PPH_{j-1}(x) - PL2_{j-1}(x)| &\leq \sum_{s=0}^3 |\tilde{a}_{j-1,s} - \hat{a}_{j-1,s}| \left| \left( x - x_{j-\frac{1}{2}} \right)^s \right| = O(h^2), \\
|f(x) - PPH_{j-1}(x)| &\leq |f(x) - PL2_{j-1}(x)| + |PL2_{j-1}(x) - PPH_{j-1}(x)| = O(h^2).
\end{aligned}$$

#### 4.2. $D_{j-1}D_j \leq 0$ .

Equations (4.6) and (4.25) and the triangular inequality lead us to

$$\begin{aligned}
\tilde{V}_{j-1} &= 0, \\
|D_{j-1} - \tilde{V}_{j-1}| &= O(1), \\
|\tilde{a}_{j-1,s} - \hat{a}_{j-1,s}| &= O(h^{2-s}), \quad s = 0, 1, 2, 3, \\
|PPH_{j-1}(x) - PL2_{j-1}(x)| &\leq \sum_{s=0}^3 |\tilde{a}_{j-1,s} - \hat{a}_{j-1,s}| \left| \left( x - x_{j-\frac{1}{2}} \right)^s \right| = O(h^2), \\
|f(x) - PPH_{j-1}(x)| &\leq |f(x) - PL2_{j-1}(x)| + |PL2_{j-1}(x) - PPH_{j-1}(x)| = O(h^2).
\end{aligned}$$

And these last chains of equations finish the proof. □

We observe that close to the jump discontinuity, that is, in the intervals  $[x_{j-1}, x_j]$  and  $[x_{j+1}, x_{j+2}]$ , we do not lose all accuracy, but we maintain at least second order accuracy. Unfortunately, in the central interval  $[x_j, x_{j+1}]$  containing the singularity this approach does not allow us to obtain any gain with respect to other reconstruction operators.

**Remark 8.** *Notice that linear reconstruction operators based on an stencil of four points typically lose the approximation order in three intervals around discontinuities, while the introduced nonlinear reconstruction operator only loses completely the approximation order in the interval containing the jump discontinuity and maintains at least second order accuracy, that is,  $O(h^2)$ , in the adjacent intervals. In the interval containing the jump discontinuity the approximation order is lost also in the nonlinear reconstruction strategy, since with point values of the function it is impossible to detect the exact position of the jump discontinuity.*

**Remark 9.** *The order reduction due to inflection points can be tackled using a translation strategy in the definition of the Harmonic mean, to avoid arguments of different signs. This strategy complicates the definition of the operator, but it has been satisfactorily introduced on various occasions [6], [20]. In practice the translation is needed not only at the interval containing the inflection point, but also in adjacent intervals.*



## 4.4 Analysis of Gibbs phenomena around jump discontinuities

In this section we are going to give a result analyzing the behavior of the proposed nonlinear reconstruction with respect to the generation of possible Gibbs effects due to the presence of jump discontinuities in the underlying function. In particular we prove the following proposition.

Before enunciating the theorem we introduce some definitions.

**Definition 16.** Given  $X^0 = \{x_i\}_{i \in \mathbb{Z}}$  a  $\sigma$  quasi-uniform grid in  $\mathbb{R}$ , we define, for  $k \in \mathbb{N}$  (the larger the  $k$  the larger the resolution), the set of nested grids given by  $X^k = \{x_i^k\}_{i \in \mathbb{Z}}$ , where  $x_{2i}^k = x_i^{k-1}$  and  $x_{2i+1}^k = \frac{x_i^{k-1} + x_{i+1}^{k-1}}{2}$ .

Let us also denote  $[f]$  the size of a jump discontinuity,  $r_j^k(x)$  the straight line joining the points  $(x_j^k, f_j^k)$  and  $(x_{j+1}^k, f_{j+1}^k)$ ,  $d_i^k(x)$ ,  $i = j - 1, j, j + 1$  the vertical distance from the reconstruction  $PPH_j^k(x)$  to the horizontal line passing through the middle point of  $(x_j^k, f_j^k)$  and  $(x_{j+1}^k, f_{j+1}^k)$ . The respective expressions come given by

$$[f] = f_{j+1}^k - f_j^k,$$

$$r_j^k(x) = \frac{f_j^k + f_{j+1}^k}{2} + \frac{f_{j+1}^k - f_j^k}{h_{j+1}^k} (x - x_{j+\frac{1}{2}}^k),$$

$$d_i^k(x) = PPH_i^k(x) - \frac{f_i^k + f_{i+1}^k}{2}.$$

We will also use  $r_{max}^k$  as the maximum distance between  $PPH_j^k(x)$  and  $r_j^k(x)$  measured perpendicularly to  $r_j^k(x)$ .

**Theorem 5.** Let  $X^k = \{x_i^k\}_{i \in \mathbb{Z}}$ ,  $k \in \mathbb{N} \cup \{0\}$  be a set of nested  $\sigma$  quasi-uniform grids in  $\mathbb{R}$  with  $\sigma < \frac{3+\sqrt{17}}{2}$ . Let  $f \in C^4(\mathbb{R})$  be a function with four continuous derivatives in all the real line with an isolated jump discontinuity at the abscissa  $\mu$  located at a certain  $[x_j^k, x_{j+1}^k]$  for each  $k$ , where  $j$  depends on  $k$ . Then,  $\exists k_0 : \forall k \geq k_0$  the reconstruction  $PPH^k(x)$  associated to the data  $f^k := (f(x_i^k))_{i \in \mathbb{Z}}$  does not generate Gibbs phenomena. In particular, the following statements hold:

1.  $\|PPH^k(x) - f(x)\|_{L^\infty} = O((h^k)^4)$  in  $(-\infty, x_{j-1}^k] \cup [x_{j+2}^k, \infty)$ ,
2.  $|d_{j-1}^k(x)| = O(h^k)$ ,
3.  $|d_{j+1}^k(x)| = O(h^k)$ ,
4.  $PPH_j^k(x)$  lies inside the rectangle  $[x_j^k, x_{j+1}^k] \times [f_j^k, f_{j+1}^k]$ ,
5.  $r_{max}^k = O(h^k)$ ,

where  $h^k := \max_{i \in \mathbb{Z}} \{h_i^k\}$ .

*Proof.* Let us consider  $k$  large enough,  $k \geq k_0$ , such that

$$\left| \frac{[f]}{h_{j+1}^k} \right| > \left| \frac{f_j^k - f_{j-1}^k}{h_j^k} \right|, \quad (4.26)$$

$$\left| \frac{[f]}{h_{j+1}^k} \right| > \left| \frac{f_{j+2}^k - f_{j+1}^k}{h_{j+2}^k} \right|. \quad (4.27)$$

Then

$$D_{j-1}^k = O(1),$$

$$D_j^k = \frac{\frac{f_{j+1}^k - f_j^k}{h_{j+1}^k} - \frac{f_j^k - f_{j-1}^k}{h_j^k}}{h_j^k + h_{j+1}^k} = O\left(\frac{[f]}{(h^k)^2}\right), \quad (4.28)$$

$$D_{j+1}^k = \frac{\frac{f_{j+2}^k - f_{j+1}^k}{h_{j+2}^k} - \frac{f_{j+1}^k - f_j^k}{h_{j+1}^k}}{h_{j+1}^k + h_{j+2}^k} = -O\left(\frac{[f]}{(h^k)^2}\right), \quad (4.29)$$

$$D_{j+2}^k = O(1).$$

and from (4.28), (4.29) and (4.6) we get

$$\begin{aligned} \operatorname{sgn}(D_j^k) &= \operatorname{sgn}([f]) \neq \operatorname{sgn}(D_{j+1}^k), \\ \tilde{V}_j^k &= 0. \end{aligned} \quad (4.30)$$

We carry out the rest of the proof addressing point after point.

**1.** Since only three intervals are affected by the jump discontinuity for construction, then,  $\forall k$

$$\|PPH^k(x) - f(x)\|_{L^\infty} = O((h^k)^4) \quad \text{in} \quad (-\infty, x_{j-1}^k] \cup [x_{j+2}^k, \infty).$$

**2.** We are going to show now that the oscillations due to the presence of the discontinuity diminish at the interval  $[x_{j-1}^k, x_j^k]$  with  $k$  increasing.

In  $[x_{j-1}^k, x_j^k]$  the PPH reconstruction amounts to

$$PPH_{j-1}^k(x) = \tilde{a}_{j-1,0}^k + \tilde{a}_{j-1,1}^k \left(x - x_{j-\frac{1}{2}}^k\right) + \tilde{a}_{j-1,2}^k \left(x - x_{j-\frac{1}{2}}^k\right)^2 + \tilde{a}_{j-1,3}^k \left(x - x_{j-\frac{1}{2}}^k\right)^3. \quad (4.31)$$

As  $|D_{j-1}^k| \leq |D_j^k|$ , the coefficients are given by (4.14) adapted to the interval  $j-1$

$$\begin{aligned} \tilde{a}_{j-1,0}^k &= \frac{f_{j-1}^k + f_j^k}{2} - \frac{(h_j^k)^2}{4} \tilde{V}_{j-1}^k, \\ \tilde{a}_{j-1,1}^k &= \frac{-f_{j-1}^k + f_j^k}{h_j^k} + \frac{(h_j^k)^2}{4h_{j-1}^k + 2h_j^k} (D_{j-1}^k - \tilde{V}_{j-1}^k), \\ \tilde{a}_{j-1,2}^k &= \tilde{V}_{j-1}^k, \\ \tilde{a}_{j-1,3}^k &= -\frac{2}{2h_{j-1}^k + h_j^k} (D_{j-1}^k - \tilde{V}_{j-1}^k). \end{aligned} \quad (4.32)$$

Taking into account property (4.7) of the harmonic mean, we can write

$$\begin{aligned} |\tilde{V}_{j-1}^k| &= |\tilde{V}_{j-1}^k(D_{j-1}^k, D_j^k)| \leq \min \left\{ \frac{1}{w_{j-1,0}^k} |D_{j-1}^k|, \frac{1}{w_{j-1,1}^k} |D_j^k| \right\} \\ &\leq \frac{1}{w_{j-1,0}^k} |D_{j-1}^k| \leq 2\sigma |D_{j-1}^k|. \end{aligned}$$

Considering (4.31), the distance  $d_{j-1}^k(x)$  can be bounded by

$$\begin{aligned} \left| d_{j-1}^k(x) \right| &= \left| PPH_{j-1}^k(x) - \frac{f_{j-1}^k + f_j^k}{2} \right| = \left| -\frac{(h_j^k)^2}{4} \tilde{V}_{j-1}^k + \tilde{a}_{j-1,1}^k \left( x - x_{j-\frac{1}{2}}^k \right) \right. \\ &\quad \left. + \tilde{a}_{j-1,2}^k \left( x - x_{j-\frac{1}{2}}^k \right)^2 + \tilde{a}_{j-1,3}^k \left( x - x_{j-\frac{1}{2}}^k \right)^3 \right| = O(h^k), \end{aligned}$$

where  $h^k := \max_{i \in \mathbb{Z}} \{h_i^k\}$ .

**3.** In  $[x_{j+1}^k, x_{j+2}^k]$ , applying arguments based on symmetry and taking into account that  $|D_{j+1}^k| \geq |D_{j+2}^k|$  we also get that  $|d_{j+1}^k(x)| = O(h^k)$ .

**4.** In  $[x_j^k, x_{j+1}^k]$ , as  $\tilde{V}_j^k = 0$  due to (4.30), the expression of  $PPH_j^k(x)$  according to (4.13), (4.14), (4.18) will be

$$PPH_j^k(x) = \frac{f_j^k + f_{j+1}^k}{2} + \tilde{a}_{j,1}^k \left( x - x_{j+\frac{1}{2}}^k \right) + \tilde{a}_{j,3}^k \left( x - x_{j+\frac{1}{2}}^k \right)^3. \quad (4.33)$$

At this point we consider two subcases depending on  $|D_j^k|$  and  $|D_{j+1}^k|$

#### 4.1 $|D_j^k| \leq |D_{j+1}^k|$

We can write

$$d_j^k(x) = \tilde{a}_{j,1}^k \left( x - x_{j+\frac{1}{2}}^k \right) + \tilde{a}_{j,3}^k \left( x - x_{j+\frac{1}{2}}^k \right)^3 = \left( x - x_{j+\frac{1}{2}}^k \right) E_j^k(x), \quad (4.34)$$

where

$$E_j^k(x) = \frac{f_{j+1}^k - f_j^k}{h_{j+1}^k} + \frac{D_j^k}{4h_j^k + 2h_{j+1}^k} \left( (h_{j+1}^k)^2 - 4(x - x_{j+\frac{1}{2}}^k)^2 \right).$$

The maximum value of the function  $d_j^k(x)$  in the interval  $[x_j^k, x_{j+1}^k]$  is either at the extremes of the interval or among any possible critical point  $x_c$  verifying  $(d_j^k)'(x_c) = 0$ . At the extremes of the interval we have  $|d_j^k(x_j^k)| = |d_j^k(x_{j+1}^k)| = \frac{1}{2} |f_{j+1}^k - f_j^k|$ , and the condition is satisfied. We are going to prove that the local reconstruction  $PPH_j^k(x)$  lies inside the rectangle  $[x_j^k, x_{j+1}^k] \times [f_j^k, f_{j+1}^k]$  since any critical point  $x_c$  of the function  $d_j^k(x)$  falls outside the interval  $[x_j^k, x_{j+1}^k]$ . For this purpose, we shall prove that  $(PPH_j^k)'(x) \neq 0 \quad \forall x \in [x_j^k, x_{j+1}^k]$ .

We start computing  $(PPH_j^k)'(x)$  and  $(PPH_j^k)''(x)$ ,

$$(PPH_j^k)'(x) = \frac{f_{j+1}^k - f_j^k}{h_{j+1}^k} + \frac{D_j^k}{4h_j^k + 2h_{j+1}^k} \left( (h_{j+1}^k)^2 - 12(x - x_{j+\frac{1}{2}}^k)^2 \right), \quad (4.35)$$

$$(PPH_j^k)''(x) = -24 \frac{D_j^k}{4h_j^k + 2h_{j+1}^k} (x - x_{j+\frac{1}{2}}^k).$$

Last equations show that  $(PPH_j^k)'(x)$  is symmetric respect to the vertical axis passing through  $x = x_{j+\frac{1}{2}}^k$  where it reaches a local maximum since  $(PPH_j^k)''(x_{j+\frac{1}{2}}^k) = 0$ .

Evaluating (4.35) at  $x_j^k$ ,  $x_{j+\frac{1}{2}}^k$  and  $x_{j+1}^k$  we obtain

$$(PPH_j^k)'(x_j) = (PPH_j^k)'(x_{j+1}) = \frac{f_{j+1}^k - f_j^k}{h_{j+1}^k} - \frac{D_j^k (h_{j+1}^k)^2}{2h_j^k + h_{j+1}^k}, \quad (4.36)$$

$$(PPH_j^k)'(x_{j+\frac{1}{2}}^k) = \frac{f_{j+1}^k - f_j^k}{h_{j+1}^k} + \frac{D_j^k (h_{j+1}^k)^2}{2(h_j^k + h_{j+1}^k)}. \quad (4.37)$$

From (4.37) and (4.30) we get

$$\text{sgn} \left( (PPH_j^k)'(x_{j+\frac{1}{2}}^k) \right) = \text{sgn}([f]). \quad (4.38)$$

To analyze the sign of  $(PPH_j^k)'(x_j)$  we replace in (4.36)  $D_j^k$  by its expression (4.28)

$$(PPH_j^k)'(x_j) = \frac{f_{j+1}^k - f_j^k}{h_{j+1}^k} - \frac{(h_{j+1}^k)^2}{(h_{j+1}^k)^2 + 3h_j^k h_{j+1}^k + 2(h_j^k)^2} \left[ \frac{f_{j+1}^k - f_j^k}{h_{j+1}^k} - \frac{f_j^k - f_{j-1}^k}{h_j^k} \right],$$

and we consider two subcases depending on the sign of  $[f]$ ,

**4.1.1**  $\text{sgn}[f] > 0$ . From (4.26),  $\frac{[f]}{h_{j+1}^k} > -\frac{f_j^k - f_{j-1}^k}{h_j^k}$ , and we get

$$\begin{aligned} (PPH_j^k)'(x_j) &> \frac{f_{j+1}^k - f_j^k}{h_{j+1}^k} - \frac{(h_{j+1}^k)^2}{(h_{j+1}^k)^2 + 3h_j^k h_{j+1}^k + 2(h_j^k)^2} 2 \frac{f_{j+1}^k - f_j^k}{h_{j+1}^k} \\ &= \frac{f_{j+1}^k - f_j^k}{h_{j+1}^k} \left[ 1 - \frac{2(h_{j+1}^k)^2}{(h_{j+1}^k)^2 + 3h_j^k h_{j+1}^k + 2(h_j^k)^2} \right] > 0, \end{aligned}$$

since

$$\frac{2(h_{j+1}^k)^2}{(h_{j+1}^k)^2 + 3h_j^k h_{j+1}^k + 2(h_j^k)^2} < 1,$$

for  $\sigma < \frac{3+\sqrt{17}}{2}$ .

**4.1.2**  $\text{sgn}[f] < 0$ . Again from (4.26),  $\frac{[f]}{h_{j+1}^k} < -\frac{f_j^k - f_{j-1}^k}{h_j^k}$ , and we get

$$\begin{aligned} (PPH_j^k)'(x_j) &< \frac{f_{j+1}^k - f_j^k}{h_{j+1}^k} - \frac{(h_{j+1}^k)^2}{(h_{j+1}^k)^2 + 3h_j^k h_{j+1}^k + 2(h_j^k)^2} 2 \frac{f_{j+1}^k - f_j^k}{h_{j+1}^k} \\ &= \frac{f_{j+1}^k - f_j^k}{h_{j+1}^k} \left[ 1 - \frac{2(h_{j+1}^k)^2}{(h_{j+1}^k)^2 + 3h_j^k h_{j+1}^k + 2(h_j^k)^2} \right] < 0, \end{aligned}$$

for  $\sigma < \frac{3+\sqrt{17}}{2}$ .

In both subcases,  $\text{sgn}\left((PPH_j^k)'(x_j^k)\right) = \text{sgn}\left((PPH_j^k)'(x_{j+1}^k)\right) = \text{sgn}([f])$ , which together with expression (4.38) allow us to write  $\text{sgn}\left((PPH_j^k)'(x)\right) = \text{sgn}([f]) \quad \forall x \in [x_j^k, x_{j+1}^k]$ , and therefore  $(PPH_j^k)'(x) \neq 0 \quad \forall x \in [x_j^k, x_{j+1}^k]$ , what amounts to say that there is not local maximum value of  $PPH_j^k(x)$  inside the interval.

## 4.2 $|D_j^k| > |D_{j+1}^k|$

In this case

$$\begin{aligned} E_j^k(x) &= \frac{f_{j+1}^k - f_j^k}{h_{j+1}^k} - \frac{D_{j+1}^k}{4h_{j+2}^k + 2h_{j+1}^k} \left( (h_{j+1}^k)^2 - 4(x - x_{j+\frac{1}{2}}^k)^2 \right), \\ (PPH_j^k)'(x) &= \frac{f_{j+1}^k - f_j^k}{h_{j+1}^k} - \frac{D_{j+1}^k}{4h_{j+2}^k + 2h_{j+1}^k} \left( (h_{j+1}^k)^2 - 12(x - x_{j+\frac{1}{2}}^k)^2 \right), \\ (PPH_j^k)''(x) &= 24 \frac{D_{j+1}^k}{4h_{j+2}^k + 2h_{j+1}^k} (x - x_{j+\frac{1}{2}}^k). \end{aligned}$$

Following a similar path to case 4.1 we arrive to

$$|d_j^k(x)| = \left| PPH_j^k(x) - \frac{f_j^k + f_{j+1}^k}{2} \right| \leq \frac{1}{2} |f_{j+1}^k - f_j^k| \quad \forall x \in [x_j^k, x_{j+1}^k],$$

$$(PPH_j^k)'(x) \neq 0 \quad \forall x \in [x_j, x_{j+1}],$$

and therefore  $PPH_j^k(x)$  remains inside the rectangle  $[x_j^k, x_{j+1}^k] \times [f_j^k, f_{j+1}^k]$ .

**5.** We start computing the points where the slope of the tangent of  $PPH_j^k(x)$  equals to the slope of the straight line  $r_j^k(x)$ . We consider two subcases,

### 5.1 $|D_j^k| \leq |D_{j+1}^k|$

In this case, the above mentioned points where the tangent of  $p_j^k(x)$  is parallel to  $r_j^k(x)$  are given by:

$$P_1 \equiv \left( x_{j+\frac{1}{2}}^k + \frac{\sqrt{3}}{3} \frac{h_{j+1}^k}{2}, \frac{f_{j+1}^k + f_j^k}{2} + \frac{\sqrt{3}}{3} \frac{f_{j+1}^k - f_j^k}{2} + \frac{\sqrt{3}}{9} \frac{D_j^k (h_{j+1}^k)^3}{2(2h_j^k + h_{j+1}^k)} \right),$$

$$P_2 \equiv \left( x_{j+\frac{1}{2}}^k - \frac{\sqrt{3}}{3} \frac{h_{j+1}^k}{2}, \frac{f_{j+1}^k + f_j^k}{2} - \frac{\sqrt{3}}{3} \frac{f_{j+1}^k - f_j^k}{2} - \frac{\sqrt{3}}{9} \frac{D_j^k (h_{j+1}^k)^3}{2(2h_j^k + h_{j+1}^k)} \right).$$

The largest distance from these points to  $r_j^k(x)$  is the maximum distance between  $PPH_j^k(x)$  and  $r_j^k(x)$  measured perpendicularly to  $r_j^k(x)$ .

For both points this distance coincides with

$$r_{max}^k = \frac{\sqrt{3}}{9} \frac{|D_j^k|}{\sqrt{(f_{j+1}^k - f_j^k)^2 + (h_{j+1}^k)^2}} \frac{(h_{j+1}^k)^4}{2(2h_j^k + h_{j+1}^k)} = O(h^k).$$

### 5.2 $|D_j^k| > |D_{j+1}^k|$

The required points  $P_1$  and  $P_2$  in this case take the form:

$$P_1 \equiv \left( x_{j+\frac{1}{2}}^k + \frac{\sqrt{3}}{3} \frac{h_{j+1}^k}{2}, \frac{f_{j+1}^k + f_j^k}{2} + \frac{\sqrt{3}}{3} \frac{f_{j+1}^k - f_j^k}{2} - \frac{\sqrt{3}}{9} \frac{D_{j+1}^k (h_{j+1}^k)^3}{2(2h_{j+2}^k + h_{j+1}^k)} \right),$$

$$P_2 \equiv \left( x_{j+\frac{1}{2}}^k - \frac{\sqrt{3}}{3} \frac{h_{j+1}^k}{2}, \frac{f_{j+1}^k + f_j^k}{2} - \frac{\sqrt{3}}{3} \frac{f_{j+1}^k - f_j^k}{2} + \frac{\sqrt{3}}{9} \frac{D_{j+1}^k (h_{j+1}^k)^3}{2(2h_{j+2}^k + h_{j+1}^k)} \right),$$

and  $r_{max}^k$  is given by

$$r_{max}^k = \frac{\sqrt{3}}{9} \frac{|D_{j+1}^k|}{\sqrt{(f_{j+1}^k - f_j^k)^2 + (h_{j+1}^k)^2}} \frac{(h_{j+1}^k)^4}{2(2h_{j+2}^k + h_{j+1}^k)} = O(h^k).$$

□

**Remark 10.** *The hypothesis in Theorem 5 concerning the use of a nested set of  $\sigma$  quasi-uniform grids amounts in practice to build the reconstruction with a small enough maximum grid size.*

In the next section we carry out some numerical experiments to check that the practical observations coincide with the theoretical results.

## 4.5 Numerical experiment

In this section we present a simple numerical test to validate the theoretical results. Our experiment computes the approximation order of the considered reconstruction in several areas corresponding with the different points in Theorem 4. In particular we measure the approximation order in the following areas, identified with the given acronyms:

$A_0$ : In the subinterval containing the discontinuity.

$A_1$ : In a region where the function is smooth without inflexion points.

$A_2$ : In a region where the function is smooth but contains a inflexion point.

$A_3$ : In a region close to the inflexion point without containing it.

$A_4$ : In the subinterval just to the right of the one containing the singularity.

Let  $X^0 = (0, 3, 8, 11, 17, 23, 25, 27, 31, 32, 36, 37.5, 38, 39.3, 40) \frac{\pi}{20}$  be a nonuniform grid in  $[0, 2\pi]$  and  $f(x)$  the following smooth function with a jump discontinuity at  $x = 1.2\pi$ , and an inflexion point at  $x = \frac{3\pi}{2}$ ,

$$f(x) := \begin{cases} \sin x & x < 1.2\pi, \\ \cos x + 10 & x \geq 1.2\pi. \end{cases}$$

Given the initial abscissas  $x_i, i \in I = \{0, \dots, 14\}$ , we consider the set of nested grids  $X^k = \{x_i^k\}_{i \in I^k}$ , where  $x_{2i}^k = x_i^{k-1}$ ,  $x_{2i+1}^k = \frac{x_i^{k-1} + x_{i+1}^{k-1}}{2}$ , and  $I^k = \{x_0^k, \dots, x_{n_k}^k\}$ , with  $n_k = 2n_{k-1} - 1$ ,  $n_0 = 14$ ,  $k = 0, 1, \dots, 7$ . For each level of resolution  $k$  we build the PPH reconstruction using the data  $(x_i^k, f(x_i^k)), i \in I_k$  computing the approximation errors in infinity norm with respect to the original function using a denser set of abscissas, that is, we compute a numerical approximation of

$$E_k := \|f(x) - PPH^k(x)\|_\infty.$$

Then, we compute the numerical approximation order as

$$p = \log_2 \frac{E_{k-1}}{E_k}, \quad k = 0, 1, \dots, 7.$$

Notice that due to Theorem 4 we can assume that for fine enough grids

$$E_k \approx C \left( h^k \right)^p, \quad \text{with } h^k := \max_{i \in I_k \setminus \{0\}} h_i^k, \quad h_i^k := x_i^k - x_{i-1}^k, \quad h^k = \frac{h^{k-1}}{2}.$$

In Tables 4.1 and 4.2 we present the errors committed by Lagrange and PPH reconstructions respectively when using as initial nodes the defined nested grids  $X^k$ . The errors appear separately for each kind of region  $A_0, A_1, A_2, A_3$  and  $A_4$ . The largest error comes near the jump discontinuity for Lagrange reconstruction, as it can be observed in the column corresponding with  $A_0$ .

$k$	Lagrange				
	$A_0$	$A_1$	$A_2$	$A_3$	$A_4$
$k = 0$	5.6495	3.7038	$7.5463 \times 10^{-1}$	$6.3455 \times 10^{-4}$	$7.5463 \times 10^{-1}$
$k = 1$	9.4448	$7.3685 \times 10^{-4}$	$4.2214 \times 10^{-5}$	$9.0640 \times 10^{-5}$	$6.1204 \times 10^{-1}$
$k = 2$	9.3578	$6.2735 \times 10^{-5}$	$3.4996 \times 10^{-6}$	$9.2479 \times 10^{-6}$	$6.1887 \times 10^{-1}$
$k = 3$	9.3587	$4.0575 \times 10^{-6}$	$3.0851 \times 10^{-7}$	$6.5454 \times 10^{-7}$	$6.2234 \times 10^{-1}$
$k = 4$	9.3591	$2.5733 \times 10^{-7}$	$2.2334 \times 10^{-8}$	$4.3080 \times 10^{-8}$	$6.2409 \times 10^{-1}$
$k = 5$	9.3593	$1.5978 \times 10^{-8}$	$1.4894 \times 10^{-9}$	$2.7567 \times 10^{-9}$	$6.2496 \times 10^{-1}$
$k = 6$	9.3594	$1.0021 \times 10^{-9}$	$9.5977 \times 10^{-11}$	$1.7424 \times 10^{-1}$	$6.2540 \times 10^{-1}$
$k = 7$	9.3595	$6.2737 \times 10^{-11}$	$6.0880 \times 10^{-12}$	$1.0951 \times 10^{-11}$	$6.2562 \times 10^{-1}$

Table 4.1: Approximation errors obtained at iteration  $k, k = 1, \dots, 7$  for the considered cases  $A_0, A_1, A_2, A_3$  and  $A_4$  using the Lagrange reconstruction.

$k$	PPH				
	$A_0$	$A_1$	$A_2$	$A_3$	$A_4$
$k = 0$	5.0072	$1.9182 \times 10^{-2}$	$8.3447 \times 10^{-3}$	$2.2239 \times 10^{-3}$	$7.3017 \times 10^{-3}$
$k = 1$	9.3051	$6.5968 \times 10^{-3}$	$7.8190 \times 10^{-4}$	$2.9306 \times 10^{-4}$	$2.3996 \times 10^{-3}$
$k = 2$	9.3588	$8.3401 \times 10^{-4}$	$2.4763 \times 10^{-4}$	$3.4429 \times 10^{-5}$	$6.1993 \times 10^{-4}$
$k = 3$	9.3591	$3.4729 \times 10^{-5}$	$3.0993 \times 10^{-5}$	$2.7653 \times 10^{-6}$	$1.5738 \times 10^{-4}$
$k = 4$	9.3593	$2.6086 \times 10^{-6}$	$3.8754 \times 10^{-6}$	$2.0098 \times 10^{-7}$	$3.9636 \times 10^{-5}$
$k = 5$	9.3594	$1.8126 \times 10^{-7}$	$4.8446 \times 10^{-7}$	$4.3976 \times 10^{-8}$	$9.9451 \times 10^{-6}$
$k = 6$	9.3595	$1.0730 \times 10^{-8}$	$6.0559 \times 10^{-8}$	$4.6559 \times 10^{-9}$	$2.4908 \times 10^{-6}$
$k = 7$	9.3595	$6.5331 \times 10^{-10}$	$7.5699 \times 10^{-9}$	$5.0457 \times 10^{-10}$	$6.2325 \times 10^{-7}$

Table 4.2: Approximation errors obtained at iteration  $k, k = 1, \dots, 7$  for the considered cases  $A_0, A_1, A_2, A_3$  and  $A_4$  using the PPH reconstruction.

In Table 4.3 we present the obtained approximation orders for the studied PPH reconstruction and just for the sake of comparison we also add the approximation orders for the classical four points piecewise Lagrange polynomial interpolation. We have computed the approximation order in the specified different regions  $A_0, A_1, A_2, A_3$  and  $A_4$ . More in concrete, in the case of region  $A_1$  we use the interval  $[2, 3]$  for the  $x$  variable, in the case of region  $A_2$  the interval  $[4, 5]$ , and in the case of region  $A_3$  the intervals  $[x_{d_k+k}, 2\pi]$ , where  $k$  indicates the resolution level and the index  $d_k$  is such that the inflexion point falls into the interval  $[x_{d_k-1}, x_{d_k}]$  for each  $k$ . We can observe that in the region  $A_0$  both reconstructions are affected by the jump discontinuity and they lose the



approximation order due mainly to the subinterval containing the discontinuity. In the region of type  $A_1$  both reconstructions attain fourth order accuracy as expected. In the case  $A_2$  the PPH reconstruction reduces the approximation order to third order due to the presence of the inflexion point. Similarly in the vicinity of the inflexion point, region  $A_3$ , the PPH reconstruction stays between  $p = 3$  and  $p = 4$ . In the adjacent intervals to the singularity, case  $A_4$  we clearly observe an improvement with respect to Lagrange interpolation, since we obtain order  $p = 2$  while Lagrange completely loses the approximation order. Notice that the order reduction produced in the regions  $A_2$  and  $A_3$  occurs in very limited areas and it can be corrected using a translation strategy (see [6],[20]) that we have not implemented in this experiment with the aim of studying the original reconstruction operator.

$k$	Lagrange					PPH				
	$A_0$	$A_1$	$A_2$	$A_3$	$A_4$	$A_0$	$A_1$	$A_2$	$A_3$	$A_4$
$k = 1$	-0.7414	12.2953	14.1257	2.8075	0.3021	-0.8940	1.5399	3.4158	2.9238	1.6054
$k = 2$	0.0133	3.5540	3.5925	3.2929	-0.0160	-0.0083	2.9836	1.6588	3.0895	1.9526
$k = 3$	-0.0001	3.9506	3.5038	3.8206	-0.0081	$-5.4 \times 10^{-5}$	4.5859	2.9982	3.6381	1.9779
$k = 4$	$6.5 \times 10^{-5}$	3.9789	3.7880	3.9254	-0.0040	$-2.9 \times 10^{-5}$	3.7348	2.9995	3.7823	1.9893
$k = 5$	$3.3 \times 10^{-5}$	4.0094	3.9064	3.9660	-0.0020	$-1.5 \times 10^{-5}$	3.8472	2.9999	2.1923	1.9948
$k = 6$	$1.6 \times 10^{-5}$	3.9950	3.9559	3.9838	-0.0010	$-7.4 \times 10^{-6}$	4.0784	3.0000	3.2396	1.9974
$k = 7$	$8.1 \times 10^{-6}$	3.9976	3.9787	3.9919	-0.0005	$-3.7 \times 10^{-6}$	4.0377	3.0000	3.2059	1.9987

Table 4.3: Approximation orders obtained at iteration  $k, k = 1, \dots, 7$  for the considered cases  $A_0, A_1, A_2, A_3$  and  $A_4$  using the PPH and Lagrange reconstructions.

In Figure 4.1 we plot the function  $f(x)$  and the Lagrange and PPH reconstructions obtained from the initial grids  $X^k, k = 0, 1, 2$ . We can see that around the singularity, Lagrange reconstruction loses the approximation order and the Gibbs phenomena appears. In this zone, PPH reconstruction performs in a more proper way, avoiding any Gibbs effects. We can see that no oscillations appear in the PPH reconstruction even for the coarsest grid. These observations can be seen more clearly in Figure 4.2 where we have plotted a zoom of this region for  $k = 3$  for both reconstruction operators Lagrange and PPH. We also point out that the oscillations due to the jump discontinuity in Lagrange reconstruction do not diminish to zero with the subdivision level. In fact, from  $k = 2$  we have checked out that the reconstruction values at the local maxima and minima of the oscillations remain almost constant.

In the jump interval the distance  $r_{max}^k$  decreases as  $k$  increases, since  $r_{max}^k = O(h^k)$ . In Table 4.4 the values for  $k = 0, 1, \dots, 7$  are shown. We can see that at a certain subdivision level the given values are approximately decreasing with the ratio  $\frac{1}{2}$ . Therefore, PPH reconstruction approaches to the straight line  $r_j^k(x)$  as  $k$  increases.

	$k = 0$	$k = 1$	$k = 2$	$k = 3$	$k = 4$	$k = 5$	$k = 6$	$k = 7$
$r_{max}^k$	$1.1126 \times 10^{-3}$	$5.4822 \times 10^{-4}$	$1.2527 \times 10^{-3}$	$6.2825 \times 10^{-4}$	$3.1452 \times 10^{-4}$	$1.5735 \times 10^{-4}$	$7.8700 \times 10^{-5}$	$3.9356 \times 10^{-5}$

Table 4.4: Distances  $r_{max}^k$  obtained at subdivision level  $k, k = 0, 1, 2, 3, 4, 5, 6, 7$ .

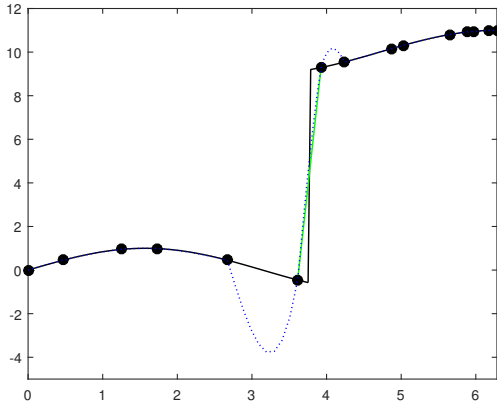
## 4.6 Conclusions

We have studied the behavior of the PPH reconstruction operator in presence of jump discontinuities for the case of working with  $\sigma$  quasi-uniform grids. For this purpose, the arithmetic and harmonic means used in the uniform case are changed for weighted means with concrete weights, so that the main properties that allow for maintaining order of approximation in smooth areas and adaptation near singularities continue being true.

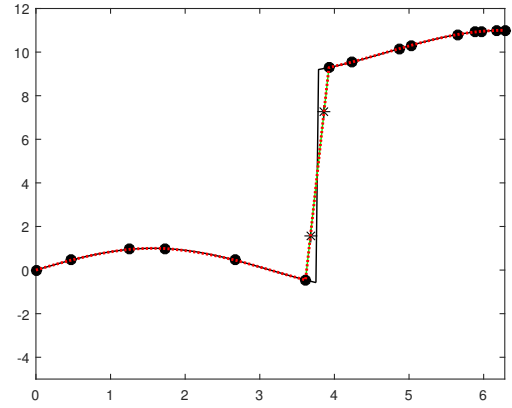
A explicit result concerning the approximation order, Theorem 4, has been proved, showing at least second order of approximation for the adjacent intervals to the one containing the jump discontinuity, and ensuring fourth order of approximation in convex (concave) parts of the function far from inflexion points. At a interval containing a inflexion point we get third order of approximation and in the vicinity the order grows progressively till fourth order.

A main result of this chapter is Theorem 5 in Section 4 proving that the presented reconstruction operator does not generate any Gibbs phenomena in the concrete sense indicated in the enunciate for  $\sigma$  quasi-uniform grids where the maximum space between nodes of the grid is small enough.

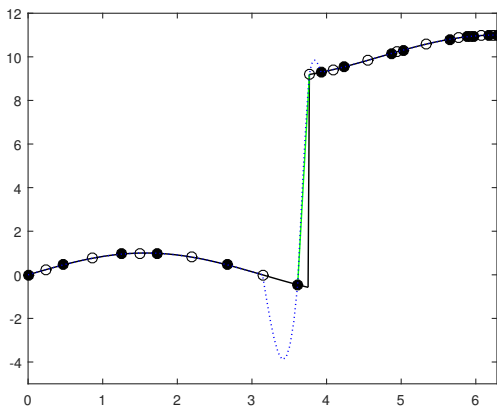
Finally we have carried out some numerical experiments to reinforce the theoretical results proven as much in Proposition 1 as in Theorem 1.



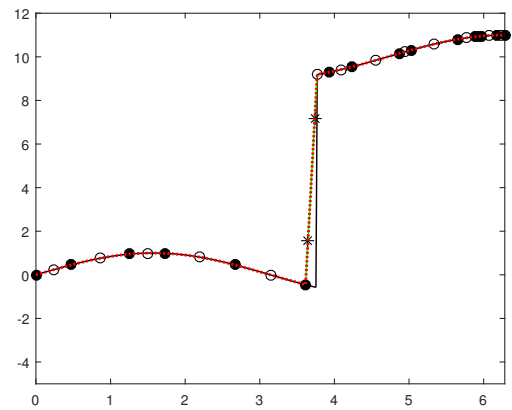
(a)



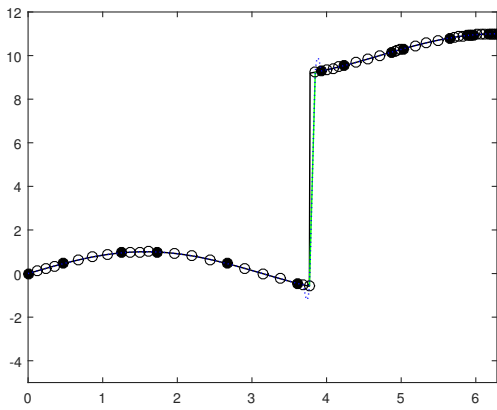
(b)



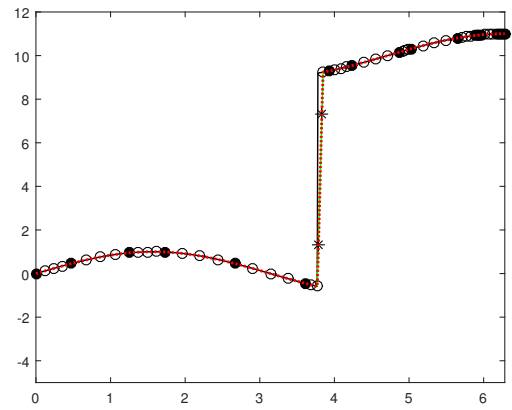
(c)



(d)

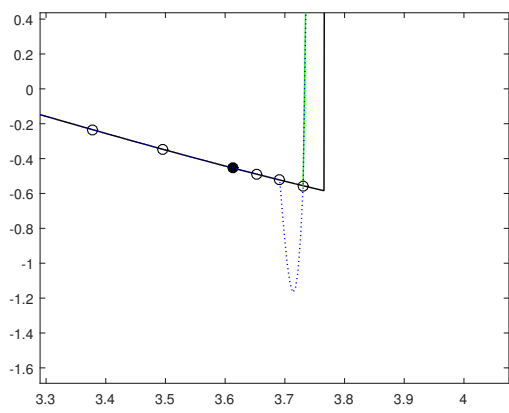


(e)

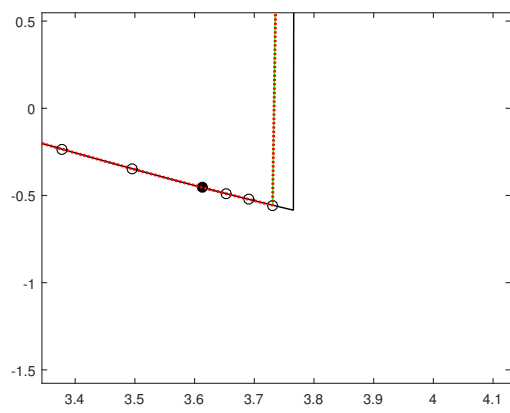


(f)

Figure 4.1: In black solid line: function  $f(x)$ , in green solid line the straight line joining the extreme points of the jump interval  $[x_j^k, x_{j+1}^k]$ , in blue dotted line: Lagrange reconstruction, in red dotted line: PPH reconstruction. Void circles stand for initial nodes, filled circles for nodes at the  $k$  subdivision level and asterisks for points  $P_1$  and  $P_2$ . (a): Lagrange  $k = 0$ , (b): PPH  $k = 0$ , (c): Lagrange  $k = 1$ , (d): PPH  $k = 1$ , (e): Lagrange  $k = 2$ , (f): PPH  $k = 2$ .



(a)



(b)

Figure 4.2: Zoom of the region around the jump discontinuity for subdivision grid level  $k = 3$ . (a): Lagrange, (b): *PPH*.

## Chapter 5

# Improving the approximation order around inflection points of the PPH nonlinear interpolatory reconstruction operator on nonuniform grids.

This chapter is the result of a fruitful collaboration, which has given rise to a fully written paper which is now submitted [17]

- Amat, S.; Ortiz, P.; Ruiz, J.; Trillo, J. C.; Yáñez, D. F. Improving the approximation order around inflection points of the PPH nonlinear interpolatory reconstruction operator on nonuniform grids. Submitted.

### 5.1 Introduction

A high quantity of reconstruction operators have emerged in the last decades to attend the demands of diverse applications in applied mathematics and industry [1, 2, 26, 25]. Normally, polynomials are considered because of their simplicity and fast computation, and more specifically piecewise polynomials in order to avoid using high degree polynomials. High order polynomials involve larger stencils to build the reconstructions, what makes them more vulnerable to be affected by the presence of potential discontinuities in the data, apart of being well known for producing spurious maxima and minima known as Runge phenomena.

Nonlinear reconstructions allow adaptation to the available data and they also permit to preserve certain properties inherent to the initial data. One of such properties is convexity, which is intimately related to curve and surface design. In this context some nonlinear operators have appeared in the literature in the past few years [6, 7, 10, 20, 4, 27]. In particular we pay attention to the Piecewise Polynomial Harmonic (PPH) reconstruction [6, 11, 32, 37, 42, 50], which was defined in nonuniform grids to preserve the convexity of the initial data under certain restrictions [42]. This reconstruction works well with data coming from strictly convex functions, but it fails to guarantee the approximation order in the vicinity of inflection points. This drawback comes directly from the heart of the definition itself of the PPH reconstruction operator, that is, the use of the weighted harmonic mean of two positive quantities. However, the problem can be solved by

using a modified mean with a translation strategy.

In this chapter we introduce the definition of what we call a translation operator. Then, we apply this operator to the weighted harmonic mean obtaining a new adapted mean which retains similar properties as the original one, what is a crucial issue in order to be inserted into the construction of the improved PPH reconstruction operator. Our main concern about improving the approximation order around inflection points is to generate a tool that retains the approximation order in the whole domain for smooth functions and maintains local convexity in the convex areas. This convexity preservation property in smooth areas was proven in [42] under certain constrains. Also in [42] is made evident that the PPH reconstruction, both in uniform and in nonuniform grids, is relevant not only as an adapted reconstruction for smooth function with isolated jump discontinuities (see [6, 43]), but as a reconstruction that preserves convexity of the initial data.

We study several possible options to work in combination with the PPH reconstruction operator. In particular we define a way of choosing the best option depending on the specific data to which it is going to be applied. Part of this work has been inspired by the ideas given in [20].

The chapter is organized as follows: In Section 5.2 we remind the nonlinear PPH reconstruction operator [42] on nonuniform grids and its application for data coming from strictly convex functions. Section 5.3 is dedicated to definition and study of the translation operator. In Section 5.4 we analyze the behavior of the improved PPH reconstruction operator with respect to the approximation order. In Section 5.5 we give a way of selecting the translation parameter depending on the data. In Section 5.6 we present some numerical tests in order to confirm the theoretical results. Finally, some conclusions are provided in Section 5.7.

## 5.2 A nonlinear PPH reconstruction operator on nonuniform grids

In this section we recall the definition of the nonlinear PPH reconstruction operator on nonuniform grids, see [42]. We include the necessary elements for the rest of the chapter. In [42] the reconstruction operator is designed to deal with strictly convex functions, albeit it is also of interest in the case of working with piecewise smooth functions affected by isolated jump discontinuities. This will be our case of interest in this section and in the rest of the chapter.

Let us define a nonuniform grid  $X = (x_i)_{i \in \mathbb{Z}}$  in  $\mathbb{R}$ . Let us also denote  $h_i := x_i - x_{i-1}$ , the nonuniform spacing between abscissae. We consider underlying piecewise continuous functions  $f(x)$  with at most a finite set of isolated jump discontinuities, and let us call  $f_i := f(x_i)$  the ordinates corresponding to the point values of the function at the given abscissae. We also introduce the following notations. In first place, the second order divided differences

$$\begin{aligned} D_j &:= f[x_{j-1}, x_j, x_{j+1}] = \frac{f_{j-1}}{h_j(h_j + h_{j+1})} - \frac{f_j}{h_j h_{j+1}} + \frac{f_{j+1}}{h_{j+1}(h_j + h_{j+1})}, \\ D_{j+1} &:= f[x_j, x_{j+1}, x_{j+2}] = \frac{f_j}{h_{j+1}(h_{j+1} + h_{j+2})} - \frac{f_{j+1}}{h_{j+1} h_{j+2}} + \frac{f_{j+2}}{h_{j+2}(h_{j+1} + h_{j+2})}, \end{aligned} \quad (5.1)$$

in second place a weighted arithmetic mean of  $D_j$  and  $D_{j+1}$  defined as

$$M_j = w_{j,0}D_j + w_{j,1}D_{j+1}, \quad (5.2)$$

with the weights

$$\begin{aligned} w_{j,0} &= \frac{h_{j+1} + 2h_{j+2}}{2(h_j + h_{j+1} + h_{j+2})}, \\ w_{j,1} &= \frac{h_{j+1} + 2h_j}{2(h_j + h_{j+1} + h_{j+2})} = 1 - w_{j,0}. \end{aligned} \quad (5.3)$$

These weights will allow us to express the third order Lagrange interpolation polynomial based on the stencil  $\{x_{j-1}, x_j, x_{j+1}, x_{j+2}\}$  in terms of  $D_j$  and  $D_{j+1}$  and their weighted arithmetic mean. Given these ingredients in [42] we can find the following definitions, and results that we will use later.

**Lemma 16.** *Let us consider the set of ordinates  $\{f_{j-1}, f_j, f_{j+1}, f_{j+2}\}$  for some  $j \in \mathbb{Z}$  at the abscissae  $\{x_{j-1}, x_j, x_{j+1}, x_{j+2}\}$  of a nonuniform grid  $X = (x_i)_{i \in \mathbb{Z}}$ . Then, the values  $f_{j-1}$  and  $f_{j+2}$  at the extremes can be expressed as*

$$f_{j-1} = \frac{-1}{\gamma_{j,-1}}(\gamma_{j,0}f_j + \gamma_{j,1}f_{j+1} + \gamma_{j,2}f_{j+2}) + \frac{M_j}{\gamma_{j,-1}}, \quad (5.4a)$$

$$f_{j+2} = \frac{-1}{\gamma_{j,2}}(\gamma_{j,-1}f_{j-1} + \gamma_{j,0}f_j + \gamma_{j,1}f_{j+1}) + \frac{M_j}{\gamma_{j,2}}, \quad (5.4b)$$

with the constants  $\gamma_{j,i}$ ,  $i = -1, 0, 1, 2$  given by

$$\begin{aligned} \gamma_{j,-1} &= \frac{h_{j+1} + 2h_{j+2}}{2h_j(h_{j+1} + h_j)(h_j + h_{j+1} + h_{j+2})}, \\ \gamma_{j,0} &= \frac{1}{2h_{j+1}(h_j + h_{j+1} + h_{j+2})} \left( \frac{h_{j+1} + 2h_j}{h_{j+1} + h_{j+2}} - \frac{h_{j+1} + 2h_{j+2}}{h_j} \right), \\ \gamma_{j,1} &= \frac{1}{2h_{j+1}(h_j + h_{j+1} + h_{j+2})} \left( \frac{h_{j+1} + 2h_{j+2}}{h_{j+1} + h_j} - \frac{h_{j+1} + 2h_j}{h_{j+2}} \right), \\ \gamma_{j,2} &= \frac{h_{j+1} + 2h_j}{2h_{j+2}(h_{j+1} + h_{j+2})(h_j + h_{j+1} + h_{j+2})}. \end{aligned} \quad (5.5)$$

**Definition 17.** *Given  $x, y \in \mathbb{R}$ , and  $w_x, w_y \in \mathbb{R}$  such that  $w_x > 0$ ,  $w_y > 0$ , and  $w_x + w_y = 1$ , we denote as  $\tilde{V}$  the following extension of the weighted harmonic mean given by the function*

$$\tilde{V}(x, y) = \begin{cases} \frac{xy}{w_x y + w_y x} & \text{if } xy > 0, \\ 0 & \text{otherwise.} \end{cases} \quad (5.6)$$

**Lemma 17.** *If  $x \geq 0$  and  $y \geq 0$ , the harmonic mean in (5.6) is bounded as follows*

$$\tilde{V}(x, y) < \min \left\{ \frac{1}{w_x}x, \frac{1}{w_y}y \right\} \leq \frac{1}{w_x}x. \quad (5.7)$$

We also include the definition of the approximation order such as it is commonly introduced in numerical analysis. We are going to use it through the remaining part of the chapter.

**Definition 18.** An expression  $e(h) = O(h^r)$ ,  $r \in \mathbb{Z}$  means that there exist  $h_0 > 0$  and  $M > 0$  such that  $\forall 0 < h \leq h_0$

$$\frac{|e(h)|}{h^r} \leq M.$$

**Lemma 18.** Let  $a > 0$  be a fixed positive real number, and let  $|x| \geq a$  and  $|y| \geq a$ . If  $|x - y| = O(h)$ , and  $xy > 0$ , then the previously defined weighted harmonic mean is also close to the weighted arithmetic mean  $M(x, y) = w_x x + w_y y$ ,

$$|M(x, y) - \tilde{V}(x, y)| = \frac{w_x w_y}{w_x y + w_y x} (x - y)^2 = O(h^2). \quad (5.8)$$

**Definition 19** (PPH reconstruction). Let  $X = (x_i)_{i \in \mathbb{Z}}$  be a nonuniform mesh. Let  $f = (f_i)_{i \in \mathbb{Z}}$  be a sequence in  $l_\infty(\mathbb{Z})$ . Let  $D_j$  and  $D_{j+1}$  be the second order divided differences, and for each  $j \in \mathbb{Z}$  let us consider the modified values  $\{\tilde{f}_{j-1}, \tilde{f}_j, \tilde{f}_{j+1}, \tilde{f}_{j+2}\}$  built according to the following rule

- **Case 1:** If  $|D_j| \leq |D_{j+1}|$

$$\begin{cases} \tilde{f}_i = f_i, & j-1 \leq i \leq j+1, \\ \tilde{f}_{j+2} = \frac{-1}{\gamma_{j,2}} (\gamma_{j,-1} f_{j-1} + \gamma_{j,0} f_j + \gamma_{j,1} f_{j+1}) + \frac{\tilde{V}_j}{\gamma_{j,2}}, \end{cases} \quad (5.9)$$

- **Case 2:** If  $|D_j| > |D_{j+1}|$

$$\begin{cases} \tilde{f}_{j-1} = \frac{-1}{\gamma_{j,-1}} (\gamma_{j,0} f_j + \gamma_{j,1} f_{j+1} + \gamma_{j,2} f_{j+2}) + \frac{\tilde{V}_j}{\gamma_{j,-1}}, \\ \tilde{f}_i = f_i, & j \leq i \leq j+2, \end{cases} \quad (5.10)$$

where  $\gamma_{j,i}$ ,  $i = -1, 0, 1, 2$  are given in (5.5) and  $\tilde{V}_j = \tilde{V}(D_j, D_{j+1})$ , with  $\tilde{V}$  the weighted harmonic mean defined in (5.6) with the weights  $w_{j,0}$  and  $w_{j,1}$  in (5.3). We define the PPH nonlinear reconstruction operator as

$$PPH(x) = PPH_j(x), \quad x \in [x_j, x_{j+1}], \quad (5.11)$$

where  $PPH_j(x)$  is the unique interpolation polynomial which satisfies

$$PPH_j(x_i) = \tilde{f}_i, \quad j-1 \leq i \leq j+2. \quad (5.12)$$

According to Definition 19, it is possible to establish a parallelism with Lagrange interpolation, in fact we can write the PPH reconstruction as

$$PPH_j(x) = \tilde{a}_{j,0} + \tilde{a}_{j,1} \left(x - x_{j+\frac{1}{2}}\right) + \tilde{a}_{j,2} \left(x - x_{j+\frac{1}{2}}\right)^2 + \tilde{a}_{j,3} \left(x - x_{j+\frac{1}{2}}\right)^3, \quad (5.13)$$

where the coefficients  $\tilde{a}_{j,i}$ ,  $i = 0, 1, 2, 3$  are calculated by imposing conditions (5.12). We explain each one of the two possible local cases, Case 1 or Case 2. The coefficients will have symmetrical expressions.

**Case 1.**  $|D_j| \leq |D_{j+1}|$ , which means that a potential singularity may lay in  $[x_{j+1}, x_{j+2}]$ . It has been proposed to replace  $f_{j+2}$  with  $\tilde{f}_{j+2}$  in equation (5.9) by changing the weighted arithmetic mean in equation (5.4b) for its corresponding weighted harmonic mean. This replacement has been



performed to carry out a witty modification of the value  $\tilde{f}_{j+2}$  in such a way that its difference with respect to the original  $f_{j+2}$  is large in presence of a discontinuity, but remains sufficiently small in smooth areas maintaining the approximation order. Lemma 17 is crucial for the adaptation in case of dealing with the presence of a jump discontinuity, while Lemma 18 plays a fundamental part in proving fourth approximation order for smooth areas of an underlying function.

In this case the coefficients  $\tilde{a}_{j,i}$ ,  $i = 0, 1, 2, 3$  of the PPH polynomial read

$$\begin{aligned}\tilde{a}_{j,0} &= \frac{f_j + f_{j+1}}{2} - \frac{h_{j+1}^2}{4} \tilde{V}_j, \\ \tilde{a}_{j,1} &= \frac{-f_j + f_{j+1}}{h_{j+1}} + \frac{h_{j+1}^2}{4h_j + 2h_{j+1}} (D_j - \tilde{V}_j), \\ \tilde{a}_{j,2} &= \tilde{V}_j, \\ \tilde{a}_{j,3} &= -\frac{2}{2h_j + h_{j+1}} (D_j - \tilde{V}_j).\end{aligned}\tag{5.14}$$

For our purposes in the next sections, we need to go deeper and examine the relation with Lagrange interpolation. In particular we get that

$$|\tilde{f}_{j+2} - f_{j+2}| = \frac{2h_{j+2}(h_{j+1} + h_{j+2})(h_j + h_{j+1} + h_{j+2})}{2h_j + h_{j+1}} |M_j - \tilde{V}_j|,\tag{5.15}$$

and considering the Lagrange interpolation polynomial written in the same form as in (5.13), that is

$$PL_j(x) = a_{j,0} + a_{j,1} \left(x - x_{j+\frac{1}{2}}\right) + a_{j,2} \left(x - x_{j+\frac{1}{2}}\right)^2 + a_{j,3} \left(x - x_{j+\frac{1}{2}}\right)^3,\tag{5.16}$$

we get that the difference of these coefficients with the ones of  $PPH_j(x)$  is given by

$$\begin{aligned}\tilde{a}_{j,0} - a_{j,0} &= \frac{h_{j+1}^2}{4} (M_j - \tilde{V}_j), \\ \tilde{a}_{j,1} - a_{j,1} &= \frac{h_{j+1}^2}{4h_j + 2h_{j+1}} (M_j - \tilde{V}_j), \\ \tilde{a}_{j,2} - a_{j,2} &= -(M_j - \tilde{V}_j), \\ \tilde{a}_{j,3} - a_{j,3} &= -\frac{2}{2h_j + h_{j+1}} (M_j - \tilde{V}_j).\end{aligned}\tag{5.17}$$

**Case 2.**  $|D_j| > |D_{j+1}|$ , which means that a possible singularity lies in  $[x_{j-1}, x_j]$ . In this case, in Definition 19, the value  $f_{j-1}$  is replaced with  $\tilde{f}_{j-1}$  by using expression (5.10). Similar comments apply in this case due to symmetry considerations. The coefficients for the polynomial (5.13) now read

$$\begin{aligned}
\tilde{a}_{j,0} &= \frac{f_j + f_{j+1}}{2} - \frac{h_{j+1}^2}{4} \tilde{V}_j, \\
\tilde{a}_{j,1} &= \frac{-f_j + f_{j+1}}{h_{j+1}} + \frac{h_{j+1}^2}{2h_{j+1} + 4h_{j+2}} (-D_{j+1} + \tilde{V}_j), \\
\tilde{a}_{j,2} &= \tilde{V}_j, \\
\tilde{a}_{j,3} &= -\frac{2}{h_{j+1} + 2h_{j+2}} (-D_{j+1} + \tilde{V}_j).
\end{aligned} \tag{5.18}$$

The expressions relating the coefficients of the PPH polynomial with the Lagrange interpolation polynomial now write

$$|\tilde{f}_{j-1} - f_{j-1}| = \frac{2h_j(h_{j+1} + h_j)(h_j + h_{j+1} + h_{j+2})}{2h_{j+2} + h_{j+1}} |M_j - \tilde{V}_j|, \tag{5.19}$$

$$\begin{aligned}
\tilde{a}_{j,0} - a_{j,0} &= \frac{h_{j+1}^2}{4} (M_j - \tilde{V}_j), \\
\tilde{a}_{j,1} - a_{j,1} &= -\frac{h_{j+1}^2}{2h_{j+1} + 4h_{j+2}} (M_j - \tilde{V}_j), \\
\tilde{a}_{j,2} - a_{j,2} &= -(M_j - \tilde{V}_j), \\
\tilde{a}_{j,3} - a_{j,3} &= \frac{2}{2h_{j+2} + h_{j+1}} (M_j - \tilde{V}_j).
\end{aligned} \tag{5.20}$$

In next section we introduce the definition of a translation operator, which is meant to solve the lost of approximation order close to the inflection points of the underlying function due to the implementation of the weighted harmonic mean 17 in the case of having arguments with different signs.

### 5.3 The translation operator

In [42] it was proven that if the data come from a piecewise smooth function with an isolated jump discontinuity which verify  $D_j D_{j+1} \leq 0$  at some interval away from the discontinuity, then the PPH reconstruction operator gives an approximation of order  $O(h^3)$  lower than  $O(h^4)$  obtained just by using the piecewise Lagrange interpolation polynomial. This fact is produced by the presence of an inflection point in the function. Also, even if  $D_j D_{j+1} > 0$ , when we are near an inflection point it happens a reduction of order towards third order due to the definition of the extended weighted harmonic mean (5.6). And a similar drawback would be observed in the two adjacent intervals to the interval that potentially contains a jump discontinuity. In these intervals the approximation order decreases to second order. Therefore, we observe three situations that may require a modification in the definition of the reconstruction operator in order to attain the

expected fourth order of approximation at the time that none of their positive qualities about adaptation to discontinuities and behavior with strictly convex functions is affected. The first and third of these situations occur due to the fact that the weighted harmonic mean used in the definition of the PPH reconstruction operator is defined with value 0 whenever the sign of the two involved arguments  $D_j$  and  $D_{j+1}$  is different or one of them is zero. The second situation has also to do with the definition of the weighted harmonic mean and more specifically with Lemma 18, since the hypothesis of this lemma are not satisfied if either or both  $D_j$  and  $D_{j+1}$  are of order  $O(h^r)$  for some  $r > 0$ .

In order to solve this problematic behavior we introduce a new adapted version of the weighted harmonic mean. We first give the definition of a translation operator  $T$ , [20].

**Definition 20.** *Given  $h > 0$ , a translation operator  $T$  is any function  $T : \mathbb{R}^2 \rightarrow \mathbb{R}$  satisfying*

1.  $T(0, 0) = 0$ ,
2.  $T(x, y) = T(y, x)$ ,
3.  $T(-x, -y) = -T(x, y)$ ,
4.  $\text{sign}(x + T(x, y))\text{sign}(y + T(x, y)) > 0, \forall (x, y) \neq (0, 0)$ ,
5. if  $(x, y) \neq (0, 0)$ , with  $|x| \leq |y|$ ,
  - a) if  $|x| = |y|, \text{sign}(x) \neq \text{sign}(y)$ , then  $\text{sign}(x + T(x, y)) > 0, \text{sign}(y + T(x, y)) > 0$ ,
  - b) otherwise,  $\text{sign}(x + T(x, y))\text{sign}(y) > 0, \text{sign}(y + T(x, y))\text{sign}(y) > 0$ ,
6.  $\min\{|x + T(x, y)|, |y + T(x, y)|\} = O(1), \forall (x, y) \neq (0, 0)$ , with  $|x| = O(h^\alpha), |y| = O(h^\alpha)$ , for some  $\alpha \geq 0$ .

Property 4 of Definition 20 avoids the division by zero in Definition 17, eliminating the case in which the sign of the arguments does not coincide. This solves the inconveniences that generates reducing the mean to zero in expression (5.6). Property 5 guarantees that the translation is done towards the largest of the arguments in absolute value. Finally, property 6 will be needed to prove similar lemmas to Lemma 17 and Lemma 18, what in turn will allow to prove adaptation in case of discontinuities and fourth order accuracy in the reconstruction respectively.

With the above definition of a translation operator  $T$ , we are now ready to present the adapted weighted harmonic mean.

**Definition 21.** *We define the translated weighted harmonic mean as*

$$J(x, y) = \tilde{V}(x + T(x, y), y + T(x, y)) - T(x, y), \quad (5.21)$$

where  $T$  is an appropriate translation operator.

From now on, we will drop the arguments of the translation operator  $T$  for the sake of simplicity. They are easily inferred by the context.

For this new mean we can give the following technical lemmas.

**Lemma 19.** *For all  $(x, y) \in \mathbb{R}^2$ , the  $J(x, y)$  mean satisfies  $J(-x, -y) = -J(x, y)$ .*

*Proof.*

$$\begin{aligned}
J(-x, -y) &= \tilde{V}(-x + T(-x, -y), -y + T(-x, -y)) - T(-x, -y) \\
&= \tilde{V}(-(x + T(x, y)), -(y + T(x, y))) + T(x, y) \\
&= -\tilde{V}(x + T(x, y), y + T(x, y)) + T(x, y) = -J(x, y).
\end{aligned}$$

□

**Lemma 20.** *For all  $(x, y) \in \mathbb{R}^2$ , the translated weighted harmonic mean is bounded as follows*

$$|J(x, y)| \leq \max \left\{ \frac{|x + T|}{w_x}, |T| \right\}. \quad (5.22)$$

*Proof.* Since  $\tilde{V}(x + T, y + T)$  and  $T$  have the same sign, then applying Lemma 17 we get

$$|J(x, y)| \leq \max \left\{ |\tilde{V}(x + T, y + T)|, |T| \right\} \leq \max \left\{ \frac{|x + T|}{w_x}, |T| \right\}.$$

□

**Lemma 21.** *Let  $a > 0$  be a fixed positive real number,  $T$  be a translation operator, and let  $(x, y) \in \mathbb{R}^2$  be such that  $|x + T| \geq a$  and  $|y + T| \geq a$ . If  $|x - y| = O(h)$ , then the translated weighted harmonic mean is a second order approximation to the weighted arithmetic mean  $M(x, y) = w_x x + w_y y$ , i.e.,*

$$|M(x, y) - J(x, y)| = \frac{w_x w_y (x - y)^2}{w_x y + w_y x + T} = O(h^2). \quad (5.23)$$

*Proof.* Using the definition of  $J(x, y)$  we get

$$|M(x, y) - J(x, y)| = |M(x, y) - \tilde{V}(x + T, y + T) + T| = |M(x + T, y + T) - \tilde{V}(x + T, y + T)|,$$

and applying Lemma 18 we have that

$$|M(x + T, y + T) - \tilde{V}(x + T, y + T)| = \frac{w_x w_y (x - y)^2}{w_x y + w_y x + T} = O(h^2).$$

□

Notice that Lemma 20 and Lemma 21 correspond to an extension of previous Lemma 17 and Lemma 18.

**Remark 11.** *The bound obtained in Lemma 20 can be improved for particular choices of the translation  $T$ , due to the fact that in the general case, one applies the triangular inequality in the proof to reach the result, and this step can be refined for a given  $T$ . See for example the definition of the translation  $\tilde{T}$  in (5.24) and its corresponding Lemma 22.*

One possible definition of translation  $T$  fulfilling previous Definition 20 is obtained by

$$\tilde{T}(x, y) = \begin{cases} s \epsilon & \text{if } xy > 0, \\ s (\min \{|x|, |y|\} + \epsilon) & \text{otherwise,} \end{cases} \quad (5.24)$$

where  $\epsilon = O(1)$  is a constant and  $s$  is defined using the sign function as

$$s = \begin{cases} \text{sign}(y) & \text{if } |x| \leq |y|, \\ \text{sign}(x) & \text{otherwise.} \end{cases}$$

The proposed new mean is then given by

$$\tilde{J}(x, y) = \tilde{V}(x + \tilde{T}, y + \tilde{T}) - \tilde{T}, \quad (5.25)$$

and verifies the following specific lemma which improves the bound in Lemma 20.

**Lemma 22.** *For all  $(x, y) \in \mathbb{R}^2$ , the translated weighted harmonic mean  $\tilde{J}$  is bounded as follows*

$$|\tilde{J}(x, y)| \leq \begin{cases} \frac{|x|}{w_x} + \frac{w_y}{w_x} \epsilon & \text{if } |x| \leq |y|, \\ \frac{|y|}{w_y} + \frac{w_x}{w_y} \epsilon & \text{otherwise.} \end{cases}$$

*Proof.* Let us suppose without loss of generality that  $|x| \leq |y|$ . We consider four possible different cases, and we prove the result separately for each case.

**Case A.**  $x \leq 0, y > 0$ . In this case  $\tilde{T} = -x + \epsilon > 0$ .

$$\tilde{J}(x, y) = \tilde{V}(\epsilon, y - x + \epsilon) + x - \epsilon.$$

Now, we observe that

$$\begin{aligned} \tilde{V}(\epsilon, y - x + \epsilon) &\geq \epsilon, \\ \tilde{V}(\epsilon, y - x + \epsilon) &< \frac{1}{w_x} \epsilon. \end{aligned}$$

If  $\tilde{V}(\epsilon, y - x + \epsilon) + x - \epsilon \geq 0$ ,

$$|\tilde{J}(x, y)| < |x| + \frac{w_y}{w_x} \epsilon.$$

If  $\tilde{V}(\epsilon, y - x + \epsilon) + x - \epsilon < 0$ ,

$$|\tilde{J}(x, y)| = \epsilon - x - \tilde{V}(\epsilon, y - x + \epsilon) \leq |x|.$$

**Case B.**  $x \geq 0, y < 0$ . In this case  $\tilde{T} = -x - \epsilon < 0$ .

$$\tilde{J}(x, y) = \tilde{V}(-\epsilon, y - x - \epsilon) + x + \epsilon.$$

Observing that

$$\begin{aligned}\tilde{V}(-\epsilon, y - x - \epsilon) &\leq -\epsilon, \\ \tilde{V}(-\epsilon, y - x - \epsilon) &> -\frac{1}{w_x}\epsilon.\end{aligned}$$

If  $\tilde{V}(-\epsilon, y - x - \epsilon) + x + \epsilon \geq 0$ ,

$$|\tilde{J}(x, y)| = \tilde{V}(-\epsilon, y - x - \epsilon) + x + \epsilon \leq |x|.$$

If  $\tilde{V}(-\epsilon, y - x - \epsilon) + x + \epsilon < 0$ ,

$$|\tilde{J}(x, y)| \leq |x| + \frac{w_y}{w_x}\epsilon.$$

**Case C.**  $x > 0, y > 0$ . In this case  $\tilde{T} = \epsilon > 0$ .

$$\tilde{J}(x, y) = \tilde{V}(x + \epsilon, y + \epsilon) - \epsilon.$$

We are going to use that in this case

$$\begin{aligned}\tilde{V}(x + \epsilon, y + \epsilon) &\geq x + \epsilon, \\ \tilde{V}(x + \epsilon, y + \epsilon) &< \frac{1}{w_x}(x + \epsilon).\end{aligned}$$

Since in this case  $\tilde{V}(x + \epsilon, y + \epsilon) - \epsilon \geq 0$ , then

$$|\tilde{J}(x, y)| < \frac{|x|}{w_x} + \frac{w_y}{w_x}\epsilon.$$

**Case D.**  $x < 0, y < 0$ . In this case  $\tilde{T} = -\epsilon < 0$ .

$$\tilde{J}(x, y) = \tilde{V}(x - \epsilon, y - \epsilon) + \epsilon.$$

In this case using that

$$\begin{aligned}\tilde{V}(x - \epsilon, y - \epsilon) &\leq x - \epsilon, \\ \tilde{V}(x - \epsilon, y - \epsilon) &> \frac{1}{w_x}(x - \epsilon),\end{aligned}$$

and observing that  $\tilde{V}(x - \epsilon, y - \epsilon) + \epsilon < 0$ , we get

$$|\tilde{J}(x, y)| < \frac{|x|}{w_x} + \frac{w_y}{w_x}\epsilon.$$

□

## 5.4 Improved PPH reconstruction operator

In this section we introduce the modified mean defined in previous section into the definition of the PPH reconstruction operator, giving rise to the following definition.

**Definition 22** (Translated PPH reconstruction). *Let  $X = (x_i)_{i \in \mathbb{Z}}$  be a nonuniform mesh. Let  $f = (f_i)_{i \in \mathbb{Z}}$  be a sequence in  $l_\infty(\mathbb{Z})$ . Let  $D_j$  and  $D_{j+1}$  be the second order divided differences in (5.1), and for each  $j \in \mathbb{Z}$  let us consider the modified values  $\{\tilde{f}_{j-1}, \tilde{f}_j, \tilde{f}_{j+1}, \tilde{f}_{j+2}\}$  built according to the following rule*

- **Case 1:** If  $|D_j| \leq |D_{j+1}|$

$$\begin{cases} \tilde{f}_i = & f_i, & j-1 \leq i \leq j+1, \\ \tilde{f}_{j+2} = & \frac{-1}{\gamma_{j,2}}(\gamma_{j,-1}f_{j-1} + \gamma_{j,0}f_j + \gamma_{j,1}f_{j+1}) + \frac{J_j}{\gamma_{j,2}}. \end{cases} \quad (5.26)$$

- **Case 2:** If  $|D_j| > |D_{j+1}|$

$$\begin{cases} \tilde{f}_{j-1} = & \frac{-1}{\gamma_{j,-1}}(\gamma_{j,0}f_j + \gamma_{j,1}f_{j+1} + \gamma_{j,2}f_{j+2}) + \frac{J_j}{\gamma_{j,-1}}, \\ \tilde{f}_i = & f_i, & j \leq i \leq j+2. \end{cases} \quad (5.27)$$

where  $\gamma_{j,i}$ ,  $i = -1, 0, 1, 2$  are given in (5.5) and  $J_j = J(D_j, D_{j+1})$ , with  $J$  the translated weighted harmonic mean defined in (5.21) or in (5.25) with the weights  $w_{j,0}$  and  $w_{j,1}$  in (5.3). We define the translated PPH nonlinear reconstruction operator as

$$PPHT(x) = PPHT_j(x), \quad x \in [x_j, x_{j+1}], \quad (5.28)$$

where  $PPHT_j(x)$  is the unique third degree interpolation polynomial which satisfies

$$PPHT_j(x_i) = \tilde{f}_i, \quad j-1 \leq i \leq j+2. \quad (5.29)$$

The coefficients for this new reconstruction operator match exactly with the expressions in (5.14) and (5.18) respectively depending on the case, except for the substitution of  $\tilde{V}_j$  for  $J_j$ .

We can prove now the following result about the order of approximation attained by the reconstruction. We want to point out that the order improves in the vicinity of inflection points due to the considered translation, which is an improvement with respect to the original reconstruction procedure, see Theorem 1 in [43].

We are going to study the approximation order of the given reconstruction for functions of class  $C^4(\mathbb{R})$  with an isolated jump discontinuity at a given point  $\mu$ . We consider only the case of working with  $\sigma$  quasi-uniform grids, according with the following definition.

**Definition 23.** *A nonuniform mesh  $X = (x_i)_{i \in \mathbb{Z}}$  is said to be a  $\sigma$  quasi-uniform mesh if there exist  $h_{min} = \min_{i \in \mathbb{Z}} h_i$ ,  $h_{max} = \max_{i \in \mathbb{Z}} h_i$ , and a finite constant  $\sigma$  such that  $\frac{h_{max}}{h_{min}} \leq \sigma$ .*

The next theorem proves full order of accuracy, that is fourth order of accuracy, in all intervals except the interval containing the singularity and the two adjacent intervals. We observe that the approximation order is reduced to third order close in the two adjacent intervals, but it is not completely lost.

**Theorem 6.** Let  $f(x)$  be a function of class  $C^4(\mathbb{R} \setminus \{\mu\})$ , with a jump discontinuity at the point  $\mu$ . Let  $X = (x_i)_{i \in \mathbb{Z}}$  be a  $\sigma$  quasi-uniform mesh in  $\mathbb{R}$ , with  $h_i = x_i - x_{i-1}$ ,  $\forall i \in \mathbb{Z}$ , and  $f = (f_i)_{i \in \mathbb{Z}}$ , the sequence of point values of the function  $f(x)$ ,  $f_i = f(x_i)$ . Let us consider  $j \in \mathbb{Z}$  such that  $\mu \in [x_j, x_{j+1}]$ . Then, the reconstruction  $PPHT(x)$  satisfies

1. In  $[x_i, x_{i+1}]$ ,  $i \neq j-1, j, j+1$ , then

$$\max_{x \in [x_i, x_{i+1}]} |f(x) - PPHT(x)| = O(h^4).$$

2. In  $[x_{j-1}, x_j] \cup [x_{j+1}, x_{j+2}]$ ,

$$\max_{x \in [x_{j-1}, x_j] \cup [x_{j+1}, x_{j+2}]} |f(x) - PPHT(x)| = O(h^2),$$

where  $h = \max_{i \in \mathbb{Z}} \{h_i\}$ .

*Proof.* We do the proof point by point.

1. Given  $x \in [x_i, x_{i+1}]$ , the reconstruction operator is built as  $PPHT(x) = PPHT_i(x)$ .

We recall that second order divided differences amount to second order derivatives at an intermediate point divided by two, i.e

$$D_i = \frac{f''(\mu_1)}{2!}, \quad D_{i+1} = \frac{f''(\mu_2)}{2!},$$

with  $\mu_1 \in (x_{i-1}, x_{i+1})$  and  $\mu_2 \in (x_i, x_{i+2})$ . Due to the properties of the translation  $T$  in Definition 20, we have that

$$D_i + \tilde{T} = O(1), \quad D_{i+1} + \tilde{T} = O(1) \text{ and } D_{i+1} - D_i = O(h),$$

and from Lemma 21 we get that

$$M_i - \tilde{J}_i = \frac{w_{i,0}w_{i,1}(D_{i+1} - D_i)^2}{w_{i,0}D_{i+1} + w_{i,1}D_i + \tilde{T}} = O(h^2). \quad (5.30)$$

Plugging this information into (5.17) if  $|D_i| \leq |D_{i+1}|$ , or into (5.20) if  $|D_i| > |D_{i+1}|$ , we get that

$$|\tilde{a}_{i,s} - a_{i,s}| = O(h^{4-s}), \quad s = 0, 1, 2, 3. \quad (5.31)$$

Thus

$$|PPHT_i(x) - PL_i(x)| \leq \sum_{s=0}^3 |\tilde{a}_{i,s} - a_{i,s}| \left| \left( x - x_{i+\frac{1}{2}} \right)^s \right| = O(h^4),$$

where  $PL_i(x)$  is the Lagrange interpolatory polynomial. Taking into account again the triangular inequality

$$|f(x) - PPHT_i(x)| \leq |f(x) - PL_i(x)| + |PL_i(x) - PPHT_i(x)| = O(h^4),$$

using that Lagrange interpolation also attains fourth order of accuracy.

2. In order to prove Point 2, let us suppose without lost of generalization, that  $x \in [x_{j-1}, x_j]$ . The other case is proven analogously. Since, by hypothesis, the function  $f(x)$  is smooth in  $[x_{j-2}, x_j]$  and



it presents a jump discontinuity in the interval  $[x_j, x_{j+1}]$ , we have  $D_{j-1} = O(1)$  and  $D_j = O(1/h^2)$ . Therefore  $|D_{j-1}| \leq |D_j|$ .

Let  $PL2_{j-1}(x)$  be the second degree Lagrange interpolatory polynomial built using the three pairs of values  $(x_{j-2}, f_{j-2})$ ,  $(x_{j-1}, f_{j-1})$ ,  $(x_j, f_j)$ .

$$PL2_{j-1}(x) = \widehat{a}_{j-1,0} + \widehat{a}_{j-1,1} \left(x - x_{j-\frac{1}{2}}\right) + \widehat{a}_{j-1,2} \left(x - x_{j-\frac{1}{2}}\right)^2,$$

where

$$\begin{aligned}\widehat{a}_{j-1,0} &= \frac{f_{j-1} + f_j}{2} - \frac{h_j^2}{4} D_{j-1}, \\ \widehat{a}_{j-1,1} &= \frac{-f_{j-1} + f_j}{h_j}, \\ \widehat{a}_{j-1,2} &= D_{j-1}.\end{aligned}\tag{5.32}$$

The difference between these coefficients and the ones of  $PPHT_{j-1}(x)$  shown in Equation (5.14) with  $J$  instead of  $\widetilde{V}$  is given by

$$\begin{aligned}\widetilde{a}_{j-1,0} - \widehat{a}_{j-1,0} &= \frac{h_j^2}{4} (D_{j-1} - J_{j-1}), \\ \widetilde{a}_{j-1,1} - \widehat{a}_{j-1,1} &= \frac{h_j^2}{4h_{j-1} + 2h_j} (D_{j-1} - J_{j-1}), \\ \widetilde{a}_{j-1,2} - \widehat{a}_{j-1,2} &= -(D_{j-1} - J_{j-1}), \\ \widetilde{a}_{j-1,3} &= -\frac{2}{2h_{j-1} + h_j} (D_{j-1} - J_{j-1}).\end{aligned}\tag{5.33}$$

Taking into account Equations (5.33), Lemma 20 and the triangular inequality we obtain

$$\begin{aligned}|J_{j-1}(D_{j-1}, D_j)| &\leq \max\left\{\frac{1}{w_{j-1,0}} |D_{j-1} + T|, |T|\right\}, \\ |D_{j-1} - J_{j-1}| &\leq |D_{j-1}| + \max\left\{\frac{1}{w_{j-1,0}} |D_{j-1} + T|, |T|\right\} = O(1), \\ |\widetilde{a}_{j-1,s} - \widehat{a}_{j-1,s}| &= O(h^{2-s}), \quad s = 0, 1, 2, 3, \\ |PPHT_{j-1}(x) - PL2_{j-1}(x)| &\leq \sum_{s=0}^3 |\widetilde{a}_{j-1,s} - \widehat{a}_{j-1,s}| \left| \left(x - x_{j-\frac{1}{2}}\right)^s \right| = O(h^2), \\ |f(x) - PPHT_{j-1}(x)| &\leq |f(x) - PL2_{j-1}(x)| + |PL2_{j-1}(x) - PPHT_{j-1}(x)| = O(h^2).\end{aligned}$$

□

**Remark 12.** *If one pays attention to the proof of point 2 in Theorem 6, and considers the definition of the particular translation proposed in (5.24) and Lemma 22, then it is easy to reach the*

conclusion that the smaller the  $\epsilon$ , the better accuracy obtained in the two intervals adjacent to the jump discontinuity. However, in order for the proof of point 1 to work,  $\epsilon$  must still be  $O(1)$ , so that it is possible to avoid the reduction of order close to inflection points where the second order divided differences could be  $O(h)$  and, therefore, Lemma 21 would not be applicable. A nonlinear choice of the value of  $\epsilon$  seems then appropriate.

**Remark 13.** In the intervals adjacent to the jump discontinuity, one can get third order of accuracy in the cases where there is a change of sign between the two consecutive second divided differences involved in either  $[x_{j-1}, x_j]$  or  $[x_{j+1}, x_{j+2}]$ , just by considering a translation of the type  $\tilde{T}$  in (5.24) with an adapted value of  $\epsilon$ , small enough in those intervals, at least  $\epsilon = O(h)$ . In this cases we will have

$$\max_{x \in [x_{j-1}, x_j] \cup [x_{j+1}, x_{j+2}]} |f(x) - PPHT(x)| = O(h^3).$$

The reason for this fact comes from the expression of the adapted mean  $\tilde{J}$  in these cases, Case A and Case B of Lemma 22, combined with the proof of the second point of Theorem 6 by estimating now the difference  $|D_{j-1} - J_{j-1}| = O(h)$ .

## 5.5 Nonlinear choice of the parameter $\epsilon$ in the translation operator

It turns out that it is better to take a small  $\epsilon$  near a potential jump discontinuity, but it must remain  $O(1)$  at zones where there is the possibility of having second order divided differences  $D_i$  of order  $O(h)$ , just as it happens close to of inflection points. This assessment is also observed in the numerical experiments.

This is the reason why we propose a strategy to choose  $\epsilon$  automatically depending on the data. Inspired by the smoothness indicators proposed in [47],[20], see Remark 14, we propose an  $\epsilon$  with the following expression,

$$\epsilon_j := \frac{h_j^\alpha}{|D_j| + |D_{j+1}| + \xi}, \quad (5.34)$$

where  $\alpha := [\beta(|D_j| + |D_{j+1}|)]$  is the integer part of  $IS_j := \beta(|D_j| + |D_{j+1}|)$ , which stands as a kind of smoothness indicator. The parameter  $\xi = h^4$  is included to avoid divisions by zero. The parameter  $\beta$  is taken into account to make the  $\epsilon$  smaller as we get apart from the inflection points. This fact will result in obtaining a reconstruction almost equal to the original PPH reconstruction in smooth areas without inflection points, allowing the preservation of convexity (see [42]). We have considered  $\beta = 1$  in our numerical experiments. The parameter  $\alpha$  is large when a jump discontinuity affects the stencil used to obtain it and, in turn, this situation will result in a very small value of  $\epsilon_j$  in that area. On the other hand, this indicator provides  $\alpha = 0$  near an inflection point for sufficiently small grid sizes and, therefore,  $\epsilon_j = O(h^{-r})$ , for some  $r > 0$ . Thus,  $\epsilon$  is guaranteed to be large in this region.

**Remark 14.** In [47] Jiang and Shu propose to obtain smoothness indicators using something similar to the total variation, but based in the  $L^2$  norm, so that the result is smoother than the total variation. The proposed formula is just a sum of the  $L^2$  norms of the derivatives of the interpolation polynomials in the cell-averages over the interval  $(x_{j-1/2}, x_{j+1/2})$ . Those indicators are more related with the localization of critical points instead of inflection points. Moreover, for our case expression (5.34) is cheaper computationally since  $D_j$  and  $D_{j+1}$  are already computed.

## 5.6 Numerical experiments

In this section we present a simple numerical test to validate the theoretical results. Our experiment computes the approximation order of the considered reconstructions in several areas corresponding with the different points in Theorem 6. In particular we measure the approximation order in the following areas, identified with the given symbols:

- $A_0$ : In the interval containing the jump discontinuity.
- $A_1$ : In a region where the function is smooth without inflection points and far away from them.
- $A_2$ : In a region where the function is smooth but contains an inflection point.
- $A_3$ : In a region close to the inflection point without containing it.
- $A_4$ : In the subinterval just to the right of the one containing the singularity.

We deal with the following piecewise polynomial reconstruction operators of third degree:

- Lagrange: piecewise centered Lagrange interpolation polynomial.
- PPH: nonlinear reconstruction operator given in Definition 19.
- PPHT,  $\epsilon = 0.5$ : translated version of the PPH reconstruction operator given in Definition 22.
- PPHT,  $\epsilon = 0.05$ : translated version of the PPH reconstruction operator given in Definition 22.
- PPHT,  $\epsilon_j$ : translated version of the PPH reconstruction operator given in Definition 22 using an adaptive value of the parameter  $\epsilon$  according to expression (5.34).

Let  $X^0 = (0, 3, 8, 11, 17, 23, 25, 27, 31, 32, 36, 37.5, 38, 39.3, 40) \frac{\pi}{20}$  be a nonuniform grid in  $[0, 2\pi]$  and  $f(x)$  the following smooth function with a jump discontinuity at  $x = 1.2\pi$ , and an inflection point at  $x = \frac{3\pi}{2}$ ,

$$f(x) := \begin{cases} \sin x & x < 1.2\pi, \\ \cos x + 10 & x \geq 1.2\pi. \end{cases}$$

This function has also inflection points at  $x = 0, \pi$ , but we will be dealing with the indicated regions, letting aside those inflection points. The results for those cases give similar conclusions and they have not been reported. In fact, the numerical tests that have been carried out with different functions presenting well separated inflection points and isolated jump discontinuities give similar results as the one shown in this article. For example, if the jump size is smaller, then the approximation errors are in turn smaller, but the approximation orders present exactly the same behavior (maybe with the need of smaller grid sizes).

In our experiment we have taken for the grid  $X^0$  the following regions  $A_0^0 = [0, 2\pi]$ ,  $A_1^0 = [2, 3]$ ,  $A_2^0 = [4, 5]$ ,  $A_3^0 = [\frac{31\pi}{20}, 6.2]$ ,  $A_4^0 = [\frac{25\pi}{20}, 4]$ . Notice that this intervals correspond to the initial grid  $X^0$  and they need to vary appropriately among the scales  $k$  to satisfy the requirements of the definition of the associated region.

Given the initial abscissas  $x_i^0, i \in I_0 = \{0, \dots, 14\}$ , we consider the set of nested grids  $X^k = \{x_i^k\}_{i \in I^k}$ , where  $x_{2i}^k = x_i^{k-1}$ ,  $x_{2i+1}^k = \frac{x_i^{k-1} + x_{i+1}^{k-1}}{2}$ , and  $I^k = \{x_0^k, \dots, x_{n_k}^k\}$ ,  $k = 0, 1, \dots, 7$ , with

$n_k = 2n_{k-1} - 1$ ,  $n_0 = 14$ . For each level of resolution  $k$ , we build the corresponding reconstruction  $R_k(x)$  using the data  $(x_i^k, f(x_i^k)), i \in I_k$  computing the approximation errors in the infinity norm with respect to the original function using a denser set of abscissas, i.e., we compute a numerical approximation of

$$E_k := \|f(x) - R_k(x)\|_\infty.$$

Then, we compute the numerical approximation order as

$$p = \log_2 \frac{E_{k-1}}{E_k}, \quad k = 1, \dots, 7.$$

Notice that due to Theorem 6 we can assume that for fine enough grids

$$E_k \approx C \left(h^k\right)^p, \quad \text{with } h^k := \max_{i \in I_k \setminus \{0\}} h_i^k, \quad h_i^k := x_i^k - x_{i-1}^k, \quad h^k = \frac{h^{k-1}}{2}.$$

In Tables 5.1, 5.3, 5.5, 5.7, 5.9 we present the errors committed by the considered reconstruction operators by using as initial nodes the defined nested grids  $X^k$ . The errors appear separately for each kind of region  $A_0, A_1, A_2, A_3$  and  $A_4$ . In Tables 5.2, 5.4, 5.6, 5.8, 5.10 appear the corresponding approximation orders.

In Tables 5.1, 5.2 we can see that neither of these methods is designed to adapt in the interval containing the jump discontinuity since it is impossible to localize exactly the discontinuity just working with the point values of the function. The largest error comes near the jump discontinuity for Lagrange reconstruction, as it can be observed in the column corresponding to this reconstruction. In the region  $A_1$  all the reconstruction operators attain fourth order of accuracy,  $p = 4$ , as it can be seen in Tables 5.3, 5.4. Regions  $A_2$  and  $A_3$  correspond to the vicinity of an inflection point, where the nonlinear PPH reconstruction operator reduces the approximation order to third order. We can observe in Tables 5.5, 5.6, 5.7, 5.8 how all the translated versions get closer to fourth order in these two regions,  $A_2$  and  $A_3$ . Albeit, the version with larger  $\epsilon$  and adapted  $\epsilon_j$  perform in a better way than with smaller  $\epsilon$  in these cases. Finally in Tables 5.9, 5.10 we can see how the nonlinear reconstruction operators reach second order of accuracy in the intervals to the right and to the left of the interval containing the jump discontinuity, while the linear Lagrange reconstruction operator completely loses the order of approximation. In the case of the adapted translated version, we get third order due to the observation given in Remark 13.

In Figure 5.1 we plot the function  $f(x)$  and the Lagrange, and PPHT (with  $\epsilon_j$  adapted) reconstructions obtained from the initial grids  $X^k, k = 0, 1, 2$ . We can see that around the singularity, Lagrange reconstruction loses the approximation order and the Gibbs phenomena appears. In this zone, PPHT reconstruction performs in a more proper way, avoiding any Gibbs effects. We can see that no oscillations appear in the PPHT reconstruction even for the coarsest grid. These observations can be seen more clearly in Figure 5.2 where we have plotted a zoom of this region for  $k = 3$  for both operators Lagrange and *PPHT*. We also point out that the oscillations due to the jump discontinuity in Lagrange reconstruction do not diminish to zero with the subdivision level.

In Figure 5.3 we analyze the numerical behavior of the truncation parameter  $\epsilon$  and the effect of the parameter  $\beta$  introduced in its definition. As we can see the large values of  $\epsilon$  correspond with the areas around the inflection points of the function and the parameter takes values very close to  $\epsilon = 0$  in the three intervals around the jump discontinuity. The effect of  $\beta$  is more noticeable as we increase its value from  $\beta = 1$  to  $\beta = 100$ , setting the value of the parameter  $\epsilon$  closer to zero for the smooth areas without inflection points. This fact makes the translated version of this reconstruction similar to the original PPH reconstruction operator in smooth convex areas.

**Remark 15.** *The numerical experiment has been carried out using a finite interval, that in principle, falls out from the scope of Theorem 6. However, the results are also true for the finite case away from the boundaries, and the proof remains exactly the same. Notice that any finite discretization of a finite interval is a  $\sigma$  quasi-uniform grid according to Definition 23. The boundaries have been treated by using non-centered third degree Lagrange polynomials, so that if we take into account that the discontinuity and the inflection point are placed far from the boundaries, they do not affect to the attained numerical approximation order.*

## 5.7 Conclusions

Using the general definition of a translation operator given in [20], and previously mentioned in [6], we have considered several specific cases. In particular, we have studied a way of choosing a translation adaptively depending on the specific data to which it is going to be applied. In turn, this translation operator has been used to extend the definition of the already existing PPH reconstruction operator on nonuniform grids [42, 43] to work appropriately with functions which are not necessarily strictly convex. We give a corresponding theorem ensuring the pursued objective of getting fourth order of approximation at the smooth parts of the function, independently of the presence or not of inflection points. Finally we have performed some numerical experiments to check the behavior of the proposed adaptation.

$k$	<i>Lagrange</i>	<i>PPH</i>	<i>PPHT, <math>\epsilon = 0.5</math></i>	<i>PPHT, <math>\epsilon = 0.05</math></i>	<i>PPHT, <math>\epsilon_j</math></i>
$k = 0$	5.6495	5.0072	4.8870	4.9125	4.9153
$k = 1$	9.4448	9.3051	9.1754	9.1740	9.1738
$k = 2$	9.3578	9.3588	9.5194	9.5194	9.5195
$k = 3$	9.3587	9.3591	9.5207	9.5208	9.5208
$k = 4$	9.3591	9.3593	9.5214	9.5214	9.5214
$k = 5$	9.3593	9.3594	9.5217	9.5217	9.5217
$k = 6$	9.3594	9.3595	9.5219	9.5219	9.5219
$k = 7$	9.3595	9.3595	9.5220	9.5220	9.5220

Table 5.1: Approximation errors  $E_k$  in the infinity norm obtained at iteration  $k, k = 0, \dots, 7$  by using the considered reconstruction operators, Lagrange PPH, PPHT with  $\epsilon = 0.5$ , PPHT with  $\epsilon = 0.05$ , and PPHT with adapted  $\epsilon_j$  in the region  $A_0$ .

$k$	<i>Lagrange</i>	<i>PPH</i>	<i>PPHT</i> , $\epsilon = 0.5$	<i>PPHT</i> , $\epsilon = 0.05$	<i>PPHT</i> , $\epsilon_j$
$k = 1$	$-7.4 \times 10^{-1}$	$-8.9 \times 10^{-1}$	$-9.1 \times 10^{-1}$	$-9.0 \times 10^{-1}$	$-9.0 \times 10^{-1}$
$k = 2$	$1.3 \times 10^{-2}$	$-8.3 \times 10^{-3}$	$-5.3 \times 10^{-2}$	$-5.3 \times 10^{-2}$	$-5.3 \times 10^{-2}$
$k = 3$	$-1.3 \times 10^{-4}$	$-5.4 \times 10^{-5}$	$-2.1 \times 10^{-4}$	$-2.0 \times 10^{-4}$	$-2.0 \times 10^{-4}$
$k = 4$	$6.5 \times 10^{-5}$	$-2.9 \times 10^{-5}$	$-1.0 \times 10^{-4}$	$-9.9 \times 10^{-5}$	$-9.9 \times 10^{-5}$
$k = 5$	$3.3 \times 10^{-5}$	$-1.5 \times 10^{-5}$	$-5.0 \times 10^{-5}$	$-5.0 \times 10^{-5}$	$-4.9 \times 10^{-5}$
$k = 6$	$1.6 \times 10^{-5}$	$-7.4 \times 10^{-6}$	$-2.4 \times 10^{-5}$	$-2.5 \times 10^{-5}$	$-2.4 \times 10^{-5}$
$k = 7$	$8.1 \times 10^{-6}$	$-3.7 \times 10^{-6}$	$-1.2 \times 10^{-5}$	$-1.2 \times 10^{-5}$	$-1.2 \times 10^{-5}$

Table 5.2: Approximation orders  $p$  in the infinity norm obtained at iteration  $k, k = 1, \dots, 7$  by using the considered reconstruction operators, Lagrange PPH, PPHT with  $\epsilon = 0.5$ , PPHT with  $\epsilon = 0.05$ , and PPHT with adapted  $\epsilon_j$  in the region  $A_0$ .

$k$	<i>Lagrange</i>	<i>PPH</i>	<i>PPHT</i> , $\epsilon = 0.5$	<i>PPHT</i> , $\epsilon = 0.05$	<i>PPHT</i> , $\epsilon_j$
$k = 0$	3.7038	$1.9182 \times 10^{-2}$	$1.4586 \times 10^{-1}$	$2.7869 \times 10^{-2}$	$4.4601 \times 10^{-2}$
$k = 1$	$7.3685 \times 10^{-4}$	$6.5968 \times 10^{-3}$	$1.4201 \times 10^{-3}$	$4.6348 \times 10^{-3}$	$9.5688 \times 10^{-4}$
$k = 2$	$6.2735 \times 10^{-5}$	$8.3401 \times 10^{-4}$	$9.4378 \times 10^{-5}$	$4.5210 \times 10^{-4}$	$6.9863 \times 10^{-5}$
$k = 3$	$4.0575 \times 10^{-6}$	$3.4729 \times 10^{-5}$	$5.8493 \times 10^{-6}$	$2.2392 \times 10^{-5}$	$4.4229 \times 10^{-6}$
$k = 4$	$2.5733 \times 10^{-7}$	$2.6086 \times 10^{-6}$	$3.6925 \times 10^{-7}$	$1.5670 \times 10^{-6}$	$2.7765 \times 10^{-7}$
$k = 5$	$1.5978 \times 10^{-8}$	$1.8126 \times 10^{-7}$	$2.3181 \times 10^{-8}$	$1.0414 \times 10^{-7}$	$1.7329 \times 10^{-8}$
$k = 6$	$1.0021 \times 10^{-9}$	$1.0730 \times 10^{-8}$	$1.4459 \times 10^{-9}$	$6.3099 \times 10^{-9}$	$1.0840 \times 10^{-9}$
$k = 7$	$6.2737 \times 10^{-11}$	$6.5331 \times 10^{-10}$	$9.0272 \times 10^{-11}$	$3.8843 \times 10^{-10}$	$6.7782 \times 10^{-11}$

Table 5.3: Approximation errors  $E_k$  in the infinity norm obtained at iteration  $k, k = 0, \dots, 7$  by using the considered reconstruction operators, Lagrange PPH, PPHT with  $\epsilon = 0.5$ , PPHT with  $\epsilon = 0.05$ , and PPHT with adapted  $\epsilon_j$  in the region  $A_1$ .

$k$	<i>Lagrange</i>	<i>PPH</i>	<i>PPHT, <math>\epsilon = 0.5</math></i>	<i>PPHT, <math>\epsilon = 0.05</math></i>	<i>PPHT, <math>\epsilon_j</math></i>
$k = 1$	12.2953	1.5399	6.6824	2.5881	5.5426
$k = 2$	3.5540	2.9836	3.9114	3.3578	3.7757
$k = 3$	3.9506	4.5859	4.0121	4.3356	3.9815
$k = 4$	3.9789	3.7348	3.9856	3.8369	3.9937
$k = 5$	4.0094	3.8472	3.9935	3.9115	4.0019
$k = 6$	3.9950	4.0784	4.0030	4.0447	3.9987
$k = 7$	3.9976	4.0377	4.0015	4.0219	3.9994

Table 5.4: Approximation orders  $p$  in the infinity norm obtained at iteration  $k, k = 1, \dots, 7$  by using the considered reconstruction operators, Lagrange PPH, PPHT with  $\epsilon = 0.5$ , PPHT with  $\epsilon = 0.05$ , and PPHT with adapted  $\epsilon_j$  in the region  $A_1$ .

$k$	<i>Lagrange</i>	<i>PPH</i>	<i>PPHT, <math>\epsilon = 0.5</math></i>	<i>PPHT, <math>\epsilon = 0.05</math></i>	<i>PPHT, <math>\epsilon_j</math></i>
$k = 0$	$7.5463 \times 10^{-1}$	$8.3447 \times 10^{-3}$	$2.3123 \times 10^{-2}$	$5.6651 \times 10^{-3}$	$2.9178 \times 10^{-3}$
$k = 1$	$4.2214 \times 10^{-5}$	$7.8190 \times 10^{-4}$	$1.9193 \times 10^{-4}$	$6.4427 \times 10^{-4}$	$6.7164 \times 10^{-5}$
$k = 2$	$3.4996 \times 10^{-6}$	$2.4763 \times 10^{-4}$	$1.8960 \times 10^{-5}$	$1.0918 \times 10^{-4}$	$5.3926 \times 10^{-6}$
$k = 3$	$3.0851 \times 10^{-7}$	$3.0993 \times 10^{-5}$	$1.2028 \times 10^{-6}$	$8.7545 \times 10^{-6}$	$4.8008 \times 10^{-7}$
$k = 4$	$2.2334 \times 10^{-8}$	$3.8754 \times 10^{-6}$	$7.5666 \times 10^{-8}$	$6.3675 \times 10^{-7}$	$3.3935 \times 10^{-8}$
$k = 5$	$1.4894 \times 10^{-9}$	$4.8446 \times 10^{-7}$	$4.7431 \times 10^{-9}$	$4.3337 \times 10^{-8}$	$2.2339 \times 10^{-9}$
$k = 6$	$9.5977 \times 10^{-11}$	$6.0559 \times 10^{-8}$	$2.9687 \times 10^{-10}$	$2.8345 \times 10^{-9}$	$1.4299 \times 10^{-10}$
$k = 7$	$6.0880 \times 10^{-12}$	$7.5699 \times 10^{-9}$	$1.8566 \times 10^{-11}$	$1.8137 \times 10^{-10}$	$9.040 \times 10^{-12}$

Table 5.5: Approximation errors  $E_k$  in the infinity norm obtained at iteration  $k, k = 0, \dots, 7$  by using the considered reconstruction operators, Lagrange PPH, PPHT with  $\epsilon = 0.5$ , PPHT with  $\epsilon = 0.05$ , and PPHT with adapted  $\epsilon_j$  in the region  $A_2$ .

$k$	<i>Lagrange</i>	<i>PPH</i>	<i>PPHT, <math>\epsilon = 0.5</math></i>	<i>PPHT, <math>\epsilon = 0.05</math></i>	<i>PPHT, <math>\epsilon_j</math></i>
$k = 1$	14.1257	3.4158	6.9126	3.1364	5.4411
$k = 2$	3.5925	1.6588	3.3395	2.5609	3.6386
$k = 3$	3.5038	2.9982	3.9784	3.6406	3.4896
$k = 4$	3.7880	2.9995	3.9907	3.7812	3.8224
$k = 5$	3.9064	2.9999	3.9957	3.8770	3.9251
$k = 6$	3.9559	3.0000	3.9980	3.9344	3.9655
$k = 7$	3.9787	3.0000	3.9990	3.9661	3.9835

Table 5.6: Approximation orders  $p$  in the infinity norm obtained at iteration  $k, k = 1, \dots, 7$  by using the considered reconstruction operators, Lagrange PPH, PPHT with  $\epsilon = 0.5$ , PPHT with  $\epsilon = 0.05$ , and PPHT with adapted  $\epsilon_j$  in the region  $A_2$ .

$k$	<i>Lagrange</i>	<i>PPH</i>	<i>PPHT, <math>\epsilon = 0.5</math></i>	<i>PPHT, <math>\epsilon = 0.05</math></i>	<i>PPHT, <math>\epsilon_j</math></i>
$k = 0$	$6.3455 \times 10^{-4}$	$2.2239 \times 10^{-3}$	$1.2150 \times 10^{-3}$	$1.9915 \times 10^{-3}$	$8.6245 \times 10^{-4}$
$k = 1$	$9.0640 \times 10^{-5}$	$2.9306 \times 10^{-4}$	$1.4797 \times 10^{-4}$	$2.5484 \times 10^{-4}$	$1.1640 \times 10^{-4}$
$k = 2$	$9.2479 \times 10^{-6}$	$3.4429 \times 10^{-5}$	$1.6629 \times 10^{-5}$	$3.0064 \times 10^{-5}$	$1.2170 \times 10^{-5}$
$k = 3$	$6.5454 \times 10^{-7}$	$2.7653 \times 10^{-6}$	$1.0760 \times 10^{-6}$	$2.3029 \times 10^{-6}$	$8.1262 \times 10^{-7}$
$k = 4$	$4.3080 \times 10^{-8}$	$2.0098 \times 10^{-7}$	$6.8410 \times 10^{-8}$	$1.6202 \times 10^{-7}$	$5.1976 \times 10^{-8}$
$k = 5$	$2.7567 \times 10^{-9}$	$4.3976 \times 10^{-8}$	$4.6111 \times 10^{-9}$	$2.2983 \times 10^{-8}$	$3.2797 \times 10^{-9}$
$k = 6$	$1.7424 \times 10^{-10}$	$4.6559 \times 10^{-9}$	$2.9178 \times 10^{-10}$	$1.8210 \times 10^{-9}$	$2.0587 \times 10^{-10}$
$k = 7$	$1.0951 \times 10^{-11}$	$5.0457 \times 10^{-10}$	$1.8375 \times 10^{-11}$	$1.3610 \times 10^{-10}$	$1.2895 \times 10^{-11}$

Table 5.7: Approximation errors  $E_k$  in the infinity norm obtained at iteration  $k, k = 0, \dots, 7$  by using the considered reconstruction operators, Lagrange PPH, PPHT with  $\epsilon = 0.5$ , PPHT with  $\epsilon = 0.05$ , and PPHT with adapted  $\epsilon_j$  in the region  $A_3$ .



$k$	<i>Lagrange</i>	<i>PPH</i>	<i>PPHT, <math>\epsilon = 0.5</math></i>	<i>PPHT, <math>\epsilon = 0.05</math></i>	<i>PPHT, <math>\epsilon_j</math></i>
$k = 1$	2.8075	2.9238	3.0376	2.9662	2.8893
$k = 2$	3.2929	3.0895	3.1535	3.0835	3.2577
$k = 3$	3.8206	3.6381	3.9500	3.7065	3.9046
$k = 4$	3.9254	3.7823	3.9753	3.8291	3.9667
$k = 5$	3.9660	2.1923	3.8910	2.8176	3.9862
$k = 6$	3.9838	3.2396	3.9821	3.6578	3.9937
$k = 7$	3.9919	3.2059	3.9891	3.7420	3.9969

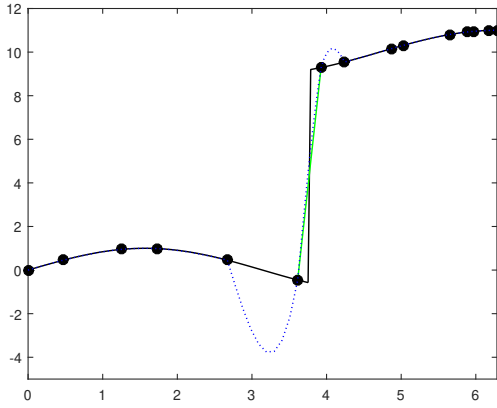
Table 5.8: Approximation orders  $p$  in the infinity norm obtained at iteration  $k, k = 1, \dots, 7$  by using the considered reconstruction operators, Lagrange PPH, PPHT with  $\epsilon = 0.5$ , PPHT with  $\epsilon = 0.05$ , and PPHT with adapted  $\epsilon_j$  in the region  $A_3$ .

$k$	<i>Lagrange</i>	<i>PPH</i>	<i>PPHT, <math>\epsilon = 0.5</math></i>	<i>PPHT, <math>\epsilon = 0.05</math></i>	<i>PPHT, <math>\epsilon_j</math></i>
$k = 0$	$7.5463 \times 10^{-1}$	$7.3017 \times 10^{-3}$	$2.3122 \times 10^{-2}$	$4.9884 \times 10^{-3}$	$2.9178 \times 10^{-3}$
$k = 1$	$6.1204 \times 10^{-1}$	$2.3996 \times 10^{-3}$	$3.3130 \times 10^{-3}$	$4.8664 \times 10^{-4}$	$1.7116 \times 10^{-4}$
$k = 2$	$6.1887 \times 10^{-1}$	$6.1993 \times 10^{-4}$	$8.0841 \times 10^{-4}$	$9.8797 \times 10^{-5}$	$1.9854 \times 10^{-5}$
$k = 3$	$6.2234 \times 10^{-1}$	$1.5738 \times 10^{-4}$	$1.9971 \times 10^{-4}$	$2.2119 \times 10^{-5}$	$2.3812 \times 10^{-6}$
$k = 4$	$6.2409 \times 10^{-1}$	$3.9636 \times 10^{-5}$	$4.9635 \times 10^{-5}$	$5.2260 \times 10^{-6}$	$2.9126 \times 10^{-7}$
$k = 5$	$6.2496 \times 10^{-1}$	$9.9451 \times 10^{-6}$	$1.2372 \times 10^{-5}$	$1.2697 \times 10^{-6}$	$3.6003 \times 10^{-8}$
$k = 6$	$6.2540 \times 10^{-1}$	$2.4908 \times 10^{-6}$	$3.0887 \times 10^{-6}$	$3.1290 \times 10^{-7}$	$4.4750 \times 10^{-9}$
$k = 7$	$6.2562 \times 10^{-1}$	$6.2325 \times 10^{-7}$	$7.7161 \times 10^{-7}$	$7.7664 \times 10^{-8}$	$5.5778 \times 10^{-10}$

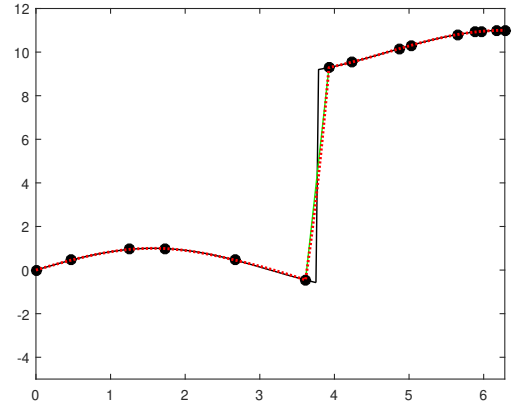
Table 5.9: Approximation errors  $E_k$  in the infinity norm obtained at iteration  $k, k = 0, \dots, 7$  by using the considered reconstruction operators, Lagrange PPH, PPHT with  $\epsilon = 0.5$ , PPHT with  $\epsilon = 0.05$ , and PPHT with adapted  $\epsilon_j$  in the region  $A_4$ .

$k$	<i>Lagrange</i>	<i>PPH</i>	<i>PPHT, <math>\epsilon = 0.5</math></i>	<i>PPHT, <math>\epsilon = 0.05</math></i>	<i>PPHT, <math>\epsilon_j</math></i>
$k = 1$	0.3021	1.6054	2.8031	3.3577	4.0914
$k = 2$	-0.0160	1.9526	2.0350	2.3003	3.1078
$k = 3$	-0.0081	1.9779	2.0172	2.1591	3.0597
$k = 4$	-0.0040	1.9893	2.0085	2.0815	3.0314
$k = 5$	-0.0020	1.9948	2.0042	2.0412	3.0161
$k = 6$	-0.0010	1.9974	2.0021	2.0207	3.0082
$k = 7$	-0.0005	1.9987	2.0010	2.0104	3.0041

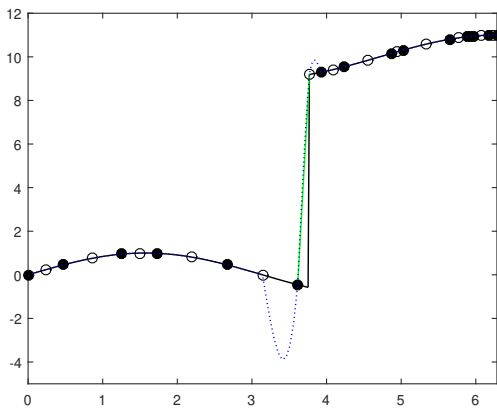
Table 5.10: Approximation orders  $p$  in the infinity norm obtained at iteration  $k, k = 1, \dots, 7$  by using the considered reconstruction operators, Lagrange PPH, PPHT with  $\epsilon = 0.5$ , PPHT with  $\epsilon = 0.05$ , and PPHT with adapted  $\epsilon_j$  in the region  $A_4$ .



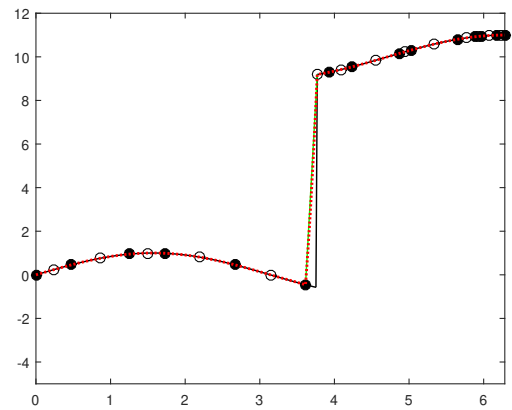
(a)



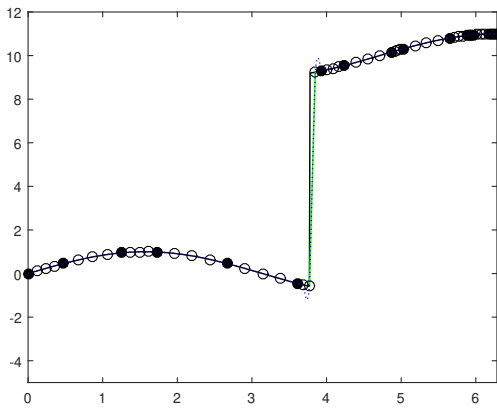
(b)



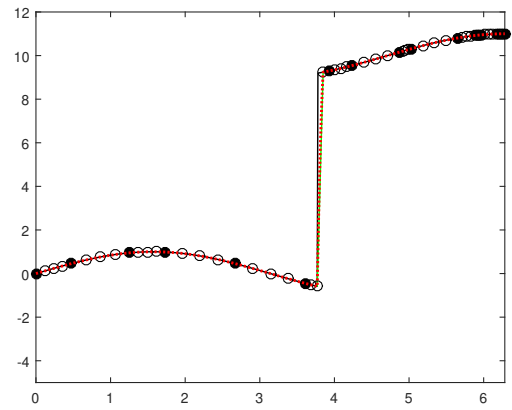
(c)



(d)

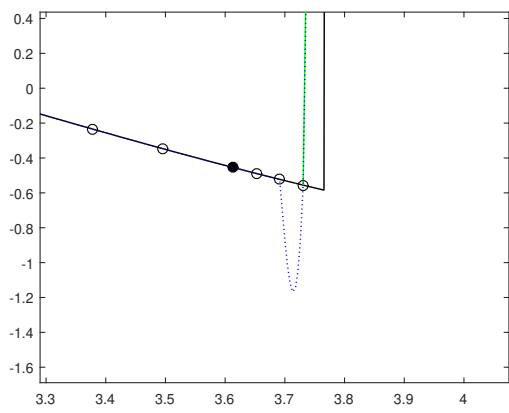


(e)

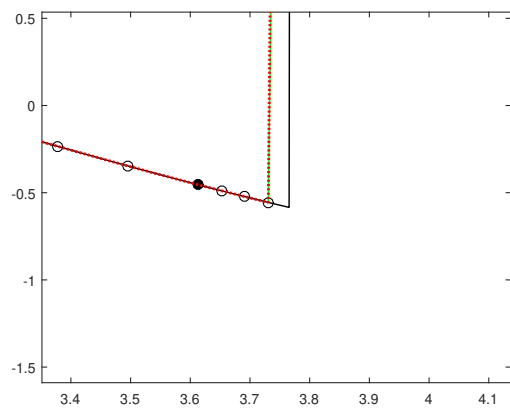


(f)

Figure 5.1: In black solid line: function  $f(x)$ . In green solid line the straight line joining the extreme points of the jump interval  $[x_j^k, x_{j+1}^k]$ . In blue dotted line: Lagrange reconstruction. In red dotted line: PPHT reconstruction with adapted  $\epsilon_j$ . Void circles stand for initial nodes, filled circles for nodes at the  $k$  subdivision level. **(a)**: Lagrange  $k = 0$ , **(b)**: PPHT  $k = 0$ , **(c)**: Lagrange  $k = 1$ , **(d)**: PPHT  $k = 1$ , **(e)**: Lagrange  $k = 2$ , **(f)**: PPHT  $k = 2$ .

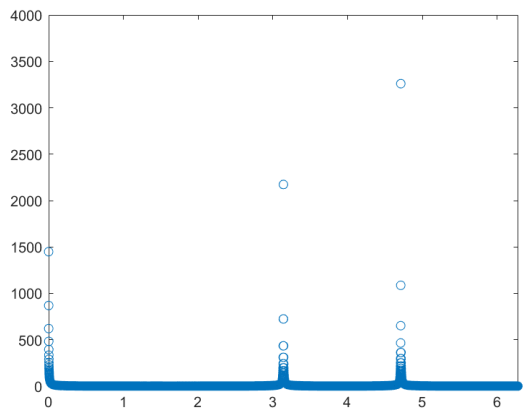


(a)

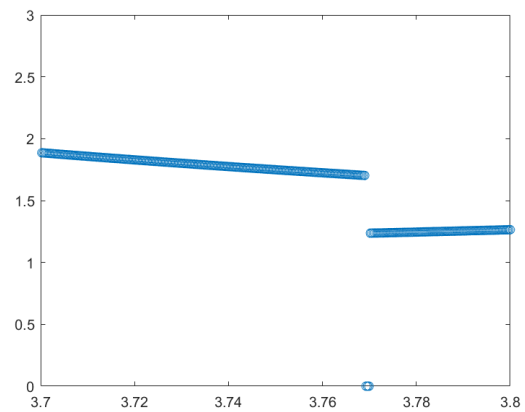


(b)

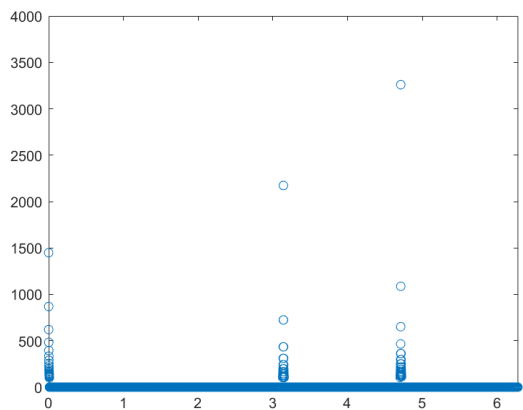
Figure 5.2: Zoom of the region around the jump discontinuity for subdivision grid level  $k=3$ . (a): Lagrange, (b): PPHT with adapted  $\epsilon_j$ .



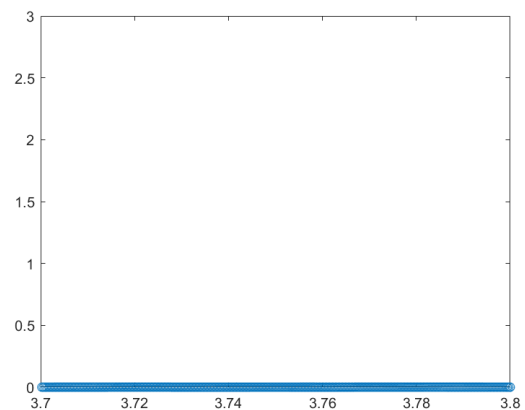
(a)



(b)



(c)



(d)

Figure 5.3: Values of the  $\epsilon$  parameter in (5.34) along different intervals for the  $x$  variable. **(a)**: for  $\beta = 1$  in the interval  $[0, 2\pi]$ , **(b)**: for  $\beta = 1$  in the interval  $[3.7, 3.8]$ , **(c)**: for  $\beta = 100$  in the interval  $[0, 2\pi]$ , **(d)**: for  $\beta = 100$  in the interval  $[3.7, 3.8]$ .

## Chapter 6

# On certain inequalities associated to curvature properties of the nonlinear PPH reconstruction operator

The contents of this chapter are wholly included in the already published paper [44]

- Ortiz, P.; Trillo, J.C. On certain inequalities associated to curvature properties of the nonlinear PPH reconstruction operator. *Journal of Inequalities and Applications*. **2019**, Paper No. 8, 13 pp, <https://doi.org/10.1186/s13660-019-1959-0>

### 6.1 Introduction

Reconstruction and subdivision operators have been studied, analyzed and implemented in computer aided geometric design giving rise to interesting applications in different fields of science. Subdivision schemes provide easy and fast algorithms for the generation of curves and surfaces from a coarse initial set of control points. They are closely related to reconstruction operators.

Starting from a given set of data, the target of the reconstruction operators is to obtain a piecewise function  $p(x)$  which interpolates or approximates the data preserving certain properties which are of interest because of some geometrical or physical reasons. One particular case is given by smoothing splines (see [23], [46]) in a given interval  $[a, b]$ . They are built through polynomial reconstruction pieces that are connected in a smooth way at the control knots and that satisfy the minimization problem

$$\min_{p \in \Pi_n} J(p) := \min_{p \in \Pi_n} \int_a^b p''(x)^2 dx + \sum_j \mu_j (p(x_j) - f_j)^2, \quad (6.1)$$

where  $\Pi_n$  stands for the polynomials of degree less or equal to  $n$ . The considered functional implies a balance, dominated by the weights  $\mu_j$ , between a low curvature term and a small value of the accumulated distance to the initial set of data  $(x_j, f_j)$ .

PPH reconstruction was firstly defined in [6], although as subdivision scheme was already introduced in [32]. Later the PPH reconstruction operator was extended to allow for the use of nonuniform meshes [41], issue that is needed to link this reconstruction with general splines. This

reconstruction is inherently a nonlinear interpolatory technique that has some remarkable characteristics. We mention those that are attractive for our purposes. In particular: a fixed centered stencil is used to build each polynomial piece, fourth order accuracy is reached in smooth convex regions, reduction to second order occurs at the vicinity of singularities but the approximation order is not completely lost as it happens in the linear case, and Gibb's effect is avoided. Also we specially remark two more properties which are going to be crucial for this reconstruction. The convexity preservation when dealing with initial discrete set of convex data [41] and a low curvature term. This last property about the curvature is part of what is going to be proven in next sections. More precisely we study the term of curvature of the functional (6.1) for the Lagrange and PPH reconstructions, in the uniform and the nonuniform case. Then, due to these suitable properties, we think that connecting the PPH reconstruction with smoothing splines could result in very interesting applications.

The chapter is organized as follows: In Section 6.2 we analyze the curvature term for the Lagrange and the PPH reconstruction on uniform meshes. In Section 6.3 we study the case of nonuniform meshes. Finally, in Section 6.4 we present some conclusions and future perspectives.

## 6.2 Study of the curvature term in uniform meshes

Let us consider the set of values  $f_{j-1}, f_j, f_{j+1}, f_{j+2}$  corresponding to subsequent ordinates at the abscissas  $x_{j-1}, x_j, x_{j+1}, x_{j+2}$  of a regular grid  $X$  with fix grid spacing  $h = x_{j+1} - x_j$ . The set of polynomials  $p(x)$  which pass through the central points  $(x_j, f_j)$  and  $(x_{j+1}, f_{j+1})$  can be written in terms of two free variables  $A$  and  $B$  as follows

$$p(x) := -\frac{1}{6}(x - x_j)(x_{j+1} - x) \left[ A \left( 1 + \frac{x_{j+1} - x}{h} \right) + B \left( 1 + \frac{x - x_j}{h} \right) \right] + \frac{x_{j+1} - x}{h} f_j + \frac{x - x_j}{h} f_{j+1}. \quad (6.2)$$

From now on, we will use the following definition of the local curvature term.

**Definition 24.** *Given a polynomial  $p(x)$  in an interval  $[x_j, x_{j+1}]$  we define the local curvature term as*

$$C(p) := \int_{x_j}^{x_{j+1}} p''(x)^2 dx. \quad (6.3)$$

In order to compute the local curvature term in Definition 24 for the set of polynomials given by (6.2) we proceed as follows. The difference between the evaluation of polynomial (6.2) and the corresponding initial data at the abscissas  $x_{j-1}, x_{j+2}$  is given by

$$p(x_{j-1}) - f_{j-1} = h^2(A - 2D_j), \quad p(x_{j+2}) - f_{j+2} = h^2(B - 2D_{j+1}), \quad (6.4)$$

where  $D_j$  and  $D_{j+1}$  are the second order divided differences

$$D_j = \frac{f_{j-1} - 2f_j + f_{j+1}}{2h^2}, \quad D_{j+1} = \frac{f_j - 2f_{j+1} + f_{j+2}}{2h^2}. \quad (6.5)$$

Computing the second derivative of the polynomial  $p(x)$  in (6.2) and introducing this computation in the *local curvature term* of expression (6.1) we get

$$C(p) := \int_{x_j}^{x_{j+1}} p''(x)^2 dx = \frac{h}{3}(A^2 + AB + B^2). \quad (6.6)$$

### 6.2.1 Curvature term for the Lagrange reconstruction

Let  $p_L(x)$  be the third degree Lagrange polynomial which interpolates the data  $(x_{j+s}, f_{j+s})$ ,  $s = -1, 0, 1, 2$ . In order to write  $p_L(x)$  in the form of polynomial (6.2) we look for the appropriate values of the parameters  $A$  and  $B$  which allow for the remaining interpolation conditions to be satisfied

$$p_L(x_{j-1}) = f_{j-1}, \quad p_L(x_{j+2}) = f_{j+2}. \quad (6.7)$$

Solving the last two equations we get

$$A_L = 2D_j, \quad B_L = 2D_{j+1}.$$

Thus, the defined curvature term (6.6) takes the form

$$C_L := C(p_L) = \frac{4h}{3}(D_j^2 + D_j D_{j+1} + D_{j+1}^2). \quad (6.8)$$

### 6.2.2 Curvature term for the PPH reconstruction

Let now  $p_H(x)$  be the PPH polynomial (see [6]). This fourth order reconstruction based also on the data  $(x_{j+s}, f_{j+s})$ ,  $s = -1, 0, 1, 2$ , basically proceeds as follows: firstly a modification of either  $f_{j-1}$  or  $f_{j+2}$  is carried out in order to avoid the bad influence of a potential singularity at  $[x_{j-1}, x_j]$  or  $[x_{j+1}, x_{j+2}]$  respectively, secondly a third order Lagrange interpolation is applied to the modified data. Then, due to this intrinsically nonlinear nature we need to consider two different cases to carry out the curvature study for  $p_H(x)$ . This is done in the following theorem.

**Theorem 7.** *The curvature term associated to the PPH polynomial  $p_H(x)$  in a uniform mesh with grid spacing  $h$  is given by*

$$C_H = \begin{cases} \frac{4hD_j^2(D_j^2 - 2D_jD_{j+1} + 13D_{j+1}^2)}{3(D_j + D_{j+1})^2} & \text{if } |D_j| \leq |D_{j+1}| \ \& \ D_j D_{j+1} > 0, \\ \frac{4hD_j^2}{3} & \text{if } |D_j| \leq |D_{j+1}| \ \& \ D_j D_{j+1} \leq 0, \\ \frac{4hD_{j+1}^2(13D_j^2 - 2D_jD_{j+1} + D_{j+1}^2)}{3(D_j + D_{j+1})^2} & \text{if } |D_j| > |D_{j+1}| \ \& \ D_j D_{j+1} > 0, \\ \frac{4hD_{j+1}^2}{3} & \text{if } |D_j| > |D_{j+1}| \ \& \ D_j D_{j+1} \leq 0, \end{cases} \quad (6.9)$$

where  $D_j$  and  $D_{j+1}$  are the second order divided differences defined as,

$$D_j = \frac{f_{j-1} - 2f_j + f_{j+1}}{2h^2}, \quad D_{j+1} = \frac{f_j - 2f_{j+1} + f_{j+2}}{2h^2}.$$

Moreover, for all cases  $C_H$  satisfies  $C_L - C_H \geq 0$ .



*Proof.* Depending on the absolute values of the second order divided differences  $D_j$  and  $D_{j+1}$  in (6.5) we analyze the following two cases:

**Case 1.**  $|D_j| \leq |D_{j+1}|$ , i.e, a potential singularity lies at  $[x_{j+1}, x_{j+2}]$ .

In this case in order to build the  $p_H(x)$  in the form of polynomial (6.2) we need to impose the following two conditions

$$p_H(x_{j-1}) = f_{j-1}, \quad p_H(x_{j+2}) = \tilde{f}_{j+2}, \quad (6.10)$$

where  $\tilde{f}_{j+2}$  represents the modified value at  $x_{j+2}$ , and it is computed by (see [6] for more details)

$$\tilde{f}_{j+2} = f_{j+2} - 4h^2 \left( \frac{D_j + D_{j+1}}{2} - \tilde{V}_j \right), \quad (6.11)$$

where  $\tilde{V}_j$  stands for the extended *Harmonic* mean defined by

$$\tilde{V}_j = \begin{cases} \frac{2D_j D_{j+1}}{D_j + D_{j+1}} & \text{if } D_j D_{j+1} > 0, \\ 0 & \text{else.} \end{cases} \quad (6.12)$$

Solving equations (6.10) for the free parameters results in

$$A_H = 2D_j, \quad B_H = 4\tilde{V}_j - 2D_j.$$

Depending on the sign of the product  $D_j D_{j+1}$ , the parameter  $B_H$  takes a different expression, and therefore the same happens for the curvature term  $C_H$  defined by  $C_H := C(p_H)$ , according to expression (6.6). We consider now the following new two cases,

**Case 1.1.**  $D_j D_{j+1} > 0$ .

In this case the term  $B_H$  reads

$$B_H = \frac{2D_j(3D_{j+1} - D_j)}{D_j + D_{j+1}},$$

and thus

$$C_H = \frac{4hD_j^2(D_j^2 - 2D_j D_{j+1} + 13D_{j+1}^2)}{3(D_j + D_{j+1})^2}.$$

It is now interesting and in fact part of our objective with this computation to compare the obtained curvature with the previous result (6.8) for the usual third order Lagrange polynomial. Performing this comparison we reach to

$$C_L - C_H = \frac{4hD_{j+1}(D_{j+1} - D_j)^2(5D_j + D_{j+1})}{3(D_j + D_{j+1})^2} \geq 0, \quad (6.13)$$

which shows clearly that the curvature term  $C_H$  for the PPH reconstruction is always lower than the corresponding curvature  $C_L$  for the Lagrange polynomial. This could be an interesting property in practical applications related with manufacturing and graphical design.

We study now the other case.

**Case 1.2.**  $D_j D_{j+1} \leq 0$ .

In this case the terms  $B_H$  and  $C_H$  read

$$B_H = -2D_j, \quad C_H = \frac{4hD_j^2}{3}.$$

Therefore the difference  $C_L - C_H$  is now

$$C_L - C_H = \frac{4hD_{j+1}(D_j + D_{j+1})}{3} \geq 0. \quad (6.14)$$

Again we see that also in this case the curvature term  $C_H$  for the PPH reconstruction is lower than the corresponding curvature  $C_L$  for the Lagrange polynomial.

**Case 2.**  $|D_j| > |D_{j+1}|$ , i.e, the potential singularity lies at  $[x_{j-1}, x_j]$ . In this second case in order to build the polynomial  $p_H(x)$  in the form (6.2) we need to impose the following two conditions

$$p_H(x_{j-1}) = \tilde{f}_{j-1}, \quad p_H(x_{j+2}) = f_{j+2}. \quad (6.15)$$

where  $\tilde{f}_{j-1}$  is the modified value at  $x_{j-1}$ . Its expression is given by (see [6] for more details)

$$\tilde{f}_{j-1} = f_{j-1} - 4h^2 \left( \frac{D_j + D_{j+1}}{2} - \tilde{V}_j \right), \quad (6.16)$$

Working in a similar way to case 1 we obtain

$$A_H = 4\tilde{V}_j - 2D_{j+1}, \quad B_H = 2D_{j+1}.$$

and depending on the sign of the product  $D_j D_{j+1}$  we consider two subcases.

**Case 2.1.**  $D_j D_{j+1} > 0$ .

Replacing  $\tilde{V}_j$  by (6.12) in the expression of  $A_H$  we get

$$A_H = \frac{2D_{j+1}(3D_j - D_{j+1})}{D_j + D_{j+1}},$$

and therefore from (6.6) we have

$$C_H = \frac{4hD_{j+1}^2(13D_j^2 - 2D_j D_{j+1} + D_{j+1}^2)}{3(D_j + D_{j+1})^2}.$$

Computing the difference between the curvature terms  $C_L$  and  $C_H$  we obtain

$$C_L - C_H = \frac{4hD_j(D_j - D_{j+1})^2(D_j + 5D_{j+1})}{3(D_j + D_{j+1})^2} \geq 0. \quad (6.17)$$

**Case 2.2.**  $D_j D_{j+1} \leq 0$ . Replacing  $\tilde{V}_j$  by (6.12) in the expression of  $A_H$  we get now

$$A_H = -2D_{j+1},$$

and therefore from (6.6) this time we have

$$C_H = \frac{4hD_{j+1}^2}{3}.$$

Finally, the difference between both curvature terms writes

$$C_L - C_H = \frac{4hD_j(D_j + D_{j+1})}{3} \geq 0. \quad (6.18)$$

□

We have just seen that for data in uniform grids, the curvature term in equation (6.1) associated to PPH reconstruction operator remains below the value of the curvature associated to Lagrange operator.

### 6.3 Study of the curvature term in nonuniform meshes

Let us consider the set of points  $f_{j-1}, f_j, f_{j+1}, f_{j+2}$  corresponding to subsequent ordinates at the abscissas  $x_{j-1}, x_j, x_{j+1}, x_{j+2}$  of a nonuniform mesh  $X$ . Let be  $h_j = x_j - x_{j-1}$ ,  $h_{j+1} = x_{j+1} - x_j$ ,  $h_{j+2} = x_{j+2} - x_{j+1}$ . Similarly to the uniform case, the set of polynomials  $p(x)$  which pass through the central points  $(x_j, f_j)$  and  $(x_{j+1}, f_{j+1})$  writes

$$\begin{aligned} p(x) := & -\frac{1}{6}(x - x_j)(x_{j+1} - x) \left[ A\left(1 + \frac{x_{j+1} - x}{h_{j+1}}\right) + B\left(1 + \frac{x - x_j}{h_{j+1}}\right) \right] \\ & + \frac{x_{j+1} - x}{h_{j+1}} f_j + \frac{x - x_j}{h_{j+1}} f_{j+1}. \end{aligned} \quad (6.19)$$

At the boundary points  $x_{j-1}, x_{j+2}$  of the interval, the distance of the polynomial to the initial data is

$$\begin{aligned} p(x_{j-1}) - f_{j-1} &= \frac{h_j(h_j + h_{j+1})}{6h_{j+1}} (A(h_j + 2h_{j+1}) + B(h_{j+1} - h_j) - 6D_j h_{j+1}), \\ p(x_{j+2}) - f_{j+2} &= \frac{h_{j+2}(h_{j+1} + h_{j+2})}{6h_{j+1}} (A(h_{j+1} - h_{j+2}) + B(2h_{j+1} + h_{j+2}) \\ &\quad - 6D_{j+1} h_{j+1}), \end{aligned} \quad (6.20)$$

where  $D_j$  and  $D_{j+1}$  are the general divided differences defined by

$$\begin{aligned} D_j &= \frac{f_{j-1}}{h_j(h_j + h_{j+1})} - \frac{f_j}{h_j h_{j+1}} + \frac{f_{j+1}}{h_{j+1}(h_j + h_{j+1})}, \\ D_{j+1} &= \frac{f_j}{h_{j+1}(h_{j+1} + h_{j+2})} - \frac{f_{j+1}}{h_{j+1} h_{j+2}} + \frac{f_{j+2}}{h_{j+2}(h_{j+1} + h_{j+2})}. \end{aligned} \quad (6.21)$$

Introducing the second derivative of (6.19) in the curvature term of (6.1) we get

$$C(p) = \int_{x_j}^{x_{j+1}} p''(x)^2 dx = \frac{h_{j+1}}{3} (A^2 + AB + B^2) = \frac{h_{j+1}}{3} ((A + B)^2 - AB). \quad (6.22)$$

### 6.3.1 Curvature term for the Lagrange reconstruction in nonuniform meshes

When  $p(x)$  is the Lagrange polynomial  $p_L(x)$ , it verifies

$$p_L(x_{j-1}) = f_{j-1}, \quad p_L(x_{j+2}) = f_{j+2}. \quad (6.23)$$

From previous conditions and equations (6.20) it results the following linear system for  $A$  and  $B$

$$\begin{aligned} A_L(h_j + 2h_{j+1}) + B_L(h_{j+1} - h_j) &= 6D_j h_{j+1}, \\ A_L(h_{j+1} - h_{j+2}) + B_L(2h_{j+1} + h_{j+2}) &= 6D_{j+1} h_{j+1}. \end{aligned} \quad (6.24)$$

Solving this system, we obtain the parameters  $A$  and  $B$  for the Lagrange polynomial

$$\begin{aligned} A_L &= \frac{2[D_j(2h_{j+1} + h_{j+2}) + D_{j+1}(h_j - h_{j+1})]}{h_j + h_{j+1} + h_{j+2}}, \\ B_L &= \frac{2[D_j(h_{j+2} - h_{j+1}) + D_{j+1}(h_j + 2h_{j+1})]}{h_j + h_{j+1} + h_{j+2}}. \end{aligned} \quad (6.25)$$

It is convenient to observe that

$$\begin{aligned} A_L + B_L &= 4M_j, \\ A_L - B_L &= \frac{6h_{j+1}(D_j - D_{j+1})}{h_j + h_{j+1} + h_{j+2}}. \end{aligned} \quad (6.26)$$

where  $M_j$  is the weighted arithmetic of  $D_j$  and  $D_{j+1}$ , that is

$$M_j = w_{j,0}D_j + w_{j,1}D_{j+1}, \quad (6.27)$$

and the weights  $w_{j,0}, w_{j,1}$  are defined by

$$\begin{aligned} w_{j,0} &= \frac{h_{j+1} + 2h_{j+2}}{2(h_j + h_{j+1} + h_{j+2})}, \\ w_{j,1} &= \frac{h_{j+1} + 2h_j}{2(h_j + h_{j+1} + h_{j+2})} = 1 - w_{j,0}. \end{aligned} \quad (6.28)$$

Plugging these values into expression (6.22) we get the curvature term  $C_L = C(p_L)$  for the Lagrange reconstruction.

### 6.3.2 Curvature term for the PPH reconstruction in nonuniform meshes

The PPH reconstruction in nonuniform meshes is defined in the interval  $[x_j, x_{j+1}]$  by using the data  $f_{j-1}, f_j, f_{j+1}, f_{j+2}$  at the abscissas  $x_{j-1}, x_j, x_{j+1}, x_{j+2}$  in the following way: depending on the relative size of  $|D_j|$  and  $|D_{j+1}|$ , we substitute either  $f_{j-1}$  for  $\tilde{f}_{j-1}$  or  $f_{j+2}$  for  $\tilde{f}_{j+2}$ . After this replacement Lagrange reconstruction is applied to the new set of data. We remark that the initial substitution is made in order to adapt to the presence of potential singularities at the same time that we maintain the fourth order accuracy of Lagrange reconstruction in smooth convex areas.

In what follows we present some expressions that we will need to derive the curvature term. For more information about these expressions see [41]. The mentioned substitutions, depending on the relative size of  $|D_j|$  and  $|D_{j+1}|$ , take the form

$$\tilde{f}_{j-1} = f_{j-1} - \frac{h_j(h_j + h_{j+1})}{w_{j,0}} (M_j - \tilde{V}_j), \quad (6.29a)$$

$$\tilde{f}_{j+2} = f_{j+2} - \frac{h_{j+2}(h_{j+1} + h_{j+2})}{w_{j,1}} (M_j - \tilde{V}_j), \quad (6.29b)$$

where  $\tilde{V}_j$  is the harmonic means of  $D_j$  and  $D_{j+1}$ , that is

$$\tilde{V}_j = \begin{cases} \frac{D_j D_{j+1}}{w_{j,0} D_{j+1} + w_{j,1} D_j} & \text{if } D_j D_{j+1} > 0, \\ 0 & \text{otherwise,} \end{cases} \quad (6.30)$$

From equations (6.27) and (6.30) we obtain

$$M_j - \tilde{V}_j = \begin{cases} \frac{w_{j,0} w_{j,1} (D_{j+1} - D_j)^2}{w_{j,0} D_{j+1} + w_{j,1} D_j} & \text{if } D_j D_{j+1} > 0, \\ M_j & \text{otherwise.} \end{cases} \quad (6.31)$$

This expression will be used later.

The divided differences  $\tilde{D}_j$  and  $\tilde{D}_{j+1}$  calculated with the PPH ordinates  $\tilde{f}_{j-1}$  and  $\tilde{f}_{j+2}$  are now given by

$$\begin{aligned} \tilde{D}_j &= \frac{\tilde{f}_{j-1}}{h_j(h_j + h_{j+1})} - \frac{f_j}{h_j h_{j+1}} + \frac{f_{j+1}}{h_{j+1}(h_j + h_{j+1})}, \\ \tilde{D}_{j+1} &= \frac{f_j}{h_{j+1}(h_{j+1} + h_{j+2})} - \frac{f_{j+1}}{h_{j+1} h_{j+2}} + \frac{f_{j+2}}{h_{j+2}(h_{j+1} + h_{j+2})}. \end{aligned} \quad (6.32)$$

and their difference with (6.21) becomes

$$\begin{aligned} D_j - \tilde{D}_j &= \frac{f_{j-1} - \tilde{f}_{j-1}}{h_j(h_j + h_{j+1})} = \frac{M_j - \tilde{V}_j}{w_{j,0}}, \\ D_{j+1} - \tilde{D}_{j+1} &= \frac{f_{j+2} - \tilde{f}_{j+2}}{h_{j+2}(h_{j+1} + h_{j+2})} = \frac{M_j - \tilde{V}_j}{w_{j,1}}. \end{aligned} \quad (6.33)$$

We are now ready to compute the curvature term associated to PPH reconstruction  $p(x) = p_H(x)$ .

**Theorem 8.** *The curvature term associated to the PPH polynomial  $p_H(x)$  in a nonuniform mesh satisfies*

1.1) If  $|D_j| \leq |D_{j+1}|$  &  $D_j D_{j+1} > 0$ ,

$$\begin{aligned} C_L - C_H &= \frac{12h_{j+1}^3 w_{j,0} w_{j,1}^2}{(2h_j + h_{j+1})^2} \left( \frac{w_{j,0} D_{j+1} + w_{j,1} D_j + D_j}{(w_{j,0} D_{j+1} + w_{j,1} D_j)^2} \right) (D_{j+1} - D_j)^3 \\ &+ 4h_{j+1} (M_j^2 - \tilde{V}_j^2). \end{aligned}$$

$$C_L - C_H \geq 0.$$

1.2) If  $|D_j| \leq |D_{j+1}|$  &  $D_j D_{j+1} \leq 0$ ,

$$C_L - C_H = \frac{8M_j h_{j+1}}{(2h_j + h_{j+1})^2} (2(h_j^2 + h_j h_{j+1} + h_{j+1}^2) M_j - 3h_{j+1}^2 D_j),$$

$C_L - C_H \geq 0$ , under one of these natural conditions:

1.2.1) If  $M_j$  and  $D_j$  have different sign.

1.2.2) If  $M_j$  and  $D_j$  have the same sign and

$$\frac{M_j}{D_j} > \frac{3h_{j+1}^2}{2(h_j^2 + h_j h_{j+1} + h_{j+1}^2)}.$$

2.1) If  $|D_j| > |D_{j+1}|$  &  $D_j D_{j+1} > 0$ ,

$$\begin{aligned} C_L - C_H &= \frac{12h_{j+1}^3 w_{j,0}^2 w_{j,1}}{(h_{j+1} + 2h_{j+2})^2} \left( \frac{w_{j,0} D_{j+1} + w_{j,1} D_j + D_{j+1}}{(w_{j,0} D_{j+1} + w_{j,1} D_j)^2} \right) (D_j - D_{j+1})^3 \\ &+ 4h_{j+1} (M_j^2 - \tilde{V}_j^2), \end{aligned}$$

$$C_L - C_H \geq 0.$$

2.2) If  $|D_j| > |D_{j+1}|$  &  $D_j D_{j+1} \leq 0$ ,

$$C_L - C_H = \frac{8M_j h_{j+1}}{(h_{j+1} + 2h_{j+2})^2} (2(h_{j+1}^2 + h_{j+1} h_{j+2} + h_{j+2}^2) M_j - 3h_{j+1}^2 D_{j+1}),$$

$C_L - C_H \geq 0$ , under one of these natural conditions:

2.2.1) If  $M_j$  and  $D_{j+1}$  have different sign.

2.2.2) If  $M_j$  and  $D_{j+1}$  have the same sign and

$$\frac{M_j}{D_{j+1}} > \frac{3h_{j+1}^2}{2(h_{j+1}^2 + h_{j+1} h_{j+2} + h_{j+2}^2)}.$$

*Proof.* We need to consider two main cases.

**Case 1.**  $|D_j| \leq |D_{j+1}|$ , i.e, the possible singularity is at  $[x_{j+1}, x_{j+2}]$

$$p_H(x_{j-1}) = f_{j-1}, \quad p_H(x_{j+2}) = \tilde{f}_{j+2}. \quad (6.34)$$

From previous conditions and equations (6.20) and (6.29b) we get the following linear system in  $A$  and  $B$

$$\begin{aligned} A_H(h_j + 2h_{j+1}) + B_H(h_{j+1} - h_j) &= 6D_j h_{j+1}, \\ A_H(h_{j+1} - h_{j+2}) + B_H(2h_{j+1} + h_{j+2}) &= 6\tilde{D}_{j+1} h_{j+1}. \end{aligned} \quad (6.35)$$

We observe that this system has the same form as the system for the Lagrange case (6.24), except for  $\tilde{D}_{j+1}$ . Its solution is

$$\begin{aligned} A_H &= \frac{2[D_j(2h_{j+1} + h_{j+2}) + \tilde{D}_{j+1}(h_j - h_{j+1})]}{h_j + h_{j+1} + h_{j+2}}, \\ B_H &= \frac{2[D_j(h_{j+2} - h_{j+1}) + \tilde{D}_{j+1}(h_j + 2h_{j+1})]}{h_j + h_{j+1} + h_{j+2}}, \end{aligned}$$

which can also be expressed as

$$\begin{aligned} A_H &= \frac{6D_j h_{j+1} + 4(h_j - h_{j+1})\tilde{V}_j}{2h_j + h_{j+1}}, \\ B_H &= \frac{-6D_j h_{j+1} + 4(h_j + 2h_{j+1})\tilde{V}_j}{2h_j + h_{j+1}}. \end{aligned} \quad (6.36)$$

From (6.36) we can easily see that

$$A_H + B_H = 4\tilde{V}_j. \quad (6.37)$$

We also point out that parameters  $A_L, B_L$  and  $A_H, B_H$  are related by

$$\begin{aligned} A_H &= A_L - \left(2 - \frac{6h_{j+1}}{2h_j + h_{j+1}}\right) (M_j - \tilde{V}_j), \\ B_H &= B_L - \left(2 + \frac{6h_{j+1}}{2h_j + h_{j+1}}\right) (M_j - \tilde{V}_j). \end{aligned} \quad (6.38)$$

Taking into account equations (6.22), (6.26), (6.37) and (6.38), we obtain the difference  $C_L - C_H$ , between Lagrange and PPH curvature terms.

$$\begin{aligned} C_L - C_H &= \frac{12h_{j+1}^3(M_j - \tilde{V}_j)}{(2h_j + h_{j+1})^2} (2w_{j,1}(D_{j+1} - D_j) - (M_j - \tilde{V}_j)) \\ &+ 4h_{j+1}(M_j^2 - \tilde{V}_j^2). \end{aligned} \quad (6.39)$$

Introducing the expression (6.31) of the difference  $M_j - \tilde{V}_j$  in previous equation, the following subcases appear:

**Case 1.1.**  $D_j D_{j+1} > 0$ .

$$\begin{aligned} C_L - C_H &= \frac{12h_{j+1}^3 w_{j,0} w_{j,1}^2}{(2h_j + h_{j+1})^2} \left( \frac{w_{j,0} D_{j+1} + w_{j,1} D_j + D_j}{(w_{j,0} D_{j+1} + w_{j,1} D_j)^2} \right) (D_{j+1} - D_j)^3 \\ &+ 4h_{j+1}(M_j^2 - \tilde{V}_j^2). \end{aligned} \quad (6.40)$$

On one side, as the sign of  $D_j$  equals to the sign of  $D_{j+1}$  then  $M_j^2 \geq \tilde{V}_j^2$ .  
On the other side, since we are in the case  $|D_j| \leq |D_{j+1}|$ , this implies that

$$(w_{j,0} D_{j+1} + w_{j,1} D_j + D_j)(D_{j+1} - D_j)^3 \geq 0.$$

Thus,  $C_L - C_H \geq 0$ .

**Case 1.2.**  $D_j D_{j+1} \leq 0$ .

$$C_L - C_H = \frac{8M_j h_{j+1}}{(2h_j + h_{j+1})^2} (2(h_j^2 + h_j h_{j+1} + h_{j+1}^2)M_j - 3h_{j+1}^2 D_j). \quad (6.41)$$

$C_L - C_H$  will be positive if  $M_j$  and  $2(h_j^2 + h_j h_{j+1} + h_{j+1}^2)M_j - 3h_{j+1}^2 D_j$  have the same sign. This happens in the following cases

1.2.1.  $M_j$  and  $D_j$  (the lower divided difference in absolute value) have different sign.

1.2.2.  $M_j$  and  $D_j$  have the same sign and  $\frac{M_j}{D_j} > \frac{3h_{j+1}^2}{2(h_j^2 + h_j h_{j+1} + h_{j+1}^2)}$ .

The last conditions are not always satisfied. However we can solve this situation by paying proper attention to the following facts:

- Case 1.2 will only take place around inflection points on the underlying function. Therefore, if we work with data corresponding to strictly convex or concave functions this case will never happen.
- Case 1.2.2 will not occur around discontinuities except for extremely nonuniform grids where  $w_{j,0} \approx 1$ , since  $M_j$  and  $D_j$  have the same sign if and only if  $|\frac{D_{j+1}}{D_j}| < \frac{w_{j,0}}{w_{j,1}}$ .
- In the supposition that for the given data condition in Case 1.2.1 is not satisfied, although this is a rare situation, then we can consider the replacement at this concrete interval of the original data  $f_{j-1}$  by  $\tilde{f}_{j-1}$  according to (6.29a) instead of  $f_{j+2}$  by  $\tilde{f}_{j+2}$  in order to attain  $C_L \geq C_H$ . This observation is easily proven because we go directly to Case 2.2.1. Thus, we give priority to the minimization of the curvature instead to the adaptation to possible singularities. Notice that as mentioned in the previous point, there should not be a singularity at the considered interval but for exceptional cases.

**Case 2.**  $|D_j| > |D_{j+1}|$ , i.e, the possible singularity is at  $[x_{j-1}, x_j]$

$$p_H(x_{j-1}) = \tilde{f}_{j-1}, \quad p_H(x_{j+2}) = f_{j+2}. \quad (6.42)$$

Previous conditions together with equations (6.20) and (6.29a) give the following linear system for  $A$  and  $B$

$$\begin{aligned} A_H(h_j + 2h_{j+1}) + B_H(h_{j+1} - h_j) &= 6\tilde{D}_j h_{j+1}, \\ A_H(h_{j+1} - h_{j+2}) + B_H(2h_{j+1} + h_{j+2}) &= 6D_{j+1} h_{j+1}. \end{aligned} \quad (6.43)$$

Its solution is

$$\begin{aligned} A_H &= \frac{2[\tilde{D}_j(2h_{j+1} + h_{j+2}) + D_{j+1}(h_j - h_{j+1})]}{h_j + h_{j+1} + h_{j+2}}, \\ B_H &= \frac{2[\tilde{D}_j(h_{j+2} - h_{j+1}) + D_{j+1}(h_j + 2h_{j+1})]}{h_j + h_{j+1} + h_{j+2}}, \end{aligned} \quad (6.44)$$

which can also be expressed as

$$\begin{aligned} A_H &= \frac{-6D_{j+1}h_{j+1} + 4(2h_{j+1} + h_{j+2})\tilde{V}_j}{h_{j+1} + 2h_{j+2}}, \\ B_H &= \frac{6D_{j+1}h_{j+1} + 4(h_{j+2} - h_{j+1})\tilde{V}_j}{h_{j+1} + 2h_{j+2}}, \end{aligned} \quad (6.45)$$

where we see that, as in Case 1,

$$A_H + B_H = 4\tilde{V}_j.$$

We also point out that parameters  $A_L, B_L$  and  $A_H, B_H$  are related by

$$\begin{aligned} A_H &= A_L - \left(2 + \frac{6h_{j+1}}{h_{j+1} + 2h_{j+2}}\right) (M_j - \tilde{V}_j), \\ B_H &= B_L - \left(2 - \frac{6h_{j+1}}{h_{j+1} + 2h_{j+2}}\right) (M_j - \tilde{V}_j). \end{aligned} \quad (6.46)$$



Taking into account equations (6.22), (6.26), (6.37) and (6.46), we also reach in this case to the expression for the difference  $C_L - C_H$ , between Lagrange and PPH curvature terms

$$\begin{aligned} C_L - C_H &= \frac{12h_{j+1}^3(M_j - \tilde{V}_j)}{(h_{j+1} + 2h_{j+2})^2} (2w_{j,0}(D_j - D_{j+1}) - (M_j - \tilde{V}_j)) \\ &+ 4h_{j+1}(M_j^2 - \tilde{V}_j^2). \end{aligned} \quad (6.47)$$

Using expression (6.31) of the difference  $M_j - \tilde{V}_j$  in previous equation, we get the subcases

**Case 2.1.**  $D_j D_{j+1} > 0$ .

$$\begin{aligned} C_L - C_H &= \frac{12h_{j+1}^3 w_{j,0}^2 w_{j,1}}{(h_{j+1} + 2h_{j+2})^2} \left( \frac{w_{j,0} D_{j+1} + w_{j,1} D_j + D_{j+1}}{(w_{j,0} D_{j+1} + w_{j,1} D_j)^2} \right) (D_j - D_{j+1})^3 \\ &+ 4h_{j+1}(M_j^2 - \tilde{V}_j^2). \end{aligned} \quad (6.48)$$

On one side,  $D_j D_{j+1} > 0$  implies  $M_j^2 \geq \tilde{V}_j^2$ .

On the other side, since  $|D_j| > |D_{j+1}|$ , then

$$(w_j D_{j+1} + w_{j,1} D_j + D_{j+1})(D_j - D_{j+1})^3 \geq 0.$$

Thus,  $C_L - C_H \geq 0$ .

**Case 2.2.**  $D_j D_{j+1} \leq 0$ .

$$C_L - C_H = \frac{8M_j h_{j+1}}{(h_{j+1} + 2h_{j+2})^2} (2(h_{j+1}^2 + h_{j+1} h_{j+2} + h_{j+2}^2) M_j - 3h_{j+1}^2 D_{j+1}). \quad (6.49)$$

$C_L - C_H$  will be positive if  $2(h_{j+1}^2 + h_{j+1} h_{j+2} + h_{j+2}^2) M_j - 3h_{j+1}^2 D_{j+1}$  have the same sign as  $M_j$ . This occurs when

2.2.1.  $M_j$  and  $D_{j+1}$  (the lower divided difference in absolute value) have different sign.

2.2.2.  $M_j$  and  $D_{j+1}$  have the same sign and  $\frac{M_j}{D_{j+1}} > \frac{3h_{j+1}^2}{2(h_{j+1}^2 + h_{j+1} h_{j+2} + h_{j+2}^2)}$ .

At this point, the same observations as in Case 1.2 can be done. That is, the last conditions are not always satisfied. However, we can solve this situation by paying proper attention to the following facts:

- Case 2.2 will only appear around inflection points. Therefore the case is avoided if we consider only data corresponding to strictly convex or concave functions.
- Case 2.2.2 will not occur around discontinuities except for extremely nonuniform grids where  $w_{j,1} \approx 1$ , since  $M_j$  and  $D_{j+1}$  have the same sign if and only if  $|\frac{D_j}{D_{j+1}}| < \frac{w_{j,1}}{w_{j,0}}$ .
- In the supposition that for the given data condition in Case 2.2.1 is not satisfied, albeit this is not a common situation, we can give priority, as it happened in Case 1.2.2, to the minimization of the curvature instead to the adaptation to possible singularities. Then, we

consider in this case the replacement at this particular interval of the original data  $f_{j+2}$  by  $\tilde{f}_{j+2}$  according to (6.29b) instead of  $f_{j-1}$  by  $\tilde{f}_{j-1}$  in order to attain  $C_L \geq C_H$ . Again, this observation is trivial to prove.

□

## 6.4 Conclusions and perspectives

We have obtained some inequalities which demonstrate that PPH reconstruction operator behaves better than usual linear Lagrange reconstruction operator regarding to curvature issues. This study complements other previous results [6], [10], [41] where it was proven that PPH reconstruction preserves also the convexity properties of the initial data. This property is also inherited by the associated subdivision scheme [37], [50].

This opens up a potential future work connecting PPH reconstruction with smoothing splines in order to obtain a PPH-type reconstruction of class  $C^2$  in the whole interval with interesting convexity preserving properties and low curvature term. Notice that piecewise PPH reconstruction is only continuous at the joint nodes.

## Chapter 7

# Analysis of PPH interpolatory subdivision scheme on $\sigma$ quasi-uniform grids.

The contents of this chapter are wholly included in the already published paper [45]

- Ortiz, P.; Trillo, J.C. Analysis of a New Nonlinear Interpolatory subdivision scheme on  $\sigma$  quasi-uniform grids. *Mathematics*. **2021**, *9*, 1320. <https://doi.org/10.3390/math9121320>

### 7.1 Introduction

Subdivision schemes are closely related to reconstruction operators. They have been used in the last few decades in many applications ranging from the numerical solution of partial differential equations to image processing and computer aided geometric design. Subdivision schemes give simple and fast algorithms to approximate the limit function from a set of initial data at a coarse resolution level. There is an immediate way of generating subdivision schemes from reconstruction operators, and more in concrete from prediction operators [5], [35]. Due to this connection, subdivision schemes inherit many of the properties of their associated reconstruction operators. In particular, the subdivision scheme will be nonlinear if the reconstruction operator is nonlinear, and it is said interpolatory if it comes from a reconstruction operator which is an interpolation.

Nonlinear subdivision schemes have emerged as good candidates to adapt to the concrete data in use. The research in this field counts with new contributions each year and receives the attention of many researchers, see for example [22], [28], [30], [38], [39]. Nonlinearity means data dependent subdivision schemes which may also involve nonlinear operations in their definition. Then, by definition, they are designed to overcome certain drawbacks that appear when dealing with their linear counterparts, such as bad behavior in presence of isolated discontinuities for instance. An example of these kind of operators was defined in [6] and was named as PPH (Piecewise Polynomial Harmonic). This scheme basically consists on a clever modification of the classical four points Lagrange subdivision scheme. Several studies have been carried out about their properties and performance in different applications, see for example [6], [10], [32]. Two main purposes of this subdivision scheme are related to dealing with data containing isolated discontinuities, reducing the undesirable effects, and preserving the convexity of the initial data, while maintaining a centered support based on four points.

In [42] the authors extend the definition of the PPH reconstruction operator to nonuniform grids. In turn, this fact allows us to extend the PPH subdivision scheme to nonuniform grids, and carry out a parallel study in this new scenario. In order to overcome some technical difficulties in the theoretical proofs, we have restricted to  $\sigma$  quasi-uniform grids for some results. The resultant scheme is quite interesting in terms of applications due to the almost  $C^1$  smoothness of the limit function, allowing to approximate accurately continuous functions with corners, and also due to appropriate properties regarding convexity preservation of the initial data, see [10]. In this chapter we focus on proving the convergence of the scheme towards an almost  $C^1$  limit function, and also we address numerically the issue of stability, which is a central issue in order to be useful for applications.

The chapter is organized as follows: Section 7.2 is devoted to remind the PPH reconstruction operator over nonuniform grids. Section 7.3 presents a short review about Harten's interpolatory multiresolution setting, which is closely connected to interpolatory subdivision schemes. In Section 7.4 we define the associated subdivision scheme, which we show that it amounts to the PPH subdivision scheme when we restrict to uniform grids. The definition is given for general nonuniform meshes, although in order to establish some theoretical results we consider  $\sigma$  quasi-uniform meshes. In section 7.5 we analyze the main issues about subdivision schemes. In particular, we prove some results about convergence, smoothness of the limit function, and convexity preservation. In section 7.6 we carry out some numerical tests to check the theoretical smoothness of the limit function, and the performance of the nonlinear subdivision scheme. Finally, we give some conclusions in section 7.7.

## 7.2 A nonlinear PPH reconstruction operator on nonuniform grids

In this section we remind the definition of the nonlinear reconstruction that will give rise to the nonlinear subdivision scheme under study in this chapter. More information about this reconstruction operator can be found in [6], [42], [43].

Let us define a nonuniform grid  $X = (x_i)_{i \in \mathbb{Z}}$ . Let us also denote  $h_i := x_i - x_{i-1}$ , the nonuniform spacing between abscissae. Let us consider the set of values  $\{f_{j-1}, f_j, f_{j+1}, f_{j+2}\}$  for some  $j \in \mathbb{Z}$  corresponding to the abscissae  $\{x_{j-1}, x_j, x_{j+1}, x_{j+2}\}$  of the nonuniform grid  $X$ .

We need to introduce the definition of the second order divided differences

$$\begin{aligned} D_j &:= f[x_{j-1}, x_j, x_{j+1}] = \frac{f_{j-1}}{h_j(h_j + h_{j+1})} - \frac{f_j}{h_j h_{j+1}} + \frac{f_{j+1}}{h_{j+1}(h_j + h_{j+1})}, \\ D_{j+1} &:= f[x_j, x_{j+1}, x_{j+2}] = \frac{f_j}{h_{j+1}(h_{j+1} + h_{j+2})} - \frac{f_{j+1}}{h_{j+1} h_{j+2}} + \frac{f_{j+2}}{h_{j+2}(h_{j+1} + h_{j+2})}, \end{aligned} \quad (7.1)$$

and the weighted arithmetic mean of  $D_j$  and  $D_{j+1}$  defined as

$$M_j = w_{j,0} D_j + w_{j,1} D_{j+1}, \quad (7.2)$$

with the weights

$$\begin{aligned} w_{j,0} &= \frac{h_{j+1} + 2h_{j+2}}{2(h_j + h_{j+1} + h_{j+2})}, \\ w_{j,1} &= \frac{h_{j+1} + 2h_j}{2(h_j + h_{j+1} + h_{j+2})} = 1 - w_{j,0}. \end{aligned} \quad (7.3)$$

We require also some definitions and lemmas that appear in [42].

**Definition 25.** Given  $x, y \in \mathbb{R}$ , and  $w_x, w_y \in \mathbb{R}$  such that  $w_x > 0$ ,  $w_y > 0$ , and  $w_x + w_y = 1$ , we denote as  $\tilde{V}$  the function

$$\tilde{V}(x, y) = \begin{cases} \frac{xy}{w_x y + w_y x} & \text{if } xy > 0, \\ 0 & \text{otherwise.} \end{cases} \quad (7.4)$$

**Lemma 23.** If  $x \geq 0$  and  $y \geq 0$ , the harmonic mean is bounded as follows

$$\tilde{V}(x, y) < \min \left\{ \frac{1}{w_x} x, \frac{1}{w_y} y \right\} \leq \frac{1}{w_x} x. \quad (7.5)$$

**Lemma 24.** Let  $a > 0$  a fixed positive real number, and let  $x \geq a$  and  $y \geq a$ . If  $|x - y| = O(h)$ , and  $xy > 0$ , then the weighted harmonic mean is also close to the weighted arithmetic mean  $M(x, y) = w_x x + w_y y$ ,

$$|M(x, y) - \tilde{V}(x, y)| = \frac{w_x w_y}{w_x y + w_y x} (x - y)^2 = O(h^2). \quad (7.6)$$

We remind the following definition for the PPH reconstruction on nonuniform meshes. The details and main properties of this reconstruction operator can be found in [42], [43].

**Definition 26** (PPH reconstruction). Let  $X = (x_i)_{i \in \mathbb{Z}}$  be a nonuniform mesh. Let  $f = (f_i)_{i \in \mathbb{Z}}$  a sequence in  $l_\infty(\mathbb{Z})$ . Let  $D_j$  and  $D_{j+1}$  be the second order divided differences, and for each  $j \in \mathbb{Z}$  let us consider the modified values  $\{\tilde{f}_{j-1}, \tilde{f}_j, \tilde{f}_{j+1}, \tilde{f}_{j+2}\}$  built according to the following rule

- **Case 1:** If  $|D_j| \leq |D_{j+1}|$

$$\begin{cases} \tilde{f}_i = f_i, & j-1 \leq i \leq j+1, \\ \tilde{f}_{j+2} = \frac{-1}{\gamma_{j,2}} (\gamma_{j,-1} f_{j-1} + \gamma_{j,0} f_j + \gamma_{j,1} f_{j+1}) + \frac{\tilde{V}_j}{\gamma_{j,2}}, \end{cases} \quad (7.7)$$

- **Case 2:** If  $|D_j| > |D_{j+1}|$

$$\begin{cases} \tilde{f}_{j-1} = \frac{-1}{\gamma_{j,-1}} (\gamma_{j,0} f_j + \gamma_{j,1} f_{j+1} + \gamma_{j,2} f_{j+2}) + \frac{\tilde{V}_j}{\gamma_{j,-1}}, \\ \tilde{f}_i = f_i, & j \leq i \leq j+2, \end{cases} \quad (7.8)$$

where  $\gamma_{j,i}$ ,  $i = -1, 0, 1, 2$  are given by

$$\begin{aligned} \gamma_{j,-1} &= \frac{h_{j+1} + 2h_{j+2}}{2h_j(h_{j+1} + h_j)(h_j + h_{j+1} + h_{j+2})}, \\ \gamma_{j,0} &= \frac{1}{2h_{j+1}(h_j + h_{j+1} + h_{j+2})} \left( \frac{h_{j+1} + 2h_j}{h_{j+1} + h_{j+2}} - \frac{h_{j+1} + 2h_{j+2}}{h_j} \right), \\ \gamma_{j,1} &= \frac{1}{2h_{j+1}(h_j + h_{j+1} + h_{j+2})} \left( \frac{h_{j+1} + 2h_{j+2}}{h_{j+1} + h_j} - \frac{h_{j+1} + 2h_j}{h_{j+2}} \right), \\ \gamma_{j,2} &= \frac{h_{j+1} + 2h_j}{2h_{j+2}(h_{j+1} + h_{j+2})(h_j + h_{j+1} + h_{j+2})}, \end{aligned} \quad (7.9)$$

and  $\tilde{V}_j = \tilde{V}(D_j, D_{j+1})$ , with  $\tilde{V}$  the weighted harmonic mean defined in (7.4) with the weights  $w_{j,0}$  and  $w_{j,1}$  in (7.3). We define  $\mathcal{R}(x)$  as the PPH nonlinear reconstruction operator given by

$$\mathcal{R}(x) = \mathcal{R}_j(x), \quad x \in [x_j, x_{j+1}], \quad (7.10)$$

where  $\mathcal{R}_j(x)$  is the unique interpolation polynomial which satisfies

$$\mathcal{R}_j(x_i) = \tilde{f}_i, \quad j-1 \leq i \leq j+2. \quad (7.11)$$

We can write the PPH reconstruction by using the middle point  $x_{j+\frac{1}{2}} = \frac{x_j+x_{j+1}}{2}$  as

$$\mathcal{R}_j(x) = \tilde{a}_{j,0} + \tilde{a}_{j,1} \left(x - x_{j+\frac{1}{2}}\right) + \tilde{a}_{j,2} \left(x - x_{j+\frac{1}{2}}\right)^2 + \tilde{a}_{j,3} \left(x - x_{j+\frac{1}{2}}\right)^3, \quad (7.12)$$

where the coefficients  $\tilde{a}_{j,i}$ ,  $i = 0, \dots, 3$  are calculated by imposing conditions (7.11). Depending on the local case, Case 1 or Case 2, the coefficients will have different expressions.

**Case 1.**  $|D_j| \leq |D_{j+1}|$ , In this case, the coefficients of the polynomial (7.12) take the form

$$\begin{aligned} \tilde{a}_{j,0} &= \frac{f_j + f_{j+1}}{2} - \frac{h_{j+1}^2}{4} \tilde{V}_j, \\ \tilde{a}_{j,1} &= \frac{-f_j + f_{j+1}}{h_{j+1}} + \frac{h_{j+1}^2}{4h_j + 2h_{j+1}} (D_j - \tilde{V}_j), \\ \tilde{a}_{j,2} &= \tilde{V}_j, \\ \tilde{a}_{j,3} &= -\frac{2}{2h_j + h_{j+1}} (D_j - \tilde{V}_j). \end{aligned} \quad (7.13)$$

**Case 2.**  $|D_j| > |D_{j+1}|$ , In this case, we obtain the following coefficients for the polynomial (7.12)

$$\begin{aligned} \tilde{a}_{j,0} &= \frac{f_j + f_{j+1}}{2} - \frac{h_{j+1}^2}{4} \tilde{V}_j, \\ \tilde{a}_{j,1} &= \frac{-f_j + f_{j+1}}{h_{j+1}} + \frac{h_{j+1}^2}{2h_{j+1} + 4h_{j+2}} (-D_{j+1} + \tilde{V}_j), \\ \tilde{a}_{j,2} &= \tilde{V}_j, \\ \tilde{a}_{j,3} &= -\frac{2}{h_{j+1} + 2h_{j+2}} (-D_{j+1} + \tilde{V}_j). \end{aligned} \quad (7.14)$$

With the previous definitions and lemmas we are now ready to introduce the PPH subdivision scheme. But before doing it, we will also remind some basic concepts of Harten's interpolatory multiresolution setting and its connection with subdivision schemes.

### 7.3 Harten's interpolatory multiresolution setting

Let us consider a set of nested grids in  $\mathbb{R}$ ,

$$X^k = \{x_i^k\}_{i \in \mathbb{Z}},$$

and the point-value discretization

$$\begin{aligned} \mathcal{D}_k : C_B(\mathbb{R}) &\rightarrow V^k \\ f &\mapsto f^k = (f_i^k)_{i \in \mathbb{Z}} = (f(x_i^k))_{i \in \mathbb{Z}}, \end{aligned} \quad (7.15)$$

where  $V^k$  is the space of real sequences related to the resolution of  $X^k$  and  $C_B(\mathbb{R})$  the set of bounded continuous functions on  $\mathbb{R}$ .

A reconstruction operator  $\mathcal{R}_k$  associated to this discretization is any right inverse of  $\mathcal{D}_k$ , which means that for all  $f^k \in V^k$ ,  $\mathcal{R}_k f^k \in C_B(\mathbb{R})$ , and  $\mathcal{D}_k \mathcal{R}_k = I$ , that is

$$\begin{aligned} \mathcal{R}_k : V^k &\rightarrow C_B(\mathbb{R}) \\ f^k &\mapsto \mathcal{R}_k f^k, \end{aligned} \quad (7.16)$$

$$(\mathcal{R}_k f^k)(x_i^k) = (f_i^k)_{i \in \mathbb{Z}} = (f(x_i^k))_{i \in \mathbb{Z}}.$$

The sequences  $\{\mathcal{D}_k\}_{k \in \mathbb{N}}$  and  $\{\mathcal{R}_k\}_{k \in \mathbb{N}}$  define a multiresolution transform [5]. The prediction operator, i.e.,  $\mathcal{D}_{k+1} \mathcal{R}_k : V^k \rightarrow V^{k+1}$ , defines a subdivision scheme. Relation (7.16) implies that the subdivision scheme is interpolatory. If  $\mathcal{R}_k$  is a nonlinear reconstruction operator, then the corresponding subdivision scheme  $\mathcal{S} := \mathcal{D}_{k+1} \mathcal{R}_k$  becomes also nonlinear.

### 7.4 A nonlinear PPH subdivision scheme on nonuniform grids

Let us consider a particular set of nonuniform nested grids  $X^k = (x_i^k)_{i \in \mathbb{Z}}$ ,  $k \geq 0$ , generated from an initial grid  $X^0$ .

**Definition 27.** Given  $X^0 = \{x_i\}_{i \in \mathbb{Z}}$  a nonuniform grid in  $\mathbb{R}$ , we define, for  $k \in \mathbb{N}$  (the larger the  $k$  the larger the resolution), the set of nested grids given by  $X^k = \{x_i^k\}_{i \in \mathbb{Z}}$ , where  $x_{2i}^k = x_i^{k-1}$  and  $x_{2i+1}^k = \frac{x_i^{k-1} + x_{i+1}^{k-1}}{2}$ .

Let us also consider  $h_i^k = x_i^k - x_{i-1}^k$ , the nonuniform spacing between abscissae. Given a set of control points  $f^k = (f_i^k)_{i \in \mathbb{Z}}$ , we define the nonlinear PPH subdivision scheme as

$$\begin{aligned} f_{2i}^{k+1} &= (\mathcal{S} f^k)_{2i} = f_i^k, \\ f_{2i+1}^{k+1} &= (\mathcal{S} f^k)_{2i+1} = \frac{f_i^k + f_{i+1}^k}{2} - \frac{(h_{i+1}^k)^2}{4} \tilde{V}_i^k, \end{aligned} \quad (7.17)$$

where  $\tilde{V}_i^k = \tilde{V}_i^k(D_i^k, D_{i+1}^k)$  is given in (7.4) and it is computed with the weights  $(w_{i,0}^k)_{i \in \mathbb{Z}}$ , and  $(w_{i,1}^k)_{i \in \mathbb{Z}}$  given in (7.3), and the second order divided differences  $D_i^k$  and  $D_{i+1}^k$  are defined in (7.1).

Notice that the expression of the subdivision scheme at odd indexes coincides with the coefficient  $\tilde{a}_0$  of the PPH reconstruction operator in (7.13) or (7.14), due to the fact that the defined subdivision scheme satisfies  $\mathcal{S} = \mathcal{D}_{k+1}\mathcal{R}_k$ . This means that the expression of the subdivision scheme is symmetric, even if the modification of the data has been carried out to the left (7.14) or to the right (7.13) for the concrete piece of the underlying reconstruction operator.

Supposing that the initial data come from a convex smooth function, then by the process of definition through its associated reconstruction operator, we get a fourth order accurate subdivision scheme. In case of having data coming from an underlying smooth function with inflexion points, the order would be reduced around these inflexion points [43]. The use of the weighted harmonic mean in Definition 7.17 guarantees certain adaptation near jump discontinuities. In presence of an isolated singularity we have two adjacent intervals where  $D_i = O(1)$  and  $D_{i+1} = O(1/(h^k)^2)$ , or  $D_i = O(1/(h^k)^2)$  and  $D_{i+1} = O(1)$ , with  $h^k := \max_{j \in \mathbb{Z}} h_j^k$ . For these cases, the harmonic mean remains of order  $\tilde{V}_i = O(1)$ . If both  $D_i$  and  $D_{i+1}$  are affected by the discontinuity, then no adaptation is taking place. But this situation happens only in the prediction of one value per scale and per discontinuity.

It is also interesting to remark that for uniform meshes, i.e.,  $h_i = h \forall i$ , then all the given expressions reduce to equivalent expressions in [6] valid only for the uniform case.

Notice that Definition 7.17 of the PPH subdivision schemes has been introduced for general nonuniform meshes. From now on, one needs to take into account that some results are true for general grids, while others require the restriction to a particular type of nonuniform meshes, that by the way, are the most common in practice.

In next section we study some main issues about the defined subdivision scheme. In particular we prove convergence, almost  $C^1$  smoothness in the limit function, and we give a result concerning convexity preservation.

## 7.5 Main properties of the PPH subdivision scheme in nonuniform meshes

We start the section with some definitions taken from [6] that will be used in the rest of the chapter.

**Definition 28.** *A nonlinear subdivision scheme is called uniformly convergent, if for every set of initial data  $f^0 \in l_\infty(\mathbb{Z})$ , there exists a continuous function  $\mathcal{S}^\infty f^0 \in C(\mathbb{R})$ , such that*

$$\lim_{k \rightarrow \infty} \|\mathcal{S}f^k - \mathcal{S}^\infty f^0(2^{-(k+1)}\cdot)\|_{l_\infty(\mathbb{Z})} = 0.$$

**Definition 29.** *A convergent nonlinear subdivision scheme is called stable, if there exists a constant  $C$  such that for every pair of initial data  $f^0, \tilde{f}^0 \in l_\infty(\mathbb{Z})$ ,*

$$\|\mathcal{S}^\infty f^0 - \mathcal{S}^\infty \tilde{f}^0\|_{L^\infty} \leq C \|f^0 - \tilde{f}^0\|_{l_\infty(\mathbb{Z})}.$$

**Definition 30.** *Let  $N \geq 0$  be a fixed integer. A nonlinear interpolatory subdivision scheme has the property of polynomial reproduction of order  $N$ , if for all  $P \in \Pi_N$ , where  $\Pi_N$  stands for the vector space of polynomials of degree less or equal to  $N$ , we have  $\mathcal{S}p = \tilde{p}$ , where  $p$  and  $\tilde{p}$  are defined by  $p_k = P(2^{-k}\cdot)$  and  $\tilde{p}_k = P(2^{-(k+1)}\cdot)$ .*



**Definition 31.** A nonlinear subdivision scheme is called bounded, if there exists a constant  $C > 0$  such that

$$\|\mathcal{S}f\|_{l_\infty(\mathbb{Z})} \leq C\|f\|_{l_\infty(\mathbb{Z})} \quad \forall f \in l_\infty(\mathbb{Z}).$$

**Definition 32.** A nonlinear subdivision scheme is called Lipschitz continuous if there exists a constant  $C > 0$  such that for every  $f, g \in l_\infty(\mathbb{Z})$  it is verified

$$\|\mathcal{S}f - \mathcal{S}g\|_{l_\infty(\mathbb{Z})} \leq C\|f - g\|_{l_\infty(\mathbb{Z})}. \quad (7.18)$$

We can now give some basic results before addressing the convergence of the scheme. In order to prove the coming theoretical results we are going to work with  $\sigma$  quasi-uniform grids, according to the following definition

**Definition 33.** A nonuniform mesh  $X = (x_i)_{i \in \mathbb{Z}}$  is said to be a  $\sigma$  quasi-uniform mesh if there exist  $h_{\min} = \min_{i \in \mathbb{Z}} h_i$ ,  $h_{\max} = \max_{i \in \mathbb{Z}} h_i$ , and a finite constant  $\sigma$  such that  $\frac{h_{\max}}{h_{\min}} \leq \sigma$ .

**Proposition 12.** The nonlinear subdivision scheme associated to the PPH reconstruction

- 1) reproduces polynomials of degree  $N \leq 2$ ,
- 2) is bounded,
- 3) is Lipschitz continuous.

*Proof.* 1) If  $f$  is a polynomial of degree less or equal to 2,

$$D_j = D_{j+1} = \tilde{V}_j,$$

therefore the proposed scheme reproduces polynomials of degree 2.

2) By definition of the PPH subdivision scheme for a given  $j \in \mathbb{Z}$  we have that

$$(\mathcal{S}f)_{2j} = f_j,$$

$$(\mathcal{S}f)_{2j+1} = \begin{cases} \frac{f_j + f_{j+1}}{2} - \frac{(h_{j+1})^2}{4} \tilde{V}_j & \text{if } D_j D_{j+1} > 0, \\ \frac{f_j + f_{j+1}}{2} & \text{otherwise.} \end{cases}$$

Using that  $|D_j| \leq \frac{4\|f\|_{l_\infty(\mathbb{Z})}}{2h_{\min}^2}$ ,  $|D_{j+1}| \leq \frac{4\|f\|_{l_\infty(\mathbb{Z})}}{2h_{\min}^2}$ , we get that

$$\left| \frac{(h_{j+1})^2}{4} \tilde{V}_j \right| \leq \frac{(h_{j+1})^2}{4} \max\{|D_{j+1}|, |D_j|\} \leq \frac{\sigma^2}{2} \|f\|_{l_\infty(\mathbb{Z})}.$$

Thus,

$$\|\mathcal{S}f\|_{l_\infty(\mathbb{Z})} \leq \left(1 + \frac{\sigma^2}{2}\right) \|f\|_{l_\infty(\mathbb{Z})},$$

and therefore the nonlinear subdivision scheme is bounded.

3) Let us consider  $\{f\}, \{g\} \in l_\infty(\mathbb{Z})$ .

Clearly

$$|(\mathcal{S}f)_{2j} - (\mathcal{S}g)_{2j}| = |f_j - g_j| \leq \|f - g\|_{l_\infty(\mathbb{Z})}.$$

Since

$$\left| \frac{f_j + f_{j+1}}{2} - \frac{g_j + g_{j+1}}{2} \right| \leq \|f - g\|_{l_\infty(\mathbb{Z})},$$

to estimate the odd components  $|(\mathcal{S}f)_{2j+1} - (\mathcal{S}g)_{2j+1}|$  we simply need to estimate the terms

$$\frac{(h_{j+1})^2}{4} \tilde{V}_j(f), \quad \frac{(h_{j+1})^2}{4} \tilde{V}_j(g),$$

or

$$\frac{(h_{j+1})^2}{4} \tilde{V}_j(f) - \frac{(h_{j+1})^2}{4} \tilde{V}_j(g),$$

according to the sign of  $D_j(f)D_{j+1}(f)$  and  $D_j(g)D_{j+1}(g)$ .

**a)** Suppose  $D_j(f)D_{j+1}(f) > 0$  and  $D_j(g)D_{j+1}(g) \leq 0$ . In particular,  $D_{j+1}(f)D_{j+1}(g) \leq 0$  or  $D_j(f)D_j(g) \leq 0$ . In the first case, we write

$$\begin{aligned} \left| \frac{(h_{j+1})^2}{4} \tilde{V}_j(f) \right| &\leq \frac{(h_{max})^2}{4} \frac{|D_{j+1}(f)|}{w_{j,1}} \\ &\leq \frac{(h_{max})^2}{4} \frac{|D_{j+1}(f) - D_{j+1}(g)|}{w_{j,1}} \\ &\leq \frac{(h_{max})^2}{4} \frac{4}{2(h_{min})^2} 2\sigma \|f - g\|_{l_\infty(\mathbb{Z})} \\ &\leq \sigma^3 \|f - g\|_{l_\infty(\mathbb{Z})}, \end{aligned}$$

and in the second case we get similarly

$$\begin{aligned} \left| \frac{(h_{j+1})^2}{4} \tilde{V}_j(f) \right| &\leq \frac{(h_{max})^2}{4} \frac{|D_j(f)|}{w_{j,0}} \\ &\leq \frac{(h_{max})^2}{4} \frac{|D_j(f) - D_j(g)|}{w_{j,0}} \\ &\leq \frac{(h_{max})^2}{4} \frac{4}{2(h_{min})^2} 2\sigma \|f - g\|_{l_\infty(\mathbb{Z})} \\ &\leq \sigma^3 \|f - g\|_{l_\infty(\mathbb{Z})}. \end{aligned}$$

**b)** Suppose now that  $D_j(f)D_{j+1}(f) > 0$  and  $D_j(g)D_{j+1}(g) > 0$ . If  $D_j(f)D_j(g) \leq 0$ , then using the same arguments as in case **a)** we obtain

$$\left| \frac{(h_{j+1})^2}{4} \tilde{V}_j(f) - \frac{(h_{j+1})^2}{4} \tilde{V}_j(g) \right| = \left| \frac{(h_{j+1})^2}{4} \tilde{V}_j(f) \right| + \left| \frac{(h_{j+1})^2}{4} \tilde{V}_j(g) \right| \leq 2\sigma^3 \|f - g\|_{l_\infty(\mathbb{Z})}.$$

If  $D_j(f)D_{j+1}(f) < 0$ , we consider the function  $Z(x, y) = \frac{xy}{w_{j,0}y + w_{j,1}x}$  defined for all  $xy > 0$ . It is easy to check that the Jacobian of the function  $Z$  verifies

$$\|J_Z(x, y)\|_\infty \leq 2\sigma.$$

Thus, the mean value theorem easily leads to

$$\begin{aligned} \left| \frac{(h_{j+1})^2}{4} \tilde{V}_j(f) - \frac{(h_{j+1})^2}{4} \tilde{V}_j(g) \right| &\leq \frac{(h_{j+1})^2}{4} 2\sigma \|(D_j(f) - D_j(g), D_{j+1}(f) - D_{j+1}(g))\|_\infty \\ &\leq \frac{(h_{j+1})^2}{h_{min}^2} \sigma \|f - g\|_{l_\infty(\mathbb{Z})} \leq \sigma^3 \|f - g\|_{l_\infty(\mathbb{Z})}. \end{aligned}$$

Clearly,  $C = 1 + 2\sigma^3$  is a convenient constant that completes the proof.  $\square$

Next lemma and proposition allow to prove the existence of a contractive scheme  $\mathcal{S}_1$  for the differences  $\delta_i := f_i - f_{i-1}$ .

**Lemma 25.** *Let  $\mathcal{D}$  be the set defined by  $\mathcal{D} := \{j \in \mathbb{Z} : D_j D_{j+1} > 0\}$  and let the expressions  $E_{1j}, E_{2j}$  and  $M$  be defined as follows*

$$E_{1j} = \frac{\frac{h_{j+1}}{4}}{(h_{j+1} + h_{j+2})(w_{j,1} + w_{j,0} \frac{D_{j+1}}{D_j})}, \quad E_{2j} = \frac{\frac{h_{j+1}}{4}}{(h_{j+1} + h_j)(w_{j,0} + w_{j,1} \frac{D_j}{D_{j+1}})},$$

$$M = \sup_{j \in \mathcal{D}} \{|E_{1j}|, |E_{2j}|\}.$$

*Then, the following inequalities are satisfied*

- 1)  $E_{1j} > 0, \quad E_{2j} > 0, \quad \forall j \in \mathcal{D},$
- 2)  $E_{1j} \leq M, \quad E_{2j} \leq M, \quad \forall j \in \mathcal{D},$
- 3)  $M \leq \frac{1}{2}.$

*Proof.* 1) and 2) are trivial. Let us see 3). Given  $j \in \mathcal{D}$ , we have

$$E_{1j} < \frac{h_{j+1}}{4} \frac{1}{w_{j,1}(h_{j+1} + h_{j+2})} < \frac{1}{2},$$

since

$$h_{j+1} < 2w_{j,1}(h_{j+1} + h_{j+2}) \Leftrightarrow 0 < h_j h_{j+1} + 2h_{j+1} h_{j+2}.$$

Analogously, we can see that  $E_{2j} < \frac{1}{2}$ .

Thus

$$M = \sup_{j \in \mathcal{D}} \{|E_{1j}|, |E_{2j}|\} \leq \frac{1}{2}.$$

□

**Proposition 13.** *Associated to the PPH nonlinear reconstruction, on non-uniform grids there exists a nonlinear subdivision scheme  $\mathcal{S}_1$  for the differences. If the grid is  $\sigma$ -quasy uniform, then  $\mathcal{S}_1$  is bounded, i.e. satisfies*

$$\|\mathcal{S}_1 \delta^k\|_{l_\infty(\mathbb{Z})} \leq \lambda_1 \|\delta^k\|_{l_\infty(\mathbb{Z})} \quad \forall f^k \in l_\infty(\mathbb{Z}),$$

where  $\delta_j^k := f_j^k - f_{j-1}^k$ , and  $\lambda_1 = \frac{1}{2} + (\sigma - 1)M$ .

Moreover, if  $\sigma < 1 + \frac{1}{2M}$ , then  $\lambda_1 < 1$  and  $\mathcal{S}_1$  is contractive.

*Proof.* a) Existence of  $\mathcal{S}_1$ .

$\mathcal{S}_1 \delta^k$  has the following expressions for even and odd indexes.

**a.1)** Even indexes

$$\delta_{2j+2}^{k+1} = f_{2j+2}^{k+1} - f_{2j+1}^{k+1} = \frac{\delta_{j+1}^k}{2} + \frac{(h_{j+1}^k)^2}{4} \tilde{V}_j^k,$$

and depending on the value of  $\tilde{V}_j$  we differentiate two cases,

**a.1.1)** If  $D_j^k D_{j+1}^k > 0$ ,

$$\begin{aligned} \frac{(h_{j+1}^k)^2}{4} \tilde{V}_j^k &= \frac{(h_{j+1}^k)^2}{4} \frac{\frac{\delta_{j+1}^k}{h_{j+1}^k} - \frac{\delta_j^k}{h_j^k}}{h_j^k + h_{j+1}^k} \frac{\frac{\delta_{j+2}^k}{h_{j+2}^k} - \frac{\delta_{j+1}^k}{h_{j+1}^k}}{h_{j+1}^k + h_{j+2}^k} \\ &\quad w_{j,0} \frac{\frac{\delta_{j+2}^k}{h_{j+2}^k} - \frac{\delta_{j+1}^k}{h_{j+1}^k}}{h_{j+1}^k + h_{j+2}^k} + w_{j,1} \frac{\frac{\delta_{j+1}^k}{h_{j+1}^k} - \frac{\delta_j^k}{h_j^k}}{h_j^k + h_{j+1}^k} \\ &= \frac{h_{j+1}^k}{4} \frac{1}{w_{j,0}(h_j^k + h_{j+1}^k) \frac{\frac{\delta_{j+2}^k}{h_{j+2}^k} - \frac{\delta_{j+1}^k}{h_{j+1}^k}}{\frac{\delta_{j+1}^k}{h_{j+1}^k} - \frac{\delta_j^k}{h_j^k}} + w_{j,1}(h_{j+1}^k + h_{j+2}^k)} \left( \frac{h_{j+1}^k}{h_{j+2}^k} \delta_{j+2}^k - \delta_{j+1}^k \right) \\ &= E_{1j}^k \left( \frac{h_{j+1}^k}{h_{j+2}^k} \delta_{j+2}^k - \delta_{j+1}^k \right). \end{aligned}$$

Then

$$\delta_{2j+2}^{k+1} = \frac{\delta_{j+1}^k}{2} + E_{1j}^k \left( \frac{h_{j+1}^k}{h_{j+2}^k} \delta_{j+2}^k - \delta_{j+1}^k \right). \quad (7.19)$$

**a.1.2)** If  $D_j^k D_{j+1}^k \leq 0$ ,

$$\delta_{2j+2}^{k+1} = \frac{\delta_{j+1}^k}{2}. \quad (7.20)$$

**a.2)** Odd indexes

$$\delta_{2j+1}^{k+1} = f_{2j+1}^{k+1} - f_{2j}^{k+1} = \frac{\delta_{j+1}^k}{2} - \frac{(h_{j+1}^k)^2}{4} \tilde{V}_j^k,$$

and again by proceeding in a similar way we get for the two different cases,

**a.2.1)** If  $D_{j+1}^k D_j^k > 0$ ,

$$\delta_{2j+1}^{k+1} = \frac{\delta_{j+1}^k}{2} - E_{2j}^k \left( \frac{h_{j+1}^k}{h_j^k} \delta_j^k - \delta_{j+1}^k \right). \quad (7.21)$$

**a.2.2)** If  $D_j^k D_{j+1}^k \leq 0$ ,

$$\delta_{2j+1}^{k+1} = \frac{\delta_{j+1}^k}{2}. \quad (7.22)$$

b)  $\mathcal{S}_1$  is bounded.

We consider again even and odd indexes.

**b.1) Even indexes**

**b.1.1)** If  $D_j^k D_{j+1}^k > 0$ , from equation (7.19) it follows

$$\begin{aligned} |\delta_{2j+2}^{k+1}| &= \left| \left( \frac{1}{2} - E_{1j}^k \right) \delta_{j+1}^k + \left( \frac{h_{j+1}^k}{h_{j+2}^k} E_{1j}^k \right) \delta_{j+2}^k \right| \leq \left| \frac{1}{2} + E_{1j}^k \left( \frac{h_{j+1}^k}{h_{j+2}^k} - 1 \right) \right| \|\delta^k\|_{l_\infty(\mathbb{Z})} \\ &\leq \left| \frac{1}{2} + (\sigma - 1)M \right| \|\delta^k\|_{l_\infty(\mathbb{Z})}, \end{aligned}$$

**b.1.2)** If  $D_j^k D_{j+1}^k \leq 0$ ,

$$|\delta_{2j+2}^{k+1}| = \frac{1}{2} |\delta_{j+1}^k| \leq \frac{1}{2} \|\delta^k\|_{l_\infty(\mathbb{Z})}.$$

**b.2) Odd indexes**

**b.2.1)** If  $D_j^k D_{j+1}^k > 0$ , from equation (7.21) it follows

$$|\delta_{2j+1}^{k+1}| \leq \left| \frac{1}{2} + E_{2j}^k \left( \frac{h_{j+1}^k}{h_j^k} - 1 \right) \right| \|\delta^k\|_{l_\infty(\mathbb{Z})} \leq \left| \frac{1}{2} + (\sigma - 1)M \right| \|\delta^k\|_{l_\infty(\mathbb{Z})},$$

**b.2.2)** If  $D_j^k D_{j+1}^k \leq 0$ ,

$$|\delta_{2j+1}^{k+1}| = \frac{1}{2} |\delta_{j+1}^k| \leq \frac{1}{2} \|\delta^k\|_{l_\infty(\mathbb{Z})}.$$

Thus

$$\sup_{j \in \mathbb{Z}} \left\{ \left| \delta_{2j+2}^{k+1} \right|, \left| \delta_{2j+1}^{k+1} \right| \right\} \leq \left( \frac{1}{2} + (\sigma - 1)M \right) \|\delta^k\|_{l_\infty(\mathbb{Z})},$$

i.e.

$$\|\delta^{k+1}\|_{l_\infty(\mathbb{Z})} \leq \lambda_1 \|\delta^k\|_{l_\infty(\mathbb{Z})},$$

with  $\lambda_1 = \frac{1}{2} + (\sigma - 1)M$ .

c) Contraction property.

The subdivision scheme  $\mathcal{S}_1$  will be contractive if

$$\frac{1}{2} + M(\sigma - 1) < 1 \quad \Leftrightarrow \quad \sigma < 1 + \frac{1}{2M}.$$

□

**Corollary 1.** For  $\sigma$ -quasy uniform grids where  $\sigma < 2$ , the scheme  $\mathcal{S}_1$  is contractive, since  $M < \frac{1}{2}$ .

We give now a simple and technical lemma to support the proof of next lemma.

**Lemma 26.**  $\left| \frac{\tilde{V}_j^k}{\gamma_{j,2}^k} \right|$  and  $\left| \frac{\tilde{V}_j^k}{\gamma_{j,-1}^k} \right|$  are bounded by  $4\sigma^2(1+\sigma) \|\delta^k\|_{l_\infty(\mathbb{Z})}$ .

*Proof.* By definition of  $\gamma_{j,2}$  in (7.9) together with property (7.5) of the harmonic mean  $|\tilde{V}_j^k| \leq \frac{|D_{j+1}^k|}{w_{j,1}^k}$ , and the expression of  $D_{j+1}^k$

$$D_{j+1}^k = \frac{\frac{\delta_{j+2}^k}{h_{j+2}^k} - \frac{\delta_{j+1}^k}{h_{j+1}^k}}{h_{j+1}^k + h_{j+2}^k},$$

we can write

$$\left| \frac{\tilde{V}_j^k}{\gamma_{j,2}^k} \right| \leq \left| \frac{D_{j+1}^k}{w_{j,1}^k \gamma_{j,2}^k} \right| = 4h_{j+2}^k \frac{(h_j^k + h_{j+1}^k + h_{j+2}^k)^2}{(h_{j+1}^k + 2h_j^k)^2} \left| \frac{\delta_{j+2}^k}{h_{j+2}^k} - \frac{\delta_{j+1}^k}{h_{j+1}^k} \right| \leq 4\sigma^2(1+\sigma) \|\delta^k\|_{l_\infty(\mathbb{Z})}. \quad (7.23)$$

The case of  $\gamma_{j,-1}$  can be derived analogously. □

We need two more lemmas that will be used in the proof of Theorem 9.

**Lemma 27.** Let  $\{\mathcal{R}_k\}$  be the sequence of nonlinear PPH reconstruction operators associated to a sequence of nested  $\sigma$  quasi-uniform grids  $\{X^k\}$  satisfying Definition 27 and  $\mathcal{S}$  the PPH interpolatory subdivision scheme. There exists  $C \in \mathbb{R}$  such that, if  $f^{k+1} = \mathcal{S}f^k$ , then  $\forall k$ ,

$$\|\mathcal{R}_{k+1}(f^{k+1}) - \mathcal{R}_k(f^k)\|_{L^\infty} \leq C \|\delta^k\|_{l_\infty(\mathbb{Z})}. \quad (7.24)$$

*Proof.* Let  $f^k \in l_\infty(\mathbb{Z})$ , and  $x \in \mathbb{R}$ . Let  $j$  be such that  $x \in [x_j^k, x_{j+1}^k]$ , and assume that  $x \in [x_{2j}^{k+1}, x_{2j+1}^{k+1}]$ . The case  $x \in [x_{2j+1}^{k+1}, x_{2j+2}^{k+1}]$  is similar.

We can write

$$\begin{aligned} |\mathcal{R}_{k+1}(f^{k+1})(x) - \mathcal{R}_k(f^k)(x)| &\leq |\mathcal{R}_{k+1}(f^{k+1})(x) - \mathcal{R}_{k+1}^{\mathcal{L}}(f^{k+1})(x)| \\ &\quad + |\mathcal{R}_{k+1}^{\mathcal{L}}(f^{k+1})(x) - \mathcal{R}_k^{\mathcal{L}}(f^k)(x)| \\ &\quad + |\mathcal{R}_k^{\mathcal{L}}(f^k)(x) - \mathcal{R}_k(f^k)(x)|, \end{aligned}$$

where  $\mathcal{R}_k^{\mathcal{L}}$  stands for the centered Lagrange reconstruction operators of the same order.

1) We prove first the bound for the second term on the right hand side.

Since  $x \in [x_{2j}^{k+1}, x_{2j+1}^{k+1}] \subset [x_j^k, x_{j+1}^k]$  we can write

$$\begin{aligned} \mathcal{R}_{k+1}^{\mathcal{L}}(f^{k+1})(x) &= \sum_{m=-1}^2 A_m(x) f_{2j+m}^{k+1}, \\ \mathcal{R}_k^{\mathcal{L}}(f^k)(x) &= \sum_{m=-1}^2 B_m(x) f_{j+m}^k, \end{aligned}$$

where

$$A_m(x) = \prod_{\substack{s=-1 \\ s \neq m}}^2 \frac{x - x_{2j+s}^{k+1}}{x_{2j+m}^{k+1} - x_{2j+s}^{k+1}}, \quad m = -1, 0, 1, 2,$$

$$B_m(x) = \prod_{\substack{s=-1 \\ s \neq m}}^2 \frac{x - x_{j+s}^k}{x_{j+m}^k - x_{j+s}^k}, \quad m = -1, 0, 1, 2.$$

According to Lemma 5 in [42]

$$|A_m(x)| \leq \sigma, \quad |B_m(x)| \leq \sigma, \quad m = -1, 0, 1, 2. \quad (7.25)$$

Here, we remind that the Lagrange polynomial bases sum to one

$$\sum_{m=-1}^2 A_m(x) = \sum_{m=-1}^2 B_m(x) = 1. \quad (7.26)$$

From now on, we drop the explicit dependence on  $x$  for the sake of clarity and write simply  $A_m, B_m$  when referring to these quantities.

Since  $f^{k+1} = \mathcal{S}f^k$ , and  $\mathcal{S}$  is interpolatory we have

$$\begin{aligned} |\mathcal{R}_{k+1}^{\mathcal{L}}(f^{k+1})(x) - \mathcal{R}_k^{\mathcal{L}}(f^k)(x)| &= |A_{-1}f_{2j-1}^{k+1} - B_{-1}f_{j-1}^k + (A_0 - B_0)f_j^k \\ &\quad + A_1f_{2j+1}^{k+1} + (A_2 - B_1)f_{j+1}^k - B_2f_{j+2}^k|, \end{aligned}$$

where

$$f_{2j-1}^{k+1} = \frac{f_{j-1}^k + f_j^k}{2} - \frac{(h_j^k)^2}{4} \tilde{V}_{j-1}^k.$$

Taking into account property (7.5) of the harmonic mean  $|\tilde{V}_{j-1}^k| \leq \frac{|D_j^k|}{w_{j-1,1}^k}$  we can write

$$\begin{aligned} \left| \frac{(h_j^k)^2}{4} \tilde{V}_{j-1}^k \right| &\leq \frac{(h_j^k)^2}{2} \frac{h_{j-1}^k + h_j^k + h_{j+1}^k}{h_j^k + 2h_{j-1}^k} \left| \frac{\delta_{j+1}^k}{h_{j+1}^k} - \frac{\delta_j^k}{h_j^k} \right| \\ &\leq \frac{1}{2} \frac{h_j^k}{h_j^k + h_{j+1}^k} \frac{h_{j-1}^k + h_j^k + h_{j+1}^k}{h_j^k + 2h_{j-1}^k} \left( \frac{h_j^k}{h_{j+1}^k} \left| \delta_{j+1}^k \right| + \left| \delta_j^k \right| \right) \leq \frac{1}{4} \sigma^2 (\sigma + 1) \|\delta^k\|_{l_\infty(\mathbb{Z})}, \end{aligned} \quad (7.27)$$

and similarly for the term in  $f_{2j+1}^{k+1}$

$$f_{2j+1}^{k+1} = \frac{f_j^k + f_{j+1}^k}{2} - \frac{(h_{j+1}^k)^2}{4} \tilde{V}_j^k.$$

Taking again into account the property (7.5) of the harmonic mean we have  $|\tilde{V}_j^k| \leq \frac{|D_j^k|}{w_{j,0}^k}$  and we can write

$$\begin{aligned} \left| \frac{(h_{j+1}^k)^2}{4} \tilde{V}_j^k \right| &\leq \frac{(h_{j+1}^k)^2}{2} \frac{h_j^k + h_{j+1}^k + h_{j+2}^k}{h_{j+1}^k + 2h_{j+2}^k} \left| \frac{\delta_{j+1}^k - \delta_j^k}{\frac{h_{j+1}^k}{h_j^k + h_{j+1}^k}} \right| \\ &\leq \frac{1}{2} \frac{h_{j+1}^k}{h_j^k + h_{j+1}^k} \frac{h_j^k + h_{j+1}^k + h_{j+2}^k}{h_{j+1}^k + 2h_{j+2}^k} \left( \left| \delta_{j+1}^k \right| + \frac{h_{j+1}^k}{h_j^k} \left| \delta_j^k \right| \right) \leq \frac{1}{4} \sigma^2 (1 + \sigma) \|\delta^k\|_{l_\infty(\mathbb{Z})}. \end{aligned} \quad (7.28)$$

Using (7.27) and (7.28) we get

$$\begin{aligned} |\mathcal{R}_{k+1}^{\mathcal{L}}(f^{k+1})(x) - \mathcal{R}_k^{\mathcal{L}}(f^k)(x)| &\leq |A_{-1} \frac{f_{j-1}^k + f_j^k}{2} - B_{-1} f_{j-1}^k \\ &\quad + (A_0 - B_0) f_j^k + A_1 \frac{f_{j+1}^k + f_j^k}{2} \\ &\quad + (A_2 - B_1) f_{j+1}^k - B_2 f_{j+2}^k| \\ &\quad + (|A_{-1}| + |A_1|) \frac{1}{4} \sigma^2 (1 + \sigma) \|\delta^k\|_{l_\infty(\mathbb{Z})}. \end{aligned}$$

The modulus of the first term at the right hand side can be rewritten as

$$\begin{aligned} &\left| \left( \frac{A_{-1}}{2} - B_{-1} \right) (f_{j-1}^k - f_j^k) + \left( A_{-1} - B_{-1} + A_0 - B_0 + \frac{A_1}{2} \right) (f_j^k - f_{j+1}^k) \right. \\ &\quad \left. + B_2 (f_{j+1}^k - f_{j+2}^k) + ((A_{-1} + A_0 + A_1 + A_2) - (B_{-1} + B_0 + B_1 + B_2)) f_{j+1}^k \right|. \end{aligned}$$

Then, using (7.25) and (7.26)

$$|\mathcal{R}_{k+1}^{\mathcal{L}}(f^{k+1})(x) - \mathcal{R}_k^{\mathcal{L}}(f^k)(x)| \leq C_1 \|\delta^k\|_{l_\infty(\mathbb{Z})}. \quad (7.29)$$

**2)** Let us estimate now  $|\mathcal{R}_k^{\mathcal{L}}(f^k)(x) - \mathcal{R}_k(f^k)(x)|$ .

$$\mathcal{R}_k(f^k)(x) = \begin{cases} B_{-1} f_{j-1}^k + B_0 f_j^k + B_1 f_{j+1}^k + B_2 \tilde{f}_{j+2}^k, & \text{if } |D_j^k| \leq |D_{j+1}^k|, \\ B_{-1} \tilde{f}_{j-1}^k + B_0 f_j^k + B_1 f_{j+1}^k + B_2 f_{j+2}^k, & \text{if } |D_j^k| > |D_{j+1}^k|. \end{cases}$$

Let us suppose, without loss of generality, that we are in the first case, i.e.  $|D_j^k| \leq |D_{j+1}^k|$ .

$$|\mathcal{R}_k^{\mathcal{L}}(f^k)(x) - \mathcal{R}_k(f^k)(x)| = |B_2 (f_{j+2}^k - \tilde{f}_{j+2}^k)|. \quad (7.30)$$

Using Definition (26) and applying the triangular inequality we get



$$|f_{j+2}^k - \tilde{f}_{j+2}^k| \leq \left| f_{j+2}^k + \frac{1}{\gamma_{j,2}^k} (\gamma_{j,-1}^k f_{j-1}^k + \gamma_{j,0}^k f_j^k + \gamma_{j,1}^k f_{j+1}^k) \right| + \left| \frac{\tilde{V}_j^k}{\gamma_{j,2}^k} \right|. \quad (7.31)$$

Taking now into account that  $\sum_{s=-1}^2 \gamma_{j,s} = 0$ , we can rewrite the first term and we can bound it as follows

$$\begin{aligned} |f_{j+2}^k - f_{j+1}^k + \left( \frac{\gamma_{j,1}^k + \gamma_{j,2}^k}{\gamma_{j,2}^k} \right) (f_{j+1}^k - f_j^k) + \left( \frac{\gamma_{j,0}^k + \gamma_{j,1}^k + \gamma_{j,2}^k}{\gamma_{j,2}^k} \right) (f_j^k - f_{j-1}^k)| \\ \leq |\delta_{j+2}^k| + \left| \frac{\gamma_{j,1}^k + \gamma_{j,2}^k}{\gamma_{j,2}^k} \right| |\delta_{j+1}^k| + \left| \frac{\gamma_{j,-1}^k}{\gamma_{j,2}^k} \right| |\delta_j^k| \leq (2 + 3\sigma^3) \|\delta^k\|_{l_\infty(\mathbb{Z})}. \end{aligned} \quad (7.32)$$

The second term at the right hand side of (7.31) can be bounded using Lemma 26.

Considering (7.30), (7.32) and Lemma 26 we have,

$$|\mathcal{R}_k^{\mathcal{L}}(f^k)(x) - \mathcal{R}_k(f^k)(x)| \leq \sigma(2 + 4\sigma^2 + 7\sigma^3) \|\delta^k\|_{l_\infty(\mathbb{Z})} = C_2 \|\delta^k\|_{l_\infty(\mathbb{Z})}. \quad (7.33)$$

For the other case,  $|D_j^k| > |D_{j+1}^k|$  using the same ideas we also get the same bound.

**3)** Let us study now  $|\mathcal{R}_{k+1}(f^{k+1})(x) - \mathcal{R}_{k+1}^{\mathcal{L}}(f^{k+1})(x)|$ .

Inequality (7.33) allows us to write

$$|\mathcal{R}_{k+1}(f^{k+1})(x) - \mathcal{R}_{k+1}^{\mathcal{L}}(f^{k+1})(x)| \leq C_2 \|\delta^{k+1}\|_{l_\infty(\mathbb{Z})},$$

Since by Proposition 13 the operator  $\mathcal{S}_1$  is bounded by  $\frac{\sigma}{2}$  we get that

$$|\mathcal{R}_{k+1}(f^{k+1})(x) - \mathcal{R}_{k+1}^{\mathcal{L}}(f^{k+1})(x)| \leq C_2 \|\mathcal{S}_1 \delta^k\|_{l_\infty(\mathbb{Z})} \leq C_3 \|\delta^k\|_{l_\infty(\mathbb{Z})}, \quad (7.34)$$

with  $C_3 = \frac{\sigma}{2} C_2$ .

Finally, joining the results in (7.29), (7.33), and (7.34) we obtain

$$|\mathcal{R}_{k+1}(f^{k+1})(x) - \mathcal{R}_k(f^k)(x)| \leq (C_1 + C_2 + C_3) \|\delta^k\|_{l_\infty(\mathbb{Z})},$$

which completes the proof. □

The following theorem uses standard arguments and previous lemmas to prove the convergence of the nonlinear PPH subdivision scheme.

**Theorem 9** (Convergence). *Let  $\{\mathcal{R}_k\}$  be the sequence of nonlinear PPH reconstruction operators associated to a sequence of nested  $\sigma$  quasi-uniform grids  $\{X^k\}$  with  $\sigma < 1 + \frac{1}{2M}$  satisfying Definition 27. Then, the associated PPH interpolatory subdivision scheme  $\mathcal{S}$  is uniformly convergent.*

*Proof.* The basis of the proof is to observe that  $\{\mathcal{R}_k(f^k)\}_{k \in \mathbb{N}}$  is a Cauchy sequence in  $C_B(\mathbb{R})$ , the space of continuous and bounded functions in  $\mathbb{R}$ .

Let be  $f^0 = f \in l_\infty(\mathbb{Z})$ .

From Lemma 27  $\exists C_1 \in \mathbb{R}$  such that, if  $f^{k+1} = \mathcal{S}f^k$ , then  $\forall k$ ,

$$\|\mathcal{R}_{k+1}(f^{k+1}) - \mathcal{R}_k(f^k)\|_{L^\infty} \leq C_1 \|\delta^k\|_{l_\infty(\mathbb{Z})}.$$

and from Proposition 13  $\exists C_2 \in \mathbb{R}$  such that

$$\|\mathcal{S}_1 \delta^k\|_{l_\infty(\mathbb{Z})} \leq C_2 \|\delta^k\|_{l_\infty(\mathbb{Z})} \quad \forall f^k \in l_\infty(\mathbb{Z}),$$

So

$$\|\mathcal{R}_{k+1}(f^{k+1}) - \mathcal{R}_k(f^k)\|_{L^\infty} \leq C_1 C_2 \|\delta^{k-1}\|_{l_\infty(\mathbb{Z})} \leq C_1 (C_2)^k \|\delta^0\|_{l_\infty(\mathbb{Z})}.$$

As  $\sigma < 1 + \frac{1}{2M}$ ,  $\mathcal{S}_1$  is contractive, which means  $(C_2 < 1)$  and  $\lim_{k \rightarrow \infty} (C_2)^k = 0$ .

Thus, given

$$\frac{\epsilon}{C_1 \|\delta^0\|_{l_\infty(\mathbb{Z})}} > 0, \quad \exists k_0 \in \mathbb{N} \text{ such that } \forall k \geq k_0, \quad |C_2^k| < \frac{\epsilon}{C_1 \|\delta^0\|_{l_\infty(\mathbb{Z})}},$$

i.e. given  $\epsilon > 0$ ,  $\exists k_0 \in \mathbb{N}$  such that  $\forall k \geq k_0$

$$\|\mathcal{R}_{k+1}(f^{k+1}) - \mathcal{R}_k(f^k)\|_{L^\infty} < C_1 \frac{\epsilon}{C_1 \|\delta^0\|_{l_\infty(\mathbb{Z})}} \|\delta^0\|_{l_\infty(\mathbb{Z})} = \epsilon.$$

which proves that  $\{\mathcal{R}_k(f^k)\}_{k \in \mathbb{N}}$  is a Cauchy sequence in  $C_B(\mathbb{R})$ .

Since  $C_B(\mathbb{R})$  equipped with the  $L^\infty$  norm is a Banach space, there exist  $\mathcal{S}^\infty(f) = \lim_{k \rightarrow \infty} \mathcal{R}_k(f^k)$ . □

In order to continue addressing the study of the degree of smoothness of the limit function, we need one more lemma.

**Lemma 28.** *Let  $\{\mathcal{R}_k\}$  be the sequence of nonlinear PPH reconstruction operators associated to a sequence of nested  $\sigma$  quasi-uniform grids  $\{X^k\}$  satisfying Definition 27. The interpolatory PPH reconstruction operators  $\mathcal{R}_k$  have the following properties:*

- 1)  $\|\mathcal{R}_k f^k\|_{L^\infty} \leq C \|f^k\|_{l_\infty(\mathbb{Z})} \quad \forall k$ .
- 2) For each level  $k \geq 1$ , for all  $x, y$  such that  $|x - y| < \lambda_1^{k-1} h_{min}^0$ , with  $\lambda_1 = \frac{1}{2} + (\sigma - 1)M < 1$ , the contractivity constant of the scheme  $\mathcal{S}_1$  of the differences and  $h_{min}^0 = \min_{j \in \mathbb{Z}} h_j^k$ , there exist a constant  $C$  such that

$$|\mathcal{R}_k(f^k)(x) - \mathcal{R}_k(f^k)(y)| \leq C \|\delta^k\|_{l_\infty(\mathbb{Z})}. \quad (7.35)$$

*Proof.* 1) The proof of this point can be found in Proposition 3 in [42].

2) We prove property 2). We write

$$\begin{aligned} |\mathcal{R}_k(f^k)(x) - \mathcal{R}_k(f^k)(y)| &\leq |\mathcal{R}_k(f^k)(x) - \mathcal{R}_k^{\mathcal{L}}(f^k)(x)| \\ &\quad + |\mathcal{R}_k^{\mathcal{L}}(f^k)(x) - \mathcal{R}_k^{\mathcal{L}}(f^k)(y)| \\ &\quad + |\mathcal{R}_k^{\mathcal{L}}(f^k)(y) - \mathcal{R}_k(f^k)(y)|. \end{aligned}$$

According to expression (7.33) inside the proof of Lemma 27 we have that

$$|\mathcal{R}_k^{\mathcal{L}}(f^k)(x) - \mathcal{R}_k(f^k)(x)| \leq C_1 \|\delta^k\|_{l_\infty(\mathbb{Z})} \quad \forall x \in \mathbb{R}. \quad (7.36)$$

Then, we focus now in the second term. Let us suppose  $x \in [x_j^k, x_{j+1}^k]$ , and let us see that  $y \in [x_s^k, x_{s+1}^k]$  with  $|s - j| \leq 4$ .

Let us take the integer number  $k_1 = \lceil 1 - (k-1) \frac{\ln(\lambda_1)}{\ln(2)} \rceil$ , such that  $\lambda_1^{k-1} \leq (\frac{1}{2})^{k_1-1}$ , and notice that  $k_1 \geq 1$ . Then, we have that

$$|x - y| \leq 2 \left(\frac{1}{2}\right)^{k_1} h_{min}^0 = \frac{2 \cdot 2^k h_{min}^0}{2^{k_1} 2^k} \leq \frac{2 \cdot 2^{1-k_1} \frac{\ln(2)}{\ln(\lambda_1)} h_{min}^0}{2^{k_1}} = 4 \cdot 2^{k_1(-\frac{\ln(2)}{\ln(\lambda_1)} - 1)} \frac{h_{min}^0}{2^k} < 4 \frac{h_{min}^0}{2^k},$$

which implies  $|s - j| \leq 4$ . We now write

$$\begin{aligned} \mathcal{R}_k^{\mathcal{L}}(f^k)(x) &= B_{-1}f_{j-1}^k + B_0f_j^k + B_1f_{j+1}^k + B_2f_{j+2}^k, \\ \mathcal{R}_k^{\mathcal{L}}(f^k)(y) &= D_{-1}f_{s-1}^k + D_0f_s^k + D_1f_{s+1}^k + D_2f_{s+2}^k. \end{aligned}$$

Then

$$\begin{aligned} |\mathcal{R}_k^{\mathcal{L}}(f^k)(x) - \mathcal{R}_k^{\mathcal{L}}(f^k)(y)| &= |B_{-1}f_{j-1}^k + B_0f_j^k + B_1f_{j+1}^k + B_2f_{j+2}^k \\ &\quad - D_{-1}f_{s-1}^k - D_0f_s^k - D_1f_{s+1}^k - D_2f_{s+2}^k|. \end{aligned}$$

Regrouping terms

$$\begin{aligned} |\mathcal{R}_k^{\mathcal{L}}(f^k)(x) - \mathcal{R}_k^{\mathcal{L}}(f^k)(y)| &= |B_{-1}(f_{j-1}^k - f_{s-1}^k) + B_0(f_j^k - f_s^k) \\ &\quad + B_1(f_{j+1}^k - f_{s+1}^k) + B_2(f_{j+2}^k - f_{s+2}^k) \\ &\quad + (B_{-1} - D_{-1})f_{s-1}^k + (B_0 - D_0)f_s^k \\ &\quad + (B_1 - D_1)f_{s+1}^k + (B_2 - D_2)f_{s+2}^k|. \end{aligned}$$

Since  $B_{-1} + B_0 + B_1 + B_2 = D_{-1} + D_0 + D_1 + D_2 = 1$ , we can plug  $f_s^k$  into the previous formula as follows

$$\begin{aligned} |\mathcal{R}_k^{\mathcal{L}}(f^k)(x) - \mathcal{R}_k^{\mathcal{L}}(f^k)(y)| &\leq |B_{-1}(f_{j-1}^k - f_{s-1}^k) + B_0(f_j^k - f_s^k) \\ &\quad + B_1(f_{j+1}^k - f_{s+1}^k) + B_2(f_{j+2}^k - f_{s+2}^k) \\ &\quad + |(B_{-1} - D_{-1})(f_{s-1}^k - f_s^k) \\ &\quad + (B_1 - D_1)(f_{s+1}^k - f_s^k) \\ &\quad + (B_2 - D_2)(f_{s+2}^k - f_s^k)|. \end{aligned}$$

Now taking into account that  $|B_i| \leq \sigma$ ,  $|D_i| \leq \sigma$ ,  $i = -1, 0, 1, 2$  according to Lemma 4 in [42], and that  $|s - j| \leq 4$ , we get

$$\begin{aligned} |\mathcal{R}_k^{\mathcal{L}}(f^k)(x) - \mathcal{R}_k^{\mathcal{L}}(f^k)(y)| &\leq (4\sigma|s - j| + |B_{-1} - D_{-1}| + |B_1 - D_1| \\ &\quad + 2|B_2 - D_2|) \|\delta^k\|_{l_\infty(\mathbb{Z})} \leq 24\sigma \|\delta^k\|_{l_\infty(\mathbb{Z})}. \end{aligned}$$

what finishes the proof. □

With all these requisites, the limit function turns out to be Hölder continuous with  $\alpha = 1$ .

**Theorem 10** (Smoothness). *Let  $\{\mathcal{R}_k\}$  be the sequence of nonlinear PPH reconstruction operators associated to a sequence of nested  $\sigma$  quasi-uniform grids  $\{X^k\}$  with  $\sigma < 1 + \frac{1}{2M}$  satisfying Definition 27. Then, the associated PPH interpolatory subdivision scheme  $\mathcal{S}$  is Hölder continuous with  $\alpha = 1$ .*

*Proof.* In order to prove a Lipschitz condition for the limit function we have that

$$|\mathcal{S}^\infty(f)(x) - \mathcal{R}_k(f^k)(x)| \leq \sum_{l \geq k} |\mathcal{R}_{l+1}(f^{l+1})(x) - \mathcal{R}_l(f^l)(x)|.$$

By using Lemma 27 and Proposition 13 we get

$$|\mathcal{S}^\infty(f)(x) - \mathcal{R}_k(f^k)(x)| \leq C_1 \|\delta^k\|_{l_\infty(\mathbb{Z})}. \quad (7.37)$$

If  $|x - y| \geq h_{min}^0$ , then, using the boundedness of the limit function  $\mathcal{S}^\infty(f)$  derived from Theorem 9, we get

$$|\mathcal{S}^\infty(f)(x) - \mathcal{S}^\infty(f)(y)| \leq 2C_2 \|f\|_{l_\infty(\mathbb{Z})} = \frac{2C_2 \|f\|_{l_\infty(\mathbb{Z})}}{h_{min}^0} h_{min}^0 \leq \frac{2C_2 \|f\|_{l_\infty(\mathbb{Z})}}{h_{min}^0} |x - y|. \quad (7.38)$$

If  $|x - y| < h_{min}^0$ , then there exists  $k \in \mathbb{N}$  such that  $\lambda_1^k h_{min}^0 < |x - y| < \lambda_1^{k-1} h_{min}^0$ . Thus, from point 2 of Lemma 28 we obtain

$$|\mathcal{R}_k(f^k)(x) - \mathcal{R}_k(f^k)(y)| \leq C_3 \|\delta^k\|_{l_\infty(\mathbb{Z})}, \quad (7.39)$$

and therefore

$$|\mathcal{S}^\infty(f)(x) - \mathcal{S}^\infty(f)(y)| \leq (2C_1 + C_3) \|\delta^k\|_{l_\infty(\mathbb{Z})}.$$

Then, from Proposition 13,

$$|\mathcal{S}^\infty(f)(x) - \mathcal{S}^\infty(f)(y)| \leq (2C_1 + C_3) \lambda_1^k \|\delta^0\|_{l_\infty(\mathbb{Z})} \leq \frac{(2C_1 + C_3) \|\delta^0\|_{l_\infty(\mathbb{Z})}}{h_{min}^0} |x - y|. \quad (7.40)$$

Finally, from (7.38) and (7.40) we deduce

$$|\mathcal{S}^\infty(f)(x) - \mathcal{S}^\infty(f)(y)| \leq C |x - y|,$$

with  $C = \max\left\{\frac{2C_2 \|f\|_{l_\infty(\mathbb{Z})}}{h_{min}^0}, \frac{(2C_1 + C_3) \|\delta^0\|_{l_\infty(\mathbb{Z})}}{h_{min}^0}\right\}$ , that is, the limit function  $\mathcal{S}^\infty(f)$  satisfies a Lipschitz condition, which completes the proof. □

We complete our theoretical study with the important issue of preservation of convexity of the initial data. In order to address this question, we introduce two definitions.

**Definition 34.** A univariate data set  $\{(x_i, f_i)\}$  is said to be strictly convex if and only if  $D_i > 0 \forall i$ , where  $D_i = \frac{f_{i-1}}{h_i(h_i+h_{i+1})} - \frac{f_i}{h_i h_{i+1}} + \frac{f_{i+1}}{h_{i+1}(h_i+h_{i+1})}$ , and  $h_i = x_i - x_{i-1}$ .

**Definition 35.** An interpolatory subdivision scheme is said to be convexity preserving if and only if the data set  $\{(x_i^k, f_i^k)\}$  is strictly convex for all level  $k$  of subdivision.

Using these definitions we can give the following theorem.

**Theorem 11 (Convexity).** Let  $\{\mathcal{R}_k\}$  be the sequence of nonlinear PPH reconstruction operators associated to a sequence of nested  $\sigma$  quasi-uniform grids  $\{X^k\}$  with  $\sigma < 1 + \frac{1}{2M}$  satisfying Definition 27. Then, the associated PPH interpolatory subdivision scheme  $\mathcal{S}$  is convexity preserving if and only if

$$2D_{i+1}^k - \frac{h_i^k}{h_i^k + h_{i+1}^k} \tilde{V}_i^k - \frac{h_{i+1}^k}{h_i^k + h_{i+1}^k} \tilde{V}_{i+1}^k > 0, \forall i \in \mathbb{Z}, \forall k \in \mathbb{N}.$$

*Proof.* The proof is based on the fact that if  $D_i^k > 0, \forall i \in \mathbb{Z}$ , at a given scale  $k \in \mathbb{N}$ , then we have that the interpolatory subdivision scheme will be convexity preserving if  $D_{2i+1}^{k+1} > 0$ , and  $D_{2i+2}^{k+1} > 0, \forall i \in \mathbb{Z}$ .

We start computing  $D_{2i+1}^{k+1} > 0$ ,

$$D_{2i+1}^{k+1} = \frac{f_{2i}^{k+1}}{h_{2i+1}^{k+1}(h_{2i+1}^{k+1} + h_{2i+2}^{k+1})} - \frac{f_{2i+1}^{k+1}}{h_{2i+1}^{k+1} h_{2i+2}^{k+1}} + \frac{f_{2i+2}^{k+1}}{h_{2i+2}^{k+1}(h_{2i+1}^{k+1} + h_{2i+2}^{k+1})}.$$

Having into account the relations between the scales  $k$  and  $k+1$  we get

$$D_{2i+1}^{k+1} = \frac{2f_i^k}{(h_{i+1}^k)^2} - \frac{4f_{2i+1}^{k+1}}{(h_{i+1}^k)^2} + \frac{2f_{i+1}^k}{(h_{i+1}^k)^2}. \quad (7.41)$$

Using that the odd points at the scale  $k+1$  are predicted by (7.17) we obtain

$$D_{2i+1}^{k+1} = \tilde{V}_i^k > 0, \quad (7.42)$$

due to the fact that  $D_i^k > 0$  and  $D_{i+1}^k > 0$ .

Computing  $D_{2i+2}^{k+1} > 0$ ,

$$D_{2i+2}^{k+1} = \frac{f_{2i+1}^{k+1}}{h_{2i+2}^{k+1}(h_{2i+2}^{k+1} + h_{2i+3}^{k+1})} - \frac{f_{2i+2}^{k+1}}{h_{2i+2}^{k+1} h_{2i+3}^{k+1}} + \frac{f_{2i+3}^{k+1}}{h_{2i+3}^{k+1}(h_{2i+2}^{k+1} + h_{2i+3}^{k+1})}.$$

Plugging now the corresponding values for  $f_{2i+1}^{k+1}$  and  $f_{2i+3}^{k+1}$  according to (7.17) into last expression we arrive to

$$D_{2i+2}^{k+1} = \frac{\frac{f_i^k + f_{i+1}^k}{2} - \frac{(h_{i+1}^k)^2}{4} \tilde{V}_i^k}{\frac{h_{i+1}^k}{2} \left( \frac{h_{i+1}^k}{2} + \frac{h_{i+2}^k}{2} \right)} - \frac{f_{2i+2}^{k+1}}{\frac{h_{i+1}^k}{2} \frac{h_{i+2}^k}{2}} + \frac{\frac{f_{i+1}^k + f_{i+2}^k}{2} - \frac{(h_{i+2}^k)^2}{4} \tilde{V}_{i+1}^k}{\frac{h_{i+2}^k}{2} \left( \frac{h_{i+1}^k}{2} + \frac{h_{i+2}^k}{2} \right)}.$$

After simple algebraical manipulations we reach to

$$D_{2i+2}^{k+1} = 2D_{i+1}^k - \frac{h_i^k}{h_i^k + h_{i+1}^k} \tilde{V}_i^k - \frac{h_{i+1}^k}{h_i^k + h_{i+1}^k} \tilde{V}_{i+1}^k.$$

Considering that we have already proven  $D_{2i+1}^{k+1} > 0$  in (7.42), in order for the interpolatory subdivision scheme to be convexity preserving it remains only to ask for  $D_{2i+2}^{k+1} > 0$ , that is

$$2D_{i+1}^k - \frac{h_i^k}{h_i^k + h_{i+1}^k} \tilde{V}_i^k - \frac{h_{i+1}^k}{h_i^k + h_{i+1}^k} \tilde{V}_{i+1}^k > 0,$$

what concludes the proof.  $\square$

**Corollary 2.** *Let  $\{\mathcal{R}_k\}$  be the sequence of nonlinear PPH reconstruction operators associated to a sequence of nested  $\sigma$  quasi-uniform grids  $\{X^k\}$  with  $\sigma < 1 + \frac{1}{2M}$  satisfying Definition 27. If  $|\tilde{V}_i^k| < 2 \min\{D_i^k, D_{i+1}^k\}, \forall i \in \mathbb{Z}, \forall k \in \mathbb{N}$ , then the associated PPH interpolatory subdivision scheme  $\mathcal{S}$  is convexity preserving.*

*Proof.* Let us consider  $D_i^k > 0, \forall i \in \mathbb{Z}$ , at a given scale  $k \in \mathbb{N}$ . We get the following chain of inequalities

$$\begin{aligned} 2D_{i+1}^k - \frac{h_i^k}{h_i^k + h_{i+1}^k} \tilde{V}_i^k - \frac{h_{i+1}^k}{h_i^k + h_{i+1}^k} \tilde{V}_{i+1}^k &> 2D_{i+1}^k - \frac{h_i^k}{h_i^k + h_{i+1}^k} 2 \min\{D_i^k, D_{i+1}^k\} \\ &- \frac{h_{i+1}^k}{h_i^k + h_{i+1}^k} 2 \min\{D_{i+1}^k, D_{i+2}^k\} \\ &\geq 2D_{i+1}^k - \frac{h_i^k}{h_i^k + h_{i+1}^k} 2D_{i+1}^k - \frac{h_{i+1}^k}{h_i^k + h_{i+1}^k} 2D_{i+1}^k = 0, \end{aligned}$$

what proves the property of convexity preservation by applying Theorem 11.  $\square$

**Corollary 3.** *Let  $\{\mathcal{R}_k\}$  be the sequence of nonlinear PPH reconstruction operators associated to a sequence of nested  $\sigma$  quasi-uniform grids  $\{X^k\}$  with  $\sigma < 1 + \frac{1}{2M}$  satisfying Definition 27. If  $\max\{\frac{D_i^k}{D_{i+1}^k}, \frac{D_{i+1}^k}{D_i^k}\} < 2, \forall i \in \mathbb{Z}, \forall k \in \mathbb{N}$ , then the associated PPH interpolatory subdivision scheme  $\mathcal{S}$  is convexity preserving.*

*Proof.* Let us consider  $D_i^k > 0, \forall i \in \mathbb{Z}$ , at a given scale  $k \in \mathbb{N}$ . Taking into account that  $\tilde{V}_i^k$  is a mean we have

$$|\tilde{V}_i^k| \leq \max\{D_i^k, D_{i+1}^k\} < 2 \min\{D_i^k, D_{i+1}^k\},$$

and therefore we can apply Corollary 2.  $\square$

**Remark 16.** *If the initial data  $f_i^0, i \in \mathbb{Z}$  come from a smooth function, we would have the hypothesis of Corollary 3 satisfied for  $h^0 = \max_{i \in \mathbb{Z}} h_i^0$  sufficiently small since*

$$\begin{aligned} \frac{D_{i+1}}{D_i} &= \frac{f''(\mu_1)}{f''(\mu_0)} = \frac{f''(\mu_0) + f'''(c)(\mu_1 - \mu_0)}{f''(\mu_0)} \\ &= 1 + \frac{f'''(c)}{f''(\mu_0)}(\mu_1 - \mu_0) < 2, \end{aligned}$$

due to the fact that  $\mu_1 - \mu_0 = O(h^0)$ , where  $\mu_0, \mu_1, c$  are intermediate points between  $x_{i-1}^k$  and  $x_{i+2}^k$ .

**Remark 17.** In the case of dealing with uniform grids, we have that  $\tilde{V}_i^k$  coincides with the classical harmonic mean, and therefore  $|\tilde{V}_i^k| < 2 \min\{D_i^k, D_{i+1}^k\}$ , and Corollary 2 applies. Thus, we have a convexity preserving interpolatory subdivision scheme for any initial data.

**Remark 18.** If instead of the weighted harmonic mean  $\tilde{V}_i^k$  we use the classical harmonic mean in the definition of the subdivision scheme given in (7.17) we immediately get a convexity preserving subdivision scheme because the hypothesis of Corollary 2 are met. However, we will reduce the approximation order to second order in this case, while the original scheme comes from a reconstruction which is fourth order accurate for strictly convex functions (see [42]).

## 7.6 Numerical experiments

In this section we carry out some numerical experiments to analyze the obtained outputs and to compare them with the expected theoretical results. Our first experiment is focused on the presented result about the smoothness of the limit function. We are going to estimate the exponent  $\alpha$  of the Hölder continuity of the limit function. In order to do it we have considered the following functions  $f(x)$  and  $g(x)$  given by

$$f(x) := \begin{cases} x(x+1)^4, & 0 \leq x \leq 0.3, \\ x(\cos(2\pi x) + 1), & 0.3 < x \leq 0.7, \\ x^4 + x, & x > 0.7, \end{cases} \quad (7.43)$$

$$g(x) := \begin{cases} -5 + 10x, & 0 \leq x \leq 0.3, \\ \cos(2\pi x) - 2 - \cos(0.6\pi), & 0.3 < x \leq 0.7, \\ x^4 + 2, & x > 0.7. \end{cases}$$

We also consider the point-value discretization  $f^0$  given by the function values at a nonuniform grid  $X_1$  with 30 points in the interval  $[0, 1]$ . Then, we carry out an estimation of the quotient

$$C := \frac{|\mathcal{S}^\infty f^0(x) - \mathcal{S}^\infty f^0(y)|}{|x - y|^\alpha}, \quad x \neq y,$$

for different levels  $k$  of refinement,  $k = 10$ ,  $k = 15$  and  $k = 17$ , and for different values of  $\alpha$ ,  $\alpha = 0.75$ ,  $\alpha = 0.99$ ,  $\alpha = 1$ ,  $\alpha = 1.1$  and  $\alpha = 1.25$ .

In Figure 7.1 we show the considered original function in solid blue and the subdivision curve after  $k = 5$  subdivision levels in dash-dotted black. In Table 7.1 we can observe that the constant  $C$  converges with the resolution levels to a fix value for  $\alpha = 1$ . For smaller values of  $\alpha$  than 1 the estimated value of  $C$  decreases with the number of resolution levels  $k$ , what means that the Hölder exponent of the subdivision scheme is higher. In turn, for larger values of  $\alpha$  than 1 the estimated value of  $C$  increases with the number of resolution levels  $k$ , what means that the Hölder exponent of the subdivision scheme must be lower. Notice that the constant  $C$  in the definition of Hölder continuity depends on  $f(x)$  but must get stable as we approach the limit function with larger and larger  $k$ . We have also carried out the same experiment varying the number and position of the grid points, and for both functions given in (7.43). We have used a nonuniform grid  $X_2$  with 20 non equally spaced abscissae. As it can be seen in Tables 7.2 and 7.3, the results are consistent

with our previous observations, getting in all cases an estimation for the Hölder exponent  $\alpha = 1$ . However, we can appreciate that the value of the constant  $C$  depends not only on the function from which the point-values are taken, but also on the starting grid, since the limit functions for different grids are pretty similar, in the sense that they approximate the underlying function with fourth order, but they are not the same.

$k$	$\alpha = 0.75$	$\alpha = 0.99$	$\alpha = 1$	$\alpha = 1.01$	$\alpha = 1.25$
10	2.7529	43.8798	49.2457	55.2677	880.9333
15	1.1575	42.3851	49.2457	57.2167	2095.2244
17	0.8574	41.8016	49.2457	58.0154	2963.0947

Table 7.1: Estimations of the  $C$  constant in the condition for Hölder continuity with exponent  $\alpha$  for approximations of the limit function with  $k$  levels of subdivision for initial data coming from 30 point-values of the function  $f(x)$  at the grid  $X_1$  of non equally spaced abscissas.

$k$	$\alpha = 0.75$	$\alpha = 0.99$	$\alpha = 1$	$\alpha = 1.01$	$\alpha = 1.25$
10	3.8460	55.9552	62.7977	70.4769	1123.3592
15	2.4247	54.0492	62.7977	72.9622	2671.8134
17	1.7569	53.7591	62.7977	73.9808	3778.5147

Table 7.2: Estimations of the  $C$  constant in the condition for Hölder continuity with exponent  $\alpha$  for approximations of the limit function with  $k$  levels of subdivision for initial data coming from 20 point-values of the function  $f(x)$  at the grid  $X_2$  of non equally spaced abscissas.

$k$	$\alpha = 0.75$	$\alpha = 0.99$	$\alpha = 1$	$\alpha = 1.01$	$\alpha = 1.25$
10	8.3078	83.2891	91.6855	100.9284	1011.8533
15	3.4930	80.4520	91.6855	104.4876	2406.6064
17	2.4699	79.3443	91.6855	105.9462	3403.4554

Table 7.3: Estimations of the  $C$  constant in the condition for Hölder continuity with exponent  $\alpha$  for approximations of the limit function with  $k$  levels of subdivision for initial data coming from 20 point-values of the function  $g(x)$  at the grid  $X_2$  of non equally spaced abscissas.

In our second experiment we just perform a comparison between the presented *PPH* subdivision scheme and the classical linear scheme with 4 points based on Lagrange interpolation. We have plotted in Figure 7.1 the subdivision curve obtained for both methods, PPH and Lagrange, after  $k = 5$  levels of subdivision and starting from the nonuniform grid  $X_1$  with 30 initial points used in the first numerical experiment and the associated point-values of the function  $f(x)$ . The original



function is also provided to compare the approximation capabilities of both subdivision methods. We see the original function in solid blue line, the Lagrange subdivision scheme in dashed red line and the PPH subdivision scheme in dash-dotted black line. As it can be appreciated in Figure 7.1 the Gibbs effects and undesirable oscillations due to the presence of a jump discontinuity are highly reduced with the PPH scheme in contrast with what happens with the linear scheme. Notice the high oscillations that appear near the jump discontinuities when using the linear scheme, what is known to happen when one implements whatever linear scheme. In Figure 7.1 to the right we have shown a zoom of the area around the first jump discontinuity to observe more clearly the behavior of the nonlinear scheme. In Figure 7.2, we also plot the results obtained with the nonuniform grid  $X_2$  with 20 non equally spaced points considered in the previous experiment. We have considered both functions  $f(x)$  and  $g(x)$ . Again, the same type of Gibbs effects appear around the jump discontinuity for the linear method. The corner is not so problematic.

In Table 7.4, we see the errors  $\|f^k - \mathcal{S}^k f^0\|_p$ ,  $p = 1, 2, \infty$ , committed by approximating the original data  $f^k$ , i.e., the right point-values of the function  $f(x)$  at the corresponding abscissas with  $\mathcal{S}^k f^0$  for  $k = 5$  subdivision levels, where  $\mathcal{S}^k f^0$  stands for the iterative application  $k$  times of the analyzed subdivision schemes, namely PPH and Lagrange, starting from the initial function point-values  $f^0$  at the given grid  $X_1$  with 30 abscissae. In Table 7.5, we give the corresponding results for the grid  $X_2$  with 20 abscissae. In Table 7.6, we consider this time the errors  $\|g^k - \mathcal{S}^k g^0\|_p$ ,  $p = 1, 2, \infty$ , for the function  $g(x)$  using the grid  $X_2$  with 20 abscissae.

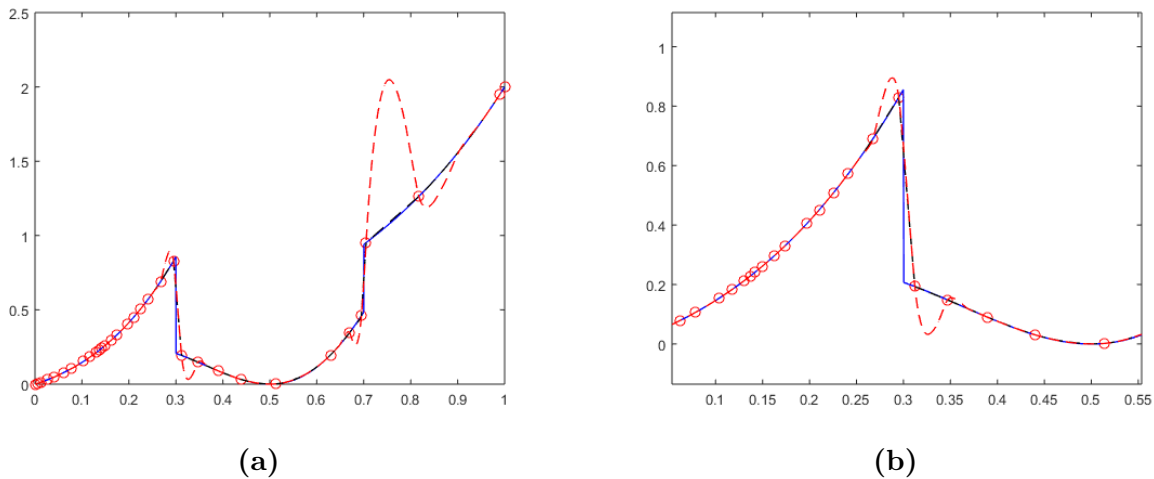


Figure 7.1: **(a)**: Comparison of the subdivision curve after  $k = 5$  subdivision levels for the Lagrange subdivision scheme, in dashed red line, and the PPH subdivision scheme in dash-dotted black line. The original function  $f(x)$  is also plotted in solid blue line. The initial control points, plotted with red circles, come from one of the nonuniform grids  $X$  considered in our two experiments, the one which consists on 30 abscissas in the interval  $[0, 1]$ . **(b)**: Zoom of the area around the first jump discontinuity.

## 7.7 Conclusions

We have defined and analyzed the PPH subdivision scheme on nonuniform grids, which is derived from its associated reconstruction operator. We have paid special attention to the case of

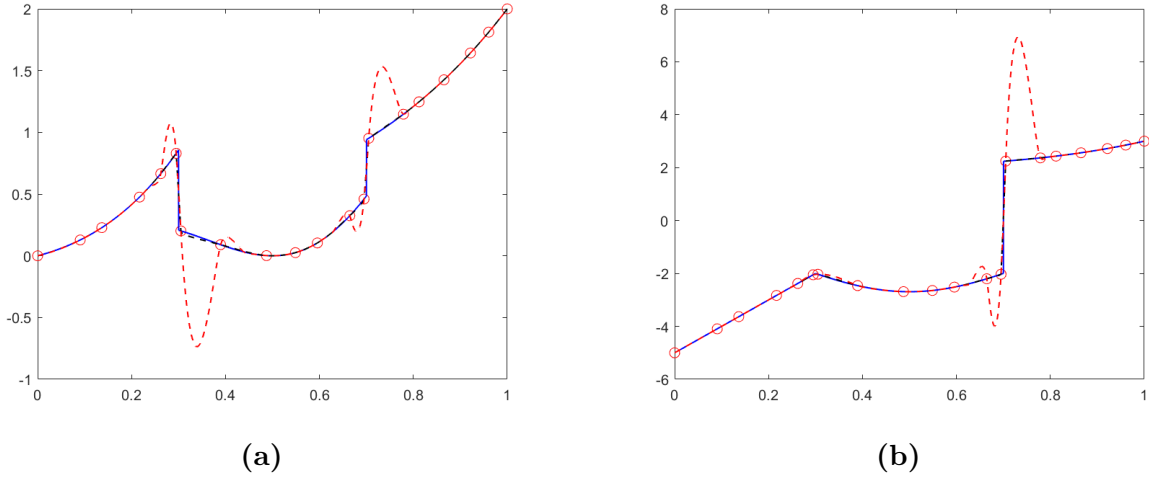


Figure 7.2: Comparison of the subdivision curve after  $k = 5$  subdivision levels for the Lagrange subdivision scheme, in dashed red line, and the PPH subdivision scheme in dash-dotted black line. The original function is also plotted in solid blue line. The initial control points, plotted with red circles, come from one of the nonuniform grids  $X$  considered in our two experiments, the one which consists on 20 abscissas in the interval  $[0, 1]$ . **(a)**: Subdivision curve for data coming from  $f(x)$ . **(b)**: Subdivision curve for data coming from  $g(x)$ .

Method	$\ f^k - S^k f^0\ _1$	$\ f^k - S^k f^0\ _2$	$\ f^k - S^k f^0\ _\infty$
PPH	0.0098	0.0454	0.4239
Lagrange	0.0388	0.1355	0.9767

Table 7.4: Subdivision errors  $\|f^k - S^k f^0\|_p$ ,  $p = 1, 2, \infty$ , committed by approximating the original data  $f^k$  with  $S^k f^0$  for  $k = 5$  subdivision levels starting from the initial function point-values  $f^0$  at the given grid  $X_1$  with 30 points.

Method	$\ f^k - S^k f^0\ _1$	$\ f^k - S^k f^0\ _2$	$\ f^k - S^k f^0\ _\infty$
PPH	0.0163	0.0529	0.3412
Lagrange	0.0809	0.1849	0.8953

Table 7.5: Subdivision errors  $\|f^k - S^k f^0\|_p$ ,  $p = 1, 2, \infty$ , committed by approximating the original data  $f^k$  with  $S^k f^0$  for  $k = 5$  subdivision levels starting from the initial function point-values  $f^0$  at the given grid  $X_2$  with 20 abscissae.

$\sigma$  quasi-uniform grids and initial data coming from strictly convex (concave) smooth functions.

We have theoretically proven some crucial issues when dealing with subdivision schemes, such as existence of a contractive scheme for the first differences, convergence, smoothness of the limit function, and preservation of the convexity properties of the initial data.

Method	$\ f^k - S^k f^0\ _1$	$\ f^k - S^k f^0\ _2$	$\ f^k - S^k f^0\ _\infty$
PPH	0.0580	0.2808	2.1087
Lagrange	0.2837	0.8468	4.6606

Table 7.6: Subdivision errors  $\|g^k - S^k g^0\|_p$ ,  $p = 1, 2, \infty$ , committed by approximating the original data  $g^k$  with  $S^k g^0$  for  $k = 5$  subdivision levels starting from the initial function point-values  $g^0$  at the given grid  $X_2$  with 20 abscissae.

In the numerical experiments section, we have carried out some experiments that reinforce the theoretical results, in particular we have observed the Hölder continuity of the limit function, giving a numerical estimation of the exponent  $\alpha$ , which coincides with the result in Theorem 10. We have also carried out another experiment to analyze the performance of the subdivision scheme with initial data which contain a numerical jump discontinuity, observing that Gibbs effects and oscillations are negligible. Finally a potential real application in  $2D$  is given by making zoom of some coarse data from geological areas corresponding with inaccessible seabeds.

## Chapter 8

# Graphical interpretation of the weighted harmonic mean of $n$ positive values and applications.

This chapter has given rise to a fully written paper which is now submitted [18]

- Amat, S. ; Ortiz, P.; Ruiz, J.; Trillo, J.C. ; Yáñez, D.F. Graphical interpretation of the weighted harmonic mean of  $n$  positive values and applications. Submitted.

### 8.1 Introduction

The arithmetic and the harmonic mean of positive numbers are present in many scientific applications ranging from statistics to numerical analysis. The harmonic mean has the property of penalizing large values, giving rise, because of this reason, to several interesting applications. Moreover, when the arguments do not differ much from each other, both means remain close, which is another crucial property in applications.

In our field of research both the arithmetic mean and the harmonic mean have been used successfully in several occasions for different applications. See for instance [48, 49] for an example in numerical conservation laws, [6, 7, 11, 50] for applications regarding signal processing and signal compression, [12, 21] for their use in image denoising and compression, and [10, 20, 37] for the case of generation of curves and subdivision.

In [42] a nonlinear reconstruction operator called PPH (Piecewise Polynomial Harmonic) was extended to nonuniform grids by using a specific weighted harmonic mean instead of the standard harmonic mean. In this chapter our aim is to introduce some necessary ingredients to extend in turn this last reconstruction operator to several dimensions. More specifically speaking, we need to dispose of an appropriate mean in several dimensions which satisfies the required basic properties, the two mentioned above, as the harmonic mean does. We carry out this study accompanied by a graphical interpretation of the weighted harmonic mean of several values, which helps to quickly understand the theoretical results.

The chapter is organized as follows: In Section 8.2 we work with the weighted arithmetic and harmonic means of two positive numbers, proving two essential results about these means which will allow us to define adapted reconstruction operators in the numerical experiments section.

These properties come accompanied with an intuitive graphical interpretation in  $2D$  according to a corresponding theoretical result that will be also proven. In Section 8.3 a similar path will be followed for the  $3D$  case, which involves working with weighted and harmonic means of three positive numbers. Section 8.4 deals with the general case of considering the weighted arithmetic and harmonic mean of  $n$  positive numbers for whatever integer value  $n \geq 2$ . In Section 8.5 we outline some applications of these results in order to define adapted reconstructions in several dimensions, and we explicitly define a new reconstruction in  $2D$  over triangular meshes adapted to discontinuities, that is, a kind of PPH reconstruction method (see [6]) on triangles. Finally, in Section 8.6 we give some conclusions.

## 8.2 About specific results on the weighted harmonic mean of two positive values

In this section we present an intuitive graphical interpretation of the weighted arithmetic and harmonic means of two positive values together with two key results about the weighted harmonic mean that justify their use in several fields of application. Among them we can mention image processing, curve and surface generation, numerical approximation of the solution of hyperbolic conservation laws apart from more traditional uses in statistics and physics. Perhaps the better known problem where the weighted harmonic mean appears is in the computation of the average speed of a vehicle that drives along a path divided into two parts of different lengths  $s_1$  and  $s_2$  at constant speed  $v_1$  and  $v_2$  respectively, that is

$$v_a = \frac{s_1 + s_2}{t_1 + t_2} = \frac{s_1 + s_2}{\frac{s_1}{v_1} + \frac{s_2}{v_2}} = \frac{1}{w_1 \frac{1}{v_1} + w_2 \frac{1}{v_2}},$$

with  $w_1 = \frac{s_1}{s_1 + s_2}$ ,  $w_2 = \frac{s_2}{s_1 + s_2}$ .

The weighted harmonic mean  $H_w$  is given in the following definition.

**Definition 36.** *Given  $a_1 > 0$ ,  $a_2 > 0$  two positive real numbers and two weights  $w_1 > 0$ ,  $w_2 > 0$  with  $w_1 + w_2 = 1$ , the weighted harmonic mean of  $a_1$  and  $a_2$  is defined by*

$$H_w(a_1, a_2) = \frac{a_1 a_2}{w_1 a_2 + w_2 a_1}.$$

We now present two particular properties, which have been already used in [43] in order to work with a nonlinear reconstruction for nonuniform grids adapted to the potential presence of jump discontinuities on the signal. The first property has to do with the adaptation in case of jump discontinuities, while the second property is related to the order of approximation attained by the nonlinear reconstruction operator, see [43] for more details.

**Lemma 29.** *If  $a_1 > 0$  and  $a_2 > 0$ , the weighted harmonic mean is bounded as follows*

$$H_w(a_1, a_2) < \min \left\{ \frac{1}{w_1} a_1, \frac{1}{w_2} a_2 \right\}. \quad (8.1)$$

**Lemma 30.** *Let  $a > 0$  a fixed positive real number, and let  $a_1 \geq a$  and  $a_2 \geq a$ . If  $|a_1 - a_2| = O(h)$ , then the weighted harmonic mean is also close to the weighted arithmetic mean  $M_w(a_1, a_2) = w_1 a_1 + w_2 a_2$ ,*

$$|M_w(a_1, a_2) - H_w(a_1, a_2)| = \frac{w_1 w_2}{w_1 a_2 + w_2 a_1} (a_1 - a_2)^2 = O(h^2). \quad (8.2)$$

A way of intuitively check these two properties graphically is by using the following interpretation. Given  $a_1, a_2$  two positive numbers and considering  $H_w$  the weighted harmonic mean of these values, we can build the following two parabolas

$$\begin{aligned} p_1(x) &= \frac{a_1 x_H - \frac{H_w}{2}}{x_H(1-x_H)} x^2 + \frac{\frac{H_w}{2} - a_1 x_H^2}{x_H(1-x_H)} x, \\ p_2(x) &= \frac{\frac{H_w}{2} + a_2(x_H - 1)}{x_H(x_H - 1)} x^2 - \frac{\frac{H_w}{2} + a_2(x_H - 1)(x_H + 1)}{x_H(x_H - 1)} x + a_2, \end{aligned} \quad (8.3)$$

where  $x_H$  is defined as the abscissa of the point where both parabolas intersect inside the trapezoid delimited by the four vertices  $(0, 0), (1, 0), (1, a_1), (0, a_2)$ . Its value is given by

$$x_H = \frac{w_1 a_2}{w_1 a_2 + w_2 a_1}. \quad (8.4)$$

**Remark 19.** Geometrically, one can build the parabolas  $p_1(x)$  and  $p_2(x)$  as the unique polynomials of degree less or equal to 2 such that they interpolate the points  $\{(0, 0), (\frac{1}{2}, (\frac{1}{4} + \frac{1}{8w_1})a_1 + (\frac{1}{4} - \frac{1}{8w_2})a_2), (1, a_1)\}$ , and  $\{(0, a_2), (\frac{1}{2}, (\frac{1}{4} - \frac{1}{8w_1})a_1 + (\frac{1}{4} + \frac{1}{8w_2})a_2), (1, 0)\}$  respectively.

In Figure 8.1 (a) we can see the representation of the trapezoid with the two parabolas intersecting at a point with abscissa  $x_H$ , for similar values of  $a_1$  and  $a_2$  and for a value of the weights  $w_1 = \frac{7}{10}, w_2 = \frac{3}{10}$ . In this case, it is appreciated a similar value of the weighted harmonic and arithmetic means. This particular situation relates with Lemma 30. In Figure 8.1 (c) we can see the case for quite different values of  $a_1$  and  $a_2$ . Now, it can be observed that the weighted harmonic mean remains much closer to the minimum value between  $a_1$  and  $a_2$  than the weighted arithmetic mean. This situation has a close relation with Lemma 29. In Figure 8.1 (b) and (d) we consider the case of having equal weights  $w_1 = w_2 = \frac{1}{2}$ , which gives rise to the usual arithmetic and harmonic means. The observations are the same as in the weighted case, although it is interesting to notice that the parabolas degenerate in the two diagonals of the trapezoid.

There are infinitely many ways of defining two parabolas which degenerate in the two diagonals for  $w_1 = w_2 = \frac{1}{2}$ , and intersect at the abscissa  $x_H$  where  $a_2 + (a_1 - a_2)x_H = H_w$ . In fact, for each ordinate of the type  $y_H = f(w_1, w_2)a_1 x_H$  with  $f(w_2, w_1) = 1$  for  $w_1 = w_2 = \frac{1}{2}$ , the parabolas interpolating the points  $\{(0, 0), (x_H, y_H), (1, a_1)\}$  and  $\{(0, a_2), (x_H, y_H), (1, 0)\}$  satisfy both requirements. In particular, we remark three particular cases because of their symmetry or simplicity.

**Case 1:**  $f(w_1, w_2) = \frac{w_2}{w_1}$ .

In this case we have

$$y_H = \frac{w_2}{w_1} a_1 x_H = \frac{w_2 a_2 a_1}{w_1 a_2 + w_2 a_1}, \quad (8.5)$$

and the parabolas take the form

$$\begin{aligned} p_1(x) &= \frac{a_1}{1-x_H} \left[ \left(1 - \frac{w_2}{w_1}\right) x^2 - \left(x_H - \frac{w_2}{w_1}\right) x \right], \\ p_2(x) &= a_2 - a_2 x. \end{aligned} \quad (8.6)$$

**Case 2:**  $f(w_1, w_2) = 1$ .

In this case we get

$$y_H = a_1 x_H, \quad (8.7)$$

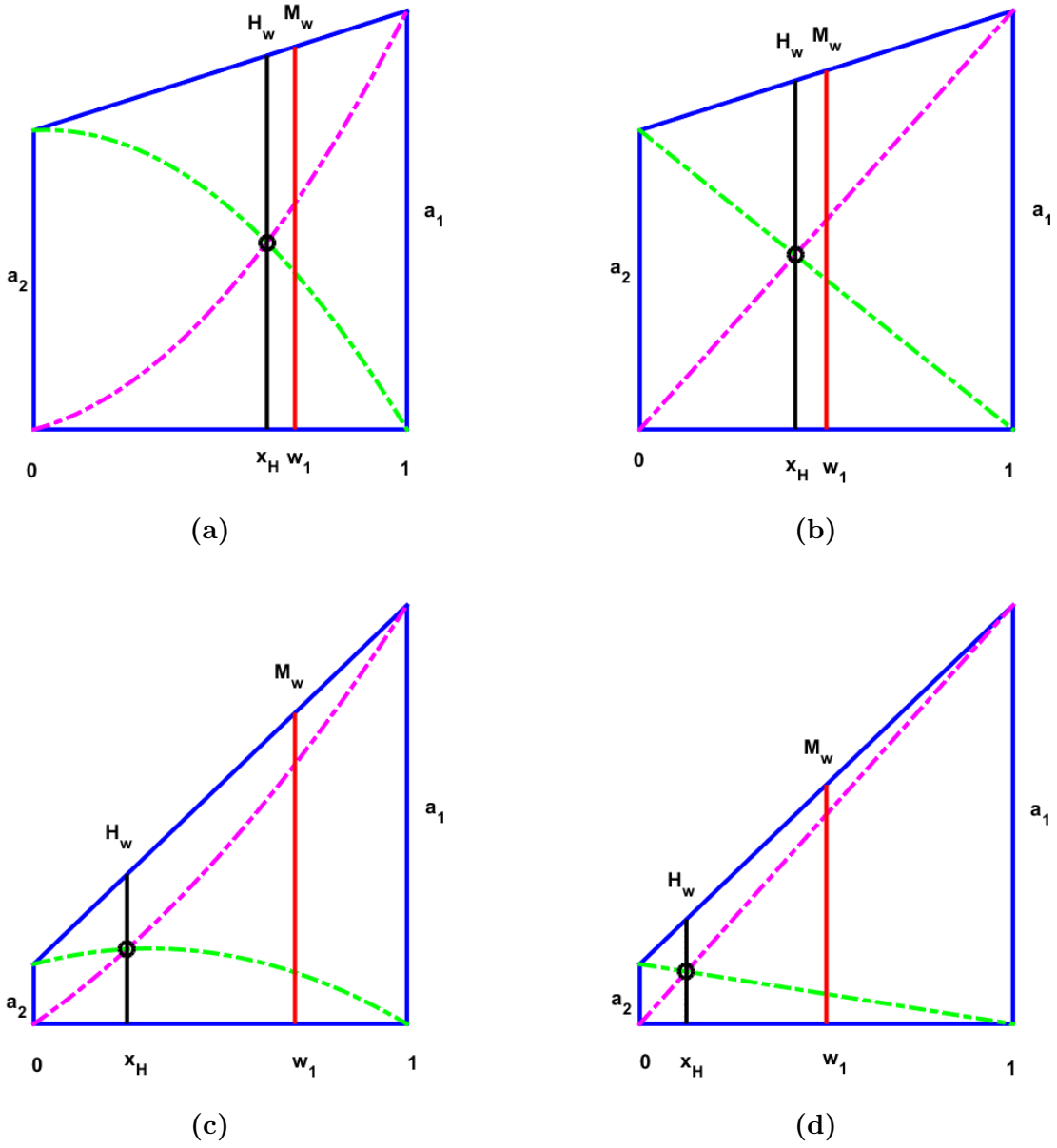


Figure 8.1: Representation of the weighted harmonic and arithmetic means. **(a)**:  $w_1 = 0.7$ ,  $w_2 = 0.3$ ,  $a_1 = 14$ ,  $a_2 = 10$ . **(b)**:  $w_1 = 0.5$ ,  $w_2 = 0.5$ ,  $a_1 = 14$ ,  $a_2 = 10$ . **(c)**:  $w_1 = 0.7$ ,  $w_2 = 0.3$ ,  $a_1 = 14$ ,  $a_2 = 2$ . **(d)**:  $w_1 = 0.5$ ,  $w_2 = 0.5$ ,  $a_1 = 14$ ,  $a_2 = 2$ . In black the weighted harmonic mean, in red the weighted arithmetic mean, in dashed magenta line the parabola  $p_1(x)$  and in dashed green line the parabola  $p_2(x)$ .

and the parabolas are given by

$$\begin{aligned}
 p_1(x) &= a_1 x, \\
 p_2(x) &= \left( \frac{a_1}{x_H - 1} + \frac{a_2}{x_H} \right) x^2 - \left( \frac{a_1}{x_H - 1} + \frac{a_2(x_H + 1)}{x_H} \right) x + a_2.
 \end{aligned} \tag{8.8}$$

**Case 3.**  $f(w_1, w_2) = \frac{1}{2w_1}$ .

In this case

$$y_H = \frac{1}{2w_1}a_1x_H, \quad (8.9)$$

and the parabolas are given in (8.3).

Notice that in the first two cases one of the parabolas remains always equal to one of the diagonals of the trapezoid for all values of  $w_1$ . Since the first and second cases are symmetrical, we will consider only first and third cases from now on. In the next section, we will present the geometrical extension of the given results to the three variables case. The proofs will be omitted because they appear later in the general  $n$ -dimensional case.

### 8.3 Geometrical interpretation of the weighted harmonic mean of three positive values

In this section we give the corresponding results about the weighted harmonic mean for the case of dealing with three positive values. These results can be generalized to  $n$  values with  $n$  a positive integer number, and we will address this situation in the next section, where we will include the proofs.

**Definition 37.** *Given  $a_1 > 0$ ,  $a_2 > 0$ ,  $a_3 > 0$  three positive real numbers and the weights  $w_1 > 0$ ,  $w_2 > 0$ ,  $w_3 > 0$  with  $w_1 + w_2 + w_3 = 1$ , their weighted harmonic mean is defined by*

$$H_w(a_1, a_2, a_3) = \frac{a_1 a_2 a_3}{w_1 a_2 a_3 + w_2 a_1 a_3 + w_3 a_1 a_2}.$$

**Lemma 31.** *If  $a_1 > 0$ ,  $a_2 > 0$ ,  $a_3 > 0$  the weighted harmonic mean is bounded as follows*

$$H_w(a_1, a_2, a_3) < \min \left\{ \frac{1}{w_1}a_1, \frac{1}{w_2}a_2, \frac{1}{w_3}a_3 \right\}. \quad (8.10)$$

**Lemma 32.** *Let  $a > 0$  a fixed positive real number, and let  $a_1 \geq a$ ,  $a_2 \geq a$ ,  $a_3 \geq a$ . If  $|a_1 - a_2| = O(h)$ ,  $|a_1 - a_3| = O(h)$ , then the weighted harmonic mean is also close to the weighted arithmetic mean  $M_w(a_1, a_2, a_3) = w_1 a_1 + w_2 a_2 + w_3 a_3$ ,*

$$\begin{aligned} |M_w(a_1, a_2, a_3) - H_w(a_1, a_2, a_3)| &= \frac{w_1 w_2 (a_1 - a_2)^2 a_3 + w_1 w_3 (a_1 - a_3)^2 a_2 + w_2 w_3 (a_2 - a_3)^2 a_1}{w_1 a_2 a_3 + w_2 a_1 a_3 + w_3 a_1 a_2} \\ &= O(h^2). \end{aligned} \quad (8.11)$$

The following two theorems are dedicated to write in a formal way the geometrical interpretation of the weighted harmonic mean, generalizing the expressions for the two variables case given in (8.3), and (8.6). The case of expressions (8.8) could be treated in a similar way, and we will not consider it, since it is a symmetrical version of case (8.6). Let us first introduce the following notations for the vertices of a straight prism with triangular base

$$\begin{aligned} B_1 &= (1, 0, 0), & B_2 &= (0, 1, 0), & B_3 &= (0, 0, 0), \\ P_1 &= (1, 0, a_1), & P_2 &= (0, 1, a_2), & P_3 &= (0, 0, a_3), \end{aligned}$$



where  $B_i, i = 1, 2, 3$ , stand for the vertices of the base and the corresponding  $P_i$  for the vertices located at the heights of the prism through the points  $B_i$  satisfying that the length of the segment between  $P_i$  and  $B_i$  is  $a_i$ . We will also use the barycenter of the points  $B_i$

$$GM_w := w_1B_1 + w_2B_2 + w_3B_3.$$

The first theorem amounts to the generalization of the expressions in (8.6) and can be written as follows.

**Theorem 12.** *Let us consider the plane  $\Pi$  which passes through the points  $P_1, P_2$  and  $P_3$  given by the equation*

$$\Pi \equiv x_1(a_3 - a_1) + x_2(a_3 - a_2) + x_3 - a_3 = 0. \quad (8.12)$$

*Let us also consider the plane  $V_3$  which passes through the points  $B_1, B_2$  and  $P_3$  given by the equation*

$$V_3 \equiv x_1 + x_2 + \frac{x_3}{a_3} = 1, \quad (8.13)$$

*and the two paraboloids  $V_1$  and  $V_2$  given by the equations*

$$\begin{aligned} V_1 &\equiv x_3 = b_1x_1^2 + (a_1 - b_1)x_1, & \text{which passes through } P_1, B_2, B_3, \\ V_2 &\equiv x_3 = b_2x_2^2 + (a_2 - b_2)x_2, & \text{which passes through } B_1, P_2, B_3, \end{aligned} \quad (8.14)$$

*where the coefficients  $b_i$  are given by*

$$b_i = \frac{H_w}{\bar{x}_i(\bar{x}_i - 1)}(w_3 - w_i), \quad i = 1, 2. \quad (8.15)$$

*Then, the system of equations formed by (8.13) and (8.14) has a unique solution  $(\bar{x}_1, \bar{x}_2, \bar{x}_3)$  given by*

$$\bar{x}_1 = w_1 \frac{H_w}{a_1}, \quad \bar{x}_2 = w_2 \frac{H_w}{a_2}, \quad \bar{x}_3 = w_3 H_w. \quad (8.16)$$

*Moreover, the height of the prism through the point  $(\bar{x}_1, \bar{x}_2, 0)$  coincides with the weighted harmonic mean  $H_w$  of  $a_1, a_2, a_3$  and the height of the prism through the barycenter of the triangular base  $GM_w = w_1B_1 + w_2B_2 + w_3B_3$  coincides with the weighted arithmetic mean.*

The second theorem deals with the generalization of expressions (8.3).

**Theorem 13.** *Let us consider the plane  $\Pi$  which passes through the points  $P_1, P_2$  and  $P_3$  given by the equation*

$$\Pi \equiv x_1(a_3 - a_1) + x_2(a_3 - a_2) + x_3 - a_3 = 0. \quad (8.17)$$

*Let us also consider the paraboloid  $V_3^*$  passing through  $B_1, B_2, P_3$  given by*

$$x_3 = a_3 + (c_1x_1(x_1 - 1) - a_3x_1) + (c_2x_2(x_2 - 1) - a_3x_2), \quad (8.18)$$

*where the coefficients  $c_i$  are given by*

$$c_i = \frac{\frac{H_w}{3} + (\bar{x}_1 + \bar{x}_2 - 1)a_3}{2\bar{x}_i(\bar{x}_i - 1)}, \quad i = 1, 2, \quad (8.19)$$

and the two paraboloids  $V_1$  and  $V_2$  given by the equations

$$\begin{aligned} V_1^* &\equiv x_3 = b_1 x_1^2 + (a_1 - b_1)x_1, & \text{which passes through } P_1, B_2, B_3, \\ V_2^* &\equiv x_3 = b_2 x_2^2 + (a_2 - b_2)x_2, & \text{which passes through } B_1, P_2, B_3, \end{aligned} \quad (8.20)$$

where the coefficients  $b_i$  are given by

$$b_i = \frac{H_w}{\bar{x}_i(\bar{x}_i - 1)} \left( \frac{1}{3} - w_i \right), \quad i = 1, 2. \quad (8.21)$$

Then, the system of equations formed by (8.18) and (8.20) has a unique solution  $(\bar{x}_1, \bar{x}_2, \bar{x}_3)$  given by

$$\bar{x}_1 = w_1 \frac{H_w}{a_1}, \quad \bar{x}_2 = w_2 \frac{H_w}{a_2}, \quad \bar{x}_3 = \frac{H_w}{3}. \quad (8.22)$$

Moreover, the height of the prism through the point  $(\bar{x}_1, \bar{x}_2, 0)$  coincides with the weighted harmonic mean  $H_w$  of  $a_1, a_2, a_3$  and the height of the prism through the barycenter of the triangular base  $GM_w = w_1 B_1 + w_2 B_2 + w_3 B_3$  coincides with the weighted arithmetic mean.

In Figures 8.2 and 8.3 we represent the situation given in Theorem 13, being the situation of Theorem 12 similar. In Figure 8.2 (a,c,e), we show the paraboloids built with the values  $a_1 = 3, a_2 = 4, a_3 = 6$ , with the weights  $w_1 = 0.2, w_2 = 0.2, w_3 = 0.6$ , and in (b,d,f), the planes obtained for the case of dealing with equal weights  $w_1 = w_2 = w_3 = \frac{1}{3}$ . These plots correspond to the situation considered in Theorem 13. We observe how the paraboloids degenerate in planes generalizing the case of the non-weighted harmonic mean.

In Figure 8.3, we show the intersection of the three paraboloids for the same values and weights. It is interesting to compare the representation of the weighted harmonic mean  $H_w$ , which coincides with the height of the prism through the point  $GH_w$  (orthogonal projection onto the base of the intersection point of the three paraboloids considered in Theorem 13), with the representation of the weighted arithmetic mean  $M_w$ , which amounts to the height of the prism through the barycenter  $GM_w$  of the vertices of the triangular base affected by the corresponding weights.

## 8.4 Results on the weighted harmonic mean of $n$ values

First, we introduce the definition of weighted harmonic mean  $H_w$  that we are going to be using

**Definition 38.** Given  $a_i > 0, i = 1, \dots, n$   $n$  positive real numbers and the weights  $w_i > 0, i = 1, \dots, n$  with  $\sum_{i=1}^n w_i = 1$ , the weighted harmonic mean is defined by

$$H_w(a_1, \dots, a_n) = \frac{1}{\sum_{i=1}^n \frac{w_i}{a_i}} = \frac{\prod_{k=1}^n a_k}{\sum_{i=1}^n w_i \prod_{\substack{k=1 \\ k \neq i}}^n a_k},$$

and the weighted arithmetic mean is defined by

$$M_w(a_1, \dots, a_n) = \sum_{i=1}^n w_i a_i.$$

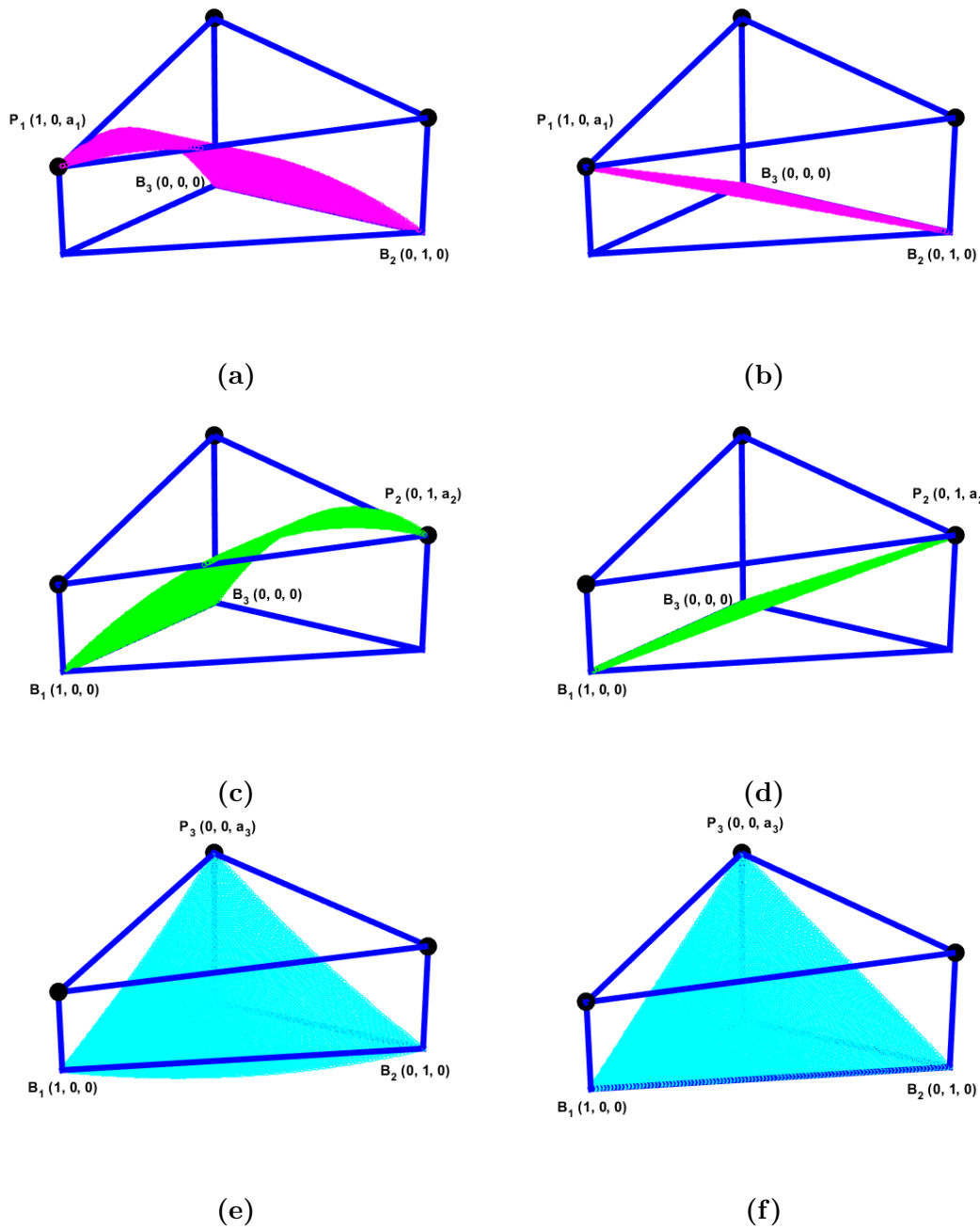


Figure 8.2: Representation of the three paraboloids considered in Theorem 13 for the representation of the harmonic mean of the values  $a_1 = 3$ ,  $a_2 = 4$ ,  $a_3 = 6$ . **(a, c, e)**: weights  $w_1 = 0.2$ ,  $w_2 = 0.2$ ,  $w_3 = 0.6$ . **(b, d, f)**: weights  $w_1 = w_2 = w_3 = \frac{1}{3}$ . **(a, b)**:  $V_1^*$ . **(c, d)**:  $V_2^*$ . **(e, f)**:  $V_3^*$ .

We now give the main two results which are crucial in applications in numerical analysis, such as we will show in the section devoted to practical cases. The first lemma has to do with the property of boundedness of the mean by the minimum of its arguments and it is used to define adaptative methods.

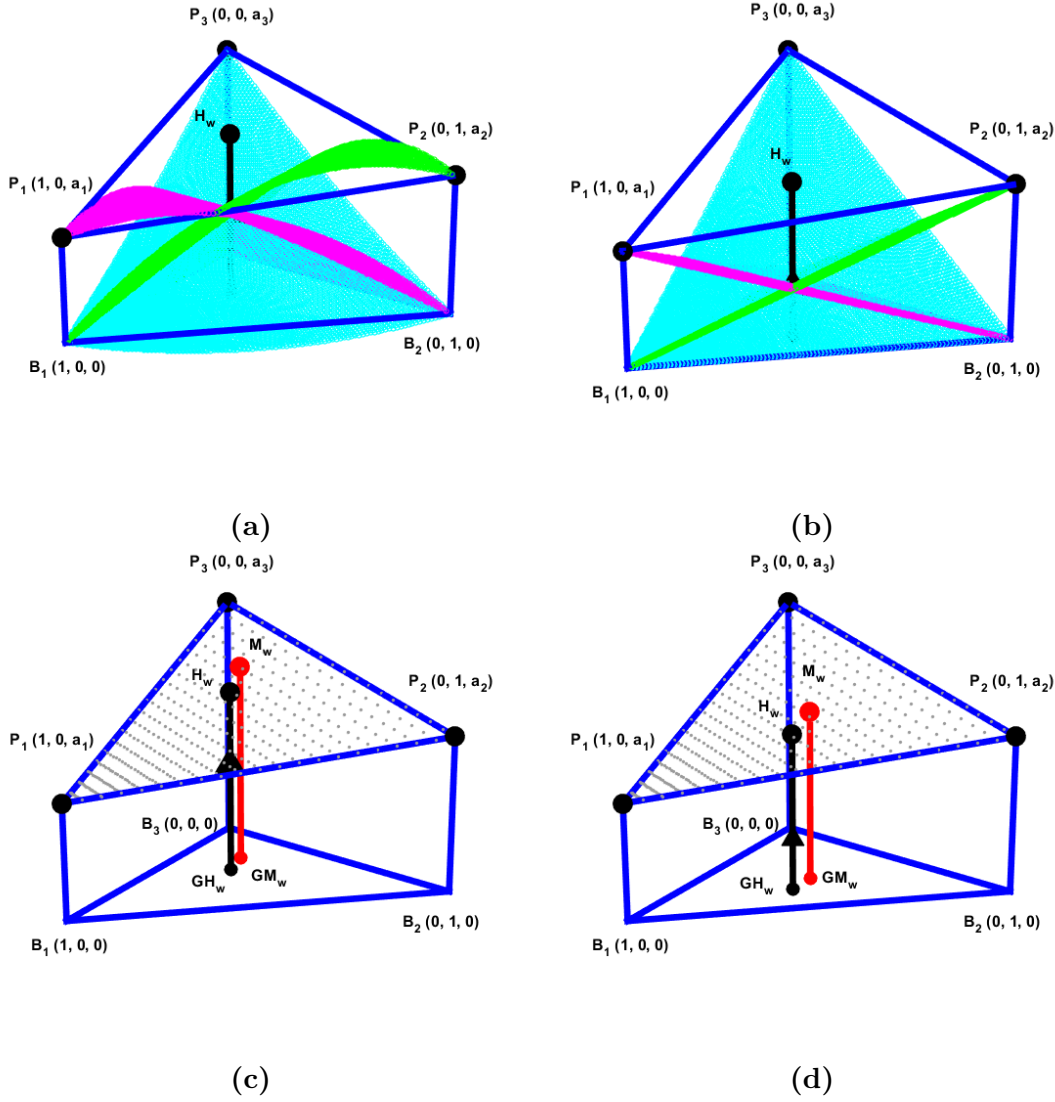


Figure 8.3: Representation of weighted harmonic mean of three positive values  $a_1 = 3$ ,  $a_2 = 4$ ,  $a_3 = 6$  as the height of the prism through the intersection point of the three paraboloids considered in Theorem 13. Comparison with the weighted arithmetic mean for the representation of the harmonic mean of the values. **(a, c)**: weights  $w_1 = 0.2$ ,  $w_2 = 0.2$ ,  $w_3 = 0.6$ . **(b, d)**: weights  $w_1 = w_2 = w_3 = \frac{1}{3}$ . **(a, b)**: Intersection of the three paraboloids. **(c, d)**: Comparison between the weighted harmonic mean and the weighted arithmetic mean.

**Lemma 33.** Let  $a_i > 0, i = 1, \dots, n$  be  $n$  positive real numbers and  $w_i > 0, i = 1, \dots, n$  the corresponding weights with  $\sum_{i=1}^n w_i = 1$ . Then, the weighted harmonic mean  $H_w$  is bounded as follows

$$H_w < \frac{a_{i_0}}{w_{i_0}} \leq \frac{a_i}{w_i}, \quad i = 1, \dots, n,$$

where  $\frac{a_{i_0}}{w_{i_0}} = \min\left\{\frac{a_1}{w_1}, \dots, \frac{a_n}{w_n}\right\}$ .

*Proof.*

$$H_w = \frac{\prod_{k=1}^n a_k}{\sum_{j=1}^n w_j \prod_{\substack{k=1 \\ k \neq j}}^n a_k} = \frac{a_{i_0}}{w_{i_0}} \frac{\prod_{\substack{k=1 \\ k \neq i_0}}^n a_k}{\sum_{j=1}^n \frac{w_j}{w_{i_0}} \prod_{\substack{k=1 \\ k \neq j}}^n a_k} < \frac{a_{i_0}}{w_{i_0}} \leq \frac{a_i}{w_i}, \quad i = 1, \dots, n.$$

□

The second lemma deals with how close remains the weighted harmonic mean to the weighted arithmetic mean when the arguments are also close among them. This property is essential to define nonlinear methods which preserve the order of approximation of their linear counterparts from which they are derived. We will also show this relation in the section dedicated to the practical examples.

**Lemma 34.** *Let  $a_i > 0, i = 1, \dots, n$  be  $n$  positive real numbers and  $w_i > 0, i = 1, \dots, n$  the corresponding weights with  $\sum_{i=1}^n w_i = 1$ . If  $a_i = O(1), \forall i = 1, \dots, n$ , and  $|a_1 - a_i| = O(h), \forall i = 2, \dots, n$ , then, the weighted harmonic mean  $H_w$  and the weighted arithmetic mean  $M_w := \sum_{i=1}^n w_i a_i$  satisfy*

$$|M_w - H_w| = O(h^2).$$

*Proof.* Using the expressions of  $H_w$  and  $M_w$  we have

$$|M_w - H_w| = \left| \sum_{i=1}^n w_i a_i - \frac{\prod_{k=1}^n a_k}{\sum_{j=1}^n w_j \prod_{\substack{k=1 \\ k \neq j}}^n a_k} \right| = \left| \frac{\sum_{i=1}^n w_i a_i \sum_{j=1}^n w_j \prod_{\substack{k=1 \\ k \neq j}}^n a_k - \prod_{k=1}^n a_k}{\sum_{j=1}^n w_j \prod_{\substack{k=1 \\ k \neq j}}^n a_k} \right|. \quad (8.23)$$

Now, paying attention to the fact that given two indices  $i_0, j_0$  such that  $1 \leq i_0 < j_0 \leq n$  we have

$$w_{i_0} a_{i_0} w_{j_0} \prod_{\substack{k=1 \\ k \neq j_0}}^n a_k = w_{i_0} a_{i_0}^2 w_{j_0} \prod_{\substack{k=1 \\ k \neq i_0, j_0}}^n a_k, \quad (8.24)$$

$$w_{j_0} a_{j_0} w_{i_0} \prod_{\substack{k=1 \\ k \neq i_0}}^n a_k = w_{i_0} a_{j_0}^2 w_{j_0} \prod_{\substack{k=1 \\ k \neq i_0, j_0}}^n a_k, \quad (8.25)$$

and just by summing up both terms in (8.24) and (8.25) we get

$$w_{i_0} a_{i_0} w_{j_0} \prod_{\substack{k=1 \\ k \neq j_0}}^n a_k + w_{j_0} a_{j_0} w_{i_0} \prod_{\substack{k=1 \\ k \neq i_0}}^n a_k = w_{i_0} w_{j_0} \prod_{\substack{k=1 \\ k \neq i_0, j_0}}^n a_k (a_{i_0}^2 + a_{j_0}^2). \quad (8.26)$$

For the case  $i_0 = j_0$  we get

$$w_{i_0} a_{i_0} w_{j_0} \prod_{\substack{k=1 \\ k \neq j_0}}^n a_k = w_{i_0}^2 \prod_{k=1}^n a_k. \quad (8.27)$$

Using the simplifications in (8.26) and (8.27) we can rewrite (8.23) as

$$|M_w - H_w| = \left| \frac{\sum_{i=1}^n w_i^2 \prod_{k=1}^n a_k + \sum_{\substack{i,j=1 \\ i < j}}^n w_i w_j (a_i^2 + a_j^2) \prod_{\substack{k=1 \\ k \neq i,j}}^n a_k}{\sum_{j=1}^n w_j \prod_{\substack{k=1 \\ k \neq j}}^n a_k} \right| = \left| \frac{\sum_{\substack{i,j=1 \\ i < j}}^n w_i w_j (a_i - a_j)^2 \prod_{\substack{k=1 \\ k \neq i,j}}^n a_k}{\sum_{j=1}^n w_j \prod_{\substack{k=1 \\ k \neq j}}^n a_k} \right| = O(h^2),$$

since by the triangular inequality we have that  $|a_i - a_j| \leq |a_i - a_1| + |a_1 - a_j| = O(h)$ .  $\square$

We introduce the following notation for the vertices of a prism in  $\mathbb{R}^n$ .

$$\begin{cases} B_i \equiv (0, \dots, 0, \frac{1}{i}, 0, \dots, 0) & i = 1, \dots, n-1, \\ B_n = (0, \dots, 0), \\ P_i \equiv (0, \dots, 0, \frac{1}{i}, 0, \dots, 0, a_i) & i = 1, \dots, n-1, \\ P_n = (0, \dots, 0, a_n), \end{cases}$$

where the points  $B_i$  represent the vertices which lay on the base of the prism and the vertices  $P_i$  are nothing more than the points located at the maximum height of the prism at the corresponding points  $B_i$  in the base and in the parallel direction to the  $x_n$  axis.

We are now ready to give the following two theorems for the weighted harmonic mean, which generalize the geometrical representations using prisms.

**Theorem 14.** *Let us consider the hyperplane  $\Pi$  which passes through the points  $P_i, i = 1, \dots, n$   $n \geq 2$ , given by the equation*

$$\Pi \equiv x_n = a_n + \sum_{i=1}^{n-1} x_i (a_i - a_n). \quad (8.28)$$

*Let us also consider the hyperplane  $V_n$  which passes through the points  $B_i, i = 1, \dots, n-1$  and  $P_n$  given by the equation*

$$V_n \equiv \sum_{i=1}^{n-1} x_i + \frac{x_n}{a_n} = 1. \quad (8.29)$$

*and the paraboloids  $V_i, i = 1, \dots, n-1$  given by the equations*

$$V_i \equiv x_n = b_i x_i^2 + (a_i - b_i) x_i, \quad (8.30)$$

*which pass through  $B_1, \dots, B_{i-1}, P_i, B_{i+1}, \dots, B_n$  respectively, where the coefficients  $b_i$  are given by*

$$b_i = \frac{H_w}{\bar{x}_i (\bar{x}_i - 1)} (w_n - w_i), \quad i = 1, \dots, n-1. \quad (8.31)$$

*Then, the system of equations formed by (8.29) and (8.30) has a unique solution  $(\bar{x}_1, \dots, \bar{x}_n)$  given by*

$$\bar{x}_i = w_i \frac{H_w}{a_i}, \quad i = 1, \dots, n-1, \quad \bar{x}_n = w_n H_w. \quad (8.32)$$

*Moreover, the following two affirmations are true:*

a) The height of the prism through the point  $(\bar{x}_1, \dots, \bar{x}_{n-1}, 0)$  coincides with the weighted harmonic mean  $H_w$  of  $a_i, i = 1, \dots, n$ , that is, the point  $(\bar{x}_1, \dots, \bar{x}_{n-1}, H_w)$  belongs to the hyperplane  $\Pi$ .

b) The height of the prism through the barycenter of the base  $GM_w = \sum_{i=1}^n w_i B_i$  coincides with the weighted arithmetic mean.

*Proof.* It is immediate to check that the proposed solution satisfies (8.29) and (8.30). Let us prove that the solution is unique. By reductio ad absurdum, let us suppose that there exists another solution  $x' = (x'_1, \dots, x'_n)$  with  $x' \neq \bar{x}$ . Then, denoting  $z_i = \bar{x}_i - x'_i, i = 1, \dots, n$ , the system of equations formed by (8.29) and (8.30) can be easily transformed into

$$\sum_{i=1}^{n-1} z_i + \frac{z_n}{a_n} = 0, \quad (8.33a)$$

$$z_n - b_i z_i (\bar{x}_i + x'_i) - (a_i - b_i) z_i = 0, \quad i = 1, \dots, n-1, \quad (8.33b)$$

what amounts to a homogeneous linear system of  $n$  equations with  $n$  unknowns. If we show that this system has only the trivial solution  $z = 0$ , then we would have proven that  $\bar{x} = x'$ , what is a contradiction with the starting supposition. Therefore,  $\bar{x}$  would be the unique solution. Let us then prove that system (8.33) has  $z = 0$  as the unique solution. Again by reductio ad absurdum, let us suppose that the system has infinite solutions, that is,  $z = \sum_{k=1}^s \lambda_k v^k$ , where  $s = n - r$ , being  $r$  the rank of the coefficient matrix of the linear system,  $\lambda_k \in \mathbb{R}$ , and  $v^k, k = 1, \dots, s$ , represent a base of the kernel of the associated linear map. Let us consider the univariate set of solutions  $z = \lambda_1 v^1, \lambda_1 \in \mathbb{R}$ . By the sake of simplicity, we will drop the superindex and we will write  $z = \lambda v$ . Thus, we obtain

$$x' = \bar{x} - z = \bar{x} - \lambda v,$$

whose coordinates are given by

$$x'_i = \bar{x}_i - z_i = \bar{x}_i - \lambda v_i. \quad (8.34)$$

Plugging (8.34) into (8.33b) we get

$$\lambda v_n = b_i \lambda v_i (2\bar{x}_i - \lambda v_i) + (a_i - b_i) \lambda v_i, \quad \forall i = 1, \dots, n-1, \quad (8.35)$$

and simplifying expression (8.35) we obtain

$$-\lambda b_i v_i^2 + 2b_i v_i \bar{x}_i + (a_i - b_i) v_i - v_n = 0, \quad \forall i = 1, \dots, n-1, \quad \lambda \neq 0. \quad (8.36)$$

Now, particularizing expression (8.36) for two different values of  $\lambda, \lambda_1 \neq \lambda_2$ , and subtracting both expressions, we reach to

$$(\lambda_1 - \lambda_2) b_i v_i^2 = 0, \quad \forall i = 1, \dots, n-1. \quad (8.37)$$

We are going to prove now that there exists  $i_0 \in \{1, \dots, n-1\}$  such that  $b_{i_0} \neq 0$  and  $v_{i_0} \neq 0$ , and therefore, from (8.37), this would imply that  $\lambda_1 = \lambda_2$  what is a contradiction. Thus,  $z = 0$  would be the unique solution of the homogeneous linear system and  $\bar{x}$  would be the unique solution of the system given by (8.29) and (8.30).

Since  $v \neq 0$ ,  $\exists v_i \neq 0$  for some  $i \in \{1, \dots, n-1\}$ . Otherwise, if  $v_i = 0$ ,  $\forall i \in \{1, \dots, n-1\}$ , from (8.33a) we get  $v_n = -a_n \sum_{i=1}^{n-1} v_i = 0$  and  $v = 0$ , what is not possible. Let us denote  $I$  the set of indices for which  $v_i \neq 0$ . If we suppose that  $b_i = 0$ ,  $\forall i \in I$ , then from (8.36) we get  $a_i v_i - v_n = 0$ . Thus,  $v_i = \frac{v_n}{a_i}$ ,  $\forall i \in I$ . Also, from (8.33a)

$$\sum_{i \in I} \lambda v_i + \lambda \frac{v_n}{a_n} = 0. \quad (8.38)$$

Now, using in (8.38) the fact that  $v_i = \frac{v_n}{a_i}$ ,  $\forall i \in I$ , we get  $v_n = 0$ , and in turn,  $v = 0$ , what gives a contradiction which comes from the supposition  $b_i = 0$ ,  $\forall i \in I$ . Therefore,  $\exists i_0 \in I$ , such that  $b_{i_0} \neq 0$ .

In order to prove now point a) of the theorem, we consider the straight line parallel to the  $x_n$  axis passing through  $(\bar{x}_1, \dots, \bar{x}_{n-1}, 0)$ , that is

$$r_w \equiv \begin{cases} x_1 = \bar{x}_1, \\ \vdots \\ x_{n-1} = \bar{x}_{n-1}. \end{cases} \quad (8.39)$$

Cutting this straight line with the hyperplane  $\Pi$  we get the point  $(\bar{x}_1, \dots, \bar{x}_{n-1}, H_w)$ , which gives the enunciated result. A similar argument proves point b), just by considering in this case the straight line parallel to the  $x_n$  axis passing through the barycenter  $GM_w = \sum_{i=1}^n w_i B_i = (w_1, \dots, w_{n-1}, 0)$ , and verifying that its intersection point with the hyperplane  $\Pi$  is just the weighted arithmetic mean  $M_w = \sum_{i=1}^n w_i a_i$ .  $\square$

**Theorem 15.** *Let us consider the hyperplane  $\Pi$  which passes through the points  $P_i$ ,  $i = 1, \dots, n$ ,  $n \geq 2$ , given by the equation*

$$\Pi \equiv x_n = a_n + \sum_{i=1}^{n-1} x_i (a_i - a_n). \quad (8.40)$$

*Let us also consider the paraboloid given by  $V_n$  which passes through the points  $B_i$ ,  $i = 1, \dots, n-1$  and  $P_n$  given by the equation*

$$V_n \equiv x_n = a_n + \sum_{i=1}^{n-1} (c_i x_i^2 - (c_i + a_n) x_i), \quad (8.41)$$

*where the coefficients  $c_i$  are given by*

$$c_i = \frac{\frac{H_w}{n} + \left( \sum_{j=1}^{n-1} \bar{x}_j - 1 \right) a_n}{(n-1) \bar{x}_i (\bar{x}_i - 1)}, \quad i = 1, \dots, n-1, \quad (8.42)$$

*and the paraboloids  $V_i$ ,  $i = 1, \dots, n-1$  given by the equations*

$$V_i \equiv x_n = b_i x_i^2 + (a_i - b_i) x_i, \quad (8.43)$$



which pass through  $B_1, \dots, B_{i-1}, P_i, B_{i+1}, \dots, B_n$  respectively, where the coefficients  $b_i$  are given by

$$b_i = \frac{H_w}{\bar{x}_i(\bar{x}_i - 1)} \left( \frac{1}{n} - w_i \right), \quad i = 1, \dots, n-1. \quad (8.44)$$

Then, the system of equations formed by (8.41) and (8.43) has a unique solution  $(\bar{x}_1, \dots, \bar{x}_n)$  given by

$$\bar{x}_i = w_i \frac{H_w}{a_i}, \quad i = 1, \dots, n-1, \quad \bar{x}_n = \frac{H_w}{n}. \quad (8.45)$$

Moreover, the following two affirmations are true:

- a) The height of the prism through the point  $(\bar{x}_1, \dots, \bar{x}_{n-1}, 0)$  coincides with the weighted harmonic mean  $H_w$  of  $a_i, i = 1, \dots, n$ , that is, the point  $(\bar{x}_1, \dots, \bar{x}_{n-1}, H_w)$  belongs to the hyperplane  $\Pi$ .
- b) The height of the prism through the barycenter of the base  $GM_w = \sum_{i=1}^n w_i B_i$  coincides with the weighted arithmetic mean.

*Proof.* It is trivial to see that the proposed solution satisfies (8.41) and (8.43). Let us prove that the solution is unique. Let us suppose that there exists another solution  $x' = (x'_1, \dots, x'_n)$  with  $x' \neq \bar{x}$ . Then, denoting  $z_i = \bar{x}_i - x'_i, i = 1, \dots, n$ , the system of equations formed by (8.41) and (8.43) can be written as

$$\sum_{i=1}^{n-1} [c_i z_i (\bar{x}_i + x'_i) - (c_i + a_n) z_i] - z_n = 0, \quad (8.46a)$$

$$z_n - b_i z_i (\bar{x}_i + x'_i) - (a_i - b_i) z_i = 0, \quad i = 1, \dots, n-1, \quad (8.46b)$$

what amounts to a homogeneous linear system of  $n$  equations with  $n$  unknowns. If we show that this system has only the trivial solution  $z = 0$ , then we would have proven that  $\bar{x} = x'$ , what is a contradiction with the starting supposition. Therefore,  $\bar{x}$  would be the unique solution. Let us then prove that system (8.46) has  $z = 0$  as the unique solution. By reductio ad absurdum, let us suppose that the system has infinite solutions, that is,  $z = \sum_{k=1}^s \lambda_k v^k$ , where  $s = n - r$ , being  $r$  the rank of the coefficient matrix of the linear system,  $\lambda_k \in \mathbb{R}$ , and  $v^k, k = 1, \dots, s$ , represent a base of the Kernel of the associated linear map. Let us consider the univariate set of solutions  $z = \lambda_1 v^1, \lambda_1 \in \mathbb{R}$ . By the sake of simplicity, we will drop the superindex and we will write  $z = \lambda v$ . Thus, we obtain

$$x' = \bar{x} - z = \bar{x} - \lambda v,$$

whose coordinates are given by

$$x'_i = \bar{x}_i - z_i = \bar{x}_i - \lambda v_i. \quad (8.47)$$

Plugging (8.47) into (8.46b) we get

$$\lambda v_n = b_i \lambda v_i (2\bar{x}_i - \lambda v_i) + (a_i - b_i) \lambda v_i, \quad \forall i = 1, \dots, n-1, \quad (8.48)$$

and simplifying expression (8.48) we obtain

$$-\lambda b_i v_i^2 + 2b_i v_i \bar{x}_i + (a_i - b_i)v_i - v_n = 0, \quad \forall i = 1, \dots, n-1, \quad \lambda \neq 0. \quad (8.49)$$

Now, particularizing expression (8.49) for two different values of  $\lambda$ ,  $\lambda_1 \neq \lambda_2$ , and subtracting both expressions, we reach to

$$(\lambda_1 - \lambda_2)b_i v_i^2 = 0, \quad \forall i = 1, \dots, n-1. \quad (8.50)$$

Before continuing with the main proof, we need to prove the following statement

$$s1) \text{ sign}(c_i) = \text{sign}(c_j) \quad \forall i, j \in \{1, \dots, n-1\},$$

where  $\text{sign}(\cdot)$  denotes the sign function,

$$\text{sign}(x) := \begin{cases} 1 & x > 0, \\ -1 & x < 0, \\ 0 & x = 0. \end{cases}$$

Statement s1) is proven just by isolating the term  $H_w$  in equation  $c_i = 0$ , that is

$$\begin{aligned} c_i = 0 &\Leftrightarrow \frac{H_w}{n} = a_n \left(1 - \sum_{j=1}^{n-1} \bar{x}_j\right) = a_n - H_w \left(a_n \sum_{j=1}^{n-1} \frac{w_j}{a_j}\right) \\ &\Leftrightarrow H_w = \frac{a_n}{\frac{1}{n} + a_n \sum_{j=1}^{n-1} \frac{w_j}{a_j}} = \frac{\prod_{k=1}^n a_k}{\frac{1}{n} a_1 \dots a_{n-1} + \sum_{j=1}^{n-1} w_j \prod_{\substack{k=1 \\ k \neq j}}^n a_k}. \end{aligned} \quad (8.51)$$

Comparing expression (8.51) with the expression of  $H_w$  in Definition 38, we get that  $c_i = 0 \Leftrightarrow w_n = \frac{1}{n}$ ,  $c_i > 0 \Leftrightarrow w_n < \frac{1}{n}$ , and  $c_i < 0 \Leftrightarrow w_n > \frac{1}{n}$ .

We are ready to continue with the main proof. Since  $v \neq 0$ , the set of indices  $I$  such that  $v_i \neq 0, i \in I$ , is not empty. Let us suppose that  $b_i = 0, \forall i \in I$ . From (8.46), we get

$$v_n = a_i v_i, \quad (8.52)$$

$$v_n = \sum_{i \in I} (-\lambda c_i v_i + 2c_i \bar{x}_i - (a_n + c_i)) v_i. \quad (8.53)$$

Plugging (8.52) into (8.53) and using that  $v_i \neq 0$ , and in turn  $v_n \neq 0$ , we get that

$$\sum_{i \in I} \left(-\lambda c_i \frac{v_i}{a_i} + 2c_i \frac{\bar{x}_i}{a_i} - \frac{a_n + c_i}{a_i}\right) - 1 = 0, \quad \forall \lambda \in \mathbb{R}. \quad (8.54)$$

From equation (8.54), since it is true for all value of  $\lambda$ , taking two different values  $\bar{\lambda}_1, \bar{\lambda}_2$  we get that

$$-\bar{\lambda}_1 v_n \left(\sum_{i \in I} \frac{c_i}{a_i^2}\right) + \sum_{i \in I} \left(2c_i \frac{\bar{x}_i}{a_i} - \frac{a_n + c_i}{a_i}\right) - 1 = 0, \quad (8.55)$$

$$-\bar{\lambda}_2 v_n \left(\sum_{i \in I} \frac{c_i}{a_i^2}\right) + \sum_{i \in I} \left(2c_i \frac{\bar{x}_i}{a_i} - \frac{a_n + c_i}{a_i}\right) - 1 = 0, \quad (8.56)$$

and subtracting (8.55) and (8.56) we get

$$\sum_{i \in I} \frac{c_i}{a_i^2} = 0. \quad (8.57)$$

Taking into account statement s1), since all  $c_i$  have the same sign, it must be  $c_i = 0, i \in I$ . In turn, by using (8.53), this fact implies

$$-\sum_{i \in I} \frac{a_n v_n}{a_i} = v_n \Rightarrow v_n \left(1 + \sum_{i \in I} \frac{a_n}{a_i}\right) = 0,$$

what is not viable as  $v_n \neq 0$ , and we get a contradiction. Therefore,  $\exists i \in I$ , such that  $b_i \neq 0$ . From (8.50), this means that  $\lambda_1 = \lambda_2$  what gives again a contradiction, this time with the initial supposition. Thus,  $z = 0$  is the unique solution of the homogeneous linear system and  $\bar{x}$  is the unique solution of the system given by (8.41) and (8.43).

In order to prove now point a) of the theorem, we consider the straight line parallel to the  $x_n$  axis passing through  $(\bar{x}_1, \dots, \bar{x}_{n-1}, 0)$ , that is

$$r_w \equiv \begin{cases} x_1 = \bar{x}_1, \\ \vdots \\ x_{n-1} = \bar{x}_{n-1}. \end{cases} \quad (8.58)$$

Cutting this straight line with the hyperplane  $\Pi$  we get the point  $(\bar{x}_1, \dots, \bar{x}_{n-1}, H_w)$ , which gives the enunciated result. A similar argument proves point b), just by considering in this case the straight line parallel to the  $x_n$  axis passing through the barycenter  $GM_w = \sum_{i=1}^n w_i B_i = (w_1, \dots, w_{n-1}, 0)$ , and verifying that its intersection point with the hyperplane  $\Pi$  is just the weighted arithmetic mean  $M_w = \sum_{i=1}^n w_i a_i$ .  $\square$

**Remark 20.** *In the non-weighted case, that is, when all  $w_i = \frac{1}{n}, i = 1, \dots, n$ , all the paraboloids degenerate in diagonal hyperplanes.*

A simpler representation using only hyperplanes is also possible for the general case of dealing with the weighted harmonic mean, as it comes out directly from Remark 20 and from the observation

$$H_{\frac{1}{n}}\left(\frac{a_1}{w_1}, \dots, \frac{a_n}{w_n}\right) = nH_w(a_1, \dots, a_n), \quad (8.59)$$

where  $H_{\frac{1}{n}}$  stands for the harmonic mean with uniform weights  $w_i = \frac{1}{n}, i = 1, \dots, n$ .

More precisely, using the previous notations and defining also

$$\begin{cases} a_i^* = \frac{a_i}{w_i}, \\ P_i^* \equiv (0, \dots, 0, \frac{1}{w_i}, 0, \dots, 0, a_i^*), \quad i = 1, \dots, n-1, \\ P_n^* = (0, \dots, 0, a_n^*), \\ H_w = H_w(a_1, \dots, a_n), w = (w_1, \dots, w_n), \\ H_{\frac{1}{n}}^* = H_w(a_1^*, \dots, a_n^*), w = \left(\frac{1}{n}, \dots, \frac{1}{n}\right), \\ M_w = M_w(a_1, \dots, a_n), w = (w_1, \dots, w_n), \\ M_{\frac{1}{n}}^* = M_w(a_1^*, \dots, a_n^*), w = \left(\frac{1}{n}, \dots, \frac{1}{n}\right), \end{cases}$$

we can give the following corollary.

**Corollary 4.** *Let us consider the hyperplanes  $\Pi, \Pi^*$  which pass through the points  $P_i$ , and  $P_i^*, i = 1, \dots, n$ , respectively,  $n \geq 2$ . They are given by the equations*

$$\Pi \equiv x_n = a_n + \sum_{i=1}^{n-1} x_i(a_i - a_n), \quad (8.60)$$

$$\Pi^* \equiv x_n = \frac{a_n}{w_n} + \sum_{i=1}^{n-1} x_i\left(\frac{a_i}{w_i} - \frac{a_n}{w_n}\right). \quad (8.61)$$

Let us also consider the hyperplane  $V_n^*$  which passes through the points  $B_i, i = 1, \dots, n-1$  and  $P_n^*$  given by the equation

$$V_n^* \equiv \sum_{i=1}^{n-1} x_i + w_n \frac{x_n}{a_n} = 1. \quad (8.62)$$

and the hyperplanes  $V_i^*, i = 1, \dots, n-1$  given by the equations

$$V_i^* \equiv x_n = \frac{a_i}{w_i} x_i, \quad \text{which pass through } B_1, \dots, B_{i-1}, P_i^*, B_{i+1}, \dots, B_n. \quad (8.63)$$

Then, the system of equations formed by (8.62) and (8.63) has a unique solution  $(\bar{x}_1, \dots, \bar{x}_n)$  given by

$$\bar{x}_i = w_i \frac{H_w}{a_i}, \quad i = 1, \dots, n-1, \quad \bar{x}_n = \frac{H_{\frac{1}{n}}^*}{n} = H_w. \quad (8.64)$$

Moreover, the following two affirmations are true:

- a) *The height of the prism  $P^*$  (with vertices  $P_i^*$ ) through the point  $(\bar{x}_1, \dots, \bar{x}_{n-1}, 0)$  coincides with the harmonic mean of  $a_i^*, i = 1, \dots, n$ , that is,  $H_{\frac{1}{n}}^*$ , and the height of the prism  $P$  (with vertices  $P_i$ ) through the same point is  $\frac{1}{n} H_{\frac{1}{n}}^* = H_w$ , that is, the point  $(\bar{x}_1, \dots, \bar{x}_{n-1}, H_w)$  belongs to the hyperplane  $\Pi$ .*
- b) *The height of the prism  $P^*$  through the barycenter of the triangular base  $GM_{\frac{1}{n}} = \sum_{i=1}^n \frac{1}{n} B_i$  coincides with the arithmetic mean  $M_{\frac{1}{n}}^*$ , and the height of the prism  $P$  through the weighted barycenter of the triangular base  $GM_w = \sum_{i=1}^n w_i B_i$  coincides with the weighted arithmetic mean  $M_w$ .*

*Proof.* It is trivially derived either from Theorem 14 or from Theorem 15 just by applying the relation (8.59) and observing the Remark 20.  $\square$

In Figure 8.4 we see the representation of Corollary 4 in 2D and in 3D for a particular choice of the arguments  $a_i$  and the weights. In the upper part we see the case of two arguments. We can appreciate the relation (8.59) between the harmonic mean of the modified arguments  $a_i^*$  and the weighted harmonic mean of the original arguments  $a_i$ , which is placed at the half part of the height of the trapezoid at the abscissa where both means take place. However, no clear relation is observed between the arithmetic mean of the modified values  $M_{\frac{1}{n}}^*$  and the weighted arithmetic mean  $M_w$  of the original ones. The same appreciation runs for the case of three arguments, where the weighted harmonic mean of the original arguments locates at the third part of the height of the prism through the corresponding abscissa.

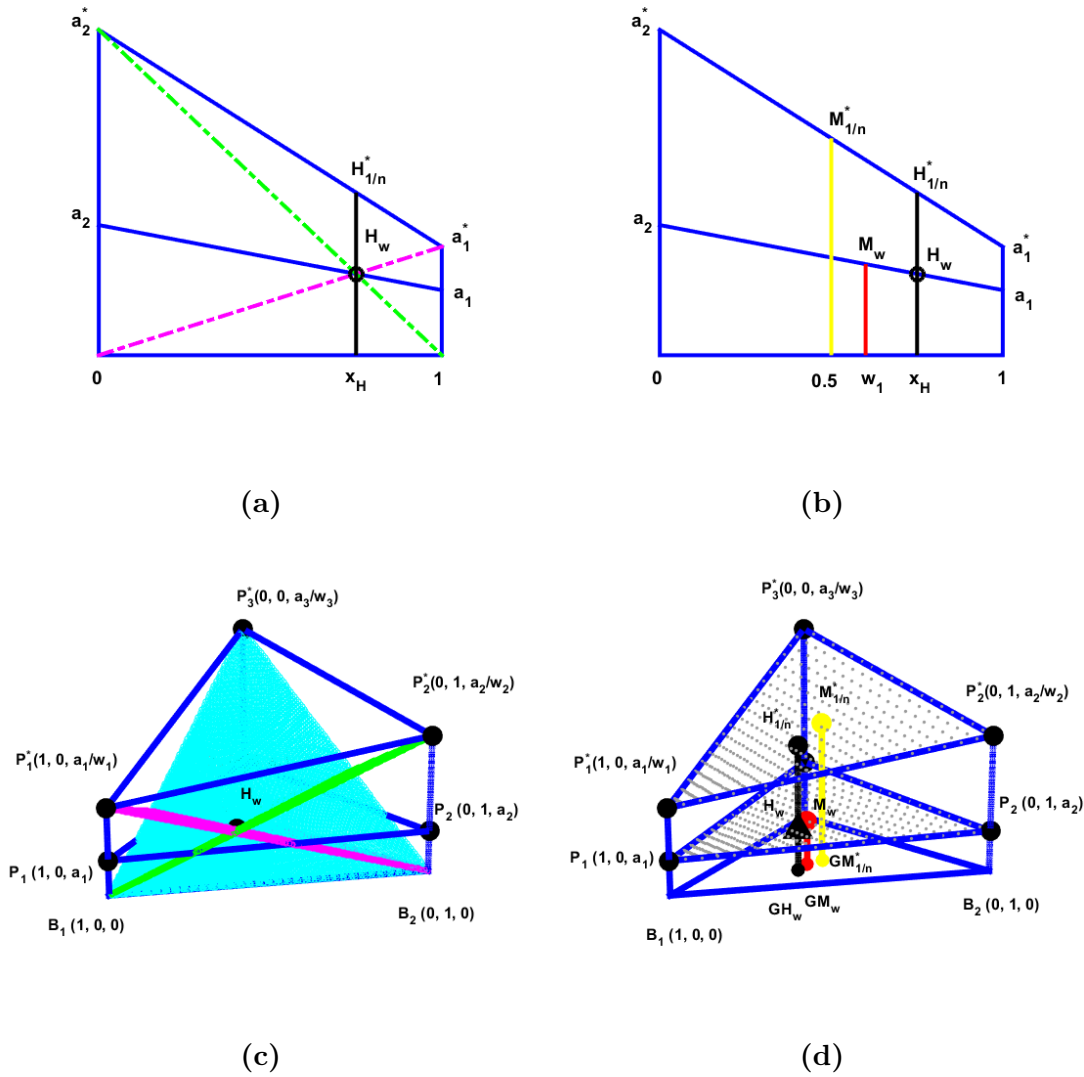


Figure 8.4: Representation of weighted harmonic mean according to Corollary 4. **(a)**: Weighted harmonic mean of the two positive values  $a_1 = 3$ ,  $a_2 = 6$ , with weights  $w_1 = 0.6$ ,  $w_2 = 0.4$ . **(b)**: Comparison among  $H_{\frac{1}{n}}^*$ ,  $H_w$ ,  $M_{\frac{1}{n}}^*$ ,  $M_w$ , in the case of two arguments. **(c)**: Weighted harmonic mean of the three positive values  $a_1 = 6$ ,  $a_2 = 7$ ,  $a_3 = 10$  with weights  $w_1 = 0.4$ ,  $w_2 = 0.3$ ,  $w_3 = 0.3$ . **(d)**: Comparison among  $H_{\frac{1}{n}}^*$ ,  $H_w$ ,  $M_{\frac{1}{n}}^*$ ,  $M_w$ , in the case of three arguments. In blue the harmonic mean, in red the weighted arithmetic mean of the original values, in yellow the arithmetic mean of the modified values.

## 8.5 Examples of application

In this section our main purpose is to point out how to use the simple theoretical results presented in previous sections to define a nonlinear reconstruction operator adapted to jump discontinuities. This application is just one possibility of use of the introduced concepts. It can be applied in many other contexts in order to define a nonlinear method from an already existing

linear method, just by writing the necessary expressions in terms of a weighted arithmetic mean of some quantities, which satisfy certain requirements having to do with satisfying the hypothesis of Lemma 34 in smooth areas of an hypothetical underlying function, acting as smoothness indicators, being just one or a few of them potentially affected by a discontinuity (and very large because of this reason), and not using these affected quantities in the rest of the expressions. Then, the fact of substituting the arithmetic mean for a corresponding harmonic mean will allow the adaptation thanks to Lemma 33, since the large values, due to the presence of a discontinuity, will be limited.

Some examples of already existing methods that use these ideas with the harmonic mean of two values can be found in several applications. Let us mention for example:

- Point values reconstructions and the related field of subdivision and multiresolution schemes, see [6, 42] and the references therein.
- The field of image processing, to define nonlinear compression methods into the cell averages framework inside Harten's multiresolution, see [12].
- Also in the field of image processing for denoising purposes, see [21].
- Generation of curves and surfaces, due to some remarkable properties of the harmonic mean in relation with the definition of convexity preserving reconstruction methods, see for example [37].
- In combination with spline reconstructions, see [20].
- In the solution of hyperbolic conservation laws, see [49, 48].

Up to our knowledge, there are no existing applications using these ideas, and involving harmonic means of 3 or more values. In what follows, we are going to present a new nonlinear adapted reconstruction method for approximating two variable functions using the point values of the function over triangular meshes. Since our aim with this definition is just to clarify the way of using the presented theory, we are going to focus on the local definition of the reconstruction operator for a given triangle of the mesh. Let us consider  $S \subseteq \mathbb{R}^2$ , the equilateral triangle with sides of length  $2h$ , with  $h > 0$  any positive real number, defined by the vertices  $A(-h, \frac{\sqrt{3}}{2}h)$ ,  $C(0, -\frac{\sqrt{3}}{2}h)$ ,  $E(h, \frac{\sqrt{3}}{2}h)$ , as shown in Figure 8.5. Let us also consider that the triangle is divided into 4 new smaller triangles:  $S_A$  of vertices  $ABF$ ,  $S_C$  of vertices  $CDB$ ,  $S_E$  of vertices  $EFD$ , and  $S_R$  of vertices  $BDF$ , just by considering the mid points of each side of the original triangle, see also Figure 8.5. We are going to describe how to build a nonlinear reconstruction inside the triangle  $S_R$  of an underlying function  $f(x, y)$ , from which we know its point values at the six mentioned points  $A, B, C, D, E, F$ . This nonlinear reconstruction will attain third order of approximation in case the underlying function  $f(x, y)$  is of class  $C^3$ , and will be adapted to the presence of jump discontinuities that affect only one of the three values  $A, C$ , or  $E$ .

Firstly, we are going to define the associated linear reconstruction, that it is going to be nothing more than the second degree interpolating polynomial that goes through the six given initial points. Let us write the polynomial around the barycenter of the triangle  $G(0, \frac{\sqrt{3}}{6}h)$  in the form

$$p(x, y) = a_{00} + a_{10}x + a_{01}(y - \frac{\sqrt{3}}{6}) + a_{20}x^2 + a_{11}x(y - \frac{\sqrt{3}}{6}) + a_{02}(y - \frac{\sqrt{3}}{6})^2. \quad (8.65)$$

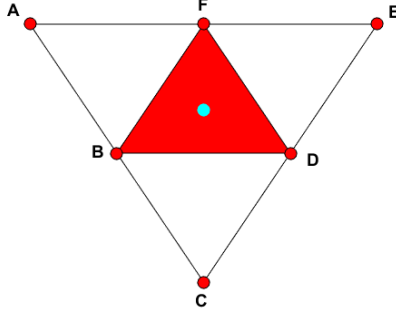


Figure 8.5: Disposition of the considered domain to build the reconstruction inside the red triangle  $S_R$  with vertices  $BDF$ , using the point values of an underlying function  $f(x, y)$  at the six points  $A, B, C, D, E, F$ .

Imposing the interpolation conditions  $p(Q_i) = f(Q_i)$ , for  $Q_i \in \{A, B, C, D, E, F\}$ , we get a linear system of equations, which has unique solution given by

$$\begin{aligned}
 a_{00} &= \frac{4}{9}(f_B + f_D + f_F) - \frac{1}{9}(f_A + f_C + f_E), \\
 a_{10} &= \frac{-f_A - 4f_B + 4f_D + f_E}{6h}, \\
 a_{01} &= \frac{\sqrt{3}}{18h}(f_A - 4f_B - 2f_C - 4f_D + f_E + 8f_F), \\
 a_{20} &= \frac{f_A - 2f_F + f_E}{2h^2}, \\
 a_{11} &= -\frac{\sqrt{3}}{3h^2}(f_A - 2f_B + 2f_D - f_E), \\
 a_{02} &= \frac{f_A - 4f_B + 4f_C - 4f_D + f_E + 2f_F}{6h^2},
 \end{aligned}$$

where  $f_{Q_i}$  denotes  $f(Q_i)$ . It is easy to prove, by using Taylor expansions, the following theorem that ensures third order of approximation of the proposed linear reconstruction.

**Theorem 16.** *Let  $f : \Omega \Rightarrow \mathbb{R}$  be a function of class  $C^3(\Omega)$ , with  $S \subseteq \Omega$ . And let  $p(x, y)$  denote the interpolating polynomial defined by (8.65) with the coefficients given by (8.66). Then, we have*

$$|f(x, y) - p(x, y)| = O(h^3), \quad \forall (x, y) \in S_R.$$

We have then accomplished the first step in the definition of the nonlinear method, that is, we have a ready to modify linear method. Secondly, we want to rewrite the coefficients of the linear reconstruction by making appear arithmetic means. Let us define  $\Delta_A$ ,  $\Delta_C$ , and  $\Delta_E$  as follows

$$\begin{aligned}
 \Delta_A &:= \frac{f_A - (f_B + f_F) + f_D}{h}, \\
 \Delta_C &:= \frac{f_C - (f_B + f_D) + f_F}{h}, \\
 \Delta_E &:= \frac{f_E - (f_D + f_F) + f_B}{h}.
 \end{aligned} \tag{8.66}$$

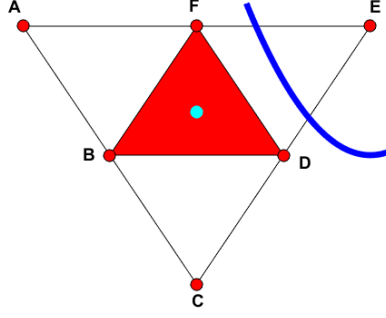


Figure 8.6: Disposition of the considered domain affected by a jump discontinuity along the blue curve.

It is immediate to prove, by using Taylor expansions, that in smooth areas of the function

$$\Delta_A = O(h), \quad \Delta_C = O(h), \quad \Delta_E = O(h), \quad (8.67)$$

$$\Delta_A - \Delta_C = O(h), \quad \Delta_A - \Delta_E = O(h), \quad \Delta_C - \Delta_E = O(h). \quad (8.68)$$

Moreover, these values  $\Delta_A$ ,  $\Delta_C$ ,  $\Delta_E$  act as smoothness indicators, a kind of divided differences, in the sense that if a jump discontinuity lies affecting one of the values  $A$ ,  $C$ , or  $E$ , then the corresponding divided difference will be  $O(\frac{1}{h})$ , while the others will remain  $O(h)$ . In Figure 8.5, we see the case of having the vertex  $E$  affected by a jump discontinuity, which takes place along a curve plotted in blue. The idea behind the method that we are going to explain is to substitute  $f_E$  for a more suitable value  $\tilde{f}_E$ , that both maintains the approximation accuracy in case of dealing with a smooth function and allows for adaptation in case of discontinuity.

The coefficients in (8.66) can be rewritten as follows

$$\begin{aligned} a_{00} &= \frac{1}{3}(f_B + f_D + f_F) - \frac{h}{3} \frac{\Delta_A + \Delta_C + \Delta_E}{3}, \\ a_{10} &= \frac{f_D - f_B}{h} - \frac{1}{6}(2\Delta_A + \Delta_C) + \frac{1}{2} \frac{\Delta_A + \Delta_C + \Delta_E}{3}, \\ a_{01} &= \frac{\sqrt{3}}{6}(\Delta_C + 2\frac{f_F - f_C}{h}) + \frac{\sqrt{3}}{6} \frac{\Delta_A + \Delta_C + \Delta_E}{3}, \\ a_{20} &= -\frac{3}{2h}\Delta_C + \frac{3}{2h} \frac{\Delta_A + \Delta_C + \Delta_E}{3}, \\ a_{11} &= -\frac{2\sqrt{3}}{h}\Delta_A + \frac{\sqrt{3}}{3h^2}(f_D - 2f_F + f_B) + \frac{\sqrt{3}}{h} \frac{\Delta_A + \Delta_C + \Delta_E}{3}, \\ a_{02} &= -\frac{1}{2h}\Delta_C + \frac{1}{2h} \frac{\Delta_A + \Delta_C + \Delta_E}{3}. \end{aligned} \quad (8.69)$$

It is important that the potentially affected value by a possible discontinuity  $f_E$ , the one that makes  $\Delta_E$  be the largest in absolute value, appears only inside the term  $\Delta_E$  and in turn  $\Delta_E$  appears only in the arithmetic mean.



Thirdly, we are going to modify the expressions of the coefficients in (8.69) implementing the substitution of the arithmetic means by adequate harmonic means. Since the values of the divided differences could be positive, negative, or zero, and we are also going to need that these quantities satisfy the hypothesis of Lemma 34, we require the redefinition of the weighted harmonic mean by using a translation strategy. In order to do so, we introduce the concept of translation operator, which will allow us to extend the definition of the weighted harmonic mean.

**Definition 39.** Given  $h > 0$ , a translation operator  $T$  is any function  $T : \mathbb{R}^3 \rightarrow \mathbb{R}$  satisfying

1.  $T(0, 0, 0) = 0$ ,
2.  $T(x, y, z) = T(\sigma(x), \sigma(y), \sigma(z))$ , where  $\sigma$  is any permutation of three elements,
3.  $T(-x, -y, -z) = -T(x, y, z)$ ,
4.  $\text{sign}(x + T(x, y, z)) = \text{sign}(y + T(x, y, z)) = \text{sign}(z + T(x, y, z))$ ,  $\forall (x, y, z) \neq (0, 0, 0)$ ,
5. if  $(x, y, z) \neq (0, 0, 0)$ , with  $|s| = \max\{|x|, |y|, |z|\}$ ,
  - a) if  $\exists s_1 : |s_1| = |s|, \text{sign}(s_1) \neq \text{sign}(s)$ , then  $\text{sign}(x + T(x, y, z)) > 0$ ,  
 $\text{sign}(y + T(x, y, z)) > 0, \text{sign}(z + T(x, y, z)) > 0$ ,
  - b) if  $\nexists s_1 : |s_1| = |s|, \text{sign}(s_1) \neq \text{sign}(s)$ , then  $\text{sign}(x + T(x, y, z))\text{sign}(s) > 0$ ,  
 $\text{sign}(y + T(x, y, z))\text{sign}(s) > 0, \text{sign}(z + T(x, y, z))\text{sign}(s) > 0$ ,
6.  $\min\{|x + T(x, y, z)|, |y + T(x, y, z)|, |z + T(x, y, z)|\} = O(1)$ ,  $\forall (x, y, z) \neq (0, 0, 0)$ , with  
 $|x| = O(h^\alpha), |y| = O(h^\alpha), |z| = O(h^\alpha)$ , for some  $\alpha \geq 0$ .

Properties 1 to 4 are meant to apply the weighted harmonic mean in mind by using basically the expression given for positive numbers. While the property 5 will play an important role to guarantee the adaptation of the method in case one of the arguments is very large due to the presence of a discontinuity. In turn, property 6 ensures that the new arguments that are going to be considered in the new definition of the mean will satisfy the hypothesis of Lemma 34.

We are now ready to redefine the weighted harmonic mean

$$J_w(a_1, a_2, a_3) = \begin{cases} H_w(a_1 + T, a_2 + T, a_3 + T) - T, & (a_1, a_2, a_3) \neq (0, 0, 0), \\ 0, & (a_1, a_2, a_3) = (0, 0, 0), \end{cases} \quad (8.70)$$

where  $T$  is any translation operator satisfying Definition 39. It is important to notice that the new mean also satisfies similar lemmas, Lemma 33 and Lemma 34, as the weighted harmonic mean. In fact, we can prove the following two lemmas.

**Lemma 35.** Let  $a_i > 0$ ,  $i = 1, 2, 3$  be real numbers and  $w_i > 0$ ,  $i = 1, 2, 3$  the corresponding weights with  $w_1 + w_2 + w_3 = 1$ . Then, the translated weighted harmonic mean  $J_w$  is bounded as follows

$$|J_w| \leq \max\left\{\frac{|a_1 + T|}{w_1}, |T|\right\}.$$

*Proof.* Since  $J_w(a_1 + T, a_2 + T, a_3 + T)$  and  $T$  have the same sign, then applying Lemma 33 we get

$$|J_w(a_1, a_2, a_3)| \leq \max\{|H_w(a_1 + T, a_2 + T, a_3 + T)|, |T|\} \leq \max\left\{\frac{|a_1 + T|}{w_1}, |T|\right\}.$$

□

**Lemma 36.** Let  $a_i > 0$ ,  $i = 1, 2, 3$  be real numbers and  $w_i > 0$ ,  $i = 1, 2, 3$  the corresponding weights with  $w_1 + w_2 + w_3 = 1$ . If  $|a_1 - a_i| = O(h)$ ,  $i = 2, 3$ , then, the translated weighted harmonic mean  $J_w$  and the weighted arithmetic mean  $M_w := w_1 a_1 + w_2 a_2 + w_3 a_3$  satisfy

$$|M_w - J_w| = O(h^2).$$

*Proof.* The case of  $(a_1, a_2, a_3) = (0, 0, 0)$  is trivial. If  $(a_1, a_2, a_3) \neq (0, 0, 0)$ , using the definition of  $J_w$  we get

$$\begin{aligned} |M_w(a_1, a_2, a_3) - J_w(a_1, a_2, a_3)| &= |M_w(a_1, a_2, a_3) - H_w(a_1 + T, a_2 + T, a_3 + T) - T| \\ &= |M_w(a_1 + T, a_2 + T, a_3 + T) - H_w(a_1 + T, a_2 + T, a_3 + T)|, \end{aligned}$$

and applying Lemma 34 we have that

$$|M_w(a_1 + T, a_2 + T, a_3 + T) - H_w(a_1 + T, a_2 + T, a_3 + T)| = O(h^2).$$

□

Thanks to the new translated version of the weighted harmonic mean in (8.70) we can finally define the modified coefficients

$$\begin{aligned} \tilde{a}_{00} &= \frac{1}{3}(f_B + f_D + f_F) - \frac{h}{3}J_{\frac{1}{3}}(\Delta_A, \Delta_C, \Delta_E), \\ \tilde{a}_{10} &= \frac{f_D - f_B}{h} - \frac{1}{6}(2\Delta_A + \Delta_C) + \frac{1}{2}J_{\frac{1}{3}}(\Delta_A, \Delta_C, \Delta_E), \\ \tilde{a}_{01} &= \frac{\sqrt{3}}{6}(\Delta_C + 2\frac{f_F - f_C}{h}) + \frac{\sqrt{3}}{6}J_{\frac{1}{3}}(\Delta_A, \Delta_C, \Delta_E), \\ \tilde{a}_{20} &= -\frac{3}{2h}\Delta_C + \frac{3}{2h}J_{\frac{1}{3}}(\Delta_A, \Delta_C, \Delta_E), \\ \tilde{a}_{11} &= -\frac{2\sqrt{3}}{h}\Delta_A + \frac{\sqrt{3}}{3h^2}(f_D - 2f_F + f_B) + \frac{\sqrt{3}}{h}J_{\frac{1}{3}}(\Delta_A, \Delta_C, \Delta_E), \\ \tilde{a}_{02} &= -\frac{1}{2h}\Delta_C + \frac{1}{2h}J_{\frac{1}{3}}(\Delta_A, \Delta_C, \Delta_E). \end{aligned} \tag{8.71}$$

The new nonlinear local reconstruction method writes then

$$\tilde{p}(x, y) = \tilde{a}_{00} + \tilde{a}_{10}x + \tilde{a}_{01}(y - \frac{\sqrt{3}}{6}) + \tilde{a}_{20}x^2 + \tilde{a}_{11}x(y - \frac{\sqrt{3}}{6}) + \tilde{a}_{02}(y - \frac{\sqrt{3}}{6})^2, \tag{8.72}$$

where the coefficients  $\tilde{a}_{00}, \tilde{a}_{10}, \tilde{a}_{01}, \tilde{a}_{20}, \tilde{a}_{11}, \tilde{a}_{02}$  are given in (8.71). It is also interesting to notice that this reconstruction amounts to modifying the value  $f_E$

$$f_E = f_B + f_D + f_F - (f_A + f_C) + 3hM_{\frac{1}{3}}(\Delta_A, \Delta_C, \Delta_E),$$

in order to get

$$\tilde{f}_E = f_B + f_D + f_F - (f_A + f_C) + 3hJ_{\frac{1}{3}}(\Delta_A, \Delta_C, \Delta_E),$$

and then considering the original interpolation problem with modified function values  $\{f_A, f_B, f_C, f_D, \tilde{f}_E\}$ . By definition, it is not difficult to prove a theorem about the adaptation of the proposed method and the third order accuracy in smooth areas.

**Theorem 17.** Let  $f : \Omega \Rightarrow \mathbb{R}$  be a function of class  $C^3(\Omega)$ , with  $S \subseteq \Omega$ . And let  $\tilde{p}(x, y)$  denote the interpolating polynomial defined by (8.72) with the coefficients given by (8.71). Then, we have

$$|f(x, y) - \tilde{p}(x, y)| = O(h^3), \quad \forall (x, y) \in S_R. \quad (8.73)$$

Moreover, if  $f$  has a jump discontinuity along a curve letting  $S \setminus S_E$  to one side and the vertex  $E$  to the other side of the curve, then we have

$$|f(x, y) - \tilde{p}(x, y)| = O(h), \quad \forall (x, y) \in S_R. \quad (8.74)$$

*Proof.* Taking into account that  $|M_{\frac{1}{3}} - J_{\frac{1}{3}}| = O(h^2)$  according to Lemma 36, from (8.69) and (8.71) we get that

$$\begin{aligned} a_{00} - \tilde{a}_{00} &= O(h^3), \\ a_{10} - \tilde{a}_{10} &= O(h^2), \quad a_{01} - \tilde{a}_{01} = O(h^2), \\ a_{20} - \tilde{a}_{20} &= O(h), \quad a_{11} - \tilde{a}_{11} = O(h), \quad a_{02} - \tilde{a}_{02} = O(h). \end{aligned} \quad (8.75)$$

Now, from the expressions of the linear reconstruction  $p(x, y)$  in (8.65) and of the nonlinear reconstruction  $\tilde{p}(x, y)$  in (8.72) we easily obtain by applying the triangular inequality that

$$\begin{aligned} |p(x, y) - \tilde{p}(x, y)| &\leq |a_{00} - \tilde{a}_{00}| + |a_{10} - \tilde{a}_{10}||x| + |a_{01} - \tilde{a}_{01}||y - \frac{\sqrt{3}}{6}| + |a_{20} - \tilde{a}_{20}||x|^2 \\ &+ |a_{11} - \tilde{a}_{11}||x||y - \frac{\sqrt{3}}{6}| + |a_{02} - \tilde{a}_{02}||y - \frac{\sqrt{3}}{6}|^2. \end{aligned} \quad (8.76)$$

Thus, using (8.75) we reach to

$$|p(x, y) - \tilde{p}(x, y)| = O(h^3). \quad (8.77)$$

Applying Theorem 16 and (8.77) we have

$$|f(x, y) - \tilde{p}(x, y)| \leq |f(x, y) - p(x, y)| + |p(x, y) - \tilde{p}(x, y)| = O(h^3),$$

which proves (8.73).

In order to prove (8.74) we start by pointing out that

$$|f(x, y) - p_1(x, y)| = O(h^2), \quad \forall (x, y) \in S_R, \quad (8.78)$$

where  $p_1(x, y)$  is given by,

$$p_1(x, y) = a_{00} + a_{10}x + a_{01}(y - \frac{\sqrt{3}}{6}).$$

Now, taking into account that due to Lemma 35,  $|J_{\frac{1}{3}}| = O(1)$ , we have

$$\begin{aligned} |p_1(x, y) - \tilde{p}(x, y)| &\leq |a_{00} - \tilde{a}_{00}| + |a_{10} - \tilde{a}_{10}||x| + |a_{01} - \tilde{a}_{01}||y - \frac{\sqrt{3}}{6}| + |\tilde{a}_{20}||x|^2 \\ &+ |\tilde{a}_{11}||x||y - \frac{\sqrt{3}}{6}| + |\tilde{a}_{02}||y - \frac{\sqrt{3}}{6}|^2 = O(h) + O(1)O(h) + O(1)O(h) = O(h). \end{aligned} \quad (8.79)$$

Thus

$$|f(x, y) - \tilde{p}(x, y)| \leq |f(x, y) - p_1(x, y)| + |p_1(x, y) - \tilde{p}(x, y)| = O(h^2) + O(h) = O(h), \quad \forall (x, y) \in S_R,$$

which finishes the proof.  $\square$

**Remark 21.** *We have defined the reconstruction in equilateral triangles using the harmonic mean of three values, but the reconstruction can be extended to whatever triangle by defining adequate weights depending on the specific form of the triangle, expressing the coefficients in terms of weighted arithmetic means instead, and then following the same track as in the given example.*

The ideas expressed in the presented new reconstruction operator can be extrapolated to higher dimensions, and into other fields of numerical analysis, such as the previously mentioned in the list at the beginning of this section. To finish this section, we present a simple numerical example that reinforces the theoretical results. Given the following two functions of two variables  $f(x, y)$  and  $g(x, y)$ ,

$$f(x, y) := \sin(x + y) + 20, \quad g(x, y) := \begin{cases} \sin(x + y) + 20, & y < -\sqrt{3}(x - \frac{5}{8}), \\ \cos(x + y) + 200, & y \geq -\sqrt{3}(x - \frac{5}{8}), \end{cases}$$

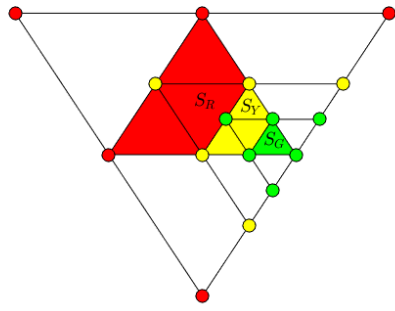
defined in the triangle  $T$  of vertices  $A(-h, \frac{\sqrt{3}}{2}h)$ ,  $C(0, -\frac{\sqrt{3}}{2}h)$ ,  $E(h, \frac{\sqrt{3}}{2}h)$ , with  $h = 0.005$ , we consider the linear reconstruction  $p(x, y)$  given by (8.65) and the nonlinear reconstruction  $\tilde{p}(x, y)$  given by (8.72) inside the triangle  $S_R$  represented in Figure 8.5, and also the same kind of reconstructions, but in the triangles  $S_Y$  and  $S_G$  with sides of length a half and a quarter of the length of the sides of the original triangle  $S_R$ . Then, we measure the errors and the approximation order of both linear and associated nonlinear method in two scenarios, i.e., with the smooth function  $f(x, y)$  and with the function  $g(x, y)$  which contains a jump discontinuity along the straight line  $y = -\sqrt{3}(x - \frac{5}{8})$ . In Figure 8.5, we see the domain of the considered functions and the representation of the reconstructions attained in the triangle  $S_R$  by both methods. One can easily observe how the linear method produces the expected Gibb phenomena around the jump discontinuity, while the nonlinear method seems to avoid it. This fact can also be appreciated in the Table 8.1, where we have measured the committed errors for the two reconstructions inside the triangle  $S_G$  when building the reconstructions for the three triangles  $S_R$ ,  $S_Y$ , and  $S_G$  respectively. We have also included the numerical approximation order computed from these errors, i.e., we have approximated the numerical order  $p$  by using

$$p \approx \log_2 \frac{E_{S_R}}{E_{S_Y}}, \quad \text{and} \quad p \approx \log_2 \frac{E_{S_Y}}{E_{S_G}},$$

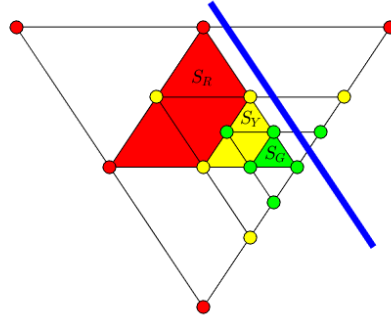
where  $E_{S_R}$ ,  $E_{S_Y}$ , and  $E_{S_G}$  stand for the approximation errors in infinity norm inside the triangle  $S_G$ , attained by the considered reconstruction operators, builded using the information relative to the indicated triangle. In the case of dealing with a smooth function, we see that the nonlinear method imitates the good behavior of its linear counterpart. This point can be appreciated as much in Figure 8.5 as in Table 8.2. We would like to remark the fact that the obtained numerical orders coincide with the expected according to Theorem 16 and Theorem 17. Also, it is remarkable the fact that the linear method completely loses any approximation order in case of the jump discontinuity and produces Gibbs effects, while these drawbacks are avoided with the proposed nonlinear method, attaining at least a first order approximation.

## 8.6 Conclusions

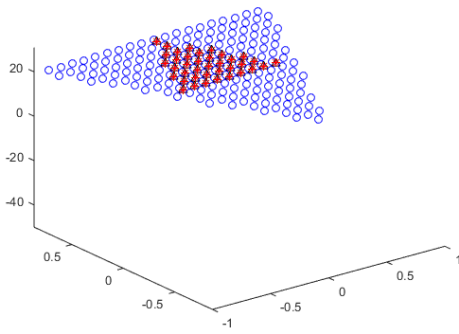
In this chapter we have presented two relevant properties of the harmonic mean that allow for new constructions of numerical methods, such as nonlinear reconstruction operators, subdivision



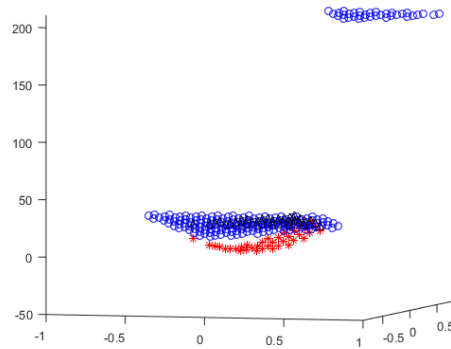
(a)



(b)



(c)



(d)

Figure 8.7: **(a)**: Disposition of the considered domain to build the linear and nonlinear reconstructions inside the triangles  $S_R$ ,  $S_Y$ , and  $S_G$ . **(b)**: Disposition of the considered domain affected by a jump discontinuity along the blue curve for which we build the linear and nonlinear reconstructions inside the triangles  $S_R$ ,  $S_Y$ , and  $S_G$ . **(c)**: Obtained reconstructions, and comparison with the original smooth function  $f(x, y)$  in the triangle  $S_R$ . **(d)**: Obtained reconstructions, and comparison with the original discontinuous function  $g(x, y)$  in the triangle  $S_R$ . With blue circles the original function, with red asterisks the linear reconstruction and with black triangles the new nonlinear reconstruction.

$p(x, y)$			$\tilde{p}(x, y)$		
<i>Triangle</i>	$\ p(x, y) - f(x, y)\ _\infty$	$p$	<i>Triangle</i>	$\ \tilde{p}(x, y) - f(x, y)\ _\infty$	$p$
$S_R$	16.9679	–	$S_R$	$7.0587 \times 10^{-7}$	–
$S_Y$	22.6243	–0.4151	$S_Y$	$4.7168 \times 10^{-7}$	0.5816
$S_G$	22.6245	$-1.3679 \times 10^{-5}$	$S_G$	$2.3545 \times 10^{-7}$	1.0024

Table 8.1: Numerical approximation errors  $\|p(x, y) - g(x, y)\|_\infty$  and  $\|\tilde{p}(x, y) - g(x, y)\|_\infty$  in infinity norm between the linear reconstruction and the original discontinuous function  $g(x, y)$  and between the nonlinear reconstruction  $\tilde{p}(x, y)$  and the original discontinuous function  $g(x, y)$  in the triangle  $S_G$  for the cases of building the reconstructions inside the triangles  $S_R$ ,  $S_Y$  and  $S_G$  of decreasing side lengths. The approximation orders  $p$  are also offered.

$p(x, y)$			$\tilde{p}(x, y)$		
<i>Triangle</i>	$\ p(x, y) - f(x, y)\ _\infty$	$p$	<i>Triangle</i>	$\ \tilde{p}(x, y) - f(x, y)\ _\infty$	$p$
$S_R$	$9.1721 \times 10^{-9}$	–	$S_R$	$8.9912 \times 10^{-9}$	–
$S_Y$	$1.6914 \times 10^{-9}$	2.4390	$S_Y$	$1.6687 \times 10^{-9}$	2.4298
$S_G$	$2.1329 \times 10^{-10}$	2.9874	$S_G$	$2.1080 \times 10^{-10}$	2.9848

Table 8.2: Numerical approximation errors  $\|p(x, y) - f(x, y)\|_\infty$  and  $\|\tilde{p}(x, y) - f(x, y)\|_\infty$  in infinity norm between the linear reconstruction and the original smooth function  $f(x, y)$  and between the nonlinear reconstruction  $\tilde{p}(x, y)$  and the original smooth function  $f(x, y)$  in the triangle  $S_G$  for the cases of building the reconstructions inside the triangles  $S_R$ ,  $S_Y$  and  $S_G$  of decreasing side lengths. The approximation orders  $p$  are also offered.

and multiresolution schemes, and solvers of hyperbolic conservation laws. These properties have been presented for any finite number of arguments, with the purpose of generating new algorithms in problems involving  $N$ -dimensional spaces. We have given some geometrical representations of both the weighted harmonic mean and the weighted arithmetic mean where the mentioned properties can be appreciated in an intuitive way. In the last part of the chapter we offer a clear and simple example on how to use these simple concepts to attain interesting and promising results in defining new methods.

## Chapter 9

# Future works and perspectives

This chapter is intended as a brief guide to continue and extend the work carried out through the production of this thesis dissertation. Science and in particular the mathematics field is so broad that many branches arise from the same stem, no matter the specific that it is. New questions always emerge as an opportunity to broaden the human understanding of underlying ideas.

Here, we simply let written the thoughts that have appeared when dealing with each particular chapter developed in this manuscript. In this way, we hope that anyone interested or maybe myself together with perhaps my thesis advisor or other colleagues will find the time, motivation, and appropriate circumstances to deepen in such items.

The remarkable points to be considered are separated in chapters as follows:

### Chapter 2

- P2.1 Extension of the general stability results of the subdivision scheme to  $\sigma$  quasi uniform grids.
- P2.2 Particularization for the more specific case of dealing with convex or concave initial data, that is the generalization of Chapter 2 to  $\sigma$  quasi uniform grids.
- P2.3 Study the possibility of imposing conditions for a local change of data in order to being able to prove the stability of PPH-like subdivision schemes that consist on a local modification of the data together with the application of an already known linear and therefore stable scheme. This study can be done as much with uniform as with nonuniform grids.

### Chapter 3

- P3.1 Definition and analysis of PPH-type reconstructions of higher order in nonuniform grids.
- P3.2 Definition of another kind of mean in such a way that following the same ideas as in this chapter, we get a reconstruction that keeps third order accuracy  $O(h^3)$  in the interval  $[x_j, x_{j+1}]$  in the case that a jump singularity is located at the interval  $[x_{j+1}, x_{j+2}]$ , instead of  $O(h^2)$ .
- P3.3 In combination with Chapter 7, calculation of the error bounds that appear in the process of approximation of the limit function of the nonuniform PPH subdivision scheme by firstly refining the initial data using some steps of PPH subdivision and then applying the nonuniform PPH reconstruction operator.

## Chapter 4

- P4.1 In combination with the definition of a translation operator in Chapter 5, analysis of the behavior respect to Gibbs phenomena of the PPH reconstruction implemented with the translation operator.

## Chapter 5

- P5.1 Analysis of the behavior respect to Gibbs phenomena of the PPH reconstruction implemented with the translation operator.

## Chapter 6

- P6.1 Analysis in more detail of the connection between the PPH reconstruction operator with smoothing splines in a given interval  $[a, b]$ , giving not only a local relation between both methods but a global one.

## Chapter 7

- P7.1 In combination with Chapter 3, calculation of the error bounds that appear in the process of approximation of the limit function of the nonuniform PPH subdivision scheme by firstly refining the initial data using some steps of PPH subdivision and then applying the nonuniform PPH reconstruction operator.
- P7.2 Analysis of the PPH subdivision scheme in nonuniform grids with respect to the elimination of the Gibbs phenomena.
- P7.3 Implementation and study the PPH subdivision scheme implemented with a translation operator.
- P7.4 Theoretical and numerical analysis of the associated PPH multiresolution scheme in nonuniform meshes. In particular such things as compression capabilities and stability of the subdivision and multiresolution schemes.
- P7.5 Definition and complete parallel developments for the case of extrapolating the ideas of the PPH reconstruction, subdivision and multiresolution schemes to the cell average setting.

## Chapter 8

- P8.1 Implementation of the proposed local reconstruction in equilateral triangles in a domain that admits a previous tessellation with equilateral triangles.
- P8.2 Extension of the PPH reconstruction on equilateral triangles to general triangles.
- P8.3 Application of similar ideas to derive non separable reconstructions directly in  $2D$  by using polyominoes. It seems possible in this context to define methods such as ENO-type, WENO-type and PPH-type methods.
- P8.4 Generalization of the previous points to higher dimensions,  $3D$ , etcetera.
- P8.5 Potential application of these algorithms into Finite Element Methods (FEM).

We hope that at least some of all these points will be successfully carried out in a near future.



# Bibliography

- [1] Amat S.; Aràndiga F.; Cohen A.; Donat R. Tensor product multiresolution analysis with error control for compact image representation. *Signal Processing* **2002**, *82(4)*, 587-608.
- [2] Amat S.; Aràndiga F.; Cohen A.; Donat R.; Garcia G.; von Oehsen M. Data compression with ENO schemes: a case study. *Applied and Computational Harmonic Analysis* **2001**, *11(2)*, 273-288.
- [3] Amat S.; Busquier S.; Trillo J.C. Stable interpolatory multiresolution in 3D. *Applied Numerical Analysis and Computational Mathematics* **2005**, *2(2)*, 177-188.
- [4] Aràndiga F.; Cohen A.; Donat R.; Dyn N.; Basarab B. Approximation of piecewise smooth functions and images by edge-adapted (ENO-EA) nonlinear multiresolution techniques. *Applied and Computational Harmonic Analysis* **2008**, *24(2)*, 225-250.
- [5] Aràndiga, F.; Donat, R. Nonlinear multi-scale decomposition: The approach of A. Harten. *Numerical Algorithms* **2000**, *23*, 175-216.
- [6] Amat, S.; Donat, R.; Liandrat, J.; Trillo, J.C. Analysis of a new nonlinear subdivision scheme. Applications in image processing. *Foundations of Computational Mathematics* **2006**, *6(2)*, 193-225.
- [7] Amat, S.; Dadourian, K.; Liandrat, J.; Trillo, J.C. High order nonlinear interpolatory reconstruction operators and associated multiresolution schemes. *Journal of Computational and Applied Mathematics* **2013**, *253*, 163-180.
- [8] Aràndiga, F.; Donat, R.; Romani, L.; Rossini, M. On the reconstruction of discontinuous functions using multiquadric RBF-WENO local interpolation techniques. *Mathematics and Computers in Simulation* **2020**, *176*, 4-24.
- [9] Amat S.; Donat R.; Trillo J.C. On specific stability bounds for linear multiresolution schemes based on piecewise polynomial Lagrange interpolation. *Journal of Mathematical Analysis and Applications* **2009**, *358(1)*, 18-27.
- [10] Amat, S.; Donat, R.; Trillo, J.C. Proving convexity preserving properties of interpolatory subdivision schemes through reconstruction operators. *Applied Mathematics and Computation* **2013**, *219(14)*, 7413-7421.
- [11] Amat S.; Liandrat J. On the stability of PPH nonlinear multiresolution. *Applied and Computational Harmonic Analysis* **2005**, *18(2)*, 198-206.

- [12] Amat S.; Liandrat J.; Ruiz J.; Trillo J.C. On a nonlinear mean and its application to image compression using multiresolution schemes. *Numerical Algorithms* **2016**, *71(4)*, 729-752.
- [13] Amat, S.; Liandrat, J.; Ruiz, J.; Trillo, J.C. On a power WENO scheme with improved accuracy near discontinuities. *SIAM Journal of Scientific Computing* **2017**, *39*, A2472-A2507.
- [14] Amir, A.; Levin, D. Quasi-interpolation and outliers removal. *Numerical Algorithms* **2018**, *78*, 805-825.
- [15] Amat S.; Moncayo M. Error bounds for a class of subdivision schemes based on the two-scale refinement equation. *Journal of Computational and Applied Mathematics* **2011**, *236(2)*, 265-278.
- [16] Amat, S.; Magreñán, A.A.; Ruiz, J.; Trillo, J.C.; Yáñez, D.F. On the use of generalized harmonic means in image processing using multiresolution algorithms. *International Journal of Computational Mathematics* **2020**, *97*, 455-466.
- [17] Amat, S.; Ortiz, P.; Ruiz, J.; Trillo, J.C.; Yáñez, D. F. Improving the approximation order around inflexion points of the PPH nonlinear interpolatory reconstruction operator on nonuniform grids. Submitted.
- [18] Amat, S. ; Ortiz, P.; Ruiz, J.; Trillo, J.C. ; Yáñez, D.F. Graphical interpretation of the weighted harmonic mean of  $n$  positive values and applications. Submitted.
- [19] Amat, S.; Ruiz, J.; Shu, C.W. On a new WENO algorithm of order  $2r$  with improved accuracy close to discontinuities. *Applied Mathematical Letters* **2020**, *105*, 106298-106309.
- [20] Amat S.; Shu C.W.; Ruiz J.; Trillo J.C. On a class of splines free of Gibbs phenomenon. *Mathematical Modelling in Numerical Analysis* **2021**, *55*, S29-S64.
- [21] Amat S.; Ruiz J.; Trillo J.C. Fast multiresolution algorithms and their related variational problems for image denoising. *Journal of Scientific Computing* **2010**, *43(1)*, 1-23
- [22] Amat S.; Ruiz J.; Trillo J.C.; Yáñez D.F. On a family of non-oscillatory subdivision schemes having regularity  $C^r$  with  $r > 1$ . *Numerical Algorithms* **2020**, *85(2)*, 543-569.
- [23] De Boor C. A practical guide to splines. *New York Springer-Verlag* **1978**.
- [24] Cohen A.; Dyn N., Matei B. Quasilinear subdivision schemes with applications to ENO interpolation. *Applied and Computational Harmonic Analysis* **2003**, *15*, 89-116.
- [25] Dyn, N.; Farkhi, E.; Keinan, S. Approximation of 3D objects by piecewise linear geometric interpolants of their 1D cross-sections. *Journal of Computational and Applied Mathematics* **2020**, *368*, 112466-112475.
- [26] Dyn, N; Gregori, J.A.; Levin, D. A 4-point interpolatory subdivision scheme for curve design. *Computer Aided Geometrical Design* **1987**, *4*, 257-268.
- [27] Dyn, N.; Kuijt, F.; Levin, D.; Van Damme, R. Convexity preservation of the four-point interpolatory subdivision scheme. *Computer Aided Geometrical Design* **1999**, *16(8)*, 789-792.

- [28] Donat R.; López Ureña S. Nonlinear stationary subdivision schemes reproducing hyperbolic and trigonometric functions. *Advances in Computational Mathematics* **2019**, *45(5-6)*, 3137-3172.
- [29] Dyn N.; Levin, D. Stationary and non-stationary binary subdivision schemes, *Mathematical Methods in Computer Aided Geometric Design II; Academic Press: Boston, MA, USA. 1991*, 209-216.
- [30] Dyn N.; Levin D.; Massopust P. Attractors of trees of maps and of sequences of maps between spaces with applications to subdivision. *Journal of Fixed Point Theory and Applications* **2020**, *22(1)* Paper No. 14, 24 pp.
- [31] Donat, R.; Yáñez, D.F. A nonlinear Chaikin-based binary subdivision scheme. *Journal of Computational and Applied Mathematics* **2019**, *349*, 379-389.
- [32] Floater M.S.; Michelli, C.A. Nonlinear stationary subdivision. *Approximation Theory: in memory of A.K. Varna*, ed: Govil N.K.; Mohapatra N.; Nashed Z.; Sharma A.; Szabados J. **1998**, *212*, 209-224.
- [33] Guessab A.; Moncayo M.; Schmeisser G. A class of nonlinear four-point subdivision schemes. *Advances in Computational Mathematics* **2012**, *37(2)*, 151-190.
- [34] Harten, A. Eno schemes with subcell resolution. *Journal of Computational Physics* **1989**, *83(1)*, 148-184 .
- [35] Harten, A. Multiresolution representation of data II. *SIAM Journal of Numerical Analysis* **1996**, *33(3)*, 1205-1256.
- [36] Jiménez, I.; Ortiz, P.; Ruiz, J.; Trillo, J. C.; Yáñez, D. F. Improving the stability bound for the PPH nonlinear subdivision scheme for data coming from strictly convex functions. *Applied Mathematics and Computations*. **2021**, <https://doi.org/10.1016/j.amc.2021.126042>
- [37] Kuijt, F.; Van Damme,R. Convexity preserving interpolatory subdivision schemes. *Constructive Approximations* **1998**, *14*, 609-630.
- [38] Levin D.; Dyn N.; Viswanathan P.V. Non-stationary versions of fixed-point theory, with applications to fractals and subdivision. *Journal of Fixed Point Theory and Applications* **2019**, *21(1)*, Paper No. 26, 25 pp.
- [39] Moosmüller C. ; Dyn N. Increasing the smoothness of vector and Hermite subdivision schemes. *IMA Journal on Numerical Analysis* **2019**, *39(2)*, 579-606.
- [40] Matei B.; Meignen S. Nonlinear and nonseparable bidimensional multiscale representation based on cell-average representation. *IEEE Transactions on Image Processing* **2015**, *24*, 4570-4580.
- [41] Ortiz, P.; Trillo, J.C. Nonlinear interpolatory reconstruction operator on non uniform grids. *arXiv* **2018**, arxiv:1811.10566.
- [42] Ortiz, P.; Trillo, J.C. On the convexity preservation of a quasi  $C^3$  nonlinear interpolatory reconstruction operator on  $\sigma$  quasi-uniform grids. *Mathematics*. **2021**, *9(4)*, 310. <https://doi.org/10.3390/math9040310>.

- [43] Ortiz P.; Trillo J.C. A piecewise polynomial harmonic nonlinear interpolatory reconstruction operator on non uniform grids: Adaptation around jump discontinuities and elimination of Gibbs phenomenon. *Mathematics*. **2021**, *9*(4), 335. <https://doi.org/10.3390/math9040335>.
- [44] Ortiz, P.; Trillo, J.C. On certain inequalities associated to curvature properties of the nonlinear PPH reconstruction operator. *Journal of Inequalities and Applications*. **2019**, Paper No. 8, 13 pp, <https://doi.org/10.1186/s13660-019-1959-0>
- [45] Ortiz, P.; Trillo, J.C. Analysis of a new nonlinear interpolatory subdivision scheme on  $\sigma$  quasi-uniform grids. *Mathematics*. **2021**, *9*, 1320. <https://doi.org/10.3390/math9121320>
- [46] Reinsch C.H. Smoothing by spline functions. *Numerische Mathematik*. **1967**, *10*, 177-183.
- [47] Shu C.W.; Osher S. Efficient implementation of essentially non-oscillatory shock-capturing schemes. *Journal of Computational Physics* **1988**, *77*(2), 439-471.
- [48] Serna S. A class of extended limiters applied to piecewise hyperbolic methods. *SIAM Journal on Scientific Computing* **2006**, *28*(1), 123-140.
- [49] Serna S.; Marquina A. Power ENO methods: a fifth-order accurate weighted power ENO method. *Journal of Computational Physics* **2004**, *194*(2), 632-658.
- [50] Trillo, J.C. Nonlinear multiresolution and applications in image processing. *PhD Thesis in the University of Valencia, Spain*. **2007**.